Dissertation

zur Erlangung des Grades
Dr. rer. nat. im Fach Physik

Probing the standard model with rare charm decays

Stefan de Boer

Dortmund, Mai 2017

Fakultät Physik

technische universität
dortmund

Gutachter der Dissertation:
Prof. Dr. Gudrun Hiller, Jun.-Prof. Dr. Joachim Brod und Prof. Dr. Svjetlana Fajfer

Vorsitzender des Promotionsausschusses:
Prof. Dr. Jan Kierfeld

Datum der mündlichen Prüfung:
18. Juli 2017

For everybody

Zusammenfassung

Diese Arbeit beinhaltet eine Studie seltener Charmzerfälle im Standardmodell (SM) und jenseits davon. Im Rahmen einer effektiven Theorie berechnen wir die SM Wilsonkoeffizienten bis zur (teils) übernächsten Korrektur zur führenden logarithmischen Ordnung in der Quantenchromodynamik. Die Berechnung umfasst Anschlussbedingungen und das Laufen der Wilsonkoeffizienten in der Renormierungsgruppen-verbesserten Störungstheorie. In der Literatur verwendete Ausdrücke konnten korrigiert werden. Weiterhin wird eine Berechnung von phänomenologisch relevanten zwei Schleifen Matrixelementen der Strom-Strom Operatoren vorgestellt. Wir erarbeiten die Phänomenologie im SM für radiative und semileptonische inklusive Zerfälle, sowie für exklusive Zerfälle $D \to Pll$ und $D \to V\gamma$, einschließlich nicht-perturbativer Effekte. Die Verzweigungsverhältnisse sind von Resonanzen dominiert, jedoch können wir verschiedene Observablen konstruieren, die eindeutig das SM prüfen, z.B. sind Asymmetrien, Winkelobservablen und Leptonflavorverletzende Zerfälle (approximate) Nulltests des SM. Effekte von Physik jenseits des SM werden modellunabhängig und mit Leptoquark Modellen analysiert, wobei verschiedene Einschränkungen und Korrelationen, z.B. mittels Flavor Strukturen, herausgearbeitet werden. Zusätzlich prüfen wir das SM anhand des Zerfalls $\Lambda_c \to p\gamma$, welcher an (zukünftigen) Experimenten zugänglich ist und untersuchen die radiativen Zerfälle in supersymmetrischen Modellen.

Abstract

This thesis comprises a study of rare charm decays in the standard model (SM) and beyond. Within an effective theory framework, we calculate the SM Wilson coefficients to (partly) next-to-next-to leading logarithmic order in quantumchromodynamics. The calculation includes matching conditions and the running of the Wilson coefficients in the renormalization group-improved perturbation theory, thereby correcting expressions used in the literature. Furthermore, a calculation of phenomenological relevant two loop matrix elements of current-current operators is presented. We work out the phenomenology in the SM for radiative and semileptonic inclusive decays as well as the exclusive decays $D \to Pll$ and $D \to V\gamma$, including non-perturbative effects. The branching ratios are dominated by resonances, yet we can construct various observables which cleanly probe the SM, e.g. asymmetries, angular observables and lepton flavor violating decays are (approximate) SM null tests. Beyond the SM physics effects are analyzed model-independently and via leptoquark models, where various constraints and correlations, e.g. through flavor patterns, are worked out. In addition, we probe the SM by means of the decay $\Lambda_c \to p\gamma$, which is accessible at (future) colliders, and investigate the radiative decays in supersymmetric models.

Acknowledgments

Ich möchte mich bei allen bedanken, die mich während der letzten Jahre begleitet und unterstützt haben. Dazu zählen insbesondere meine Eltern, Geschwister, meine Freundin und Freunde, die mir stets den Rücken frei gehalten haben.

Ein besonderer Dank gebührt meiner Doktormutter, die mir diese Arbeit erst ermöglicht hat. Dabei konnte ich von wertvollen Diskussionen und fachlichen Reisen profitieren.

Weiterhin möchte ich allen Mitarbeitern der Lehrstühle T3 und T4 für physikalischen Input danken. Während meiner Zeit am Lehrstuhl habe ich viele Menschen kennen lernen dürfen, die eine motivierende, spannende, unkomplizierte und gesellige Arbeitsatmosphäre geschaffen haben. Obgleich manch einer bereits die Gruppe verlassen hat, werden viele schöne Erinnerungen bleiben. An dieser Stelle sei auch dem Sekretariat und den Admin(ion)s für ihre Hilfe bei nicht-physikalischen Angelegenheiten gedankt. Ein besonderes Lob gilt allen, die Teile dieser Arbeit korrekturgelesen haben sowie für die vielen nützlichen Kommentare.

Ich möchte den Koautoren der dieser Arbeit zugrunde liegenden Publikationen für eine lehrreiche Zeit und eine fruchtbare Zusammenarbeit danken. Diese Zusammenarbeit wurde vom DFG Forschungsverbund FOR 1873 “Quark Flavour Physics and Effective Field Theories” finanziell unterstützt.

Finally, a summary for the English-speaking colleagues: Thank you for a fascinating, interesting and joyful time.

Publications

This thesis is based on the following publications by the author:

- Stefan de Boer and Gudrun Hiller. "Flavor and new physics opportunities with rare charm decays into leptons". In: *Phys. Rev.* D93.7 (2016), p. 074001. DOI: 10.1103/PhysRevD.93.074001. arXiv: 1510.00311 [hep-ph]
- Stefan de Boer, Bastian Müller, and Dirk Seidel. "Higher-order Wilson coefficients for $c \to u$ transitions in the standard model". In: *JHEP* 08 (2016), p. 091. DOI: 10.1007/JHEP08(2016)091. arXiv: 1606.05521 [hep-ph]
- Stefan de Boer and Gudrun Hiller. "Rare radiative charm decays within the standard model and beyond". In: (2017). arXiv: 1701.06392 [hep-ph]
- Stefan de Boer. "Two loop virtual corrections to $b \to (d, s)\ell^+\ell^-$ and $c \to u\ell^+\ell^-$ for arbitrary momentum transfer". In: (2017). arXiv: 1707.00988 [hep-ph]

and the conference proceedings:

- Stefan de Boer. "Rare Semileptonic Charm Decays". In: *7th International Workshop on Charm Physics (Charm 2015) Detroit, MI, USA, May 18-22, 2015*. 2015. arXiv: 1510.00496 [hep-ph]. URL: http://inspirehep.net/record/1395977/files/arXiv:1510.00496.pdf
- Stefan de Boer. "Opportunities with (semi)leptonic rare charm decays". In: *Proceedings, 51st Rencontres de Moriond on Electroweak Interactions and Unified Theories: La Thuile, Italy, March 12-19, 2016*. 2016, pp. 569–572. arXiv: 1605.03415 [hep-ph]. URL: http://inspirehep.net/record/1457615/files/arXiv:1605.03415.pdf

Contents

1. Introduction

The physics of particles is a field with an inspiring past of intriguing developments. The purpose of elementary particle physics is to describe nature at its fundamental level, where matter and interactions emerge. The present theory of particle physics is based on the one hand on quantum field theory with its abstract mathematical structure and on the other hand on the tangible concept of symmetries, condensed in the standard model (SM).

Whereas the last decades can be assigned to the theoretical formulation and experimental confirmation of the SM, nowadays weight is shifted towards the search of beyond the standard model (BSM) physics. In particular, the observation of the Higgs boson in 2012 [7, 8], as predicted by the Higgs mechanism introduced in 1964 [9–12], completes the SM. Further theoretical predictions have been observed subsequently by experiments, e.g. the charm quark was predicted in 1964 [13] and discovered in 1974 [14, 15]. Nowadays, the SM is established as the theory of particle physics due to the interplay of theory and experiment. On the other side, experiments have confronted theory with observations that are not grounded in the SM.

A shortcoming of the SM is the absence of neutrino masses, which are necessary for neutrino oscillations as observed in 1998 and 2001 [16, 17]. Cosmological observations show that ordinary matter is accompanied with dark matter [18], where the latter constitutes five times the mass-energy of the universe as ordinary matter, which is even less than dark energy constitutes. As a first guess dark matter is a BSM particle or it may be part of a modified description of gravity. Besides, gravity is not part of the SM, which would be desirable in view of a unified theory, in addition to a unification of the strong and electroweak (EW) theories. Furthermore, the baryon asymmetry in the early universe requires sizable charge parity (CP) violation, which follows from the Sakharov conditions [19], but cannot be accounted for in the SM. Interestingly, the cosmological observations can be related to particle physics, thus connecting the largest and smallest scales. Nonetheless, particle experiments themselves also challenge the SM. The muon anomalous magnetic moment is the most precisely calculated and measured observable, see [20] for a review. The measurement is largely in agreement with the SM calculation but exhibits a $3.6\,\sigma$ discrepancy [21] at the high precision level. Recently several SM anomalies were revealed in b physics, see [22] for a discussion and, additionally, [23] for a measurement of the lepton flavor ratio in $B^0 \to K^{*0}ll$ decays. These deviations are indirect hints for BSM physics. Indirect searches at low energies generically require a high degree of theoretical precision and experimental sensitivity. On the other hand,

indirect searches allow to probe physics at scales beyond the reach of complementary direct searches at high energies.

Physics of rare decays with charmed particles give rise to such probes. The current situation of rare charm decays may be compared to the one of b physics several years ago, when a broad program, including high precision calculations, developments of new methods, and experimental observations of various modes, has been waiting ahead. Nonetheless, the setting for rare charm physics is intrinsically exceptional: Firstly, the decays are particularly rare, hence experimentally hardly accessible. In fact, apart from a single radiative mode that was observed only in 2016 [24], solely upper limits on branching ratios down to the ten ppb level have been obtained [25]. Various experiments have been and still are involved in the experimental charm program, e.g. $D^0 - \bar{D}^0$ mixing was observed from 2007 onwards by the BaBar, Belle, CDF, and LHCb collaborations [26–29]. Furthermore, charm decays hold a privileged position in lattice calculations, see, e.g., [30]. Secondly, common theoretical frameworks can only be cautiously employed for charm decays. The charm mass may not be large enough for a heavy quark expansion, nor small enough to employ chiral perturbation theory, and is slightly above the non-perturbative scale. Nevertheless, as each coin has two sides, one may turn apparent drawbacks into a virtue - a guideline that we will follow throughout this thesis - i.e. charm decays uniquely probe quantum chromodynamics (QCD). Furthermore, they uniquely probe the up-type sector, as the u quark is stable and decays of the t quark are even more challenging, see e.g. [31] for a review. Specifically, the hints at violation of lepton flavor universality (LFU) in b decays mentioned above should also emerge in charm physics, accompanied with a clean SM prediction, as QCD uncertainties cancel. Thus, charm decays are necessarily linked to an answer of the conceptional question of flavor in the SM: Why are the observed patterns of masses and mixing in the fermion sector the way they are and what is the origin of three copies of fermions? In fact, the flavor sector constitutes most of the parameters of the SM, yet their structure is an unanswered question. A minimal extension to a fourth generation of fermions is excluded, see [32] for a review.

This thesis consists of three chapters followed by the conclusion and outlook in chapter 5. The chapters cover the following topics:

- In chapter 2 we review flavor in the SM and introduce the effective theory which is utilized throughout this thesis. It is based on an operator product expansion (OPE), where we calculate the corresponding Wilson coefficients [33] in the SM to (partly) next-to-next-to leading logarithmic (NNLL) order in QCD. This calculation includes a two step matching as well as the running in renormalization group (RG)-improved perturbation theory. Along we settle the issue of different calculations existing in the literature. We further calculate effective Wilson coefficients that encode perturbative matrix elements to (partly) next-to-next-to leading order (NNLO). Finally, we discuss quantum electrodynamics (QED) contributions.

- Chapter 3 is dedicated to a phenomenological study of rare charm decays in the SM. We consider inclusive radiative and semileptonic decays. Furthermore, we analyze various observables in exclusive $D \to Pll$ and $D \to V\gamma$ decays, where P and V denote a pseudoscalar and vector meson, respectively. Non-perturbative effects are taken into account. Of particular interest are (approximate) SM null tests which provide a testing ground for BSM physics. Finally, we review several other semileptonic modes.

- BSM physics effects are studied in chapter 4. We utilize a model-independent approach, leptoquark (LQ) models and supersymmetric (SUSY) models for radiative decays. We analyze semileptonic and radiative D decays as well as the baryonic decay $\Lambda_c \to p\gamma$. Correlations are worked out, including constraints on LQ models and flavor patterns.

Details on the renormalization group equation (RGE) and constraints on LQ models are compiled in the appendix. Additionally, to make this thesis more self-contained, the latter comprises parameters, distributions and observables, form factors, resonant decays and chiral Fierz identities.

2. Standard model Wilson coefficients

The main objects analyzed in this thesis are Wilson coefficients. They are part of an effective field theory which is valid below a certain scale, e.g. the EW scale in the SM. For an introduction to effective field theories see, e.g., [34]. The physics above that scale is reflected in these Wilson coefficients. An example of an effective theory is Fermi's theory of the weak interaction. Back then the W boson was not known, indeed its dynamical nature is negligible at low energies due to its heavy mass. Within this bottom-up approach, the W boson enters through coefficients, the Wilson coefficients. Nowadays, we utilize a top-down approach to calculate the Wilson coefficients in the SM, as it is experimentally established. The same effective theory will be utilized in chapter 4 to explore BSM physics. Within this framework, different models, including the SM, are parametrized in a unified way, allowing for a comparison. In this chapter, which is based on [2], we calculate the SM Wilson coefficients. We start with a review of flavor in the SM in the next section. If one is solely interested in phenomenological applications of the SM Wilson coefficients, one is referred to chapter 3.

2.1. Flavor in the standard model

The SM of particle physics is a renormalizable quantum field theory with the local gauge group $SU(3)_C \otimes SU(2)_L \otimes U(1)_Y$. The $SU(3)_C$ group encodes the theory of QCD [35–38]. The EW symmetry group $SU(2)_L \otimes U(1)_Y \to U(1)_{\text{QED}}$ is spontaneously broken to QED, due to a non-trivial vacuum that breaks the symmetry of the Lagrangian [39, 40], and see e.g. [41] for Salam's contribution. In table 2.1 the fermions of the SM and their group representations are given. For the experimentally measured masses see appendix A.

In the SM a change of flavor is only possible via charged currents. The $W_\mu^\pm$ bosons couple to left handed quark currents $J_\mu^\pm$ via

$$\begin{aligned} \mathcal{L}_{\text{SM}} \supset \frac{e}{\sqrt{2}\sin\theta_w} \left(W_+^\mu J_\mu^+ + W_-^\mu J_\mu^- \right) , \\ J_\mu^+ = V_{ij} \bar{u}_L^i \gamma^\mu d_L^j , \quad J_\mu^- = V_{ij}^\dagger \bar{d}_L^i \gamma^\mu u_L^j , \end{aligned} \tag{2.1}$$

where e is the electromagnetic coupling and θ_w denotes the weak mixing/Weinberg angle. Here V is the Cabibbo–Kobayashi–Maskawa (CKM) matrix [42, 43], which describes the

field	$SU(3)_C$	$SU(2)_L$	Y_w	T_3	q
$\begin{pmatrix} u \\ d \end{pmatrix}_L, \begin{pmatrix} c \\ s \end{pmatrix}_L, \begin{pmatrix} t \\ b \end{pmatrix}_L$	**3**	**2**	1/6	$1/2$ $-1/2$	$2/3$ $-1/3$
$\begin{pmatrix} \nu_e \\ e \end{pmatrix}_L, \begin{pmatrix} \nu_\mu \\ \mu \end{pmatrix}_L, \begin{pmatrix} \nu_\tau \\ \tau \end{pmatrix}_L$	**1**	**2**	$-1/2$	$1/2$ $-1/2$	0 -1
$u_R\,, c_R\,, t_R$	**3**	**1**	2/3	0	2/3
$d_R\,, s_R\,, b_R$	**3**	**1**	$-1/3$	0	$-1/3$
$e_R\,, \mu_R\,, \tau_R$	**1**	**1**	-1	0	-1

Table 2.1.: The SM fermions, their group representations and charges. The weak hypercharge is defined as $Y_w = (q - T_3)$, where q denotes the electric charge in units of the proton charge, and T_3 is the third component of the weak isospin. The labels L and R refer to left and right handed fields, respectively.

rotation between eigenvectors of the weak interaction and the mass eigenstates, as given by Yukawa interactions. We write the CKM matrix as

$$V = \begin{pmatrix} V_{ud} & V_{us} & V_{ub} \\ V_{cd} & V_{cs} & V_{cb} \\ V_{td} & V_{ts} & V_{tb} \end{pmatrix} \tag{2.2}$$

and refer to appendix A for its experimental data. The CKM matrix obeys the unitarity condition $VV^\dagger = 1$ and it is the only source of flavor and CP violation in the SM since $V \neq 1$ and $V \in \mathbb{C}$, respectively. For the latter we neglect a possible very small strong CP phase, due to a non-trivial topology of the QCD vacuum.

On the other hand, neutral currents via the Z boson preserve flavor. Hence, flavor changing neutral current (FCNC) transitions are only induced at loop level in the SM, as shown in figure 2.1. In fact, the absence of tree level FCNC transitions in the SM leads to the postulation of the Glashow–Iliopolus–Maiani (GIM) mechanism [44].

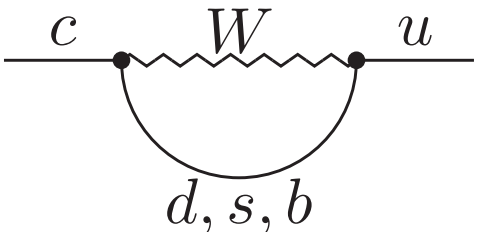

Figure 2.1.: A FCNC in the SM. The dots represent insertions of the corresponding entries of the CKM matrix.

The FCNC transitions inducing rare charm decays involve the mass ratios $m_d : m_s : m_b : m_W \sim 0.00006 : 0.001 : 0.05 : 1$. Utilizing the unitarity condition one can estimate the generic $c \to u$ amplitude as

$$\begin{aligned}\mathcal{A}(c \to u) &= V_{cd}^* V_{ud}\, f(m_d^2/m_W^2) + V_{cs}^* V_{us}\, f(m_s^2/m_W^2) + V_{cb}^* V_{ub}\, f(m_b^2/m_W^2) \\ &= V_{cs}^* V_{us} \left(f(m_s^2/m_W^2) - f(m_d^2/m_W^2)\right) \\ &+ V_{cb}^* V_{ub} \left(f(m_b^2/m_W^2) - f(m_d^2/m_W^2)\right) \end{aligned} \tag{2.3}$$

with the loop function $f(m_q^2/m_W^2) \sim \frac{1}{16\pi^2}\frac{m_q^2}{m_W^2}$. The first term is GIM suppressed, while the second term is suppressed by means of the CKM hierarchy $V_{cb}^* V_{ub} \simeq \lambda^4$, where $\lambda \simeq 0.225$ [45], employing the Wolfenstein parametrization [46]. Thus, we estimate $\mathcal{A}(c \to u) \sim \mathcal{O}(10^{-8})$. Note that the involved CP violating phases are small. Hence, charm FCNC transitions are rare in the SM as loop and GIM/CKM suppressed. Indeed, the estimated amplitude is enhanced by QCD effects, which are calculated in the next sections.

2.2. Effective weak Lagrangian

The formulation utilized throughout this thesis is an effective low-energy theory based on the OPE. The effective Lagrangian at leading order (LO) in the Fermi coupling G_F is given as [2, 47, 48]

$$\mathcal{L}_{\text{eff}} = \mathcal{L}_{\text{QCD}\otimes\text{QED}}|_{\{f:m_f<\mu\}} + \mathcal{L}_{\text{eff}}^{\text{weak}}\,, \tag{2.4}$$

where the Lagrangian of QCD and QED is restricted to fermions f with masses m below a mass scale μ. The QCD $\otimes$ QED Lagrangian contains the covariant derivative $D_\mu = (\partial_\mu + ig_s T^a \mathcal{A}_\mu^a + ieqA_\mu)$, where T^a are the $SU(3)_C$ generators normalized to $\text{Tr}[T^a T^b] = \delta^{ab}/2$. Furthermore, g_s is the strong coupling, $\mathcal{A}_\mu^a$ and A_μ denote the gluon

and electromagnetic fields, respectively, and q is the electric charge in units of the proton charge. The effective weak Lagrangian describing $c \to ull$ transitions reads

$$\mathcal{L}_{\text{eff}}^{\text{weak}}\big|_{m_W \geq \mu > m_b} = \frac{4G_F}{\sqrt{2}} \sum_{q \in \{d,s,b\}} V_{cq}^* V_{uq} \left(C_1(\mu) P_1^{(q)} + C_2(\mu) P_2^{(q)} \right) , \tag{2.5}$$

$$\mathcal{L}_{\text{eff}}^{\text{weak}}\big|_{m_b > \mu \geq m_c} = \frac{4G_F}{\sqrt{2}} \sum_{q \in \{d,s\}} V_{cq}^* V_{uq} \left(C_1(\mu) P_1^{(q)} + C_2(\mu) P_2^{(q)} + \sum_{i=3}^{10} C_i(\mu) P_i \right) , \tag{2.6}$$

where the sum is over light down-type quark fields. The Wilson coefficients C_i and the operators P_i, see eqs. (2.7-2.16) for their definitions, are discussed below.

In the effective Lagrangian approach, heavy fields with masses $M > (\mu_W, \mu_b)$ for the corresponding thresholds are integrated out and absorbed in the Wilson coefficients. This is done by equating the amputed, one-particle-irreducible off-shell Green's functions in the full, e.g. the SM, and the effective theory with single insertions of the operators P_i. An expansion is done at LO in the EW gauge couplings and external momenta/light quark masses squared divided by the squared masses of the particles, which are integrated out. Hence, masses of the light fields are consistently set to zero.

The effective weak Lagrangian, eqs. (2.5, 2.6), depends on the scale. The matching at the scale μ_W induces solely the operators $P_{1,2}$, whereas only due to a second matching, where the b quark is integrated out, the additional operators P_{3-10} emerge. This procedure can be compared to the running of couplings and masses in a mass independent renormalization scheme, where corrections at flavor thresholds are included by hand. The matching will be described in detail in the next sections. Furthermore, the Wilson coefficients C_i and the operators are each scale dependent, yet physical observables are scale independent. In fact, the scale dependence of the Wilson coefficients and operator matrix elements do not cancel to a certain order in perturbation theory. The residual scale dependence is related to the RGE, which is employed to evaluate the Wilson coefficients at different scales. For an introduction to the RGE see, e.g., [49]. The RGE allows to sum logarithms of the form $(\alpha \ln[\mu_0/\mu])^n$ for $n \in \mathbb{N}$ and $\alpha = g^2/(4\pi)$, where g denotes the coupling, to all orders in α. In particular, large logarithms are resummed, e.g. for $\mu_0 \sim m_W$ and $\mu \sim m_b$ in eq. (2.5). The RGE and its solution is presented in appendix B. It follows that the residual scale dependence probes higher order terms in the perturbative expansion by varying the scale, yet a scheme dependence remains. In QCD, the Wilson coefficients $C_{1,2}$ in eqs. (2.5, 2.6) are quark universal and the quark dependence is solely given by CKM matrix. At higher order in QED this does not hold. In the current chapter we focus on QCD effects, as its coupling α_s is much larger than the QED coupling α_e at low energies. As we include expression to order α_s^2 leading QED effects may, however, become of similar size. This will be considered in section 2.7. The Wilson coefficients are, furthermore, universal for all $c \to ull$ processes. This also includes processes induced by $c \to u\gamma$, $c \to ug$, and $c\bar{u} \to q\bar{q}$ transitions as well as for the effective

Wilson coefficients introduced in section 2.6. However, note that additional effects can be absorbed in Wilson coefficients, but are process dependent, e.g. weak annihilation and spectator interaction, see section 3.3.1.

The basis of local off-shell physical SM operators of dimension less than six consists of [2, 50–52]

$$P_1^{(q)} = (\bar{u}_L \gamma_{\mu_1} T^a q_L)(\bar{q}_L \gamma^{\mu_1} T^a c_L)\,, \tag{2.7}$$

$$P_2^{(q)} = (\bar{u}_L \gamma_{\mu_1} q_L)(\bar{q}_L \gamma^{\mu_1} c_L)\,, \tag{2.8}$$

$$P_3 = (\bar{u}_L \gamma_{\mu_1} c_L) \sum_{\{q:m_q<\mu\}} (\bar{q}\gamma^{\mu_1} q)\,, \tag{2.9}$$

$$P_4 = (\bar{u}_L \gamma_{\mu_1} T^a c_L) \sum_{\{q:m_q<\mu\}} (\bar{q}\gamma^{\mu_1} T^a q)\,, \tag{2.10}$$

$$P_5 = (\bar{u}_L \gamma_{\mu_1}\gamma_{\mu_2}\gamma_{\mu_3} c_L) \sum_{\{q:m_q<\mu\}} (\bar{q}\gamma^{\mu_1}\gamma^{\mu_2}\gamma^{\mu_3} q)\,, \tag{2.11}$$

$$P_6 = (\bar{u}_L \gamma_{\mu_1}\gamma_{\mu_2}\gamma_{\mu_3} T^a c_L) \sum_{\{q:m_q<\mu\}} (\bar{q}\gamma^{\mu_1}\gamma^{\mu_2}\gamma^{\mu_3} T^a q)\,, \tag{2.12}$$

$$P_7 = \frac{e}{g_s^2} m_c\, \bar{u}_L \sigma^{\mu_1\mu_2} c_R F_{\mu_1\mu_2}\,, \tag{2.13}$$

$$P_8 = \frac{1}{g_s} m_c\, \bar{u}_L \sigma^{\mu_1\mu_2} T^a c_R G^a_{\mu_1\mu_2}\,, \tag{2.14}$$

$$P_9 = \frac{e^2}{g_s^2} (\bar{u}_L \gamma_{\mu_1} c_L) \left(\bar{l}\gamma^{\mu_1} l\right)\,, \tag{2.15}$$

$$P_{10} = \frac{e^2}{g_s^2} (\bar{u}_L \gamma_{\mu_1} c_L) \left(\bar{l}\gamma^{\mu_1}\gamma_5 l\right)\,. \tag{2.16}$$

Here, $q_{L/R} = \frac{1}{2}(1 \mp \gamma_5)q$ are chiral quark fields, $\sigma^{\mu_1\mu_2} = \frac{i}{2}[\gamma^{\mu_1}, \gamma^{\mu_2}]$, and $F_{\mu_1\mu_2} = (\partial_{\mu_1} A_{\mu_2} - \partial_{\mu_2} A_{\mu_1})$ and $G^a_{\mu_1\mu_2} = (\partial_{\mu_1} \mathcal{A}^a_{\mu_2} - \partial_{\mu_2} \mathcal{A}^a_{\mu_1} - g_s f^{abc} \mathcal{A}^b_{\mu_1} \mathcal{A}^c_{\mu_2})$ are the electromagnetic and chromomagnetic field strength tensors, respectively. The gauge-invariant physical operators, eqs. (2.7-2.16), consist of current-current operators $P_{1,2}$, QCD penguin operators P_{3-6}, magnetic moment operators $P_{7,8}$, and semileptonic operators $P_{9,10}$. They are build from light fields only. The operator basis also includes the operators $P'_7 = \frac{e}{g_s^2}\, m_c\, \bar{u}_R \sigma^{\mu_1\mu_2} c_L F_{\mu_1\mu_2}$ and $P'_8 = \frac{1}{g_s}\, m_c\, \bar{u}_R \sigma^{\mu_1\mu_2} T^a c_L G^a_{\mu_1\mu_2}$, whose Wilson coefficients are suppressed by m_u/m_c with respect to $C_{7,8}$ in the SM, and are neglected, as light quark masses are neglected. Furthermore, we do not consider electromagnetic penguin operators, which are the QED equivalents of P_{3-6}. For completeness, also one dimension five operator may be added to the operator basis, which violates lepton number and is thus omitted [53]. The choice of the operator basis is not unique and we will give a more suitable one for phenomenological analyses in chapter 3. The definitions

given by eqs. (2.7-2.16) are, however, common for higher order calculations as we discuss next.

In the basis of eqs. (2.7-2.16) Dirac traces of γ_5 are absent at the LO in the Fermi coupling and to all orders in QCD. This feature allows to consistently anticommute γ_5 within dimensional regularization [50], see [54] for other prescriptions. However, no such traces are present in the SM diagrams. Other choices of operator bases and the mappings between different ones are (partly) given in [2, 52, 55]. We extend this description by noting that the mapping onto the "traditional" operator basis, see e.g. [56], is given by the action of the rotation matrix R [55] on the $P_{1-6} \to P_9$ mixing at LO and the mixing [52] onto operators $\alpha_s/(4\pi)P_{7,8}^{\text{eff}}$, see section 2.6, at next-to leading order (NLO). The normalization of the dipole and semileptonic operators, eqs. (2.13-2.16), allows to count diagrams in orders of α_s equivalent to the number of loops in the SM diagrams [51], e.g. the LO mixing of P_{1-6} onto P_9 is of order α_s^0.

To regularize ultraviolet (UV) divergences, dimensionally non-physical "evanescent" operators have to be included, which vanish algebraically in four dimension. They are equivalently defined in [50–52, 55, 57], while three loop evanescent operators are given in [55]. Additionally, non-physical gauge-invariant and gauge-variant operators that vanish by the QCD⊗QED equations of motion (EOM) up to a total derivative, emerge due to QCD renormalization. The EOM-vanishing operators are given in [52] and are equivalently defined in [51, 55]. Matrix elements of the non-physical operators between physical states vanish if the infrared (IR) regularization does not break symmetries and the calculation is performed without an expansion in external momenta. Moreover, the Becchi–Rouet–Stora–Tyutin (BRST) variation of certain operators induce non-physical BRST-exact operators as counterterms. These are, however, not relevant up to three loop for the operators P_i [52, 55, 57].

In the following sections we will calculate the SM Wilson coefficients at (partly) NNLL order in QCD,

$$C_i(\mu) = C_i^{(0)}(\mu) + \frac{\alpha_s(\mu)}{4\pi} C_i^{(1)}(\mu) + \left(\frac{\alpha_s(\mu)}{4\pi}\right)^2 C_i^{(2)}(\mu) + \mathcal{O}\left(\alpha_s^3(\mu)\right) , \tag{2.17}$$

following the definitions made in eqs. (2.5-2.16). The matching at μ_W at fixed order in perturbation theory is at NNLO, while the matching at μ_b is at NLO. The running of the Wilson coefficients is calculated in the RG-improved perturbation theory at NNLL order. It is obtained from a calculation at one loop order higher than the actual matching calculation, which guarantees the scheme independence of physical observables at the order the matching is performed. Finally, effective Wilson coefficients are introduced and calculated at (partly) NNLO. The combination of different orders in different steps is not consistent, yet as will be shown, the missing NNLO calculations are numerically small in phenomenological applications. To regularize UV divergences we use the mass independent dimensional regularization scheme, which does not break power counting and the mass independent modified minimal subtraction ($\overline{\text{MS}}$) renormalization scheme.

2.3. Matching at $\mu \sim m_W$

As already mentioned in the previous section, only $C_{1,2}$ are induced at the EW scale in the SM. This follows from a consistent implementation of the effective weak theory and is elaborated in this section. The numerical values of the Wilson coefficients, in particular of C_9, depend on the correct treatment of light quark fields.

At the scale $\mu \sim m_W$ the t quark, H boson, Z boson, and W boson are integrated out simultaneously. This does not induce large logarithms as the involved masses are of similar size. Indeed, a sequential integration of the t quark and the bosons would break the $SU(2)_L \otimes U(1)_Y$ gauge symmetry, introducing Wess-Zumino terms.

The NNLO QCD matching at $\mu_W \sim m_W$ is given as [2, 51, 55]

$$C_1(\mu_W) = \frac{\alpha_s(\mu_W)}{4\pi}\left(15 + 6\ln\frac{\mu_W^2}{m_W^2}\right) + \left(\frac{\alpha_s(\mu_W)}{4\pi}\right)^2 \times \left(-T\left[\frac{m_t^2}{m_W^2}\right] + \frac{7987}{72} + \frac{17}{3}\pi^2 + \frac{475}{6}\ln\frac{\mu_W^2}{m_W^2} + 17\ln^2\frac{\mu_W^2}{m_W^2}\right), \tag{2.18}$$

$$C_2(\mu_W) = 1 + \left(\frac{\alpha_s(\mu_W)}{4\pi}\right)^2\left(\frac{127}{18} + \frac{4}{3}\pi^2 + \frac{46}{3}\ln\frac{\mu_W^2}{m_W^2} + 4\ln^2\frac{\mu_W^2}{m_W^2}\right) \tag{2.19}$$

with

$$T[x] = -(16x+8)\sqrt{4x-1}\,\mathrm{Cl}_2\left[2\sin^{-1}\frac{1}{2\sqrt{x}}\right] + \left(16x + \frac{20}{3}\right)\ln x + 32x + \frac{112}{9}, \tag{2.20}$$

and the Clausen function of order two

$$\mathrm{Cl}_2[x] = \mathrm{Im}[\mathrm{Li}_2[\exp[ix]]], \qquad \mathrm{Li}_2[x] = -\int_0^x \mathrm{d}t \frac{\ln[1-t]}{t}. \tag{2.21}$$

With respect to [2], additional terms $\sim \ln[\mu_W^2/m_W^2]$ are provided that vanish for $\mu_W = m_W$ but are used in this thesis to estimate the scale uncertainty. The other Wilson coefficients $C_{3-10}(\mu_W)$ are zero due to the CKM unitarity. Corresponding matching diagrams involve, e.g. two loop diagrams with a t quark.

The vanishing of $C_{3-10}(\mu_W)$ is treated differently in the literature. The approach presented here is the same as in [47, 48]. Contrary [58–60] start with non-vanishing Wilson coefficients $C_{3-10}(\mu_W)$. They are driven by non-vanishing light quark masses, e.g. via [61]

$$\sum_{q\in\{d,s,b\}} V_{cq}^* V_{uq} C_9^{(q)}(\mu_W) \simeq V_{cs}^* V_{us}\frac{-2}{9}\ln\frac{m_s^2}{m_d^2} \simeq -0.29, \tag{2.22}$$

thus breaking the GIM mechanism. We add that the electromagnetic Wilson coefficient in [58–60] was adopted from [61], which is, however, only valid for $b \to s\gamma$ transitions.

The corresponding expressions for $c \to u\gamma$ transitions are given in [62], yet a correct treatment implies $C_7(\mu_W) = 0$. The non-vanishing Wilson coefficients follow from a fixed order calculation, which is valid on its own but not in the context of the OPE, where the light quark fields form the operators, but do not contribute to the Wilson coefficients. The light quark masses have to be consistently set to zero, or used as an expansion parameter if they enter the definitions of operators, e.g. for P_7. Indeed, this prescription was used in [61], which provides the basic expressions for the results in [58–60]. In particular, the numerical value in eq. (2.22) is driven by a large logarithm arising from the light quark masses. Employing the RGE the fixed order calculation is improved and these spurious logarithms are resummed, see also [2].

Nevertheless, non-vanishing $C_{3-10}(\mu_W)$ are possible within the OPE if the CKM unitarity is broken. However, the corresponding Wilson coefficients are not enhanced by large logarithms. Here we provide their expressions proportional to $(V_{cd}^* V_{ud} + V_{cs}^* V_{us} + V_{cb}^* V_{ub}) = -\Delta V_{cu}$ extracted from [51]

$$
\begin{aligned}
C_3(\mu_W) &= \left(\frac{\alpha_s(\mu_W)}{4\pi}\right)^2 \left(-\frac{680}{243} - \frac{20}{81}\pi^2 - \frac{68}{81}\ln\frac{\mu_W^2}{m_W^2} - \frac{20}{27}\ln^2\frac{\mu_W^2}{m_W^2}\right) , \\
C_4(\mu_W) &= \frac{\alpha_s(\mu_W)}{4\pi}\left(-\frac{7}{9} + \frac{2}{3}\ln\frac{\mu_W^2}{m_W^2}\right) \\
&\quad + \left(\frac{\alpha_s(\mu_W)}{4\pi}\right)^2 \left(\frac{950}{243} + \frac{10}{81}\pi^2 + \frac{124}{27}\ln\frac{\mu_W^2}{m_W^2} + \frac{10}{27}\ln^2\frac{\mu_W^2}{m_W^2}\right) , \\
C_5(\mu_W) &= \left(\frac{\alpha_s(\mu_W)}{4\pi}\right)^2 \left(\frac{68}{243} + \frac{2}{81}\pi^2 + \frac{14}{81}\ln\frac{\mu_W^2}{m_W^2} + \frac{2}{27}\ln^2\frac{\mu_W^2}{m_W^2}\right) , \\
C_6(\mu_W) &= \left(\frac{\alpha_s(\mu_W)}{4\pi}\right)^2 \left(\frac{85}{162} + \frac{5}{108}\pi^2 + \frac{35}{108}\ln\frac{\mu_W^2}{m_W^2} + \frac{5}{36}\ln^2\frac{\mu_W^2}{m_W^2}\right) , \\
C_7(\mu_W) &= \frac{\alpha_s(\mu_W)}{4\pi}\left(-\frac{23}{36}\right) + \left(\frac{\alpha_s(\mu_W)}{4\pi}\right)^2 \left(\frac{713}{243} + \frac{4}{81}\ln\frac{\mu_W^2}{m_W^2}\right) , \\
C_8(\mu_W) &= \frac{\alpha_s(\mu_W)}{4\pi}\left(-\frac{1}{3}\right) + \left(\frac{\alpha_s(\mu_W)}{4\pi}\right)^2 \left(\frac{91}{324} - \frac{4}{27}\ln\frac{\mu_W^2}{m_W^2}\right) , \\
C_9(\mu_W) &= \frac{\alpha_s(\mu_W)}{4\pi}\left(\frac{1}{4\sin^2\theta_w} + \frac{38}{27} - \frac{4}{9}\ln\frac{\mu_W^2}{m_W^2}\right) + \left(\frac{\alpha_s(\mu_W)}{4\pi}\right)^2 \\
&\quad \times \left(\frac{1}{\sin^2\theta_w} + \frac{524}{729} - \frac{128}{243}\pi^2 - \frac{16}{3}\ln\frac{\mu_W^2}{m_W^2} - \frac{128}{81}\ln^2\frac{\mu_W^2}{m_W^2}\right) , \\
C_{10}(\mu_W) &= \frac{\alpha_s(\mu_W)}{4\pi}\left(-\frac{1}{4\sin^2\theta_w}\right) + \left(\frac{\alpha_s(\mu_W)}{4\pi}\right)^2 \left(-\frac{1}{\sin^2\theta_w}\right) .
\end{aligned}
\tag{2.23}
$$

However, we will take the CKM unitarity to be intact and consequently $C_{3-10}(\mu_W) = 0$. Effects of a breaking of the CKM unitarity will be considered in section 2.7.

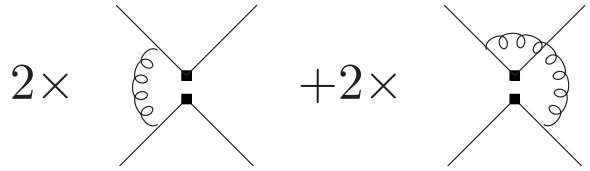

Figure 2.2.: One loop diagrams contributing to the mixing of O_1 and O_2 in QCD. The boxes denote the insertion of the current-current operator O_2. The multiplicative factors follow from symmetry. The second diagram is non-planar.

The next step is to evolve the Wilson coefficients, governed by the RGE. Its solution is given in appendix B, for which the anomalous dimension matrix (ADM) is needed, which is provided in appendix B.2.

2.4. Anomalous dimension and loop integrals in a nutshell

In this section we show how the anomalous dimension is obtained from renormalization. We calculate the ADM for current-current operators at LO QCD. Along we compute basic one loop integrals, including finite terms. The current section contains solely sample calculations and serves as an introduction into some technical aspects. For the actual calculation of the Wilson coefficients one is referred to the next sections.

In the following, we calculate the mixing of current-current operators from renormalization, hence derive the LO ADM. For simplicity, we work with operators in the traditional basis, that is

$$O_1 = ((\overline{u}_L)_\alpha \gamma_\mu (q_L)^\beta)((\overline{q}_L)_\beta \gamma^\mu (c_L)^\alpha)\,, \quad O_2 = ((\overline{u}_L)_\alpha \gamma_\mu (q_L)^\alpha)((\overline{q}_L)_\beta \gamma^\mu (c_L)^\beta)\,, \tag{2.24}$$

where α and β denote color indices. The resulting one loop diagrams are shown in figure 2.2. The purpose is to calculate these diagrams and to express the results in terms of tree level matrix elements of O_1 and O_2, giving rise to the matching between operators.

The first diagram in d dimensions yields, neglecting external quark momenta,

$$\begin{aligned}
\mathcal{A}_1 &= \frac{4G_F}{\sqrt{2}} V_{cq}^* V_{uq} \int \frac{\mathrm{d}k^d}{(2\pi)^d} \left(\bar{u}_\alpha (i g_s \gamma_\mu T^a) \frac{i\not{k}}{k^2} (\gamma_\nu P_L) q^\alpha \right) \frac{-i}{k^2} \\
&\quad \times \left(\bar{q}_\beta (i g_s \gamma^\mu T^a) \frac{i(-\not{k})}{k^2} (\gamma^\nu P_L) c^\beta \right) \\
&= i \frac{4G_F}{\sqrt{2}} V_{cq}^* V_{uq}\, g_s^2 \int \frac{\mathrm{d}k^d}{(2\pi)^d} \frac{k^\rho k^\sigma}{k^6} (\bar{u}_\alpha \gamma^\mu T^a \gamma_\rho \gamma_\nu P_L q^\alpha)(\bar{q}_\beta \gamma_\mu T^a \gamma_\sigma \gamma^\nu P_L c^\beta) \\
&= i \frac{4G_F}{\sqrt{2}} V_{cq}^* V_{uq}\, g_s^2 \int \frac{\mathrm{d}k^d}{(2\pi)^d} \frac{k^2/d}{k^6} (\bar{u}_\alpha \gamma^\mu T^a \gamma_\rho \gamma_\nu P_L q^\alpha)(\bar{q}_\beta \gamma_\mu T^a \gamma^\rho \gamma^\nu P_L c^\beta)\,.
\end{aligned} \tag{2.25}$$

We neglect the mass dependence from the integral in d dimension, as it does not contribute to the divergence at one loop. The last line follows from the symmetry of the integral, i.e. $\int \frac{\mathrm{d}k^d}{(2\pi)^d} k^\rho k^\sigma / k^6 \propto \eta^{\rho\sigma}$, where the proportionality constant is determined by a contraction with the metric $\eta_{\rho\sigma}$.

After a Wick-rotation the integral is evaluated to

$$\begin{aligned}\int \frac{\mathrm{d}k^d}{(2\pi)^d}\frac{1}{k^4} &= \int \frac{\mathrm{d}k^d}{(2\pi)^d}\left[\frac{1}{k^2(k^2-m^2)} - \frac{m^2}{k^4(k^2-m^2)}\right] \\ &= \frac{i(\Gamma[2-d/2]_{\mathrm{UV}} - \Gamma[2-d/2]_{\mathrm{IR}})}{(4\pi)^{d/2}}\end{aligned} \tag{2.26}$$

with an arbitrary mass m and $\Gamma[\epsilon] = 1/\epsilon - \gamma + \mathcal{O}(\epsilon)$, where γ denotes the Euler constant. The evaluation of this and a more general class of integrals will be done at the end of the current section. In eq. (2.26) the UV and IR divergences are separated. They cancel within dimensional regularization. In fact, the IR divergences are the same in the full and the effective theory. We keep only the UV divergences as needed for the anomalous dimension.

The generators T^a in the fundamental representation obey the relation

$$(T^a)_{ij}(T^a)_{kl} = \frac{1}{2}\left(\delta_{il}\delta_{kj} - \frac{1}{N}\delta_{ij}\delta_{kl}\right) \tag{2.27}$$

which follows from building an $SU(N)$ invariant as well as the properties $(T^a)_{ii}(T^a)_{kl} = 0$ and $(T^aT^a)_{il} = (N^2-1)/(2N)\delta_{il}$. In fact, eq. (2.27) is the source of the mixing of the operators O_1 and O_2.

Using the identity $(\bar{u}_1\gamma^\mu\gamma^\rho\gamma^\nu P_L u_2)(\bar{u}_3\gamma_\mu\gamma_\rho\gamma_\nu P_L u_4) = d^2(\bar{u}_1\gamma^\mu P_L u_2)(\bar{u}_3\gamma_\mu P_L u_4)$ for Dirac spinors one obtains

$$\begin{aligned}\mathcal{A}_1 &= -\frac{4G_F}{\sqrt{2}}V_{cq}^*V_{uq}\,g_s^2\frac{\Gamma[2-d/2]}{(4\pi)^{d/2}}\frac{d}{2} \\ &\quad\times\left((\bar{u}_\beta\gamma_\mu P_L q^\alpha)(\bar{q}_\alpha\gamma^\mu P_L c^\beta) - \frac{1}{N}(\bar{u}_\alpha\gamma_\mu\ P_L q^\alpha)(\bar{q}_\beta\gamma^\mu P_L c^\beta)\right) \\ &= -\frac{4G_F}{\sqrt{2}}V_{cq}^*V_{uq}\frac{g_s^2}{(4\pi)^2}\Gamma[\epsilon] \\ &\quad\times\left(2(\bar{u}_\beta\gamma_\mu P_L q^\alpha)(\bar{q}_\alpha\gamma^\mu P_L c^\beta) - \frac{2}{N}(\bar{u}_\alpha\gamma_\mu\ P_L q^\alpha)(\bar{q}_\beta\gamma^\mu P_L c^\beta)\right),\end{aligned} \tag{2.28}$$

where $d = 4-2\epsilon$. In the calculation we use the anticommutation relation $\{\gamma^5, \gamma^\mu\} = 0$.

The second diagram yields

$$\begin{aligned}\mathcal{A}_2 &= \frac{4G_F}{\sqrt{2}}V_{cq}^*V_{uq}\int\frac{\mathrm{d}k^d}{(2\pi)^d}\left(\bar{u}_\alpha(ig\gamma_\mu T^a)\frac{i\not{k}}{k^2}(\gamma_\nu P_L)q^\alpha\right)\frac{+i}{k^2}\left(\bar{q}_\beta(ig\gamma^\nu T^a)\frac{i(-\not{k})}{k^2}(\gamma^\mu P_L)c^\beta\right)\\ &= \frac{4G_F}{\sqrt{2}}V_{cq}^*V_{uq}\frac{g_s^2}{(4\pi)^2}\Gamma[\epsilon]\\ &\times\left(\frac{1}{2}(\bar{u}_\beta\gamma_\mu P_L q^\alpha)(\bar{q}_\alpha\gamma^\mu P_L c^\beta)-\frac{1}{2N}(\bar{u}_\alpha\gamma_\mu\ P_L q^\alpha)(\bar{q}_\beta\gamma^\mu P_L c^\beta)\right)\end{aligned} \tag{2.29}$$

which follows from $(\bar{u}_1\gamma^\mu\gamma^\rho\gamma^\nu P_L u_2)(\bar{u}_3\gamma_\nu\gamma_\rho\gamma_\mu P_L u_4) = d(\bar{u}_1\gamma^\mu P_L u_2)(\bar{u}_3\gamma_\mu P_L u_4)$.

The sum of these amplitudes for $N = 3$, written in terms of the tree level matrix elements of the operators $\langle O_i\rangle^{(0)}$, is

$$2\times\mathcal{A}_1 + 2\times\mathcal{A}_2 = \frac{4G_F}{\sqrt{2}}V_{cq}^*V_{uq}\frac{g_s^2}{(4\pi)^2}\Gamma[\epsilon]\left(\langle O_1\rangle^{(0)} - 3\langle O_2\rangle^{(0)}\right). \tag{2.30}$$

The same calculation can be repeated for the operator O_1 by an appropriate interchange of the color indices.

Upon renormalization

$$O_i = Z_{ij}^{-1}(O_j)_r\,, \tag{2.31}$$

where r denotes renormalized quantities, the renormalization matrix is obtained as

$$Z = 1 + \frac{\alpha_s}{4\pi}\frac{1}{\epsilon}\begin{pmatrix}1 & -3\\ -3 & 1\end{pmatrix}. \tag{2.32}$$

The ADM can be found from the renormalization matrix as [52]

$$\gamma_{ij} = 2\beta(\epsilon,\alpha_s)Z_{ik}\frac{\mathrm{d}}{\mathrm{d}\alpha_s}Z_{kj}^{-1} \tag{2.33}$$

with

$$\beta(\epsilon,\alpha_s) = \alpha_s(-\epsilon+\beta(\alpha_s))\,,\qquad \beta(\alpha_s) = -\sum_{i=0}^{\infty}\left(\frac{\alpha_s}{4\pi}\right)^{i+1}\beta_i(n_f)\,, \tag{2.34}$$

where β_i are given by eq. (B.5) and n_f denotes the number of flavors.

Finally, we obtain

$$\gamma = \frac{\alpha_s}{4\pi}\begin{pmatrix}2 & -6\\ -6 & 2\end{pmatrix}. \tag{2.35}$$

This result agrees with the one given in appendix B.2 after an appropriate change of the operator basis, as described in section 2.2.

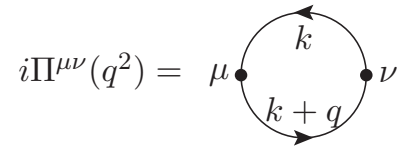

Figure 2.3.: The fermionic one loop correlation function. The external momentum associated with the vertices μ and ν is denoted by k.

In the following, we turn to the computation of the fermionic one loop correlation function $\Pi^{\mu\nu}$, shown in figure 2.3.

We obtain

$$\begin{aligned} i\Pi^{\mu\nu}(q^2) &= -\mu^{4-d}\int \frac{\mathrm{d}^d k}{(2\pi)^d}\mathrm{Tr}\left[\frac{i(\not{k}+\not{q}+m)}{(k+q)^2-m^2}(-i\gamma^\mu)\frac{i(\not{k}+m)}{k^2-m^2}(-i\gamma^\nu)\right] \\ &= -\mu^{4-d}\int \frac{\mathrm{d}^d k}{(2\pi)^d}\int_0^1 \mathrm{d}z \frac{\mathrm{Tr}\left[(\not{k}+\not{q}+m)\gamma^\mu(\not{k}+m)\gamma^\nu\right]}{\left((k+zq)^2+z(1-z)q^2-m^2\right)^2} \\ &= -\mu^{4-d}\int_0^1 \mathrm{d}z \int \frac{\mathrm{d}^d l}{(2\pi)^d} \\ &\times \frac{2dz(1-z)(q^2 g^{\mu\nu}-q^\mu q^\nu)-d(l^2+z(1-z)q^2-m^2)g^{\mu\nu}+2dl^\mu l^\nu}{\left(l^2+z(1-z)q^2-m^2\right)^2}\,, \end{aligned} \tag{2.36}$$

where $l = k + zq$ and employing the symmetry of the integral.

Writing, in euclidean form, $I_n = \int \mathrm{d}^d k/(k^2+m^2)^n$ we obtain from integration by parts (IBP) identities [63] the linear difference equation

$$(d-2n)I_n + 2nm^2 I_{n+1} = 0 \tag{2.37}$$

the solution of which is, incorporating the mass dimension,

$$I_n \propto \left(m^2\right)^{d/2-n}\frac{\Gamma[n-d/2]}{\Gamma[n]}\,. \tag{2.38}$$

As a boundary condition we use I_1, that is

$$\begin{aligned} I_1 &= \frac{2\pi^{d/2}}{\Gamma[d/2]}\int_0^\infty \mathrm{d}r \frac{r^{d-1}}{r^2+m^2} \\ &= \frac{2\pi^{d/2}}{\Gamma[d/2]}\frac{m^{d-2}}{2}\int_0^1 \mathrm{d}s\, s^{1-d/2-1}(1-s)^{d/2-1} \\ &= \frac{\pi^{d/2}m^{d-2}}{\Gamma[d/2]}\frac{\Gamma[1-d/2]\Gamma[d/2]}{\Gamma[1-d/2+d/2]}\,, \end{aligned} \tag{2.39}$$

where $r = m\sqrt{1/s-1}$. It follows that

$$I_n = \pi^{d/2}\left(m^2\right)^{d/2-n}\frac{\Gamma[n-d/2]}{\Gamma[n]} \tag{2.40}$$

as well as the integrals

$$\int \mathrm{d}^d k \frac{k^2}{(k^2+m^2)^n} = \frac{d}{2n} I_{n-1}\,, \qquad \int \mathrm{d}^d k \frac{k^\mu k^\nu}{(k^2+m^2)^n} = \frac{g^{\mu\nu}}{2n} I_{n-1}\,. \tag{2.41}$$

Finally, one obtains

$$\begin{aligned} i\Pi^{\mu\nu}(q^2) &= -\mu^{4-d}\int_0^1 \mathrm{d}z\, 2dz(1-z)\left(q^2 g^{\mu\nu} - q^\mu q^\nu\right)\frac{i}{16\pi^2}\left(\frac{4\pi}{m^2 - z(1-z)q^2}\right)^\epsilon \Gamma[\epsilon] \\ &= -i\left(q^2 g^{\mu\nu} - q^\mu q^\nu\right)\left(\frac{1}{12\pi^2}\left(\frac{1}{\epsilon} - \frac{1}{2} - \gamma + \ln[4\pi]\right)\right. \\ &\quad \left. + \frac{1}{2\pi^2}\int_0^1 \mathrm{d}z\, z(1-z)\ln\frac{\mu^2}{m^2 - z(1-z)q^2}\right), \end{aligned} \tag{2.42}$$

where $d = 4-2\epsilon$. Note that $P_{L/R}$ insertions on the fermion lines do not induce additional contributions, as the corresponding terms $\propto \gamma_5$ vanish.

2.5. Matching at $\mu \sim m_b$

While evolving the Wilson coefficients $C_{1,2}$ from μ_W to μ_c, the intermediate scale μ_b is crossed. This results in a matching of the $n_f = 5$ quark onto the $n_f = 4$ quark effective theory without the b quark. To be consistent, the matching should be done at NNLO. However, only the NLO matching is fully known and part of the NNLO matching remains missing. Nevertheless, the effect of the latter is additionally suppressed in phenomenological applications due to the GIM mechanism, see chapter 3. In contrast to the matching at μ_W all the SM operators P_{1-10} are induced at μ_b. This is illustrated in figure 2.4, where the diagrams relevant for the matching onto P_4 and P_9 at NLO are shown.

The LO matching reads $C_i^{(0)}|_{n_f=4} = C_i^{(0)}|_{n_f=5}$ for any Wilson coefficient. The matching onto $P_{1,2}$ yields $C_{1,2}^{(1)}|_{n_f=4} = C_{1,2}^{(1)}|_{n_f=5}$ at NLO. Furthermore, we obtain from the one loop matching

$$C_4^{(1)}|_{n_f=4} = \frac{1}{9}\left(1 - \ln\frac{\mu_b^2}{m_b^2}\right)C_1^{(0)}|_{n_f=5} - \frac{2}{3}\left(1 - \ln\frac{\mu_b^2}{m_b^2}\right)C_2^{(0)}|_{n_f=5}\,, \tag{2.43}$$

$$C_9^{(1)}|_{n_f=4} = -\frac{8}{27}\left(1 - \ln\frac{\mu_b^2}{m_b^2}\right)C_1^{(0)}|_{n_f=5} - \frac{2}{9}\left(1 - \ln\frac{\mu_b^2}{m_b^2}\right)C_2^{(0)}|_{n_f=5}\,, \tag{2.44}$$

$$C_{3,5-8,10}^{(1)}|_{n_f=4} = 0\,. \tag{2.45}$$

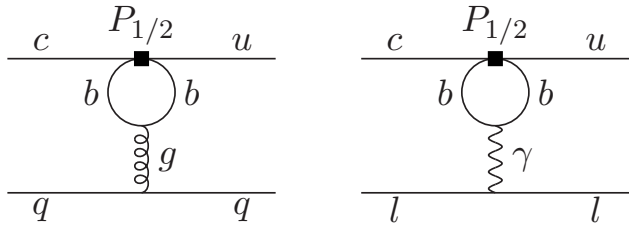

Figure 2.4.: Diagrams relevant for the NLO matching of $P_{1/2}$ onto P_4 (left) and P_9 (right) at μ_b.

These results can be checked against the matching known from kaon decays. Approximating $q^2 = 0$ in equation (C.3) of [64], a mapping via the inverse of equation (87) and equations (97), (98), (A.8) of [55] yields the same $C_{3-6}^{(1)}|_{n_f=4}$, as $C_1^{(0)}|_{n_f=5}$ vanishes. In addition, we find the same $C_9^{(1)}|_{n_f=4}$ by mapping the coefficients in [65] via the inverse of equation (A.8) of [55] and taking into account the quark charges. Part of the NNLO matching is obtained by the replacements $C_{1,2}^{(0)}|_{n_f=5} \to C_{1,2}^{(1)}|_{n_f=5}$ in eqs. (2.43, 2.44).

At two loop the matching onto $P_{1,2}$ can be extracted from [66]. We obtain for $C = (C_1, C_2)^T$

$$\begin{aligned} C^{(2)}|_{n_f=4} = C^{(2)}|_{n_f=5} + \frac{2}{3}\ln\frac{\mu_b^2}{m_b^2}\, C^{(1)}|_{n_f=5} \\ + \left(R^{-1}\left(A^{(2)} + \frac{2}{3}\ln\frac{\mu_b^2}{m_b^2} Z'^{(1,0)}_{QQ}\right) R\right)^T C^{(0)}|_{n_f=5} \end{aligned} \tag{2.46}$$

with

$$\begin{aligned} A^{(2)} &= \begin{pmatrix} -\frac{2}{3}\left(\frac{59}{36} + \frac{1}{3}\ln\frac{\mu_b^2}{m_b^2} + \ln^2\frac{\mu_b^2}{m_b^2}\right) & 0 \\ 0 & \frac{4}{3}\left(\frac{59}{36} + \frac{1}{3}\ln\frac{\mu_b^2}{m_b^2} + \ln^2\frac{\mu_b^2}{m_b^2}\right) \end{pmatrix}, \\ R &= \begin{pmatrix} 1 & \frac{2}{3} \\ -1 & \frac{1}{3} \end{pmatrix}, \quad Z'^{(1,0)}_{QQ} = \begin{pmatrix} -\frac{5}{3} & -\frac{8}{9} \\ -4 & 0 \end{pmatrix}. \end{aligned} \tag{2.47}$$

Note that all functions are linear in number of flavors at this order. One explicitly obtains

$$C_1^{(2)}|_{n_f=4} = C_1^{(2)}|_{n_f=5} + \frac{2}{3}\ln\frac{\mu_b^2}{m_b^2}\,C_1^{(1)}|_{n_f=5} + \left(\frac{59}{54} + \frac{148}{81}\ln\frac{\mu_b^2}{m_b^2} + \frac{2}{3}\ln^2\frac{\mu_b^2}{m_b^2}\right) C_1^{(0)}|_{n_f=5} + \left(-\frac{59}{18} - \frac{104}{27}\ln\frac{\mu_b^2}{m_b^2} - 2\ln^2\frac{\mu_b^2}{m_b^2}\right) C_2^{(0)}|_{n_f=5}\,, \tag{2.48}$$

$$C_2^{(2)}|_{n_f=4} = C_2^{(2)}|_{n_f=5} + \frac{2}{3}\ln\frac{\mu_b^2}{m_b^2}\,C_2^{(1)}|_{n_f=5} + \left(-\frac{59}{81} + \frac{176}{243}\ln\frac{\mu_b^2}{m_b^2} - \frac{4}{9}\ln^2\frac{\mu_b^2}{m_b^2}\right) C_1^{(0)}|_{n_f=5} - \frac{220}{81}\ln\frac{\mu_b^2}{m_b^2}\,C_2^{(0)}|_{n_f=5}\,. \tag{2.49}$$

This result is new with respect to [2]. We confirm the terms $\sim C_i^{(2)}|_{n_f=5}$, $\sim C_i^{(1)}|_{n_f=5}$, and $\sim \ln^2[\mu_b^2/m_b^2]\,C_i^{(0)}|_{n_f=5}$ by an explicit calculation. In particular, the terms $\sim C_i^{(1)}|_{n_f=5}$ follow from coupling renormalization, whereas mass renormalization is a higher order effect [67].

2.6. Effective Wilson coefficients at $\mu \sim m_c$

Evaluating the Wilson coefficients down to μ_c, as described in appendix B, concludes the calculation of the Wilson coefficients. Their numerical values are provided in section 2.9. One is left with matrix elements of the operators. We can calculate certain matrix elements in perturbation theory, giving rise to "effective" Wilson coefficients, considered in this section. They account for effects of light quarks, where we still approximate $m_{u,d} = 0$, but use a non-zero strange quark mass. In this way the number of matrix elements is reduced. In particular, we calculate $\langle P_{1-6,8}\rangle \sim \langle P_{7,9,10}\rangle^{(0)}$, where the perturbative coefficients of the tree level matrix elements are absorbed into redefined Wilson coefficients, the effective Wilson coefficients. Note that effective Wilson coefficients are actually not Wilson coefficients as they encode low energy physics. Perturbative effective Wilson coefficients are process universal as well as independent of the operator basis, regularization and renormalization scheme [68].

From the previous sections, the Wilson coefficient C_{10} vanishes due to the chiral structure of the operators which also holds for the effective Wilson coefficient, $C_{10}^{\text{eff}} = 0$, to all orders in QCD. In addition, the LO effective Wilson coefficients are

$$C_7^{\text{eff}(0)} = 0\,, \tag{2.50}$$

$$C_9^{\text{eff}(0)} = C_9^{(0)}\,. \tag{2.51}$$

At NLO we get

$$C_9^{\text{eff}(1)}|_{P_1^{(q)}} = \frac{8}{27}\left(1 - L(m_q^2, q^2)\right) C_1^{(0)}\,, \quad C_9^{\text{eff}(1)}|_{P_2^{(q)}} = \frac{2}{9}\left(1 - L(m_q^2, q^2)\right) C_2^{(0)}\,, \tag{2.52}$$

where the label $q \in \{d, s\}$. Furthermore,

$$\begin{aligned} L(m^2, q^2) &= 6 \int_0^1 \mathrm{d}z\, z(1-z) \ln \frac{\mu_c^2}{m^2 - q^2 z(1-z)} \\ &= \frac{5}{3} + \ln \frac{\mu_c^2}{m^2} + x - \frac{1}{2}(2+x)|1-x|^{1/2} \begin{cases} \ln \frac{1+\sqrt{1-x}}{1-\sqrt{1-x}} - i\pi & x < 1 \\ 2 \tan^{-1}\left[\frac{1}{\sqrt{x-1}}\right] & x > 1 \end{cases} , \\ L(m^2 = 0, q^2) &= \frac{5}{3} + \ln \frac{\mu_c^2}{q^2} + i\pi \,. \end{aligned} \tag{2.53}$$

where $x = (2m)^2/q^2$, $q^2 = (p_c - p_u)^2 = (p_+ + p_-)^2$ with momenta p, and we use $\tan^{-1}[1/\sqrt{x-1}] = -\frac{i}{2}(\ln[(1+\sqrt{1-x})/(1-\sqrt{1-x})] - i\pi)$. The calculation is analogous to the one described in the previous sections.

For the operators P_{3-6} we have to keep in mind that they encode a sum over all light quark fields. For $P_{4,6}$ only c and u quarks contribute, giving

$$\begin{aligned} C_9^{\mathrm{eff}(1)}|_{P_4} &= -\frac{16}{27} \left(\sum_{q=c,u} \left[1 - L(m_q^2, q^2)\right] \right) C_4^{(0)} \,, \\ C_9^{\mathrm{eff}(1)}|_{P_6} &= -\frac{256}{27} \left(\sum_{q=c,u} \left[1 - L(m_q^2, q^2)\right] \right) C_6^{(0)} \,. \end{aligned} \tag{2.54}$$

For $P_{3,5}$, restricting to a single light quark in the loop, we obtain

$$\begin{aligned} C_9^{\mathrm{eff}(1)}|_{P_3^{(q)}} &= \left(4 q_q L(m_q^2, q^2) + \delta_{uf} \frac{4}{3} q_u (L(m_q^2, q^2) - 1) \right) C_3^{(0)} \,, \\ C_9^{\mathrm{eff}(1)}|_{P_5^{(q)}} &= \left(40 q_q L(m_q^2, q^2) + \delta_{uf} \frac{64}{3} q_u \frac{1}{2} (L(m_q^2, q^2) - 1) \right) C_5^{(0)} \,, \end{aligned} \tag{2.55}$$

where q_i denotes the charge and summing all light quarks gives

$$\begin{aligned} C_9^{\mathrm{eff}(1)}|_{P_3} &= -\frac{4}{9} \left(\sum_{q=c,u} \left[1 - 7 L(m_q^2, q^2)\right] + 3 \sum_{q=s,d} L(m_q^2, q^2) \right) C_3^{(0)} \,, \\ C_9^{\mathrm{eff}(1)}|_{P_5} &= -\frac{8}{9} \left(\sum_{q=c,u} \left[8 - 38 L(m_q^2, q^2)\right] + 15 \sum_{q=s,d} L(m_q^2, q^2) \right) C_5^{(0)} \,. \end{aligned} \tag{2.56}$$

As we have made the quark charge dependence explicit, with $C_9^{\mathrm{eff}(1)}|_{P_{1,2}^{(q)}, P_{4,6}} \sim q_u$, we can check our results against the ones known from b decays. We find agreement with the results in [56], when approximating massless u, d and s quarks.

Summing up the contributions from each operator insertion, we find for massless u, d quarks and $q \in \{d, s\}$

$$\begin{aligned} C_9^{\text{eff}(1)}|_q = {} & C_9^{(1)} + \frac{8}{27}C_1^{(0)} + \frac{2}{9}C_2^{(0)} - \frac{8}{9}C_3^{(0)} - \frac{32}{27}C_4^{(0)} - \frac{128}{9}C_5^{(0)} - \frac{512}{27}C_6^{(0)} \\ & + L(m_c^2, q^2)\left(\frac{28}{9}C_3^{(0)} + \frac{16}{27}C_4^{(0)} + \frac{304}{9}C_5^{(0)} + \frac{256}{27}C_6^{(0)}\right) \\ & + L(m_s^2, q^2)\left(-\frac{4}{3}C_3^{(0)} - \frac{40}{3}C_5^{(0)}\right) \\ & + L(0, q^2)\left(\frac{16}{9}C_3^{(0)} + \frac{16}{27}C_4^{(0)} + \frac{184}{9}C_5^{(0)} + \frac{256}{27}C_6^{(0)}\right) \\ & + \left(\delta_{qs}L(m_s^2, q^2) + \delta_{qd}L(0, q^2)\right)\left(-\frac{8}{27}C_1^{(0)} - \frac{2}{9}C_2^{(0)}\right). \end{aligned} \tag{2.57}$$

Coming back to the discussion of the fixed order calculation around eq. (2.22) we add that penguin diagrams are double-counted in the effective Wilson coefficients, as e.g. done in [58–60, 69, 70].

Concerning C_7^{eff} at NLO, the contribution from P_{3-6} yields [71]

$$C_7^{\text{eff}(1)} = C_7^{(1)} + \sum_{i=1}^{6} y_i^{(7)} C_i^{(0)} \tag{2.58}$$

and we obtain from [52] by multiplying $y^{(7)}$ with the charge ratio $q_u/q_d = -2$

$$y^{(7)} = \begin{pmatrix} 0 & 0 & \frac{2}{3} & \frac{8}{9} & \frac{40}{3} & \frac{160}{9} \end{pmatrix}, \qquad y^{(8)} = \begin{pmatrix} 0 & 0 & 1 & -\frac{1}{6} & 20 & -\frac{10}{3} \end{pmatrix}. \tag{2.59}$$

Analogously, $y^{(8)}$ contributes to $C_8^{\text{eff}} = C_8^{(1)} + \sum_{i=1}^{6} y_i^{(8)} C_i^{(0)}$, which is part of the NNLO contribution,

$$\begin{aligned} C_7^{\text{eff}(2)}|_q = {} & C_7^{(2)} + \sum_{i=1}^{6} y_i^{(7)} C_i^{(1)} \\ & + \sum_{i=1}^{2} {}_{iq}C_7^{\text{eff}(2)} + \sum_{i=3}^{6}\left(r_i - \frac{\gamma_{i7}^{(1)\text{eff}}}{2}\ln\frac{\mu_c^2}{m_c^2}\right) C_i^{(0)} + F_8^{(7)}(q^2/m_c^2) C_8^{\text{eff}}. \end{aligned} \tag{2.60}$$

Multiplying again by the charge ratio the function F_8 is obtained from [72] as

$$\begin{aligned} F_8^{(7)}(\rho) = {} & \frac{8\pi^2}{27}\frac{(2+\rho)}{(1-\rho)^4} - \frac{8}{9}\frac{\left(11 - 16\rho + 8\rho^2\right)}{(1-\rho)^2} - \frac{16}{9}\frac{\sqrt{\rho}\sqrt{4-\rho}}{(1-\rho)^3}\left(9 - 5\rho + 2\rho^2\right)\arcsin\frac{\sqrt{\rho}}{2} \\ & - \frac{32}{3}\frac{(2+\rho)}{(1-\rho)^4}\arcsin^2\frac{\sqrt{\rho}}{2} - \frac{16}{9}\frac{\rho}{(1-\rho)}\ln\rho - \frac{32}{9}\ln\frac{\mu_c^2}{m_c^2} - \frac{16}{9}\pi i. \end{aligned} \tag{2.61}$$

The calculation of F_8 is done in the pole mass scheme, however, the result is the same in the $\overline{\text{MS}}$ mass to the order considered here. Furthermore,

$$C_7^{\text{eff}(2)}|_{P_2^{(q)}} = f(m_q^2/m_c^2) C_2^{(0)}\,, \tag{2.62}$$

where the function f at $q^2 = 0$ can be taken from [47],

$$\begin{aligned} f(\rho) = f_0 - \frac{1}{243}\big(&576\pi^2\rho^{\frac{3}{2}} + (3672 - 288\pi^2 - 1296\zeta_3 + (1944 - 324\pi^2)\ln\rho + 108\ln^2\rho \\ &+ 36\ln^3\rho)\rho + (324 - 576\pi^2 + (1728 - 216\pi^2)\ln\rho + 324\ln^2\rho + 36\ln^3\rho)\rho^2 \\ &+ (1296 - 12\pi^2 + 1776\ln\rho - 2052\ln^2\rho)\rho^3\big) - \frac{4\pi i}{81}\big((144 - 6\pi^2 + 18\ln\rho + 18\ln^2\rho) \\ &\times\rho + (-54 - 6\pi^2 + 108\ln\rho + 18\ln^2\rho)\rho^2 + (116 - 96\ln\rho)\rho^3\big) \\ &+ \mathcal{O}\left((\rho\ln\rho)^4\right)\,. \end{aligned} \tag{2.63}$$

The constant term f_0 is neglected in [47] as it is GIM suppressed. We obtain this term from [73] as

$$\begin{aligned} f_0 &= -\frac{16}{27\epsilon}q_u\left(1 + 2\epsilon\ln\frac{\mu_c^2}{m_c^2}\right) + q_u\left(\frac{100}{81} + \frac{8}{27}\pi i\right) - \frac{2}{\epsilon}q_d\left(1 + 2\ln\frac{\mu_c^2}{m_c^2}\right) \\ &\quad + q_d\left(-\frac{29}{3} - \frac{4}{3}\pi i\right) + \frac{2}{3}\frac{4}{3}q_u\frac{1}{\epsilon}\left(1 + \epsilon\ln\frac{\mu_c^2}{m_c^2}\right) + \frac{1}{\epsilon}\left(2q_d - \frac{8}{27}q_u\right) \\ &= -\frac{92}{81}\ln\frac{\mu_c^2}{m_c^2} + \frac{983}{243} + \frac{52}{81}\pi i\,. \end{aligned} \tag{2.64}$$

Additionally, we find

$$C_7^{\text{eff}(2)}|_{P_1^{(q)}} = -\frac{1}{6}f(m_q^2/m_c^2)C_1^{(0)} \tag{2.65}$$

due to the color structure $\sum_{a,b} T^a T^b T^a T^b / (\sum_a T^a T^a) = (-\frac{2}{9})/(\frac{4}{3})$ which is derived by using $\sum_a T^a_{\mu\nu} T^a_{\rho\sigma} = (-1/6\,\delta_{\mu\nu}\delta_{\rho\sigma} + 1/2\,\delta_{\mu\sigma}\delta_{\nu\rho})$. Furthermore, we obtain along the calculation of [74] at $q^2 = 0$

$$\begin{aligned} r_3 &= -\frac{4784}{243} - \frac{16\pi}{3\sqrt{3}} - \frac{64}{9}X_b + 2a(1) - 4b(1) - \frac{112}{81}i\pi\,, \\ r_4 &= \frac{1270}{729} + \frac{8\pi}{9\sqrt{3}} + \frac{32}{27}X_b - \frac{1}{3}a(1) - \frac{10}{3}b(1) - 4b(m_s^2/m_c^2) + \frac{248}{243}i\pi\,, \\ r_5 &= -\frac{113360}{243} - \frac{64\pi}{3\sqrt{3}} - \frac{256}{9}X_b + 32a(1) - 64b(1) - \frac{1792}{81}i\pi\,, \\ r_6 &= -\frac{60980}{729} + \frac{32\pi}{9\sqrt{3}} + \frac{128}{27}X_b + \frac{20}{3}a(1) - \frac{88}{3}b(1) + 6a(m_s^2/m_c^2) - 40b(m_s^2/m_c^2) \\ &\quad + \frac{1520}{243}i\pi\,, \end{aligned} \tag{2.66}$$

with $X_b \simeq -0.1684$,

$$\begin{aligned} a(\rho) = \frac{16}{9}\Bigg(& \left(\frac{5}{2} - \frac{1}{3}\pi^2 - 3\zeta_3 + \left(\frac{5}{2} - \frac{3}{4}\pi^2\right)\ln\rho + \frac{1}{4}\ln^2\rho + \frac{1}{12}\ln^3\rho\right)\rho + \left(\frac{7}{4} + \frac{2}{3}\pi^2\right. \\ & \left. - \frac{1}{2}\pi^2\ln\rho - \frac{1}{4}\ln^2\rho + \frac{1}{12}\ln^3\rho\right)\rho^2 + \left(-\frac{7}{6} - \frac{1}{4}\pi^2 + 2\ln\rho - \frac{3}{4}\ln^2\rho\right)\rho^3 + \left(\frac{457}{216}\right. \\ & \left. - \frac{5}{18}\pi^2 - \frac{1}{72}\ln\rho - \frac{5}{6}\ln^2\rho\right)\rho^4 + \left(\frac{35101}{8640} - \frac{35}{72}\pi^2 - \frac{185}{144}\ln\rho - \frac{35}{24}\ln^2\rho\right)\rho^5 \\ & + \left(\frac{67801}{8000} - \frac{21}{20}\pi^2 - \frac{3303}{800}\ln\rho - \frac{63}{20}\ln^2\rho\right)\rho^6 + i\pi\Bigg(\left(2 - \frac{1}{6}\pi^2 + \frac{1}{2}\ln\rho + \frac{1}{2}\ln^2\rho\right)\rho \\ & + \left(\frac{1}{2} - \frac{1}{6}\pi^2 - \ln\rho + \frac{1}{2}\ln^2\rho\right)\rho^2 + \rho^3 + \frac{5}{9}\rho^4 + \frac{49}{72}\rho^5 + \frac{231}{200}\rho^6\Bigg)\Bigg) \\ & + \mathcal{O}\left(\rho^7\ln^2\rho\right), \end{aligned} \tag{2.67}$$

and

$$\begin{aligned} b(\rho) = -\frac{8}{9}\Bigg(& \left(-3 + \frac{1}{6}\pi^2 - \ln\rho\right)\rho - \frac{2}{3}\pi^2\rho^{3/2} + \left(\frac{1}{2} + \pi^2 - 2\ln\rho - \frac{1}{2}\ln^2\rho\right)\rho^2 \\ & + \left(-\frac{25}{12} - \frac{1}{9}\pi^2 - \frac{19}{18}\ln\rho + 2\ln^2\rho\right)\rho^3 + \left(-\frac{1376}{225} + \frac{137}{30}\ln\rho + 2\ln^2\rho + \frac{2}{3}\pi^2\right)\rho^4 \\ & + \left(-\frac{131317}{11760} + \frac{887}{84}\ln\rho + 5\ln^2\rho + \frac{5}{3}\pi^2\right)\rho^5 + \left(-\frac{2807617}{97200} + \frac{16597}{540}\ln\rho + 14\ln^2\rho\right. \\ & \left. + \frac{14}{3}\pi^2\right)\rho^6 + i\pi\left(-\rho + (1 - 2\ln\rho)\rho^2 + \left(-\frac{10}{9} + \frac{4}{3}\ln\rho\right)\rho^3 + \rho^4 + \frac{2}{3}\rho^5 + \frac{7}{9}\rho^6\right)\Bigg) \\ & + \mathcal{O}\left(\rho^7\ln^2\rho\right). \end{aligned} \tag{2.68}$$

Note that $x_{4,6}$ in equation (6.16) of [74] implicitly depends on the number of quarks. Due to a typing error $\sim Q_d^2$, i.e. the appearance of the charge squared, we can not check the divergent and finite rational terms of $x_{4,6}$ given in equation (6.18) of [74] via their equation (6.16). Finally, the effective anomalous dimensions read

$$\gamma_{37}^{(1)\text{eff}} = -\frac{128}{81}, \quad \gamma_{47}^{(1)\text{eff}} = \frac{592}{243}, \quad \gamma_{57}^{(1)\text{eff}} = \frac{12928}{81}, \quad \gamma_{67}^{(1)\text{eff}} = \frac{40288}{243}. \tag{2.69}$$

For convenience, the $P_{3-6} \to P_{7,8}$ mixing can be absorbed in an effective ADM. The corresponding basis is chosen in [2].

At NNLO we further obtain

$$\begin{aligned} C_9^{\text{eff}(2)}|_q = C_9^{(2)} &+ \frac{8}{27}C_1^{(1)} + \frac{2}{9}C_2^{(1)} - \frac{8}{9}C_3^{(1)} - \frac{32}{27}C_4^{(1)} - \frac{128}{9}C_5^{(1)} - \frac{512}{27}C_6^{(1)} \\ &+ L(m_c^2, q^2)\left(\frac{28}{9}C_3^{(1)} + \frac{16}{27}C_4^{(1)} + \frac{304}{9}C_5^{(1)} + \frac{256}{27}C_6^{(1)}\right) \\ &+ L(m_s^2, q^2)\left(-\frac{4}{3}C_3^{(1)} - \frac{40}{3}C_5^{(1)}\right) \\ &+ L(0, q^2)\left(\frac{16}{9}C_3^{(1)} + \frac{16}{27}C_4^{(1)} + \frac{184}{9}C_5^{(1)} + \frac{256}{27}C_6^{(1)}\right) \\ &+ \left(\delta_{qs}L(m_s^2, q^2) + \delta_{qd}L(0, q^2)\right)\left(-\frac{8}{27}C_1^{(1)} - \frac{2}{9}C_2^{(1)}\right) \\ &+ F_8^{(9)}(q^2/m_c^2)C_8^{\text{eff}} \end{aligned} \tag{2.70}$$

with

$$\begin{aligned} F_8^{(9)}(\rho) = &-\frac{16\pi^2}{27}\frac{(4-\rho)}{(1-\rho)^4} + \frac{16}{9}\frac{(5-2\rho)}{(1-\rho)^2} + \frac{32}{9}\frac{\sqrt{4-\rho}}{\sqrt{\rho}(1-\rho)^3}\left(4+3\rho-\rho^2\right)\arcsin\frac{\sqrt{\rho}}{2} \\ &+ \frac{64}{3}\frac{(4-\rho)}{(1-\rho)^4}\arcsin^2\frac{\sqrt{\rho}}{2} + \frac{32}{9}\frac{1}{(1-\rho)}\ln\rho \end{aligned} \tag{2.71}$$

which is obtained from [72] by multiplying with the charge ratio.

In eq. (2.70) the two loop mixing of P_{1-6} into P_9 is missing. The contributions from $P_{1,2}$, also into P_7, which extends eq. (2.63) to $q^2 \neq 0$, is subject of the next section. The effective Wilson coefficients are discussed in chapter 3 in the context of phenomenological applications.

2.6.1. Two loop QCD matrix elements of current-current operators

This section is devoted to the calculation of the two loop QCD matrix elements of $P_{1/2}$ into $P_{7,9}$. The result is valid for a more general class of heavy to light transitions with arbitrary momentum transfer and mass of the internal quark-antiquark pair, whereas the mass of the light external quark is neglected. This includes the transitions $c \to u(q\bar{q})$ with $q = d, s$, which are studied in this thesis, and also $b \to (s, d)(q\bar{q})$ with $q = c, u$, where $(q\bar{q})$ is annihilated and a photon is emitted, which may then couple to a lepton pair. The calculation uses the recent works [75] and [76] for the master integrals (MIs) and numerical evaluation, respectively.

Several calculations were performed for $b \to (s, d)$ transitions: In [77] and [78] $b \to s$ and $b \to d$ transitions, respectively, were computed for small q^2. The calculation of $b \to s$ transitions for large q^2 was accomplished in [72]. A seminumerical approach was employed in [79] to present results based on $b \to s$ transitions for the full q^2 range. In [80]

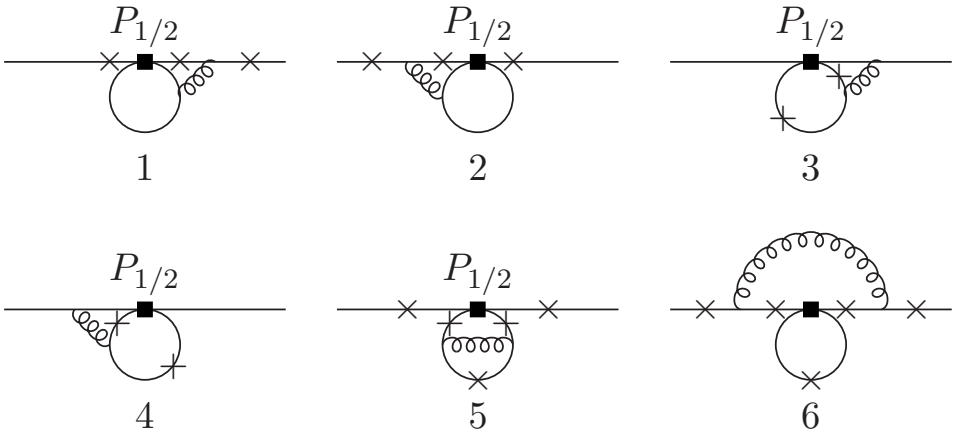

Figure 2.5.: Diagrams for heavy to light transitions at two loop QCD. The boxes denote operator insertions of $P_{1/2}$. The crosses indicate the emission of a photon, which may then couple to a lepton pair.

$b \to d$ transitions for any q^2 range were computed, extending [78]. For $c \to u$ transitions no such calculations were performed to date.

In the following, we outline our calculation. The analytical expressions and their numerical evaluation will be given in [4]. Also the relevance for $b \to (d, s)$ transitions will be considered there. In this thesis we are concerned with the impact for $c \to u$ transitions.

The diagrams relevant for heavy to light transitions at two loop QCD are shown in figure 2.5. Each of the six subsets of diagrams represents a class which is gauge invariant. The sixth class preserves the operator structure of P_9. Hence, it is commonly considered as a correction of the matrix element of P_9 [77], see e.g. section 3.1.2 for inclusive decays. Nonetheless, we have checked that in this class only the diagram with a photon from the loop of the quark-antiquark pair is non-zero and factorizes into two one loop integrals. It is the only diagram with IR and collinear singularities. The latter can be regulated by a non-zero mass of the external light quark.

We calculate the diagrams in figure 2.5 with insertions of P_2. Insertions of P_1 are then given by color factors due to additional generators in the definition of the operator: The expressions for the first four and last two classes are multiplied with $-1/6$ and $4/3$, respectively.

The matrix element for an off-shell photon γ^* can be decomposed as [80]

$$\begin{aligned}\langle\gamma^*(q,\mu)u(p_u)|P_2|c(p_c)\rangle &= \langle u(p_u)|\bar{u}X^\mu c|c(p_c)\rangle \\ &= \left(\frac{\alpha_s}{4\pi}\right)^2 F^{(q)}(q^2)\langle u(p_u)|\bar{u}_L q^\mu c_L|c(p_c)\rangle \\ &+ \left(\frac{\alpha_s}{4\pi}\right)^2 F^{(7)}(q^2)\langle u(p_u)|\bar{u}_L \sigma^{\mu\nu} q_\nu c_L|c(p_c)\rangle \\ &+ \left(\frac{\alpha_s}{4\pi}\right)^2 F^{(9)}(q^2)\langle u(p_u)|\bar{u}_L(q^2\gamma^\mu - q^\mu \not{q})c_L|c(p_c)\rangle\,, \qquad (2.72)\end{aligned}$$

where X^μ is the sum of the amputed diagrams in figure 2.5. Here $q^\mu = (p_c - p_u)^\mu$.

The scalar form factors $F^{(i)}$ are given as [80]

$$F^{(i)}(q^2) = \mathrm{Tr}[P_i^\mu X_\mu] \qquad (2.73)$$

with the projectors

$$P_i^\mu = (\not{p}_c + m_c)(C_{i1}q^\mu + C_{i2}p_c^\mu + C_{i3}\gamma^\mu)\not{p}_u\,. \qquad (2.74)$$

The factors $(\not{p}_c + m_c)$ and $\not{p}_u$ reflect the on-shell conditions for the external quarks. We find the coefficients

$$\begin{aligned}C_{q1} &= \frac{1}{(m_c^2 - q^2)q^2}\,, \quad C_{q2} = 0\,, \quad C_{q3} = 0\,, \\ C_{91} &= C_{93}\frac{(d-2)m_c^3 + dm_c q^2}{m_c^2 q^2 - q^4}\,, \\ C_{92} &= C_{93}\frac{2(d-1)m_c}{-m_c^2 + q^2}\,, \\ C_{93} &= \frac{1}{(d-2)(m_c^2 - q^2)^2}\,, \\ C_{71} &= C_{72}\frac{-dm_c^4 q^2 + 2m_c^2 q^4 + (d-2)q^6}{2m_c^4 q^2 + 2(d-3)m_c^2 q^4 - 2(d-2)q^6}\,, \\ C_{72} &= -i\frac{2m_c^2 + 2(d-2)q^2}{(d-2)(m_c^2 - q^2)^3}\,, \\ C_{73} &= C_{72}\frac{m_c(m_c^2 - q^2)^2}{-2m_c^4 - 2(d-3)m_c^2 q^2 + 2(d-2)q^4}\,. \qquad (2.75)\end{aligned}$$

Here the dimension is $d = 4-2\epsilon$. The contribution to the effective Wilson coefficients $C_{7,9}^{\mathrm{eff}}$ from the two loop matrix element $\langle ull|P_2|c\rangle$ are given by multiplying the renormalized $F^{(7,9)}$ with $ie/(2m_c)$ and e, respectively. The form factor $F^{(q)}$ vanishes for each class by gauge invariance, which we have checked.

For the calculation we utilize the computer programs `FORM 4.0` [81] and `REDUZE 2` [82]. We use the former for algebraic manipulations, e.g. the tensor algebra, and the latter

is used for the reduction to MIs. We compute some reductions by hand to reduce the number of integrals that are fed into `REDUZE 2`. It is based on the Laporta algorithm [83] which employs IBP identities [63] and Lorentz invariance (LI) identities [84]. See, e.g., section 2.4 for a calculation using IBP identities. Indeed, LI identities can be written as linear combinations of IBP identities [85]. Thus, we have calculated relations for each diagram based on LI identities by hand and checked them against the reduction tables built with `REDUZE 2`.

We find that the following diagrams in figure 2.5 vanish: In the fifth class, both diagrams with photons attached to the external lines vanish. The diagram with a photon emitted from the charm quark line in the first class is zero. For $F^{(7)}$ all diagrams with photons attached to the external lines vanish. Furthermore, all diagrams of the fifth class vanish for $F^{(7)}$. This implies that the $\langle P_1 \rangle$ induced dipole form factor is given by $-1/6\, F^{(7)}$.

As for the set of the MIs, we match a subset of the integrals calculated in [75]. A canonical set is given in [72], where the MIs are calculated for large q^2, yet the set of integrals is not minimal. While matching their set onto the MIs taken from [75], we find additional relations among the former, e.g. for the integral I_{d23} and the one of equation (A12) in [72]. Additionally, we do not encounter the integrals of equations (A5), (A8), and (A14) in [72]. Note that in the latter equation the diagram and the integral representation do not coincide.

With the MIs from [75] the calculation of the unrenormalized form factors is completed. The prescription for the renormalization is given in, e.g., [77]. Accordingly, the operator renormalization constants are written as

$$\begin{aligned} Z_{ij} &= \delta_{ij} + \delta Z_{ij}\,, \\ \delta Z_{ij} &= \frac{\alpha_s}{4\pi}\left(a_{ij}^{01} + \frac{1}{\epsilon} a_{ij}^{11}\right) + \frac{\alpha_s^2}{(4\pi)^2}\left(a_{ij}^{02} + \frac{1}{\epsilon} a_{ij}^{12} + \frac{1}{\epsilon^2} a_{ij}^{22}\right) + \mathcal{O}(\alpha_s^3)\,. \end{aligned} \tag{2.76}$$

Extending the set of physical operators P_{1-10} by the evanescent operators $E_{11,12}$ defined as

$$E_{11} = (\bar{u}_L \gamma_{\mu_1}\gamma_{\mu_2}\gamma_{\mu_3} T^a q_L)\,(\bar{q}_L \gamma^{\mu_1}\gamma^{\mu_2}\gamma^{\mu_3} T^a c_L) - 16 P_1\,, \tag{2.77}$$

$$E_{12} = (\bar{u}_L \gamma_{\mu_1}\gamma_{\mu_2}\gamma_{\mu_3} q_L)\,(\bar{q}_L \gamma^{\mu_1}\gamma^{\mu_2}\gamma^{\mu_3} c_L) - 16 P_2\,. \tag{2.78}$$

the coefficients a_{ij} are compactly written as

$$a^{11}|_{i=1,2} = \begin{pmatrix} -2 & \frac{4}{3} & 0 & -\frac{1}{9} & 0 & 0 & 0 & 0 & -\frac{8}{9} q_d & 0 & \frac{5}{12} & \frac{2}{9} \\ 6 & 0 & 0 & \frac{2}{3} & 0 & 0 & 0 & 0 & -\frac{2}{3} q_d & 0 & 1 & 0 \end{pmatrix}, \tag{2.79}$$

and

$$-6\,a_{17}^{12} = a_{27}^{12} = 2q_d - \frac{8}{27}q_u\,, \quad a_{19}^{12} = -\frac{2}{9}q_d - \frac{44}{243}q_u\,, \quad a_{29}^{12} = \frac{16}{3}q_d + \frac{88}{81}q_u\,, \tag{2.80}$$

$$a_{19}^{22} = \frac{92}{9}q_d - \frac{16}{27}n_f\,q_d + \frac{8}{81}q_u\,, \quad a_{29}^{22} = \frac{14}{3}q_d - \frac{4}{9}n_f\,q_d - \frac{16}{27}q_u\,. \tag{2.81}$$

Here n_f is the number of flavors and $q_{u,d}$ are the charges of the external/up- and internal/down-type quarks, respectively. The coefficients $a_{ij}^{11,22}$ can be found from the LO ADM $\gamma^{(0)}$, given in appendix B.2, and the coefficients a_{ij}^{12} from [57],

$$a^{11} = \frac{1}{2}\gamma^{(0)}\,, \qquad a^{12} = \frac{1}{4}\gamma^{(1)} + \frac{1}{2}\hat{b}\cdot\hat{c}\,, \qquad a^{22} = \frac{1}{8}\gamma^{(0)}\cdot\gamma^{(0)} - \frac{1}{4}\beta_0\gamma^{(0)}\,, \tag{2.82}$$

where the mixing via the evanescent operators is

$$\hat{b}|_{i=1,2} = \begin{pmatrix} \frac{5}{12} & \frac{2}{9} \\ 1 & 0 \end{pmatrix}\,, \qquad\qquad \hat{c}|_{j=9} = \begin{pmatrix} \frac{32}{9}q_d \\ \frac{8}{3}q_d \end{pmatrix}\,. \tag{2.83}$$

Accordingly, the counterterm form factors $F_{i\to(7,9)}^{\mathrm{ct}(7,9)}$, due to the mixing of $P_{1/2}$ into $P_{7,9}$, and the one loop renormalization of g_s in the definition of P_9, are [77, 78]

$$F_{i\to7}^{\mathrm{ct}(7)} = -\frac{a_{i7}^{12}}{\epsilon}\,, \qquad\qquad F_{i\to9}^{\mathrm{ct}(9)} = -\left(\frac{a_{i9}^{22}}{\epsilon^2} + \frac{a_{i9}^{12}}{\epsilon}\right) - \frac{a_{i9}^{11}\beta_0}{\epsilon^2}\,. \tag{2.84}$$

Here $\beta_0 = 11 - \frac{2}{3}n_f$. We find that the n_f dependence cancels in $F_{i\to9}^{\mathrm{ct}(9)}$, thus also for all counterterms.

The counterterms $F_{i\to4\mathrm{quark}}^{\mathrm{ct}(7,9)}$, due to the mixing of $P_{1/2}$ into four-quark operators P_j, are defined by [77]

$$\sum_j \frac{\alpha_s}{4\pi}\frac{1}{\epsilon}a_{ij}^{11}\langle ull|P_j|c\rangle_{1l} = -\left(\frac{\alpha_s}{4\pi}\right)^2\left(F_{i\to4\mathrm{quark}}^{\mathrm{ct}(7)}\langle P_7\rangle_{\mathrm{tree}} + F_{i\to4\mathrm{quark}}^{\mathrm{ct}(9)}\langle P_9\rangle_{\mathrm{tree}}\right)\,, \tag{2.85}$$

where $1l$ labels one loop matrix elements. We calculate them to $\mathcal{O}(\epsilon)$ and for insertions of $P_{1,2,4}$, $E_{11,12}$ according to eqs. (2.85) and (2.79), respectively. Therefore, we write

$$\begin{aligned} l_1(m_q^2) = \left(\frac{\mu^2}{m_q^2}\right)^\epsilon \int_0^1 \mathrm{d}z(1-z)z\Bigg(&-\frac{6}{\epsilon} + 6 - 6\ln\frac{1}{1-z(1-z)q^2/m_q^2} - \frac{\pi^2}{2}\epsilon \\ &+ 6\epsilon\ln\frac{1}{1-z(1-z)q^2/m_q^2} - 3\epsilon\ln^2\frac{1}{1-z(1-z)q^2/m_q^2}\Bigg)\,. \end{aligned} \tag{2.86}$$

Here μ is a mass scale. Note that $\int_0^1 \mathrm{d}z(1-z)z = 1/6$. In the massless limit, $m_q^2 \to 0$,

$$\begin{aligned}
\int_0^1 \mathrm{d}z(1-z)z \ln \frac{1}{1-z(1-z)q^2/m^2} &\to \frac{5}{18} - \frac{1}{6}\ln\frac{q^2}{m_q^2} + i\frac{\pi}{6}\,, \\
\int_0^1 \mathrm{d}z(1-z)z \ln^2 \frac{1}{1-z(1-z)q^2/m^2} &\to \frac{28}{27} + i\frac{5\pi}{9} - \frac{2\pi^2}{9} - \frac{5}{9}\ln\frac{q^2}{m_q^2} - i\frac{\pi}{3}\ln\frac{q^2}{m_q^2} \\
&\quad + \frac{1}{6}\ln^2\frac{q^2}{m_q^2}\,,
\end{aligned} \tag{2.87}$$

where the residual m_q^2 dependence cancels to $\mathcal{O}(\epsilon)$ in eq. (2.86). Thus, the matrix elements are

$$\begin{aligned}
\langle ull|P_1|c\rangle_{1l} &= -\frac{8}{9}q_d l_1(m_q^2)\frac{\alpha_s}{4\pi}\langle P_9\rangle_{\text{tree}}\,, \\
\langle ull|P_2|c\rangle_{1l} &= \frac{3}{4}\langle ull|P_1|c\rangle_{1l}\,, \\
\langle ull|P_4|c\rangle_{1l} &= -\frac{4}{3}q_u\left(\frac{\mu^2}{m_c^2}\right)^{\epsilon}\left(-1-\epsilon\int_0^1 \mathrm{d}z\ln\frac{1}{1-z(1-z)q^2/m_c^2}\right)\frac{\alpha_s}{4\pi}\langle P_7\rangle_{\text{tree}} \\
&\quad - \frac{8}{9}q_u\left(l_1(m_c^2)+l_1(0)\right)\frac{\alpha_s}{4\pi}\langle P_9\rangle_{\text{tree}}\,, \\
\langle ull|E_{11}|c\rangle_{1l} &= -4\left(-\frac{8}{9}q_d\right)\left(\frac{\mu^2}{m_q^2}\right)^{\epsilon}\int_0^1 \mathrm{d}z(1-z)z\left(-6-6\epsilon\ln\frac{1}{1-z(1-z)q^2/m_q^2}\right) \\
&\quad \times \frac{\alpha_s}{4\pi}\langle P_9\rangle_{\text{tree}}\,, \\
\langle ull|E_{12}|c\rangle_{1l} &= \frac{3}{4}\langle ull|E_{11}|c\rangle_{1l}\,.
\end{aligned} \tag{2.88}$$

We have checked that expanding the matrix elements in small q^2 and in the limit $m_q^2 \to 0$ yields the results in [77] and [80], respectively.

Following [77], the renormalization of the mass m_q is given by the replacement $m_q \to Z_{m_q} m_q$ in $\langle ull|P_{1,2}|c\rangle_{1l}$ of eq. (2.88). The mass renormalization constants in the $\overline{\text{MS}}$ and the pole mass scheme are [51]

$$\begin{aligned}
Z_m^{\overline{\text{MS}}} &= 1 + \frac{\alpha_s}{4\pi}\left(-\frac{4}{\epsilon}\right) + \mathcal{O}(\alpha_s^2)\,, \\
Z_m^{\text{pole}} &= 1 + \frac{\alpha_s}{4\pi}\left(-\frac{4}{\epsilon} - 4\ln\frac{\mu^2}{m^2} - \frac{16}{3}\right) + \mathcal{O}(\alpha_s^2)\,.
\end{aligned} \tag{2.89}$$

Expanding the matrix elements at $\mathcal{O}(\alpha_s/(4\pi))$ and $\mathcal{O}(\epsilon^0)$ gives the counterterms $F_{i,m_q}^{\text{ct}(9)}$ and $F_{i,m_q}^{\text{ct}(7)} = 0$. We have checked for both schemes that expanding the counterterm $F_{i,m_q}^{(9)}$ in small q^2 yields the results in [77].

Finally, the renormalized form factors are given by subtracting $F_i^{\text{ct}(7,9)} = (F_{i\to 7,9}^{\text{ct}(7,9)} + F_{i\to 4\text{quark}}^{\text{ct}(7,9)} + F_{i,m_q}^{\text{ct}(7,9)})$ from the unrenormalized form factors. Note that mass and wave function renormalization is a higher order effect [80]. We have checked that $F_i^{\text{ct}(7)}|_{\epsilon^0}$ agrees with the results in [79]. However, we did not check $F_i^{\text{ct}(9)}|_{\epsilon^0}$, as [79] computed inclusive decays, including corrections to the matrix element of P_9 from the last diagram in figure 2.5 which we excluded.

For the numerical evaluation we use the computer package `lieevaluate` [76]. The MIs given in terms of harmonic polylogarithms (HPLs) are written as generalized/Goncharov polylogarithms (GPLs) [75] that are fed into `lieevaluate`. Other packages for the numerical evaluation of GPLs are found in [86, 87]. Details on the numerical evaluation will be given in [4]. [1]

We find that subtracting the counterterm form factors from the unrenormalized form factors, the $1/\epsilon^2$ and $1/\epsilon$ divergences cancel numerically. We have checked our calculation against the ones of [72, 77, 80] for $b \to (d, s)$ transitions, finding numerical agreement for any q^2 as well as different scales, mass schemes, and parameters. For $c \to u\gamma$ transitions [47] calculated $C_7^{\text{eff}}(q^2 = 0)$ from the two loop matrix element of P_2, see also section 2.6. Adding the constant terms given in [1] we have checked the calculations, finding numerical agreement. However, we did not check the finite unrenormalized form factors in figure 4 of [79] as we did not see which scale is shown.

Note that the computation of two loop matrix elements presented here is not restricted to SM calculations, see section 4.2.1 for an example in LQ models. Furthermore, the two loop matching of $P_{1,2}$ onto $P_{7,9}$ at μ_b, see section 2.5, can be calculated as described in the current section. For the impact of the two loop matrix elements of $P_{1/2}$ in phenomenological applications for rare charm decays we refer to chapter 3.

2.7. Electromagnetic effects

Electromagnetic effects may become important, as $\alpha_e/(4\pi) \sim (\alpha_s/(4\pi))^2$. In principle, we have to enlarge the operator basis to account for QED penguin operators. However, as we are interested in the leading effects we concentrate on QED corrections to $P_{1,2}$ as they are still the only operators present at μ_W. We also take into account the mixing of $P_{9,10}$ in QED, because of a non-vanishing mixing into P_{10}.

We obtain the leading QED correction to the Wilson coefficients at μ_W from [88] as

$$C_1^{\text{QED}}(\mu_W) = 0 + \mathcal{O}(\alpha_e\alpha_s, \alpha_e^2)\,, \tag{2.90}$$

$$C_2^{\text{QED}}(\mu_W) = \frac{\alpha_e}{4\pi}\left(-\frac{7}{3} - \frac{4}{3}\ln\frac{\mu_W^2}{M_Z^2}\right) + \mathcal{O}(\alpha_e\alpha_s, \alpha_e^2)\,, \tag{2.91}$$

[1] We would like to acknowledge the authors of [75] for providing additional code on their work, which we use for checks. We thank Tobias Huber for useful discussions.

where the LO matching is already given by eqs. (2.18, 2.19), which are to be added. The corresponding LO QED ADM can be obtained from [88, 89] as

$$\gamma_0^{\text{QED}}\big|_{1,2} = \begin{pmatrix} -8/3 & 0 \\ 0 & -8/3 \end{pmatrix} . \tag{2.92}$$

The one loop running of α_e is given by

$$\alpha_e(\mu) = \alpha_e(\mu_0)\left(1 + \frac{\beta_e^{(0)}}{4\pi}\alpha_e(\mu_0)\ln\frac{\mu_0^2}{\mu^2}\right)^{-1} , \quad \beta_e^{(0)} = \left(\left(n_u q_u^2 + n_d q_u^2\right)3 + 3q_e^2\right) , \tag{2.93}$$

where $q_e = -1$ denotes the charge of the electron in units of the proton charge. Neglecting matching effects at μ_b, we find that $C_{1,2}^{\text{QED}}(\mu_c)$ are equal to the QCD induced $C_{1,2}(\mu_c)$ within one percent.

The QED Wilson coefficients $C_{9,10}^{\text{QED}}(\mu_b)$ are equal to those given in eqs. (2.44, 2.45). The operators $P_{1,2}$ do not mix into P_9 at this order in QED and the mixing of $P_{9,10}$ is governed by

$$\gamma_0^{\text{QED}}\big|_{9,10} = \begin{pmatrix} -16 - 2\beta_e^{(0)} & 8 \\ 8 & -2\beta_e^{(0)} \end{pmatrix} . \tag{2.94}$$

It follows that $C_9^{\text{QED}}(\mu_c)$ is equal to the QCD induced $C_9(\mu_c)$ within three percent and $C_{10}^{\text{QED}}(\mu_c) < 0.01\, C_9(\mu_c)$.

We conclude that QED effects are negligible with respect to the results from QCD. In particular, one can still approximate a vanishing C_{10}.

Moreover, one can limit effects from a violation of the CKM unitarity, in which case C_{10} would be non-zero. The corresponding Wilson coefficients are already given in section 2.3, parametrized by ΔV_{cu}. Neglecting the matching effects at μ_b we find that $C_{10}(m_c) \simeq 1.1\Delta V_{cu}$. From the experimental data, see appendix A, one obtains $|\Delta V_{cu}| = -0.000\,014 \pm 0.000\,005$, hence C_{10} is negligible.

2.8. Non-perturbative effects

This section is devoted to an estimate of universal non-perturbative effects from the QCD vacuum condensate. The intention is to get an impression of the size of effects not calculated so far. Specifically, we do not use the results obtained in the current section for later analyses, where we include non-perturbative effects within different frameworks.

We absorb QCD vacuum condensate effects of the light quark fields in the function $L(m^2, q^2)$ entering C_9^{eff} and defined by eq. (2.53). This follows from the similar structure of $L(m^2, q^2)$ and the fermionic one loop correlation function, see section 2.4, for which

the OPE at high q^2 is given in [90, 91] for the QCD vacuum condensate. Matching the contributions, we obtain the corrections to $L(m^2, q^2)$ as

$$L^{\text{QCDvc}} = -\frac{m^4}{q^4}\left(1+\ln\frac{\mu^2}{m^2}\right) + 8\pi^2\frac{\langle m\bar{q}q\rangle}{q^4}\left(1+\frac{4}{3}\frac{m^2}{q^2}\right) + \frac{\pi}{3}\frac{\langle\alpha_s G^2\rangle}{q^4}\left(1-\frac{4}{3}\frac{m^2}{q^2}\right) - \frac{8\pi^2}{3}\frac{\langle g\bar{q}Gq\rangle}{q^5}\frac{m^3}{q^3}\,. \tag{2.95}$$

The condensates include quark and gluon fields. A term $\langle G^3\rangle$ is absent as its coefficient is zero for light quarks. The absence of dimension two operators follows from gauge-invariance and is in agreement with lattice computations [92]. We neglect condensates of dimension higher than six and effects of a heavy c quark. The latter are GIM suppressed and can be included from [90, 91].

The condensates in eq. (2.95) are non-normal-ordered, as required for a consistent OPE [91]. A normal-ordering does not affect the gluon and quark-gluon condensates, but the quark-quark condensate mixes with the unit operator. We neglect renormalization effects, but note that the gluon condensate is renormalization scale independent and mixing is suppressed by light quark masses. The LO mixing can be found in [91].

The condensates are [93–95]

$$\begin{aligned}
&\langle\Omega|m_l\bar{l}l|\Omega\rangle(\mu=2\,\text{GeV}) = -(7.63\pm0.04)\times10^5\,\text{GeV}^4\,,\\
&\langle\Omega|m_s\bar{s}s|\Omega\rangle(\mu=2\,\text{GeV}) = -(2.26\pm0.34)\times10^{-3}\,\text{GeV}^4\,,\\
&\langle\Omega|\alpha_s\,G^{\mu\nu,a}G^a_{\mu\nu}|\Omega\rangle = \pi(0.037\pm0.015)\,\text{GeV}^4\,,\\
&\langle\Omega|g_s\,\bar{q}\sigma^{\mu\nu}T^aG^a_{\mu\nu}q|\Omega\rangle(\mu=2\,\text{GeV}) = -(0.434\pm0.004)^5\,\text{GeV}^5\,,
\end{aligned} \tag{2.96}$$

where $l\in\{u,d\}$ and Ω labels the vacuum. The approximations $\langle m_l\bar{l}l\rangle = -f_\pi^2m_\pi^2/4$ and $\langle\bar{s}s\rangle/\langle\bar{l}l\rangle = 1$ [94] hold. We use the gluon condensate extracted from e^+e^- annihilation data via QCD sum rules [95], as the corresponding lattice computations inherently suffer from large uncertainties [94], e.g. $\langle\alpha_sG^2\rangle_{\text{lattice}} = \pi(0.077\pm0.087)\,\text{GeV}^4$ [92].

Evaluating L^{QCDvc}, we find that $L^{\text{QCDvc}}(m=0)\simeq L(m=m_s)$ and $L^{\text{QCDvc}}(m=m_s)\simeq L(m=0)$. We conclude that non-perturbative effects cannot be neglected.

2.9. Summary of the standard model Wilson coefficients

We have calculated the effective SM Wilson coefficients defined in section 2.2 at partly NNLL order in QCD. The missing pieces are the NNLO matching of $P_{1,2}$ onto P_{3-9} at μ_b, see section 2.5, as well as the NNLO effective Wilson coefficients of P_7, for $q^2\neq0$, and P_9 from P_{3-6}, see section 2.6. We will find in chapter 3 that these pieces are numerically small in phenomenological applications. The consistent matching at μ_W, given at NNLO in section 2.3, settles the issue of different calculations existing in the literature. The

$\times(\alpha_s/(4\pi))^i$	$C_1^{(i)}$	$C_2^{(i)}$	$C_3^{(i)}$	$C_4^{(i)}$	$C_5^{(i)}$
$i=0$	-1.0231	1.0919	-0.0036	-0.0601	0.0003
$i=1$	0.3195	-0.0549	-0.0024	-0.0309	0.0000
$i=2$	0.0756	-0.0036	-0.0019	-0.0007	0.0001
$\times(\alpha_s/(4\pi))^i$	$C_6^{(i)}$	$C_7^{(i)}$	$C_8^{(i)}$	$C_9^{(i)}$	$C_{10}^{(i)}$
$i=0$	0.0007	0	0	-0.0030	0
$i=1$	0.0002	0.0035	-0.0020	-0.0063	0
$i=2$	0.0003	0.0002	-0.0003	-0.0036	0

Table 2.2.: SM Wilson coefficients $(\alpha_s/(4\pi))^i\, C^{(i)}(\mu_c = m_c)$, as defined section in 2.2.

running and mixing is described by the RGE, see appendix B.1 for its solution yielding the Wilson coefficients at next-to-next-to-next-to leading logarithmic (NNNLL) order and appendix B.2 for the ADM to NNLO and partly from four loop calculations. As a novel aspect we have calculated the NNLO effective Wilson coefficients of $P_{7,9}$ from $P_{1,2}$ in section 2.6.1. This calculation will also be of use in section 4.2.1 and for b physics.

We have calculated the leading QED effects in section 2.7, finding that they can be neglected. In section 2.8 we have made an attempt to include non-perturbative effects from the QCD vacuum condensate within the OPE at high q^2. We have found that non-perturbative effects are not negligible on general grounds.

We conclude the current chapter by giving the Wilson coefficients at $\mu_c = m_c$ in table 2.2 for the parameters listed in appendix A. The NNLO QCD running and decoupling at flavor thresholds is taken from [67]. The low-energy value for α_e is used, which is consistent with the solution of the QCD-QED RGE [89]. For the Wilson coefficients in different operator bases and a comparison with the Wilson coefficients from b decays, see [2]. Neglecting the matching at μ_b the NNNLL Wilson coefficients of the dipole operators are $C_7|_{\text{NNNLL}} = 0.0003$ and $C_8|_{\text{NNNLL}} = -0.0003$. The effective Wilson coefficients will be discussed in the next chapter.

3. Phenomenology in the standard model

For a phenomenological analysis it is convenient to work in a different basis than the one introduced in chapter 2 to directly compare the SM with physics beyond. In view of chapter 4, we enlarge the basis by operators that are not present in the SM but may be induced by BSM physics. Matrix elements of the effective weak Lagrangian at μ_c then read

$$\langle \mathcal{L}_{\text{eff}}^{\text{weak}} \rangle = \frac{4G_F}{\sqrt{2}} \frac{\alpha_e}{4\pi} \sum_i \left(C_i \langle Q_i \rangle + C_i' \langle Q_i' \rangle \right) , \tag{3.1}$$

where the operators of dimension six relevant for charm FCNC transitions are written as

$$Q_7 = \frac{m_c}{e} (\bar{u}\sigma^{\mu\nu} P_R c) F_{\mu\nu} , \qquad Q_7' = \frac{m_c}{e} (\bar{u}\sigma^{\mu\nu} P_L c) F_{\mu\nu} , \tag{3.2}$$

$$Q_9 = (\bar{u}\gamma_\mu P_L c) \left(\bar{l}\gamma^\mu l\right) , \qquad Q_9' = (\bar{u}\gamma_\mu P_R c) \left(\bar{l}\gamma^\mu l\right) , \tag{3.3}$$

$$Q_{10} = (\bar{u}\gamma_\mu P_L c) \left(\bar{l}\gamma^\mu \gamma_5 l\right) , \qquad Q_{10}' = (\bar{u}\gamma_\mu P_R c) \left(\bar{l}\gamma^\mu \gamma_5 l\right) , \tag{3.4}$$

$$Q_S = (\bar{u} P_R c) \left(\bar{l} l\right) , \qquad Q_S' = (\bar{u} P_L c) \left(\bar{l} l\right) , \tag{3.5}$$

$$Q_P = (\bar{u} P_R c) \left(\bar{l}\gamma_5 l\right) , \qquad Q_P' = (\bar{u} P_L c) \left(\bar{l}\gamma_5 l\right) , \tag{3.6}$$

$$Q_T = \frac{1}{2} (\bar{u}\sigma^{\mu\nu} c) \left(\bar{l}\sigma_{\mu\nu} l\right) , \qquad Q_{T5} = \frac{1}{2} (\bar{u}\sigma^{\mu\nu} c) \left(\bar{l}\sigma_{\mu\nu}\gamma_5 l\right) . \tag{3.7}$$

Here $P_{L/R} = \frac{1}{2}(1 \mp \gamma_5)$, $\sigma^{\mu\nu} = \frac{i}{2}[\gamma^\mu, \gamma^\nu]$ and the remaining notation is the same as in section 2.2. The primed operators are obtained from the unprimed ones by flipping the chirality. Contributions from P_{1-6}' given by the replacement $q_L \to q_R$ in eqs. (2.7-2.12) are absorbed into effective Wilson coefficients as for P_{1-6}. Furthermore, we can introduce a lepton flavor label for the dilepton operators, but as the SM preserves LFU we do not write them in the current chapter. For decays involving anti-charm quarks one uses the hermitian conjugated expressions.

For simplicity of notation, we call the (effective) Wilson coefficients C_i, and do not write the scale dependence whenever we refer to μ_c. The same notation was used in chapter 2 for a different operator basis. We emphasize that in the current and the following chapter C_i will refer to the Wilson coefficients of the operator basis given here. The relation to the effective SM Wilson coefficients calculated in chapter 2 is

$$C_{7,9} = \sum_{q \in \{d,s\}} V_{cq}^* V_{uq} \frac{4\pi}{\alpha_s(\mu_c)} C_{7,9}^{\text{eff}(q)}(\mu_c) . \tag{3.8}$$

Recall that $C_{10} = 0$, $C_7' \sim m_u/m_c \simeq 0$, $C_{9,10}' = 0$ as well as $C_{S,P,T,T5}^{(\prime)} = 0$ from the previous chapter. Effects from

$$Q_8 = \frac{g_s m_c}{e^2}(\bar{u}\sigma^{\mu\nu}T^a P_R c)G^a_{\mu\nu}\,, \qquad Q_8' = \frac{g_s m_c}{e^2}(\bar{u}\sigma^{\mu\nu}T^a P_L c)G^a_{\mu\nu} \tag{3.9}$$

are absorbed into $C_{7,9}^{(\prime)}$. With the notation introduced above, the SM Wilson coefficients are known to $\mathcal{O}(\alpha_s)$, where C_9 starts at $\mathcal{O}(\alpha_s^{-1})$. One should keep in mind that weak phases and strong phases from the CKM matrix and the matrix elements absorbed in the effective Wilson coefficients, respectively, are both part of the Wilson coefficients. The weak phases, however, are small due to the CKM structure, see appendix A.

The factor $1/2$ in the definitions of $Q_{T,T5}$ is introduced to compensate for a double counting in $\mu \leftrightarrow \nu$. Note that $\sigma_{\mu\nu}\gamma_5 = \frac{i}{2}\epsilon_{\mu\nu\rho\sigma}\sigma^{\rho\sigma}$ which implies that $Q_T = \frac{1}{2}(\bar{u}\sigma^{\mu\nu}\gamma_5 c)(\bar{l}\sigma_{\mu\nu}\gamma_5 l)$, and $Q_{T5} = \frac{1}{2}(\bar{u}\sigma^{\mu\nu}\gamma_5 c)(\bar{l}\sigma_{\mu\nu} l)$, hence no primed tensor operators are needed. The mixing of the scalar, pseudoscalar, tensor, and pseudotensor operators, respectively, $Q_{S,P,T,T5}^{(\prime)}$ is each closed at one loop QCD. The running of their Wilson coefficients is, due to the parity invariance of QCD, [96]

$$C_i(\mu)^{(\prime)} = \left(\frac{\alpha_s(\mu_0)}{\alpha_s(\mu)}\right)^{-\gamma_i^{(0)}/(2\beta_0)} C_i^{(\prime)}(\mu_0)\,, \qquad \gamma^{(0)} = \mathrm{diag}\left(-8, -8, \frac{8}{3}, \frac{8}{3}\right)\,, \tag{3.10}$$

where β_0 is given by eq. (B.5). The anomalous dimension of $C_{S,P}^{(\prime)}$ is the same as the one of the of $\overline{\mathrm{MS}}$ mass.

For physical observables we switch to the on-shell and renormalized pole mass scheme. Its relation to the $\overline{\mathrm{MS}}$ mass scheme is [67]

$$\frac{m_{\mathrm{pole}}(\mu)}{m_{\overline{\mathrm{MS}}}(\mu)} = \left(1 + \frac{\alpha_s}{4\pi}\left(\frac{16}{3} + 4\ln\frac{\mu^2}{m^2_{\overline{\mathrm{MS}}}}\right)\right)\,. \tag{3.11}$$

Ratios of masses are scheme independent but care has to be taken of expressions involving q^2/m^2, and m_c due to the definitions of $Q_7^{(\prime)}$, where $m_c\, C_7^{(\prime)}$ are mass scheme independent.

The SM Wilson coefficients are shown in figures 3.1 and 3.2. We observe the following: At $q^2 = (2m_s)^2$ a discontinuity represents the $s\bar{s}$ intermediate quark state. Furthermore, the full calculation of chapter 2 can be approximated by the contributions from matrix elements of $P_{1,2}$ to the effective Wilson coefficients of $P_{7,9}$. This feature reflects the GIM mechanism which is broken by a non-zero strange quark mass entering these matrix elements. The remaining contributions are subject to GIM suppression, which also holds for the pieces which are missing towards a complete NNLL calculation in chapter 2. These pieces mainly come from QCD penguin operators, for which the Wilson coefficients are additionally suppressed in the SM. We conclude that for phenomenological purposes the one and two loop matrix elements of $P_{1,2}$ into $P_{7,9}$ are numerically equivalent to a

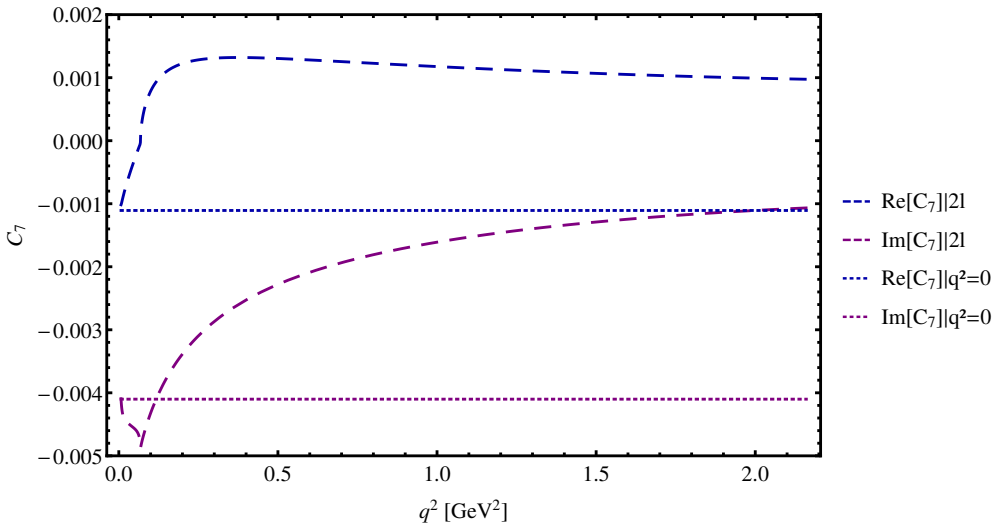

Figure 3.1.: SM Wilson coefficient C_7. The real (blue, upper) and imaginary (purple, lower) parts are shown. The label "2l" (dashed) indicates the two loop result of the calculation from section 2.6.1, whereas "$q^2 = 0$" (dotted) shows $C_7(q^2 = 0)$ from [47]. Indeed, "2l" represents the full NNLL result as obtained in chapter 2, see text, and for vanishing q^2 it agrees with "$q^2 = 0$".

complete NNLL calculation of $C_{7,9}$. Specifically, the two loop matrix elements give the leading contribution. However, this should not be seen as a breakdown of perturbativity, as the other contributions are more strongly GIM suppressed. Moreover, the one loop matrix elements are suppressed by cancellations from C_1 and C_2. The $q\bar{q}$ pair in the loop is color-singlet suppressed at one loop, whereas it forms a color-octet pair at two loop due to the additional gluon, giving rise to additional color factors. Indeed, from the SM Wilson coefficients in table 2.2 a breakdown of the perturbation series cannot be concluded.

The q^2 dependence of C_7 shows significant deviations from its value at $q^2 = 0$. This should be kept in mind, as $C_7(q^2 = 0)$ was used on the full q^2 range for $c \to ull$ induced decays in literature till today. For $c \to u\gamma$ induced decays, however, $C_7(q^2 = 0)$ can be obtained by eq. (2.62),

$$C_7(q^2 = 0) \simeq -0.0011 - 0.0041i\,. \tag{3.12}$$

In this chapter, which is based on [1] and [3], predictions for inclusive decays will be presented, see the next section. Exclusive decays, including form factors, non-perturbative effects, and different observables, will be the topic of sections 3.2 and 3.3 for $D \to Pll$ and $D \to V\gamma$, respectively. Other exclusive modes will be considered in section 3.4.

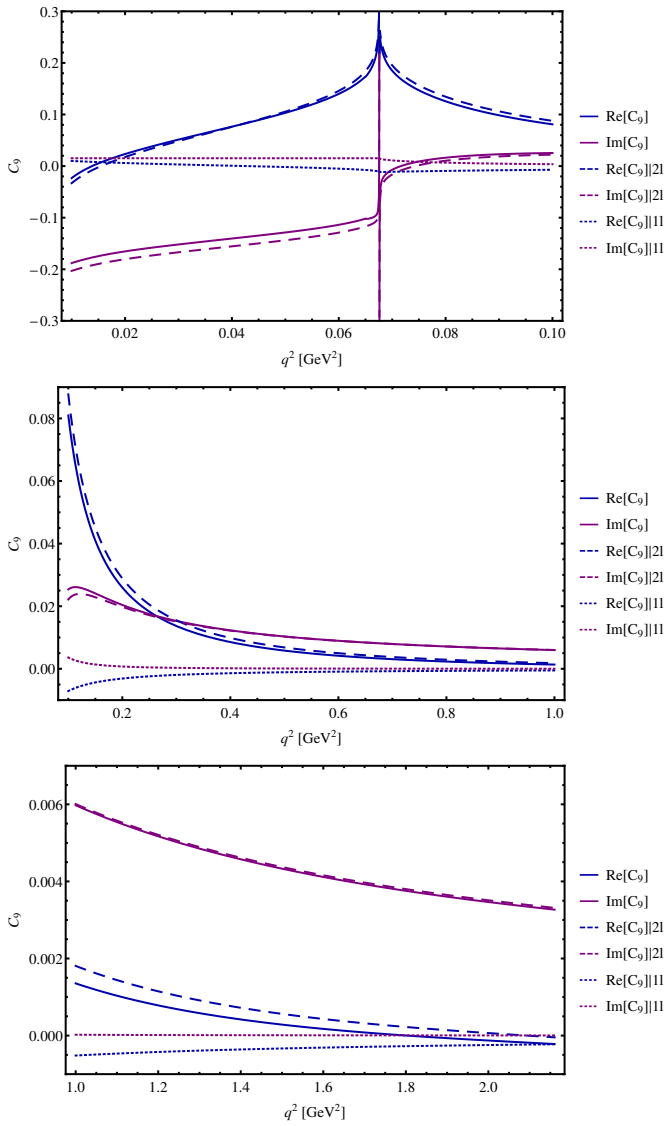

Figure 3.2.: SM Wilson coefficient C_9. The q^2 ranges are split corresponding to different orders of C_9. The real (blue) and imaginary (purple) parts are shown. The label "2l" (dashed) indicates the two loop result of the calculation from section 2.6.1. The label "1l" (dotted) indicates the one loop matrix element of $P_{1,2}$ resulting in an effective Wilson coefficient of P_9, see text. Indeed, the sum of "2l" and "1l" represents the full NNLL (solid) result as obtained in chapter 2, see text.

mode	branching ratio	norm	$\alpha_s(m_Z)$	m_c	m_s	μ_W	μ_c
$D^+ \to X_u\gamma$	4.6×10^{-8}	$\pm 4\%$					
$D^0 \to X_u\gamma$	2.3×10^{-8}	$\pm 4\%$	$^{+11}_{-10}\%$	$^{+13}_{-12}\%$	$^{+24}_{-21}\%$	$\pm 7\%$	$^{+82}_{-37}\%$
$D_s^+ \to X_u\gamma$	2.8×10^{-8}	$\pm 18\%$					

Table 3.1.: Branching ratios of $D \to X_u\gamma$ decays in the SM. The normalization is given by $\mathcal{B}(D \to X_d e\nu)$ and the other uncertainties apply for all modes. We vary $m_{W,b}/2 \leq \mu_{W,b} \leq 2m_{W,b}$, $m_c/\sqrt{2} \leq \mu_c \leq \sqrt{2}m_c$, and all other parameters according the intervals given in appendix A.

3.1. Inclusive decays

As a direct application of the SM Wilson coefficients calculated in chapter 2 and discussed above, we study inclusive $c \to u\gamma$ and $c \to ull$ decays in sections 3.1.1 and 3.1.2, respectively.

3.1.1. Inclusive $D \to X_u\gamma$ decays

The inclusive $c \to u\gamma$ branching ratio can be expressed as [47]

$$\mathcal{B}_{D\to X_u\gamma} = \frac{\alpha_e}{\pi}\frac{6|C_7|^2}{|V_{cd}^* V_{ud}|^2}\mathcal{B}(D \to X_d e\nu)\,. \tag{3.13}$$

Here X_u denotes a not fully specified final hadronic state containing a u quark. The branching ratio of $c \to d$ induced $D \to X_d e\nu$ decays is chosen as a normalization to reduce parametric uncertainties. Also renormalization scheme and scale uncertainties entering in the charm quark mass are reduced by this choice. The branching ratios, as obtained for the parameters listed in appendix A, are given in table 3.1. The difference between the modes follows from the normalization. Additionally, we give all individual non-negligible uncertainties, of at least one percent. We vary $m_i/2 \leq \mu_i \leq 2m_i$, only for μ_c we choose $m_c/\sqrt{2} \leq \mu_c \leq \sqrt{2}m_c$. This choice follows as $\mu_c = m_c/2$ would be close to the non-perturbative region and $\mu_c = 2m_c > m_b/2 = \mu_b$ would reverse the ordering of the c and b quarks, which is inconsistent with matching of the b quark. The largest uncertainty arises from the variation of the scale μ_c, yielding an uncertainty of a factor $\sim 1/2$ to ~ 2 for the branching ratios. The branching ratios are in agreement with the ones found in [47]. No experimental data are currently available.

The CP conjugated modes yield approximately the same branching ratios. This follows from the GIM mechanism and the structure of the CKM matrix, which is the only source of CP violation in the SM. Nonetheless, strong phases are sizable, see figures 3.1, 3.2.

Note that effects from $D^0 - \bar{D}^0$ mixing are small [97]. Considering untagged CP averaged branching ratios doubles the numbers provided in table 3.1.

An additional observable is the photon polarization, defined as the difference between the right-handed and left-handed quark currents. Due to a dominantly left handed polarization the SM prediction for the photon polarization is -1.

The predictions made here can be further improved, analogue to b physics: One can evaluate contributions from $c \to d\bar{d}u\gamma$ transitions, see [98], and one can calculate Brodsky–Lepage–Mackenzie (BLM) corrections, as done for b decays [99] (and references therein). Furthermore, one can include power corrections $\sim \frac{\Lambda_{\text{QCD}}}{m_c}$, see [100] (and references therein). Additionally, energy moments and power corrections to them can be calculated as well, see e.g. [101]. See [102], for non-local operators $\sim \frac{\Lambda_{\text{QCD}}}{m_c}$. However, This class of corrections will be numerically small as C_8 is GIM suppressed. Also kinematical cuts on the photon energy spectrum yield power corrections, see [100] for a review in b physics.

We will consider power corrections for exclusive radiative decays in section 3.3. Power corrections, e.g. spectator interactions, and resonant effects do, in fact, dominate the branching ratios, but were not taken into account for the inclusive predictions. A comparison of the inclusive branching ratio $\sim \mathcal{O}(10^{-8})$, see table 3.1, which is an upper limit on exclusive branching ratios, with a measurement of the exclusive decay $D^0 \to \rho^0\gamma$, i.e. $\mathcal{B}(D^0 \to \rho^0\gamma) = (1.77 \pm 0.30 \pm 0.07) \times 10^{-5}$ [24], points towards large corrections.

We will address this issue for exclusive radiative decays within the SM and BSM in section 3.3 and chapter 4, respectively. Similar observations will be made for $c \to ull$ induced decays. However, inclusive dilepton decays are instructive and will be analyzed in the next section.

3.1.2. Inclusive $D \to X_u ll$ decays

We refer to appendix C.1 for the distributions and observables relevant for $D \to X_u ll$ decays. They are obtained by means of a heavy quark expansion (HQE), where perturbative corrections to the matrix elements as well as power corrections can be included.

The q^2 distribution of the decay $D^+ \to X_u^+ e^+ e^-$ is shown in figure 3.3. We plot distributions for matrix elements to NNLO and, additionally, with non-vanishing lepton masses as well as power corrections. One observes that the effect of a non-zero lepton mass is small apart from the very low q^2 range, where it renders the branching ratio to be finite. Indeed, the SM respects LFU and the lepton flavor ratio $\mathcal{B}(c \to u\mu\mu)/\mathcal{B}(c \to uee)$ is solely broken due to kinematical effects. The decay $c \to u\tau\tau$ is kinematically forbidden. For vanishing lepton, i.e. electron, masses and in the limit $q^2 \to 0$ on-shell photons, thus $c \to u\gamma$ transitions, are probed.

At high q^2, the relative power corrections diverge and the distribution becomes negative. As in b decays [103] the HQE breaks down for $q^2 \gtrsim m_c^2/2$, as the soft momentum and soft mass hadronic system is non-perturbative. Analogue to b decays [103] no resum-

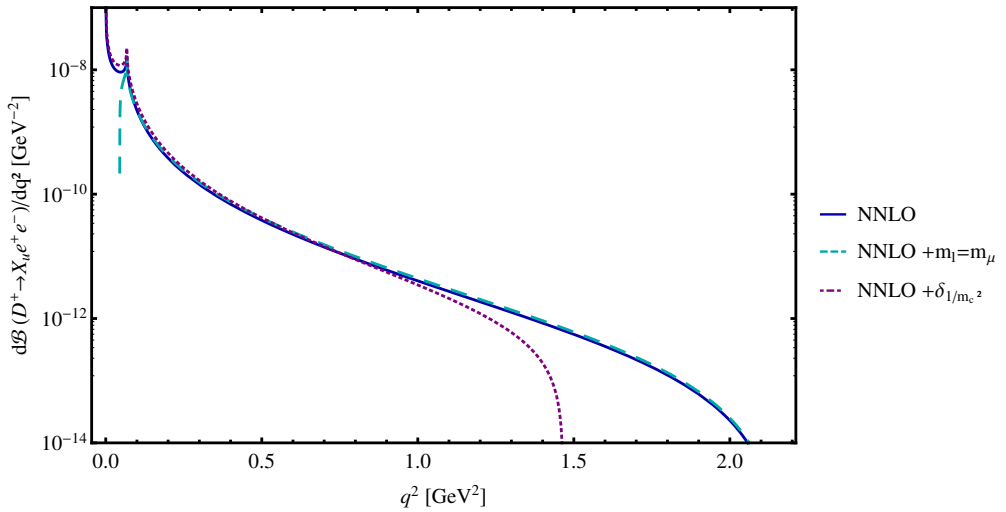

Figure 3.3.: The q^2 distribution of the branching ratio of the decay $D^+ \to X_u^+ e^+ e^-$. We plot distributions for matrix elements to NNLO (solid blue) and, additionally, with a non-zero muon lepton mass (dashed cyan) as well as power corrections (dotted purple).

mation into a light-cone distribution function, as for $D \to X_u \gamma$ and $D \to X_u l \nu_l$ decays, is possible. However, the fully integrated branching ratio is dominated by the low q^2 range, where power corrections are small. Note that for the power corrected distribution a kinematical cut on the hadron mass should be employed, which in turn induces $\frac{\Lambda_{\rm QCD}}{m_c}$ corrections. Nevertheless, the high q^2 range is theoretically accessible as the inclusive decay degenerates into only a few exclusive modes, e.g. $D \to \pi ll$ which will be studied in the next section. In principle, one can perform an expansion in inverse powers of $m_{\rm heavy}^{\rm eff} = m_c(1 - \sqrt{q^2_{\rm min}})$, where $q^2_{\rm min} \sim m_c^2/2$ to calculate the inclusive branching ratio at high q^2, see [79] for b decays. A HQE for charm decays was used to calculate the D meson lifetime, showing that predictions within the HQE and the perturbation theory are consistent with measurements, although, subleading corrections are sizable [104]. Analogously, calculations of subleading corrections in charm mixing do not signal a breakdown of the HQE [105]: It was found that formally leading contributions are more strongly GIM suppressed than subleading corrections, analogously to what we have observed for rare charm decays within the perturbation theory.

In principle, one can include additional non-perturbative effects by means of the OPE at high q^2 via quark-hadron duality, a dispersion relation, and $e^+e^- \to$ hadrons data following [103, 106, 107]. Furthermore, one can obtain the hadronic spectrum and its moments, giving rise to non-perturbative parameters, analogue to b decays [108].

mode	branching ratio	norm	$\alpha_s(m_Z)$	μ_W	μ_c
$D^+ \to X_u\mu^+\mu^-$	4.4×10^{-10}	$\pm 19\%$			
$D^0 \to X_u\mu^+\mu^-$	1.7×10^{-10}	$\pm 9\%$	$^{+14}_{-13}\%$	$^{+14}_{-11}\%$	$^{+104}_{-41}\%$
$D_s \to X_u\mu^+\mu^-$	1.6×10^{-10}	$\pm 7\%$			

Table 3.2.: Fully integrated ranching ratios of $D \to X_u ll$ decays in the SM. The results are obtained from eq. (C.12) with NNLO matrix elements for massive leptons. Power corrections are not taken into account, see text. The normalization is given by $\mathcal{B}(D \to X\mu\nu)$ and the other uncertainties apply for all modes. We vary $m_{W,b}/2 \leq \mu_{W,b} \leq 2m_{W,b}$, $m_c/\sqrt{2} \leq \mu_c \leq \sqrt{2}m_c$, and all other parameters according to the intervals given in appendix A. We do not vary $m_{c,s}$ as they were fixed in the calculation of the two loop matrix elements for simplicity.

The $D \to X_u\mu\mu$ branching ratios are given in table 3.2. The difference between the modes follows from the normalization, i.e. $\mathcal{B}(D \to X\mu\nu)$. As in the radiative case, the uncertainties are dominated by the scale μ_c, which induces an uncertainty of a factor $\sim 1/2$ to ~ 2. We do not consider electrons as their branching ratios depend on a cut in the q^2 distribution, see figure 3.3. Moreover, a q^2-cut is experimentally required to reduce jet-like X_u, which yields power corrections, as in b decays, e.g., [109]. As can be seen from figure 3.3 the branching ratios with electrons are equal to the muonic case apart from very low q^2, where branching ratios with electrons increase.

Comparing with the branching ratios obtained in [1], where the two loop matrix elements for P_9 were not taken into account, one finds that the branching ratios given in table 3.2 are only slightly increased: The enhancement of C_9 is suppressed by a small phase space, whereas the branching ratio on most of the phase-space is shifted to smaller values due to cancellations between C_7 and C_9.

In the literature the branching ratios were found to vary by two orders of magnitude [48, 58, 59, 110]. We agree with the results obtained in [48, 110] (see [111] for updated plots). The discrepancy with [58, 59] is driven by eq. (2.22).

Apart from a CP asymmetry which is approximately zero, also the leptonic forward-backward asymmetry, see appendix C, vanishes. These null tests follow from the vanishing of the Wilson coefficient C_{10} in the SM. If C_{10} would be non-vanishing, a zero point, where the forward-backward asymmetry changes sign, could be induced. Such a point is observed in b decays.

In addition to the forward-backward asymmetry, one can define the leptonic left-right asymmetry and the leptonic longitudinal/normal polarization asymmetries, see appendix C. Also the latter observables are zero as $C_{10} = 0$. Again, zero points could

be induced if C_{10} would be non-zero. All four zero points, including the one from the forward-backward asymmetry, would be driven by the same Wilson coefficients, but multiplied with different phase space factors.

Furthermore, the leptonic transverse polarization asymmetries of $l^{\pm}$ are given in appendix C. They come with a non-vanishing combination of SM Wilson coefficients but are lepton mass suppressed, which in turn is softened by a pole for low q^2. The difference between the l^+ and l^- transverse polarization asymmetries is again a null-test which can be broken by a non-vanishing C_{10}.

3.1.3. Summary of inclusive decays

In the previous sections on inclusive decays we have learnt the following: The main uncertainty in the perturbative calculation is due the scale $\mu_c \sim m_c$, i.e. higher order effects. The branching ratios calculated at NNLO are found as $\mathcal{B}(c \to u\gamma) \sim \mathcal{O}(10^{-8})$, see section 3.1.1, and $\mathcal{B}(c \to u\mu\mu) \sim \mathcal{O}(10^{-11})$, see section 3.1.2. The GIM mechanism which drives the smallness of the perturbative contributions, also renders CP asymmetries small. Additionally, due to the vanishing C_{10} several observables are approximate null-tests. As already found in section 2.8 non-perturbative effects, e.g. power corrections, should be taken care off. Indeed, comparing the measured branching ratio of $D^0 \to \rho^0\gamma$ with inclusive branching ratios calls for additional dynamics at work. While including power corrections to the branching ratio of $c \to ull$, the breakdown of the HQE at high q^2 was evident. To address these issues we will consider exclusive decays in the next sections.

3.2. The decay $D \to Pll$

The exclusive decay of a pseudoscalar D meson into a pseudoscalar P meson and a lepton pair has the simplest spin structure of rare charm decays. Furthermore, $D \to Pll$ decays constitute the only mode for inclusive decays at sufficiently high q^2. Experimentally, the most stringent limits are obtained for this mode and on the theoretical side several observables are calculable. Despite possible large uncertainties, clean SM predictions can be obtained, which can then be confronted with experiments as well as BSM physics. The decay $D \to Pll$ is hence the first way to be taken in probing the SM with rare charm decays. Note that the decay $D \to P\gamma$ with an on-shell photon is forbidden due to the spin of the photon.

The decay distribution is worked out in appendix C.2 and form factors, which describe the hadronic matrix elements for exclusive decays, will be considered in the next section. In section 3.2.2 resonance effects will be taken into account and the phenomenology in the SM will be worked out in section 3.2.3.

3.2.1. Form factors

The heavy-to-light transition form factors as defined in appendix C.2 read

$$\langle P(p_P)|\bar{u}\gamma^\mu c|D(p_D)\rangle = f_+(q^2)\left(p^\mu - \frac{m_D^2 - m_P^2}{q^2}q^\mu\right) + f_0(q^2)\frac{m_D^2 - m_P^2}{q^2}q^\mu\,, \tag{3.14}$$

$$\langle P(p_P)|\bar{u}\sigma^{\mu\nu} c|D(p_D)\rangle = i f_T(q^2)(p^\mu q^\nu - q^\mu p^\nu)\,, \tag{3.15}$$

where $q^\mu = (p_D - p_P)^\mu = (p_+ + p_-)^\mu$, and $p^\mu = (p_D + p_P)^\mu$. If the pseudoscalar P is neutrally charged, the form factors $f_{+,0,T}$ are multiplied by the isospin factor of the $u\bar{u}$ content in P, e.g. $1/\sqrt{2}$ for $P = \pi^0$. In particular, $f_+(0) = f_0(0)$ to avoid a singularity in eq. (3.14) for $q^2 \to 0$. For vanishing lepton masses $q^\mu[\bar{l}\gamma_\mu l] = 0$ due to the lepton EOM, thus f_0 is absent. Moreover, f_0 is irrelevant in the SM as C_{10} is vanishing.

The form factors are of hadronic nature and presently only calculable on the lattice. Firstly, we reduce the number of independent form factors by use of the heavy quark spin symmetry. The remaining single form factor is extracted from $D \to Pl\nu$ decays by means of isospin symmetry.

By employing the heavy quark spin symmetry within the heavy quark effective theory (HQET) [112] form factors are related at large q^2, $q^2 \sim m_c^2 \gg \Lambda_{\text{QCD}}^2$, that is at low hadronic recoil [113]. In this case the momentum of a softly interacting heavy quark can be decomposed as $p_c^\mu = m_c v^\mu + k^\mu$ with $|k| \sim \Lambda_{\text{QCD}}$. Within the HQET h_v is the heavy charm quark with velocity $v_\mu = (p_D)_\mu/m_D$, where $\not{v} h_v = h_v$. Matching the quark currents gives $\bar{u}\gamma^\mu c = \bar{u}\gamma^\mu h_v + \mathcal{O}(\alpha_s, \frac{\Lambda_{\text{QCD}}}{m_c})$ and $\bar{u}\sigma^{\mu\nu} c = \bar{u}\sigma^{\mu\nu} h_v + \mathcal{O}(\alpha_s, \frac{\Lambda_{\text{QCD}}}{m_c})$ [114]. Multiplying eq. (3.14) with v_μ and q_μ, yields up to power corrections, respectively,

$$\begin{aligned}
\langle \bar{u} h_v\rangle &= f_+ \frac{m_D^2 + p_D\cdot p_P}{m_D} + (-f_+ + f_0)\frac{m_D^2 - m_P^2}{q^2}\frac{m_D^2 - p_D\cdot p_P}{m_D}\,,\\
\langle \bar{u} c\rangle &= f_+ \frac{m_D^2 - m_P^2}{m_D} + (-f_+ + f_0)\frac{m_D^2 - m_P^2}{q^2}\frac{m_D^2 + m_P^2 - 2p_D\cdot p_P}{m_D}\,.
\end{aligned} \tag{3.16}$$

Thus, the leading form factor relations at low recoil follow as

$$f_0(q^2) = f_+(q^2)\left(1 - \frac{q^2}{m_D^2 - m_P^2}\right) + \mathcal{O}\left(\frac{\Lambda_{\text{QCD}}}{m_c}\right)\,. \tag{3.17}$$

For the tensor form factor we multiply eq. (3.15) with v_ν yielding

$$v_\nu\langle \bar{u}\sigma^{\mu\nu} h_v\rangle = i f_T\left(p^\mu \frac{m_D^2 - p_D\cdot p_P}{m_D} - q^\mu \frac{m_D^2 + p_D\cdot p_P}{m_D}\right) \tag{3.18}$$

$$= i\langle \bar{u}\gamma^\mu h_v\rangle - i\langle \bar{u} v^\mu h_v\rangle \tag{3.19}$$

$$\begin{aligned}
&= i\Bigg(f_+\left(p^\mu - v^\mu\frac{m_D^2 + p_D\cdot p_P}{m_D}\right) + (-f_+ + f_0)\frac{m_D^2 - m_P^2}{q^2}\\
&\times\left(q^\mu - v^\mu\frac{m_D^2 - p_D\cdot p_P}{m_D}\right)\Bigg)
\end{aligned} \tag{3.20}$$

up to power corrections. This implies

$$f_T 2m_D = f_+ - (-f_+ + f_0)\frac{m_D^2 - m_P^2}{q^2} \tag{3.21}$$

and combined with eq. (3.17) the second leading form factor relation at low recoil follows as

$$f_T(q^2) = f_+(q^2)\frac{1}{m_D} + \mathcal{O}\left(\frac{\Lambda_{\rm QCD}}{m_c}\right) . \tag{3.22}$$

These relations are also valid at large hadronic recoil, i.e. low q^2, as derived in the HQET/large energy effective theory (LEET) [115, 116]. We point out that power corrections enter as $\sim \frac{C_7}{C_9}\frac{\Lambda_{\rm QCD}}{m_c}$, which are suppressed once the two loop calculation of the current-current matrix elements are taken into account, see section 2.6.1, and figures 3.1, 3.2. This would not be the case without the two loop calculation.

Perturbative corrections, which break the heavy quark symmetry can be included at low and large recoil. At low recoil, they are obtained from the HQET [1, 114],

$$f_0(q^2) = 0 + \mathcal{O}\left(\frac{\Lambda_{\rm QCD}}{m_c}, \alpha_s^2\right) , \tag{3.23}$$

$$f_T(q^2) = \frac{m_D}{q^2}\left(1 - \frac{\alpha_s}{\pi}\frac{1}{3}\ln\frac{\mu_c^2}{m_c^2}\right) f_+(q^2) + \mathcal{O}\left(\frac{\Lambda_{\rm QCD}}{m_c}, \alpha_s^2\right) . \tag{3.24}$$

The pole in the form factor relation of eq. (3.24) is of kinematical origin. In the calculation of the corrections, the QCD EOM induce the matrix element $\langle \bar{u} i \overleftarrow{D}_\mu (1+\gamma_5) h_v \rangle$, which is power suppressed, hence neglected, yet it can be calculated in the chiral perturbation theory as done in b decays [117].

At large recoil, perturbative QCD vertex corrections can be included from [118] as

$$f_0(q^2) = \frac{2E}{m_D}\left(1 + \frac{\alpha_s}{\pi}\left(\frac{2}{3} + \frac{2}{3}\frac{2E}{m_D - 2E}\ln\frac{2E}{m_D}\right)\right) f_+(q^2) , \tag{3.25}$$

$$f_T(q^2) = \frac{1}{m_D}\left(1 + \frac{\alpha_s}{\pi}\left(-\frac{2}{3}\frac{2E}{m_D - 2E}\ln\frac{2E}{m_D} - \frac{1}{3}\ln\frac{\mu_c^2}{m_c^2}\right)\right) f_+(q^2) , \tag{3.26}$$

where the energy $E = (m_D^2 + m_P^2 - q^2)/(2m_D)$. Here $m_P \sim \Lambda_{\rm QCD}$ will be consistently set to zero. Note that $2E/(m_D - 2E)\ln[2E/(m_D)] \to 1$, as $q^2 \to 0$, and $m_P \simeq 0$, implying $f_0|_{\alpha_s^1} \simeq 0$, i.e. α_s corrections vanish at large recoil, as for the low recoil relation.

To obtain the full q^2 dependence of the form factor relations for f_T we take eq. (3.22) and interpolate the corrections from eqs. (3.24) and (3.26) for $m_P = 0$. The form factor f_0 is also provided by lattice computations [119] (preliminary [120, 121]). It turns out that the lattice result for f_0 is non-zero at low recoil, as opposed to its corresponding

HQET prediction, eq. (3.23). This can be attributed to large power corrections as the leading order relation is vanishing. Experiments have only restricted access to f_0 as it is suppressed by the lepton mass. Therefore, we take the f_0 from the lattice computation, where we estimate the uncertainty from [119] as $\lesssim 10\%$.

We are left with the single form factor f_+. It can be parametrized by a conformal map of the branch cut in the q^2 plane onto a circle, $|z| < 1$, via [97]

$$z(q^2, t_0) = \frac{\sqrt{t_+ - q^2} - \sqrt{t_+ - t_0}}{\sqrt{t_+ - q^2} + \sqrt{t_+ - t_0}}, \qquad t_\pm = (m_D \pm m_P)^2, \tag{3.27}$$

and some $t_0 < t_+$ which is chosen as

$$t_0 = t_+ \left(1 - \sqrt{1 - \frac{t_-}{t_+}}\right). \tag{3.28}$$

One obtains $|z| \leq 0.171$ as the radius of convergence on the full q^2 range. The form factor can be expanded as a series around $q^2 = t_0$,

$$f_+(q^2) = \frac{1}{P(q^2)\phi(q^2, t_0)} \sum_{i=0}^{\infty} a_i(t_0) \left(z(q^2, t_0)\right)^i, \tag{3.29}$$

where $a_i \in \mathbb{R}$, and $\phi(q^2, t_0)$ is analytic in the complex q^2 plane, apart from a cut from t_+ to ∞. It reads [122]

$$\begin{aligned}\phi(q^2, t_0) =& \sqrt{\frac{\pi m_c^2}{3}} \left(\sqrt{t_+ - q^2} + \sqrt{t_+ - t_0}\right) \frac{t_+ - q^2}{(t_+ - t_0)^{1/4}} \\ &\times \frac{\left(\sqrt{t_+ - q^2} + \sqrt{t_+ - t_-}\right)^{3/2}}{\left(\sqrt{t_+ - q^2} + \sqrt{t_+}\right)^5}\end{aligned} \tag{3.30}$$

and resonances below the continuum threshold at t_+ are subtracted via

$$P(q^2) = 1. \tag{3.31}$$

The parameters a_i are bounded by unitarity constraints from the correlation function [122]. For a series up to $i = 3$ they are given by the HFAG [97] for $D \to \pi$ transitions from experimental fits to $D \to \pi l \nu$ decays. Defining $r_i \equiv a_i/a_0$, the parameters read [97]

$$f_+(0)\,|V_{cd}| = 0.1426 \pm 0.0019\,, \quad r_1 = -1.95 \pm 0.18\,, \quad r_2 = -0.52 \pm 1.21\,, \tag{3.32}$$

where a_0 is fixed by $f_+(0)$. We use the isospin masses $m_i = (m_{i^+} + m_{i^0})/2$. From lattice computations we learn that the spectator quark dependence of f_+ is less than two

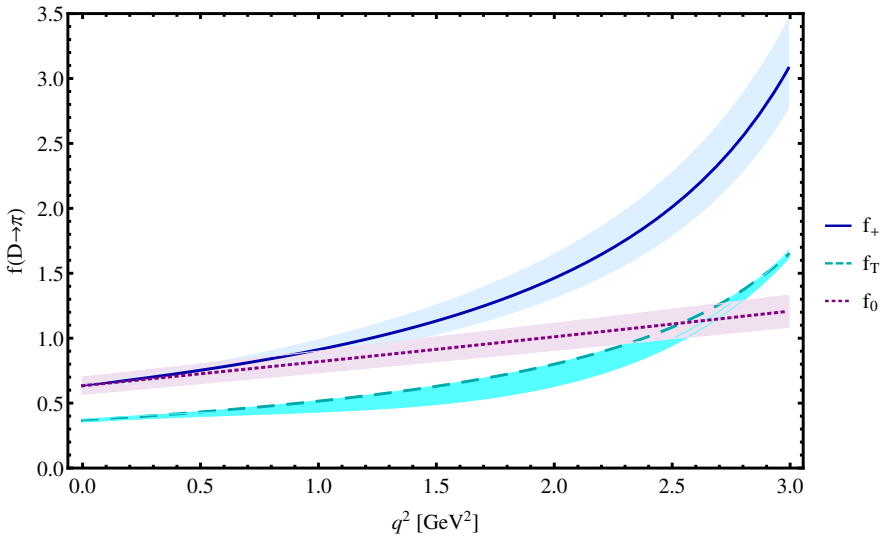

Figure 3.4.: Form factors for $D \to \pi$ transitions. The bands represent the parametric uncertainties for f_+, scale uncertainty for f_T, and estimated uncertainties for f_0, see text. The parametric uncertainties for f_T are not shown, following the ones of f_+.

percent on most of the q^2 range [119]. Hence, we take the same form factors for $D_s \to K$ transitions, while adjusting the masses. Moreover, f_+ is provided by lattice computations [119] (preliminary [120]), consistent with the experimental fits, yet the preliminary lattice calculation of [121] yields a smaller form factor at high q^2.

The form factors for $D \to \pi$ transitions are shown in figure 3.4. For a different definition of f_T, the corresponding relation, and plot, see [1].

3.2.2. Non-perturbative effects

We include resonant effects in a phenomenological approach as described in the following. The relevant resonances for $D \to PR(\to l^+l^-)$ decays are the pseudoscalars $\eta^{(\prime)}$ as well as the vectors ρ/ω, and ϕ. We employ a constant width, relativistic Breit-Wigner parametrization for the amplitude

$$-i\mathcal{A}|_R = \frac{G_F \alpha_e}{2\sqrt{2}\pi} \frac{a_R e^{i\delta_R}}{q^2 - m_R^2 + i m_R \Gamma_R} \bar{l}(p_+) \not{p}_D l(p_-)\,, \tag{3.33}$$

where $a_R \in \mathbb{R}^+$ is a constant fit parameter, and δ_R is an unknown strong phase.

The parametrizations of eq. (3.33) $\sim (p^\mu + q^\mu)$ and of eq. (C.42) $\sim (p^\mu - (m_D^2 - m_P^2)/q^2 q^\mu)$ are equivalent for vanishing lepton masses as $q_\mu(\bar{l}\gamma^\mu l) \sim m_l$. This holds also

for non-zero masses as C_{10} is vanishing. Hence, one can include effects of the resonances compactly in $C_{9,P}$ as

$$C_9^R = a_\rho e^{i\delta_\rho}\left(\frac{1}{q^2-m_\rho^2+im_\rho\Gamma_\rho}-\frac{1}{3}\frac{1}{q^2-m_\omega^2+im_\omega\Gamma_\omega}\right)+\frac{a_\phi e^{i\delta_\phi}}{q^2-m_\phi^2+im_\phi\Gamma_\phi}\,,$$
$$C_P^R = \frac{a_\eta e^{i\delta_\eta}}{q^2-m_\eta^2+im_\eta\Gamma_\eta}+\frac{a_{\eta'}}{q^2-m_{\eta'}^2+im_{\eta'}\Gamma_{\eta'}} \tag{3.34}$$

as the resonances decay electromagnetically, thus conserve parity. Here we relate the decays $D^+\to\pi^+\omega$ and $D^+\to\pi^+\rho$ by means of isospin symmetry as in [110] to reduce the number of parameters.

The matrix elements of pseudoscalar and vector particles are not independent but related by the EOM. Note that generically $|C^R|^2 \to |a_R|^2\pi/(m_R\Gamma_R)\delta(q^2-m_R^2)$ as $m_R\Gamma_R\to 0$, which, in particular, holds for $\eta^{(\prime)}$. The corresponding contributions from light $q\bar{q}$ pairs in the loop to the SM Wilson coefficients will consistently be omitted to avoid a double-counting. In the notation of eq. (3.34) CKM factors are implicit. We consider them separately wherever needed, e.g. for CP asymmetries.

As we are mainly concerned with $D^+\to\pi^+V(\to\mu\mu)$ decays we give their fit parameters only. Approximating $\mathcal{B}(D^+\to\pi^+(R\to\mu\mu))\simeq\mathcal{B}(D^+\to\pi^+R)\mathcal{B}(R\to\mu\mu)$, which is e.g. measured for $R=\phi$ [21], and taking the branching ratios from measurements, see appendix A, one obtains

$$a_\rho = (0.17\pm0.02)\,\mathrm{GeV}^2\,,\quad a_\omega = (0.032^{+0.006}_{-0.007})\,\mathrm{GeV}^2\,,\quad a_\phi = (0.24^{+0.05}_{-0.06})\,\mathrm{GeV}^2\,,$$
$$a_\eta = (0.00060^{+0.00004}_{-0.00005})\,\mathrm{GeV}^2\,,\quad a_{\eta'}\sim 0.0007\,\mathrm{GeV}^2\,. \tag{3.35}$$

The branching ratio for η' is not measured and cannot be approximated by the one from $\mathcal{B}(\eta'\to ee)$ as the branching ratio of a pseudoscalar decaying into dileptons is proportional to the lepton mass. Here it is obtained from unitarity [123] as

$$\mathcal{B}(\eta'\to\mu\mu)\sim\mathcal{B}(\eta'\to\gamma\gamma)\,\frac{\alpha_e^2}{2}\left(\frac{m_\mu}{m_{\eta'}}\right)^2\Bigg/\sqrt{1-\frac{(2m_\mu)^2}{m_{\eta'}^2}}$$
$$\times\ln^2\left[\left(1+\sqrt{1-\frac{(2m_\mu)^2}{m_{\eta'}^2}}\right)\Bigg/\left(1-\sqrt{1-\frac{(2m_\mu)^2}{m_{\eta'}^2}}\right)\right] \tag{3.36}$$

yielding $\mathcal{B}(\eta'\to\mu\mu)\sim 10^{-7}$ which is in agreement with the findings in [124, 125]. Compared to [1] the fitted parameter a_ω is new due to a recent measurement. The isospin relation $|a_\omega|=|a_\rho|/3$ slightly overestimates the fitted parameters. However, as can be seen from eq. (3.35) the ρ and ϕ are the dominant resonances, due to their total width and branching ratio, respectively. Hence, the approximations made here do not affect the phenomenology away from the ω and η' peaks. If we relax the condition of

constant widths and parameters, e.g., replace $(\Gamma_R, a_R) \to (\Gamma_R, a_R)\sqrt{q^2}/m_R$, the fitted parameters obtained in eq. (3.35) stay approximately the same. Resonances with spin higher than one are not included as their branching ratios are not measured, yet their decays to electrons are seen [21].

We observe some discrepancies with respect to the literature: In [126] equation (16) should be $\lambda_s a_\phi = 1.23 \pm 0.05$. The work of [60] is based on the fitted parameters of [127] (and updates thereof, e.g. [128]) multiplied by form factors, which was not done in the fitting of [127] (and updates thereof). In [129] the pseudoscalar η is treated as a scalar particle which results in a non-vanishing SM forward-backward asymmetry there, but is not the case for pseudoscalars. Resonant decays described within a chiral theory [70] give a similar q^2 shape, yet light penguin diagrams are double counted. Note that the decay of a ρ is hardly accessible in lattice computations due to the large total width of the ρ.

Apart from this phenomenological approach one can employ different approaches to include non-perturbative effects. One is to perform an OPE at high q^2 via quark-hadron duality, a dispersion relation, and $e^+e^- \to$ hadrons data as for inclusive decays, see [114, 130–133] for b decays. Furthermore, non-perturbative effects can be calculated, as done in b physics, via QCD factorization [134], and the soft collinear effective theory (SCET) [135] (and references therein) at low q^2. At large q^2, power corrections $\sim 1/m_c^2$ due to hard spectator interactions (HSIs) and weak annihilation (WA) $\sim 1/m_c^3$ via QCD penguin operators emerge within the OPE, see [131] for b physics. Analogous calculations for rare charm decays may be done elsewhere.

3.2.3. Phenomenology

For $D \to Pll$ decays only upper limits on the branching ratios are measured, with the most stringent one for $D^+ \to \pi^+\mu^+\mu^-$. The q^2 distribution of the latter, as derived in appendix C, is shown in figure 3.5. The perturbative contribution along with the resonance distribution as obtained in the previous section, and the experimental limit are plotted. One observes that the resonances dominate, apart from very low q^2, where perturbative contributions are of similar size. The resonant uncertainties mainly stem from the unknown relative phases, only near the resonance the uncertainties of the fitting parameters become noticeable. Towards high q^2 the SM induced branching ratio decreases. Compared to [1] we observe a similar behavior as already noticed for the inclusive study when taking the two loop matrix elements into account: The enhancement of C_9 is visible at very low q^2, whereas on most of the phase-space cancellations between C_7 and C_9 take place. The experimental limit is obtained assuming a model dependent phase space interpolation of the low and high q^2 ranges, and neglecting resonant interferences [136]. The experimentally defined binnings are $\sqrt{q^2} \in [0.250, 0.525]\,\text{GeV}$ and $\sqrt{q^2} \geq 1.25\,\text{GeV}$ to cut on the η and ϕ resonances, respectively. The resonant distribution at high q^2 is driven by the uncertainties of the unknown phases of ρ and ϕ. Once the uncertainties of the measured resonant distribution is reduced, a fit will provide fur-

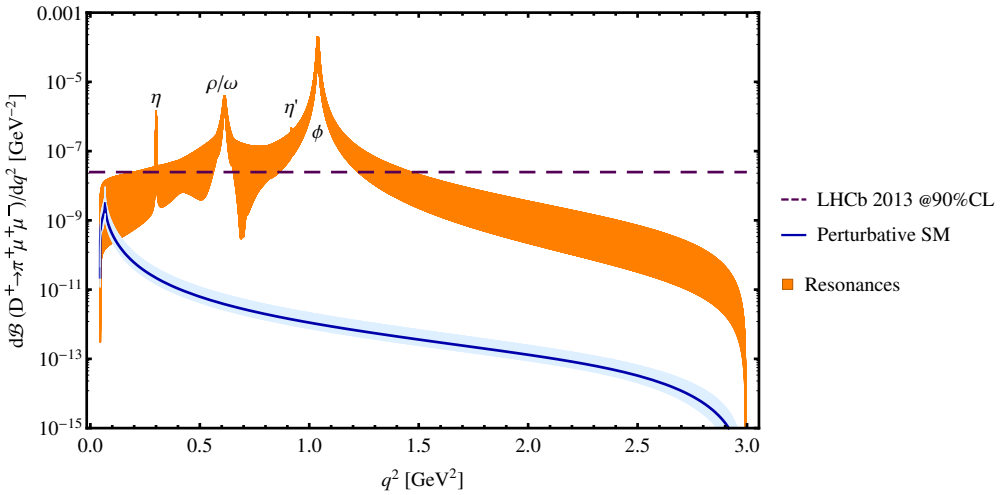

Figure 3.5.: The q^2 distribution of the branching ratio of $D^+ \to \pi^+\mu^+\mu^-$. The non-resonant 90% confidence/credibility level (CL) experimental limit, shown as a dashed purple line, is taken from [136]. The solid blue line is the perturbative contribution and the blue band shows its μ_c uncertainty, where $m_c/\sqrt{2} \leq \mu_c \leq \sqrt{2}m_c$. The orange band represents the resonances, where the phases are varied independently within $[-\pi, \pi]$.

ther information, e.g. about the phases. Note that the resonant distribution is similar to the one in figure 4 of [136]. In principle, one can fit the experimentally data on the resonant distribution, which requires less uncertainties than what is presently available to be meaningful. Finally, note that the contribution from a decay via a resonant K^0 around $m^2_{K^0} \simeq 0.25\,\mathrm{GeV}^2$, induced by charged currents, is barely visible as its branching ratio $\sim \mathcal{O}(10^{-10})$ [21] . A decay via a resonant π^0 to muons is forbidden since no phase space is available.

In view of the experimentally defined ranges we give the perturbative contributions to the branching ratios for FCNC induced $D_{(s)} \to (\pi, \eta^{(\prime)}, K)ll$ decays integrated on the full, low and high q^2 ranges in table 3.3. For the full q^2 range we only deal with muons in the final state, due to the same reasons as discussed in section 3.1.2. For $D \to \eta'$ decays the high q^2 range is not available because no phase space is left. Reminding that the scale μ_c induces the dominant uncertainty we ignore other uncertainties, but the ones from the normalization and from the form factors, which provide additional sources of uncertainties. We observe that μ_c yields still the largest uncertainty, i.e. a factor $\sim 1/2$ to ~ 2. Compared to [1] it is reduced due to the inclusion of the two loop matrix elements. In principle, one can choose the decay $D \to Pl\nu$, see e.g. [137] for its distribution, for the normalization to reduce parametric uncertainties. The parametric uncertainties are, nevertheless, small. The predictions for decays into electrons are significantly below the

experimental limits $\mathcal{B}(D^0 \to \pi^0 e^+ e^-) < 4.5 \times 10^{-5}$, $\mathcal{B}(D^0 \to \eta e^+ e^-) < 1.1 \times 10^{-4}$ and $\mathcal{B}(D_s^+ \to K^+ e^+ e^-) < 3.7 \times 10^{-6}$ [136]. For $D^+ \to \pi^+ e^+ e^-$ the BESIII collaboration [138] (preliminary) found the improved upper limit $\mathcal{B}(D^+ \to \pi^+ e^+ e^-) < 0.3 \times 10^{-6}$.

mode	$\mathcal{B}$	norm	μ_c	form factors	exp. limit
$D^+ \to \pi^+ \mu^+ \mu^-$	8.2×10^{-11}	$\pm 1\%$	$^{+121}_{-45}\%$	$\pm 5\%$	7.3×10^{-8}
$D^0 \to \pi^0 \mu^+ \mu^-$	1.6×10^{-11}	$\pm 1\%$	$^{+121}_{-45}\%$	$\pm 5\%$	1.8×10^{-4}
$D^0 \to \eta \mu^+ \mu^-$	4.0×10^{-12}	$\pm 1\%$	$^{+120}_{-45}\%$	$^{+5}_{-4}\%$	5.3×10^{-4}
$D^0 \to \eta' \mu^+ \mu^-$	3.7×10^{-12}	$\pm 1\%$	$^{+122}_{-46}\%$	$^{+5}_{-4}\%$	–
$D_s \to K^+ \mu^+ \mu^-$	3.8×10^{-11}	$\pm 2\%$	$^{+121}_{-45}\%$	$\pm 5\%$	2.1×10^{-5}

mode	$\mathcal{B}\|_{(\text{low } q^2)}$	norm	μ_c	form factors	exp. limit
$D^+ \to \pi^+ \mu^+ \mu^-$	6.1×10^{-11}	$\pm 1\%$	$^{+117}_{-41}\%$	$^{+5}_{-4}\%$	2.0×10^{-8}
$D^+ \to \pi^+ e^+ e^-$	7.2×10^{-11}	$\pm 1\%$	$^{+118}_{-41}\%$	$^{+5}_{-4}\%$	–
$D^0 \to \pi^0 \mu^+ \mu^-$	1.2×10^{-11}	$\pm 1\%$	$^{+117}_{-41}\%$	$^{+5}_{-4}\%$	–
$D^0 \to \pi^0 e^+ e^-$	1.4×10^{-11}	$\pm 1\%$	$^{+118}_{-41}\%$	$^{+5}_{-4}\%$	–
$D^0 \to \eta \mu^+ \mu^-$	3.0×10^{-12}	$\pm 1\%$	$^{+118}_{-41}\%$	$^{+5}_{-4}\%$	–
$D^0 \to \eta e^+ e^-$	3.5×10^{-12}	$\pm 1\%$	$^{+118}_{-41}\%$	$^{+5}_{-4}\%$	–
$D^0 \to \eta' \mu^+ \mu^-$	2.9×10^{-12}	$\pm 1\%$	$^{+118}_{-41}\%$	$^{+5}_{-4}\%$	–
$D^0 \to \eta' e^+ e^-$	3.4×10^{-12}	$\pm 1\%$	$^{+119}_{-42}\%$	$^{+5}_{-4}\%$	–
$D_s \to K^+ \mu^+ \mu^-$	2.8×10^{-11}	$\pm 2\%$	$^{+117}_{-41}\%$	$^{+5}_{-4}\%$	–
$D_s \to K^+ e^+ e^-$	3.3×10^{-11}	$\pm 2\%$	$^{+118}_{-41}\%$	$^{+5}_{-4}\%$	–

mode	$\mathcal{B}\|_{(\text{high } q^2)}$	norm	μ_c	form factors	exp. limit
$D^+ \to \pi^+ l^+ l^-$	1.4×10^{-13}	$\pm 1\%$	$^{+93}_{-33}\%$	$^{+28}_{-19}\%$	2.6×10^{-8}
$D^0 \to \pi^0 l^+ l^-$	2.6×10^{-14}	$\pm 1\%$	$^{+91}_{-34}\%$	$^{+26}_{-19}\%$	–
$D^0 \to \eta l^+ l^-$	1.3×10^{-16}	$\pm 1\%$	$^{+92}_{-33}\%$	$^{+24}_{-18}\%$	–
$D_s \to K^+ l^+ l^-$	2.0×10^{-14}	$\pm 2\%$	$^{+97}_{-35}\%$	$^{+25}_{-19}\%$	–

Table 3.3.: Branching ratios of $D \to Pll$ decays for the perturbative contribution in the SM, integrated on the ranges $\sqrt{q^2} \geq 2m_\mu$, $\sqrt{q^2} \in [0.250, 0.525]\,\text{GeV}$, and $\sqrt{q^2} \geq 1.25\,\text{GeV}$, where the latter two are labeled "low q^2" and "high q^2", respectively. We normalize to the total width and vary $m_c/\sqrt{2} \leq \mu_c \leq \sqrt{2}m_c$, and the form factors according to the uncertainties obtained in section 3.2.1. The experimental limits for the non-resonant branching ratios at 90% CL are taken from [21], and the LHCb collaboration [136] for $D^+ \to \pi^+\mu^+\mu^-$.

In table 3.3 we provide additional predictions for $P = \eta^{(\prime)}$ with respect to [1]. The modes $D^0 \to \eta^{(\prime)}ll$ are actually not independent as η and η' mix electromagnetically. However, experiments show that $\eta \simeq \eta_8$ and $\eta' \simeq \eta_1$ [21]. Here, the form factors are multiplied with $1/\sqrt{6}$ and $1/\sqrt{3}$ for the flavor octet η_8 and the flavor singlet η_1, respectively, to account for the isospin factors. The smallest branching ratio is predicted for the decay $D^0 \to \eta'\mu^+\mu^-$ due to a reduced phase space. This, on the other hand, restricts resonant decays. In particular a decay via an on-shell ϕ is forbidden. Only the decay $D^0 \to \eta\eta'$ is measured so far, and experimental information on resonant decays via ρ and ω are missing. Nevertheless, it may constitute an interesting mode for future studies.

The experimental sensitivity for the LHCb is extrapolated in [139]: The branching ratios of $D^+ \to \pi^+\mu^+\mu^-$ will be probed down to $\mathcal{O}(10^{-9})$. This will allow to probe resonances, the very low q^2 and high q^2 ranges, see figure 3.5.

The branching ratios found in the literature reveal a discrepancy analogue to one discussed for inclusive decays in section 3.1.2. Again, we agree with the calculations performed in [110], which updates their previous work [70]. We disagree with the latter reference, where the sum of branching ratios of the exclusive modes is larger than the one from the inclusive decays. We further disagree with the calculation of [60] as discussed around eq. (2.22).

However, the SM predictions for the branching ratios are dominated by resonances, which are accompanied with large uncertainties, including inherent modeling uncertainties. In the following, we study designed observables, which reduce the SM contribution, thus its uncertainties, to enhance the predictive power. Definitions and expressions are given in appendix C.2.

The CP asymmetry is small in the SM given the perturbative contribution. For the decay $D^+ \to \phi\pi^+$ no evidence for CP violation is found [140]. As the decay of a ϕ into a lepton pair is of electromagnetic nature, we conclude that the resonant CP asymmetry is not sizable. Nevertheless, the combination of perturbative and resonant contributions may catalyze the CP asymmetries [126], see appendix C.2 for the relevant expressions. The crucial observation is that resonances allow to evade the otherwise strong GIM mechanism. In particular, this effect may be sizable on the ϕ resonance as shown in figure 3.6. There, we included the ρ and ϕ resonances with unknown strong phases. Effects due to additional resonances are negligible. Normalizing the resonant catalyzed

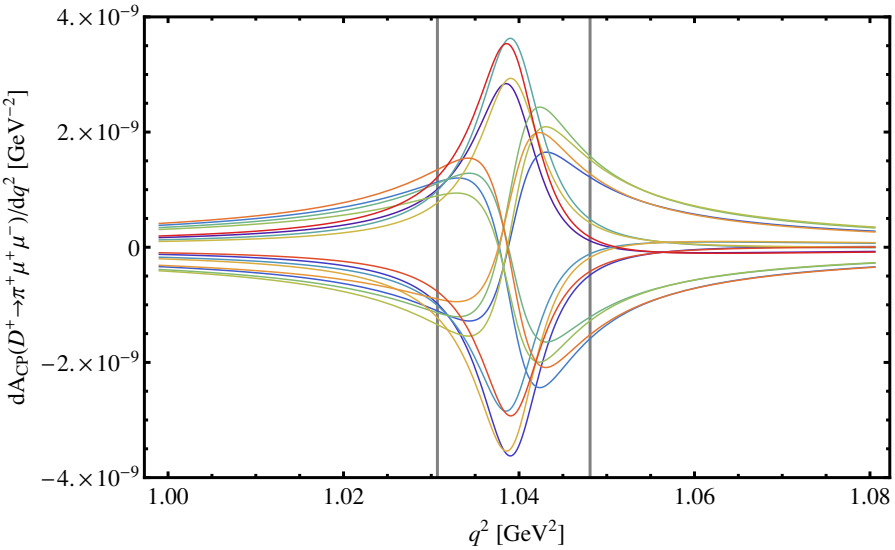

Figure 3.6.: Resonance catalyzed CP asymmetry $\mathrm{d}A_{CP}/\mathrm{d}q^2$ of $D^+ \to \pi^+\phi(\to \mu^+\mu^-)$ in the SM close to the ϕ resonance. We vary the strong phases $\delta_{\phi,\rho} \in \{0, \pi/2, 3\pi/2, \pi\}$, independently, shown by different colors. The vertical lines indicate $(m_\phi \pm \Gamma_\phi)^2$.

CP asymmetry to $\int_{(2m_\mu)^2}^{(m_D-m_\pi)^2} \mathrm{d}q^2(\mathrm{d}\mathcal{B}_{D^+\to P^+ll}/\mathrm{d}q^2 + \mathrm{d}\mathcal{B}_{D^-\to P^-ll}/\mathrm{d}q^2)$ yields less than 5×10^{-3} for any q^2. The CP asymmetry remains small in the SM due to small phases of the CKM factors.

The lepton forward-backward asymmetry, see eq. (C.54), is zero in the SM. This is also true for resonant decays including pseudoscalar resonances. Technically, the forward-backward asymmetry singles out odd powers of $\cos\theta$. Higher orders in $\cos\theta$ which allow for a non-zero forward-backward asymmetry, are estimated to be subleading: Firstly, operators of dimension larger than six are suppressed by powers of external momenta or masses with respect to the EW scale. Secondly, electromagnetic effects, e.g. the two photon diagram $\sim p_D \cdot (p_+ - p_-) \sim u$ [141, 142], are suppressed by $\alpha_e/(4\pi)$.

Combining the forward-backward asymmetry and the CP asymmetry results in the lepton forward-backward CP asymmetry, see eq. (C.55). It is zero in the SM as the forward-backward asymmetry is zero itself. If the latter would not be zero, the forward-backward CP asymmetry would still vanish in limit of CP symmetric Wilson coefficients.

The flat term is basically vanishing in the limit $m_l \to 0$. The only non-vanishing contribution arises from the pseudoscalar resonances, see eq. (C.57). The total widths of $\eta^{(\prime)}$ are small, thus the pseudoscalar resonances can be cut. An integration of both, the numerator and denominator, i.e. the decay rate, over $\sqrt{q^2} \geq 1.25\,\mathrm{GeV}$ yields a SM contribution < 0.001.

At the kinematical endpoint $q^2_{\rm max} = (m_D - m_P)^2$ the branching ratio, the flat term and the forward-backward asymmetry are predicted to be 1/2, 1 and 0, respectively [143]. This follows from the distributions given in appendix C.2 with $\lambda(m_D^2, m_P^2, q^2_{\rm max}) = 0$. The endpoint relations can be broken by (pseudo-)scalar operators. Note that the effects of the narrow pseudoscalar resonances $\eta^{(\prime)}$ are negligible at high q^2.

Finally, we comment on observables that may become interesting for future analyses. The observable $(\Gamma(D^+ \to \pi^+ l^+ l^-) - \frac{|V_{cd}|^2}{|V_{cs}|^2}\frac{m^5_{D^+}}{m^5_{D_s}}\Gamma(D_s^+ \to \pi^+ l^+ l^-))$ is less sensitive to WA. The current experimental limit on the WA induced mode is $\mathcal{B}(D_s \to \pi^+\mu^+\mu^-) < 4.1 \times 10^{-7}$ at CL=90% [21], leaving the WA reduced observable for future studies.

From table 3.3 the lepton flavor ratio is determined to be approximately one at high q^2. The lepton flavor ratio probes C_{10} for LFU couplings, see eq. (C.58). A possible breaking of LFU would be basically due to the SM operators [144]. Resonant decays preserve LFU as they couple electromagnetically, which is consistent with measurements [21]. A non-conservation of LFU implies lepton flavor violation (LFV) [145] if the family number is not conserved [144]. However, a test of LFU requires to increase measurements with electrons in the final state by a few orders of magnitude, which is beyond current experiments.

3.3. The decay $D \to V\gamma$

The $D \to V$ form factors are deferred to appendix D. For the exclusive decay of a pseudoscalar D meson into a vector V meson and a lepton pair only the form factors $T = T_1(0) = T_2(0)$, $V(0)$ and $A_1(q^2)$ are needed. Following appendix D we use

$$\begin{aligned} T &= 0.7(1 \pm 0.20)\,, \quad V(0) = 0.9(1 \pm 0.25)\,, && (D \to (\rho, \omega)\gamma) \\ T &= 0.7(1 \pm 0.25)\,, \quad V(0) = 0.9(1 \pm 0.30)\,, && (D_s \to K^*\gamma) \end{aligned} \tag{3.37}$$

and

$$\begin{aligned} A_1^{(c\to u)}(q^2) &= \frac{0.6}{1 - 0.5\, q^2/m_D^2}(1 \pm 0.15)\,, \\ A_1^{(D\to K^*, D_s\to\phi)}(q^2) &= \frac{0.6}{1 - 0.5\, q^2/m_D^2}(1 \pm 0.15)\,, \end{aligned} \tag{3.38}$$

which are multiplied by $1/\sqrt{2}$ for $D^0 \to (\rho^0, \omega)\gamma$ decays due to isospin. The form factors $V(0)$ and $A_1(q^2)$ only enter the resonant model, described in the following.

We include resonances as modeled in [146, 147], see appendix E. This model is a hybrid of factorization, heavy quark effective theory and chiral theory. Relating the intrinsic parameters to measured ones includes implicitly a breaking of $SU(3)$ flavor symmetry. For the predictions made we vary the parameters within their uncertainties.

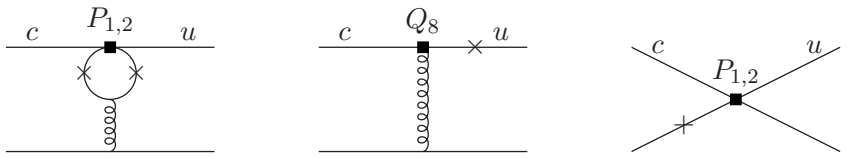

Figure 3.7.: The leading HSI (first and second) and WA (third) corrections to $c \to u\gamma$ transitions. The crosses and boxes indicate the emission of a photon and operator insertions, respectively.

In particular, the unknown strong phases give the largest uncertainties, followed by the ones of the coefficients $a_{1,2}$.

Despite its smaller number of observables, radiative decays provide a complementary phenomenology, see section 3.3.2, to rare semileptonic decays analyzed in the previous section. In particular, the only observed decay involving charm FCNC transitions is $D^0 \to \rho^0\gamma$, for which the branching ratio and the CP asymmetry are measured. Furthermore, the predictability of the SM contribution to these observables is enhanced as mode dependent corrections to the SM Wilson coefficients can be included, see the next section. Additionally to rare charm decays, we consider WA modes.

3.3.1. Perturbative and non-perturbative corrections

The total width for $D \to V\gamma$ decays can be written as [148]

$$\Gamma = \frac{m_D^3}{32\pi}\left(1 - \frac{m_V^2}{m_D^2}\right)^3 \left(|A_{\rm PC}|^2 + |A_{\rm PV}|^2\right) , \tag{3.39}$$

where the parity conserving (PC) and parity violating (PV) amplitudes read

$$A_{\rm PC/PV} = \frac{\sqrt{\alpha_e 4\pi} G_F m_c}{2\sqrt{2}\pi^2}(A_7 \pm A_7')T\,. \tag{3.40}$$

Here the coefficients $A_7^{(\prime)} = C_7^{(\prime)} + ...$ include the SM Wilson coefficients and the ellipses indicate perturbative and non-perturbative corrections, as well as BSM contributions studied in chapter 4. Note that A_7 and A_7' do not mix in eq. (3.39). For numerical purposes $(-0.00151 - (0.00556i)_{\text{CP-even}} + (0.00005i)_{\text{CP-odd}}) \leq C_7 \leq (-0.00088 - (0.00327i)_{\text{CP-even}} + (0.00002i)_{\text{CP-odd}})$, varying $m_c/\sqrt{2} \leq \mu_c \leq \sqrt{2}m_c$ and the CP phases are decomposed. In the next section we consider corrections from HSIs and WA, shown in figure 3.7. Diagrams, which are not shown, are additionally power suppressed.

Hard spectator interactions and weak annihilation

The expressions for the HSI diagrams within QCD factorization can be adopted from b physics [149] (and [134, 150, 151]). We follow [149] to obtain the leading corrections, at $\mathcal{O}(\alpha_s^1(\frac{\Lambda_{\rm QCD}}{m_c})^0)$,

$$C_7^{\rm HSI} = \frac{\alpha_s(\mu_h)}{4\pi}\left(\sum_{q\in\{d,s\}} V_{cq}^* V_{uq}\left(-\frac{1}{6}C_1(\mu_h) + C_2(\mu_h)\right) H_1^{(q)} + C_8(\mu_h) H_8\right), \quad (3.41)$$

where the hard scale $\mu_h \sim \sqrt{\Lambda_{\rm QCD} m_c}$. Here $C_{1,2,8}$ are taken at leading order due to additional non-factorisable diagrams at higher orders. Furthermore, taking into account the charge ratios,

$$\begin{aligned} H_1^{(q)} &= \frac{4\pi^2 f_D f_V^\perp}{27 T m_D \lambda_D}\int_0^1 \mathrm{d}v\, h_V^{(q)}(\bar v)\,\Phi_{V\perp}(v)\,, \\ h_V^{(q)} &= \frac{4m_q^2}{m_c^2 \bar v^2}\Bigg(\mathrm{Li}_2\left[\frac{2}{1-\sqrt{(\bar v - 4m_q^2/m_c^2 + i\epsilon])/\bar v}}\right] \\ &\quad + \mathrm{Li}_2\left[\frac{2}{1+\sqrt{(\bar v - 4m_q^2/m_c^2 + i\epsilon])/\bar v}}\right]\Bigg) - \frac{2}{\bar v}\,, \quad (3.42) \\ H_8 &= -\frac{32\pi^2 f_D f_V^\perp}{27 T m_D \lambda_D}\int_0^1 \mathrm{d}v \frac{\Phi_{V\perp}(v)}{v}\,, \quad (3.43) \end{aligned}$$

where $\bar v = 1 - v$, and the dilogarithm Li_2 is given by eq. (2.21). We use $m_d = 0$. The (transverse) decay constants $f_i^{(\perp)}$ are given in appendix A. The transverse distribution at leading twist can be expressed to first order in Gegenbauer polynomials as

$$\Phi_{V\perp} = 6v\bar v\left(1 + a_1^{V\perp} 3(v-\bar v) + a_2^{V\perp}\frac{3}{2}\left(5(v-\bar v)^2 - 1\right)\right), \quad (3.44)$$

For $D_{(s)} \to (\rho, \omega, K^{*+})\gamma$ decays we use the Gegenbauer moments [152] (and references therein)

$$\begin{aligned} a_1^{\rho\perp} &= 0\,, & a_2^{\rho\perp} &= 0.14 \pm 0.06\,, \\ a_1^{\omega\perp} &= 0\,, & a_2^{\omega\perp} &= 0.14 \pm 0.12\,, \\ a_1^{K^*\perp} &= -0.04 \pm 0.03\,, & a_2^{K^*\perp} &= 0.10 \pm 0.08 \end{aligned} \quad (3.45)$$

at $\mu = 1\,\mathrm{GeV}$, where the sign of $a_1^{K^*\perp}$ is fixed by $K^{*+} = (u\bar s)$ [153]. Here we neglect isospin breaking in the ρ. The running of the Gegenbauer moments can be found in, e.g., [150].

The parameter λ_D is defined as

$$\frac{m_D}{\lambda_D} = \int_0^1 \mathrm{d}\xi \frac{\Phi_D(\xi)}{\xi}\,, \tag{3.46}$$

that is the first negative moment of the leading twist distribution Φ of the light-cone momentum fraction ξ of the spectator quark within the D meson. In b physics, the first negative moment of the B meson light-cone distribution amplitude is measured as $\lambda_B^{\mathrm{HQET}} > 0.172\,\mathrm{GeV}$ at 90% CL [154], a positive light-cone wave function yields $\lambda_B^{\mathrm{HQET}} \leq 4/3\,\bar{\Lambda}$ [155], and by means of light-cone sum rules $\lambda_B^{\mathrm{QCD}} \lesssim \bar{\Lambda}$ [156, 157]. Here $\bar{\Lambda} = (m_B - m_b) + \mathcal{O}(\Lambda^2_{\mathrm{QCD}}/m_b)$, and $\lambda_B^{\mathrm{HQET}} > \lambda_B^{\mathrm{QCD}}$ at one loop QCD [158]. In the heavy quark limit $\lambda_D^{\mathrm{HQET}} \sim \lambda_B^{\mathrm{HQET}}$. We use $\lambda_D \sim \Lambda_{\mathrm{QCD}} \sim \mathcal{O}(0.1\,\mathrm{GeV})$.

Taking $\mu_h = 1\,\mathrm{GeV}$ for simplicity, varying the Gegenbauer moments, and decay constants one obtains

$$\begin{aligned}
C_7^{\mathrm{HSI},\rho} &\in [0.00051 + 0.0014i, 0.00091 + 0.0020i] \times \frac{\mathrm{GeV}}{\lambda_D}\,,\\
C_7^{\mathrm{HSI},\omega} &\in [0.00030 + 0.0010i, 0.00098 + 0.0020i] \times \frac{\mathrm{GeV}}{\lambda_D}\,,\\
C_7^{\mathrm{HSI},K^{*+}} &\in [0.00032 + 0.0013i, 0.00096 + 0.0022i] \times \frac{\mathrm{GeV}}{\lambda_D}\,.
\end{aligned} \tag{3.47}$$

We do not vary the form factor since it cancels in the amplitude. Chromomagnetic contributions will be discussed more generally in section 3.3.1. Contributions due to additional operators, which are subleading, can be adopted from [159].

The WA contribution is a power correction. Following [149, 160], we obtain the leading contribution, at $\mathcal{O}(\alpha_s^0(\frac{\Lambda_{\mathrm{QCD}}}{m_c})^1)$, for $D^0 \to (\rho^0, \omega)\gamma$, $D^+ \to \rho^+\gamma$ and $D_s \to K^{*+}\gamma$ decays

$$\begin{aligned}
C_7^{\mathrm{WA},\rho^0} &= -\frac{2\pi^2 q_u f_D f_{\rho^0}^{(d)} m_\rho}{T m_{D^0} m_c \lambda_D} V_{cd}^* V_{ud} \left(\frac{4}{9}C_1 + \frac{1}{3}C_2\right)\,,\\
C_7^{\mathrm{WA},\omega} &= \frac{2\pi^2 q_u f_D f_\omega^{(d)} m_\omega}{T m_{D^0} m_c \lambda_D} V_{cd}^* V_{ud} \left(\frac{4}{9}C_1 + \frac{1}{3}C_2\right)\,,\\
C_7^{\mathrm{WA},\rho^+} &= \frac{2\pi^2 q_d f_D f_\rho m_\rho}{T m_{D^+} m_c \lambda_D} V_{cd}^* V_{ud}\, C_2\,,\\
C_7^{\mathrm{WA},K^{*+}} &= \frac{2\pi^2 q_d f_{D_s} f_{K^*} m_{K^*}}{T m_{D_s} m_c \lambda_D} V_{cs}^* V_{us}\, C_2\,.
\end{aligned} \tag{3.48}$$

Again, $C_{1,2}$ is taken at leading order, $q_u = 2/3$ and $q_d = -1/3$ are the up-type and down-type quark charges, respectively, in units of the proton charge. The isospin factor of T is canceled by the one of $f_V^{(d)}$, which is the contribution from d quarks to the form factor, and given in appendix A. We neglect WA contributions due to QCD penguin

operators as they are additionally GIM suppressed as well as further subleading terms, which are calculated in b physics [159, 160]. These include non-local corrections, which are shown to be additionally power suppressed by means of QCD sum rules in b physics [159]. The overall sign for ρ^0 follows from isospin. It is due the relative sign of the d quarks generated via WA and the u quarks in $\langle Q_7 \rangle$.

Varying the decay constants and $\mu_c \in [m_c/\sqrt{2}, \sqrt{2} m_c]$ one obtains

$$\begin{aligned} C_7^{\mathrm{WA},\rho^0} &\in [-0.010, -0.0011] \times \frac{\mathrm{GeV}}{\lambda_D}\,, \\ C_7^{\mathrm{WA},\omega} &\in [0.0097, 0.0011] \times \frac{\mathrm{GeV}}{\lambda_D}\,, \\ C_7^{\mathrm{WA},\rho^+} &\in [0.029, 0.038] \times \frac{\mathrm{GeV}}{\lambda_D}\,, \\ C_7^{\mathrm{WA},K^{*+}} &\in [-0.034, -0.047] \times \frac{\mathrm{GeV}}{\lambda_D}\,. \end{aligned} \tag{3.49}$$

Note that WA contributions to the neutral modes is subject to large uncertainties stemming from the color suppressed combination of Wilson coefficients.

We add that one can calculate non-factorisable power corrections, which also induce A_7', by means of light-cone sum rules, as done in b physics [153]. However, α_s corrections vanish at leading twist in the limit of massless quarks in the V meson [161]. Corrections to A_7', as well as to A_7, are additionally power suppressed. Nevertheless, effects due to $c \to u\gamma g$ transitions via a soft gluon coupling to the Q_2 induced quark loop and the V meson can be estimated following [162] as

$$C_7'^{(c\to u\gamma g)} \sim \frac{1}{3} C_2 \left(V_{cd}^* V_{ud}\, f^{(c\to u\gamma g)}(m_d^2/m_c^2) + V_{cs}^* V_{us}\, f^{(c\to u\gamma g)}(m_s^2/m_c^2) \right) \frac{\Lambda_{\mathrm{QCD}}}{m_c}\,. \tag{3.50}$$

This contribution is $\sim \mathcal{O}(10^{-4})$ if the expansion coefficients of $f^{(c\to u\gamma g)}$ in m_q^2/m_c^2 are of order one. Effects from Q_1 and QCD penguin operators induced quark loops are further color suppressed and additionally GIM suppressed, respectively. In principle, one can calculate $f^{(c\to u\gamma g)}$ by means of light-cone sum rules, as done in b physics in [153].

We conclude that $|C_7^{\mathrm{WA},V^+}| > |C_7^{\mathrm{WA},V^0}| \gtrsim |C_7^{\mathrm{HSI}}| > |C_7|$. Hence, form factors are irrelevant in the SM, but may become important in BSM models. The SM uncertainties are driven by μ_c and λ_D. Due to the absence of further calculations, we take $|A'_{7,\mathrm{SM}}/A_{7,\mathrm{SM}}| \lesssim 0.2$ for simplicity, where weak phases follow from CKM factors, that is $A'_{7,\mathrm{SM}} = A'_{7,\mathrm{SM}}(V_{cd}^* V_{ud}, V_{cs}^* V_{us})$.

Chromomagnetic effects

In the SM chromomagnetic effects are GIM suppressed $\sim \mathcal{O}(10^{-5})$, which renders the impact from $\langle Q_8^{(\prime)} \rangle$ small. However, $\langle Q_8^{(\prime)} \rangle$ effects may become relevant in BSM scenarios.

From eq. (3.41) the $\langle Q_8^{(\prime)} \rangle$ HSI contributions follow as

$$\begin{aligned}
C_7^{(\prime)\mathrm{HSI},\rho}\big|_{\langle Q_8^{(\prime)}\rangle} &\in -\frac{\mathrm{GeV}}{\lambda_D} \times [0.031, 0.042] \times C_8^{(\prime)}\,, \\
C_7^{(\prime)\mathrm{HSI},\omega}\big|_{\langle Q_8^{(\prime)}\rangle} &\in -\frac{\mathrm{GeV}}{\lambda_D} \times [0.024, 0.040] \times C_8^{(\prime)}\,, \\
C_7^{(\prime)\mathrm{HSI},K^{*+}}\big|_{\langle Q_8^{(\prime)}\rangle} &\in -\frac{\mathrm{GeV}}{\lambda_D} \times [0.031, 0.039] \times C_8^{(\prime)}\,.
\end{aligned} \tag{3.51}$$

Independently, from light cone sum rules (LCSR) the $\langle Q_8^{(\prime)} \rangle$ gluon spectator interaction (GSI) contributions [152] (and [163]) are obtained as

$$\begin{aligned}
C_7^{(\prime)\mathrm{GSI},\rho^0} &\in -[0.068 + 0.048i, 0.14 + 0.10i] \times C_8^{(\prime)}\,, \\
C_7^{(\prime)\mathrm{GSI},\omega} &\in -[0.018 - 0.024i, 0.036 - 0.048i] \times C_8^{(\prime)}\,, \\
C_7^{(\prime)\mathrm{GSI},\rho^+} &\in -[0.057 + 0.040i, 0.12 + 0.083i] \times C_8^{(\prime)}\,, \\
C_7^{(\prime)\mathrm{GSI},K^{*+}} &\in -[0.017 - 0.020i, 0.034 - 0.040i] \times C_8^{(\prime)}\,.
\end{aligned} \tag{3.52}$$

The LCSR calculation extends the calculation by means of QCD factorization. Note that the latter actually breaks down at subleading power for $\langle Q_8^{(\prime)} \rangle$ HSIs due to a logarithmic singularity for a soft spectator quark [159]. Nevertheless, eqs. (3.52) and (3.51) are similar for $\lambda_D \sim \mathcal{O}(0.1\,\mathrm{GeV})$, yet they may come with different real and imaginary parts.

Furthermore, a similar contribution, as obtained from the perturbative matrix element, is

$$C_7^{(\prime)}\big|_{\langle Q_8^{(\prime)}\rangle} \simeq (-0.12 - 0.17i) C_8^{(\prime)}\,. \tag{3.53}$$

We conclude that chromomagnetic effects contribute as $C_7^{(\prime)}\big|_{\langle Q_8^{(\prime)}\rangle} \sim (-0.1 - 0.1i) C_8^{(\prime)}$, which is negligible in the SM.

Weak annihilation modes

Extending section 3.3.1 we calculate the WA contributions to WA modes in this section. They are not induced due to HSI nor by FCNC transitions, hence BSM effects are negligible. Hence, WA modes probe the SM and the employed theoretical frameworks.

We obtain the coefficients for the WA modes $D^0 \to (\phi, \bar{K}^{*0}, K^{*0})\gamma$, $D^+ \to K^{*+}\gamma$ and $D_s \to \rho^+\gamma$ as

$$\begin{aligned}
C_7^{D^0\to\phi\gamma} &= \frac{2\pi^2 q_u f_D f_\phi m_\phi}{T m_{D^0} m_c \lambda_D} V_{cs}^* V_{us} \left(\frac{4}{9} C_1^{(\bar{u}s)(\bar{s}c)} + \frac{1}{3} C_2^{(\bar{u}s)(\bar{s}c)}\right), \\
C_7^{D^0\to\bar{K}^{*0}\gamma} &= \frac{2\pi^2 q_u f_D f_{K^*} m_{K^{*0}}}{T m_{D^0} m_c \lambda_D} V_{cs}^* V_{ud} \left(\frac{4}{9} C_1^{(\bar{u}d)(\bar{s}c)} + \frac{1}{3} C_2^{(\bar{u}d)(\bar{s}c)}\right), \\
C_7^{D^0\to K^{*0}\gamma} &= \frac{V_{cd}^* V_{us}}{V_{cs}^* V_{ud}} C_7^{D^0\to\bar{K}^{*0}\gamma}, \\
C_7^{D^+\to K^{*+}\gamma} &= \frac{2\pi^2 q_d f_D f_{K^*} m_{K^{*+}}}{T m_{D^+} m_c \lambda_D} V_{cd}^* V_{us} C_2^{(\bar{u}s)(\bar{d}c)}, \\
C_7^{D_s\to\rho^+\gamma} &= \frac{2\pi^2 q_d f_{D_s} f_\rho m_\rho}{T m_{D_s} m_c \lambda_D} V_{cs}^* V_{ud} C_2^{(\bar{u}d)(\bar{s}c)}.
\end{aligned} \tag{3.54}$$

Here we indicate the operator structure, yet as QCD is flavor symmetric $C_{1,2}^{(\bar{q}_1 q_2)(\bar{q}_3 c)} = C_{1,2}^{(0)}$. Note that the form factor T is decay dependent, however, $\frac{\text{GeV}}{m_c T} \sim 1$ cancels in the amplitude. The mode $D^0 \to \phi\gamma$ actually receives a contribution from the decay $D^0 \to \rho^0\gamma$. This will be taken care of in section 3.3.2.

Varying the decay constants and $\mu_c \in [m_c/\sqrt{2}, \sqrt{2}m_c]$ one obtains

$$\begin{aligned}
C_7^{D^0\to\phi\gamma} &\in [-0.016, -0.0013] \times \frac{\text{GeV}}{\lambda_D} \frac{\text{GeV}}{m_c T}, \\
C_7^{D^0\to\bar{K}^{*0}\gamma} &\in [-0.051, -0.0044] \times \frac{\text{GeV}}{\lambda_D} \frac{\text{GeV}}{m_c T}, \\
C_7^{D^0\to K^{*0}\gamma} &\in [0.0028, 0.00023] \times \frac{\text{GeV}}{\lambda_D} \frac{\text{GeV}}{m_c T}, \\
C_7^{D^+\to K^{*+}\gamma} &\in [0.0082, 0.0070] \times \frac{\text{GeV}}{\lambda_D} \frac{\text{GeV}}{m_c T}, \\
C_7^{D_s\to\rho^+\gamma} &\in [-0.16, -0.13] \times \frac{\text{GeV}}{\lambda_D} \frac{\text{GeV}}{m_c T}.
\end{aligned} \tag{3.55}$$

3.3.2. Phenomenology

The branching ratios for $c \to u\gamma$ induced modes are given in table 3.4 for the different approaches, two loop QCD, HSI plus WA, and the resonant model, along with experimental data. For comparison, also the branching ratios from the resonant model as found in [146, 147] are provided. Furthermore, predictions from pole diagrams and the vector meson dominance mechanism [164], and QCD sum rules [165] are listed. An update of [164] is given in [166], yet their predictions differ partially by an order of magnitude from [164], thus we do not list them. Note that the sum of the two loop QCD predictions are

branching ratio	$D^0 \to \rho^0\gamma$	$D^0 \to \omega\gamma$
two loop QCD	$[0.14 - 2.0] \times 10^{-8}$	$[0.14 - 2.0] \times 10^{-8}$
HSI+WA	$[0.11 - 3.8] \times 10^{-6}$	$[0.078 - 5.2] \times 10^{-6}$
resonant	$[0.041 - 1.17] \times 10^{-5}$	$[0.042 - 1.12] \times 10^{-5}$
[146, 147]	$(0.1 - 1) \times 10^{-5}$	$(0.1 - 0.9) \times 10^{-5}$
[164]	$(0.1 - 0.5) \times 10^{-5}$	0.2×10^{-5}
[165]	3.8×10^{-6}	–
exp. data	$(1.77 \pm 0.31) \times 10^{-5}$	$< 2.4 \times 10^{-4}$
branching ratio	$D^+ \to \rho^+\gamma$	$D_s \to K^{*+}\gamma$
two loop QCD	$[0.75 - 1.0] \times 10^{-8}$	$[0.32 - 5.5] \times 10^{-8}$
HSI+WA	$[1.6 - 1.9] \times 10^{-4}$	$[1.0 - 1.4] \times 10^{-4}$
resonant	$[0.038 - 1.15] \times 10^{-4}$	$[0.98 - 8.77] \times 10^{-5}$
[146, 147]	$(0.4 - 6.3) \times 10^{-5}$	$(1.2 - 5.1) \times 10^{-5}$
[164]	$(2 - 6) \times 10^{-5}$	$(0.8 - 3) \times 10^{-5}$
[165]	4.6×10^{-6}	–
exp. data	–	–

Table 3.4.: Branching ratios of $D \to V\gamma$ decays in the SM. We normalize to the total width and vary the form factors, decay constants, widths, Gegenbauer moments, relative strong phases and $\mu_c \in [m_c/\sqrt{2}, \sqrt{2}m_c]$. The branching ratios from HSI plus WA scale as $(0.1\,\text{GeV}/\lambda_D)^2$. The experimental data at CL=90% are from [24], where we add uncertainties in quadrature, and from [21]. The branching ratios from [165] are given without uncertainties and are obtained by taking $a_1 = 1.3$ and $a_2 = -0.55$ [167].

below, yet close to the inclusive branching ratios of table 3.1. However, corrections to the two loop QCD calculation are dominant. The branching ratios from HSI plus WA are smaller than/similar to the resonant branching ratios for neutral/charged $c \to u\gamma$ modes. The resonant branching ratios cover the ranges found in [146, 147, 164, 165]. Note that the hierarchies of various amplitudes are dominated by CKM factors and color counting, which is taken care of in both approaches. Nonetheless, SM predictions are slightly to low to explain the measured $D^0 \to \rho^0\gamma$ branching ratio. Only for $\lambda_D < 0.1\,\text{GeV}$ in the QCD based approach the SM prediction can be sufficiently large, which indicates sizable $\frac{\Lambda_{\text{QCD}}}{m_c}$ and/or α_s corrections.

The predictions are compiled in figure 3.8, where the branching ratios of $D \to \rho\gamma$ as a function of λ_D are shown. A measurement of the $D^+ \to \rho^+\gamma$ branching ratio would allow to constrain λ_D. The contributions from the QCD based approach to the decay $D^0 \to \rho^0\gamma$ are subject to large uncertainties due to possible cancellations.

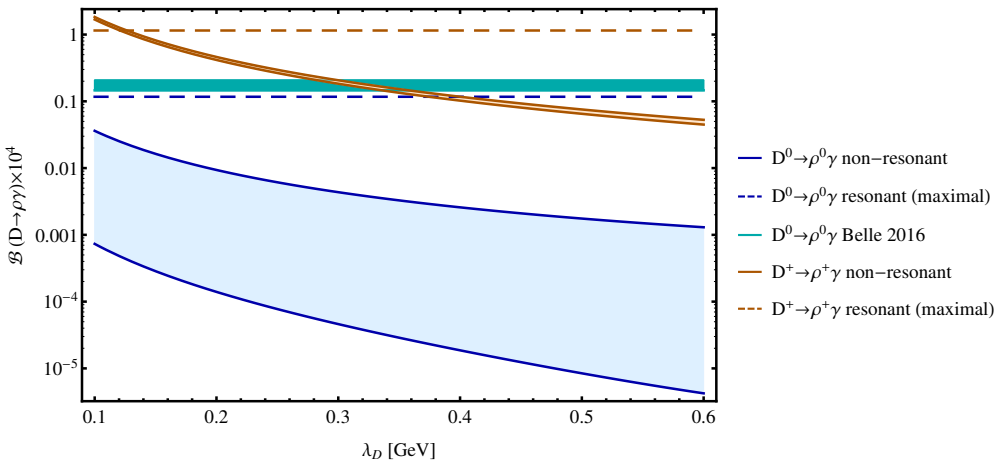

Figure 3.8.: Branching ratios of $D \to \rho\gamma$ decays as a function of λ_D. The blue and orange curves are for $D^0 \to \rho^0\gamma$ and $D^+ \to \rho^+\gamma$, respectively. The dashed lines show the maximal predictions as obtained from the resonant model. The solid filled curves are the non-resonant predictions, from two loop QCD and HSI plus WA. The experimental data from [24] are depicted as a cyan band. We vary the form factors, decay constants, widths, Gegenbauer moments, relative strong phases and $\mu_c \in [m_c/\sqrt{2}, \sqrt{2}m_c]$.

The uncertainties in the QCD based approach for $D^0 \to \rho^0\gamma$ and $D^+ \to \rho^+\gamma$ decays are anticorrelated implying large isospin violation. One obtains $\mathcal{B}_{D^+\to\rho^+\gamma} \simeq [44, 2900] \times \mathcal{B}_{D^0\to\rho^0\gamma}$, which is relaxed in the resonant model, giving $\mathcal{B}_{D^+\to\rho^+\gamma} \simeq [0.3, 280] \times \mathcal{B}_{D^0\to\rho^0\gamma}$. Note that isospin is already broken by the lifetimes $\tau(D^0)/\tau(D^+) \simeq 0.4$.

In addition to the branching ratio of $D^0 \to \rho^0\gamma$ its CP asymmetry is measured as [24]

$$A_{CP} = 0.056 \pm 0.152 \pm 0.006\,. \tag{3.56}$$

The CP asymmetry is mostly direct, analogous to the time-integrated CP asymmetry in $D^0 \to K^+K^-$ [168], thus we neglect the small indirect contribution [3].

The CP asymmetry along with the branching ratio is shown in figure 3.9. One sees that in the QCD based approach $|A_{CP}| \lesssim 2 \times 10^{-2}$ if $\mathcal{B} \gtrsim 10^{-9}$, and $|A_{CP}| \lesssim 2 \times 10^{-3}$, if $\mathcal{B} \gtrsim 10^{-6}$. The latter case is closer to the data for the branching ratio and can be obtained for, e.g., $\lambda_D \lesssim 0.3$. Sizable CP asymmetries are only possible for small branching ratios due to cancellations. In the resonant model one obtains $A_{CP} \lesssim 10^{-3}$, which vanishes in the $SU(3)$ flavor limit.

The CP asymmetry for $D^0 \to \omega\gamma$ is similar to the A_{CP} of $D^0 \to \rho^0\gamma$. For $D^+ \to \rho^+\gamma$ and $D_s \to K^{*+}\gamma$ the CP asymmetries are $\lesssim 2 \times 10^{-3}$ within the QCD based approach, whereas CP asymmetries $\lesssim 3 \times 10^{-4}$ are predicted in the resonant model.

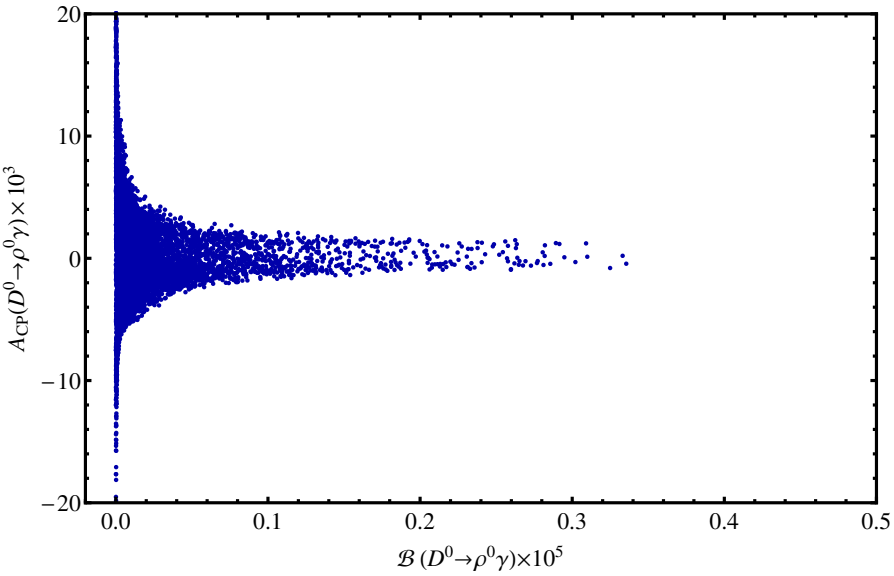

Figure 3.9.: The distributions of the CP asymmetry and the branching ratio for $D^0 \to \rho^0\gamma$ in the QCD based approach. We vary the form factor, decay constants, widths, Gegenbauer moments, relative strong phases and $\mu_c \in [m_c/\sqrt{2}, \sqrt{2}m_c]$. Furthermore, we assume $\lambda_D \in [0.1, 0.6]\,\text{GeV}$ and $|A_7'(V_{cd}^* V_{ud}, V_{cs}^* V_{us})/A_7| \lesssim 0.2$. The experimental data on the CP asymmetry and the branching ratio, respectively, do cover and are beyond the shown range.

Another observable is the photon polarization, defined as

$$P_\gamma = \frac{|A_7'|^2 - |A_7|^2}{|A_7'|^2 + |A_7|^2}\,. \tag{3.57}$$

In the QCD based approach $P_\gamma \lesssim -0.92$. Within the resonant model $|A_7'/A_7|$ cannot be predicted, hence no prediction for the photon polarization is given. One may get further information once WA in the QCD based approach is matched onto the resonant model.

Weak annihilation modes

The branching ratios of the WA modes are presented in table 3.5. Predictions from the QCD based approach and the resonant model are provided along with experimental data. For comparison, the branching ratios from the resonant model as found in [146, 147], from pole diagrams and the vector meson dominance mechanism [164], and QCD sum rules [165] are listed. They give consistent SM predictions. Again, an update of [164] is given in [166] with sizable deviations from [164], thus not listed. One observes that the branching ratios for the neutral WA modes in the resonant model are larger than the ones from the QCD based approach, similar to what was observed in the previous section for $D^0 \to \rho^0\gamma$. On the other hand this pattern is reversed for the charged WA modes. The measurements for $D^0 \to \bar{K}^{*0}\gamma$ by Belle and BaBar differ by 2.2σ, yet are in the range of the SM predictions, whereas the measurements and the SM prediction for $D^0 \to \phi\gamma$ are consistent.

Furthermore, CP asymmetries are measured as $A_{CP}(D^0 \to \phi\gamma) = -0.094 \pm 0.066$ and $A_{CP}(D^0 \to \bar{K}^{*0}\gamma) = -0.003 \pm 0.020$ [24], where uncertainties are added in quadrature. The predictions for all WA modes are zero due to a single weak phase. A slight tension thus emerges for $D^0 \to \phi\gamma$ decays. However, due to a small $(d\bar{d} + u\bar{u})$ admixture in the ϕ [21], one can approximate $A_{CP}^{(D^0\to\phi\gamma)} \sim \mathcal{O}(0.01)A_{CP}$ [3], where A_{CP} is the $D^0 \to \rho^0\gamma$ CP asymmetry. Furthermore, due to $\pi\pi \to KK$ scattering at the ϕ mass, a Breit-Wigner ansatz gives $A_{CP}^{(D^0\to\phi\gamma)} \sim \mathcal{O}(0.1)A_{CP}$. Hence, $A_{CP}^{(D^0\to\phi\gamma)} \lesssim 10^{-3}$ in the SM and the measured data on $D^0 \to \rho^0\gamma$ imply $A_{CP}^{(D^0\to\phi\gamma)} \lesssim 10^{-2}$. Thus, $A_{CP}^{(D^0\to\phi\gamma)}$ may contain information from BSM physics. Similar observation were made in [148].

We conclude that despite some discrepancies in the experimental data, they are in agreement with the calculations supporting the theoretical frameworks utilized. Furthermore, they suggest that the SM predictions are close to their upper limits. Concerning the QCD based approach sizable corrections are needed. Further information can be gained from measurements of the charges WA modes.

branching ratio	$D^0 \to \phi\gamma$	$D^0 \to \bar{K}^{*0}\gamma$	$D^0 \to K^{*0}\gamma$
WA	$[0.0074 - 1.2] \times 10^{-5}$	$[0.011 - 1.6] \times 10^{-4}$	$[0.032 - 4.4] \times 10^{-7}$
resonant	$[0.24 - 2.8] \times 10^{-5}$	$[0.26 - 4.6] \times 10^{-4}$	$[0.076 - 1.3] \times 10^{-6}$
[146, 147]	$(0.4 - 1.9) \times 10^{-5}$	$(6 - 36) \times 10^{-5}$	$(0.03 - 0.2) \times 10^{-5}$
[164]	$(0.1 - 3.4) \times 10^{-5}$	$(7 - 12) \times 10^{-5}$	0.01×10^{-5}
[165]	–	1.8×10^{-4}	–
Belle	$(2.76 \pm 0.21) \times 10^{-5}$	$(4.66 \pm 0.30) \times 10^{-4}$	–
BaBar	$(2.81 \pm 0.41) \times 10^{-5}$	$(3.31 \pm 0.34) \times 10^{-4}$	–

branching ratio	$D^+ \to K^{*+}\gamma$	$D_s \to \rho^+\gamma$
WA	$[0.73 - 1.1] \times 10^{-5}$	$[1.8 - 2.9] \times 10^{-3}$
resonant	$[0.48 - 7.6] \times 10^{-6}$	$[0.11 - 1.3] \times 10^{-3}$
[146, 147]	$(0.03 - 0.44) \times 10^{-5}$	$(20 - 80) \times 10^{-5}$
[164]	$(0.1 - 0.3) \times 10^{-5}$	$(6 - 38) \times 10^{-5}$
[165]	–	4.7×10^{-5}
Belle	–	–
BaBar	–	–

Table 3.5.: Branching ratios of WA modes in the SM. We vary the decay constants, lifetimes and $\mu_c \in [m_c/\sqrt{2}, \sqrt{2}m_c]$. The WA predictions from the QCD based approach scale as $(0.1\,\mathrm{GeV}/\lambda_D)^2$. The branching ratios from [165] are obtained by taking $a_1 = 1.3$ and $a_2 = -0.55$ [167]. The experimental data are taken from Belle [24] and BaBar [169], where we add uncertainties in quadrature and for the latter update the normalization [21].

3.4. Summary of exclusive decays

The branching ratios of $D \to Pll$ and $D \to V\gamma$ decays are dominated by non-perturbative physics. For the reference mode $D^+ \to \pi^+\mu^+\mu^-$ resonant decays are orders of magnitude above the perturbative predictions in the SM, see section 3.2.3. However, at very low q^2 they are competitive and at high q^2, above the resonances, resonant decays are an order of magnitude below the current experimental limit. In particular, angular observables and CP asymmetries are clean observables, i.e. (approximate) null tests of the SM, even when including contributions from resonant decays. Similarly, for the reference mode $D^0 \to \rho^0\gamma$ non-perturbative physics are dominating the branching ratio, see section 3.3. Again, the CP asymmetry is an approximate null test of the SM. Moreover, WA modes serve as a test for the theoretical frameworks and, indeed, show agreement for the measured modes. However, in the QCD based approach sizable perturbative/power corrections are needed. For $D^0 \to \rho^0\gamma$ the experimental data on the branching ratio is slightly above the SM predictions and the statistically driven uncertainty on the CP asymmetry is presently not indicative. Nonetheless, future measurements may reveal a gap with respect to the SM predictions, which will then be filled with BSM physics. This will be studied in the next chapter. Before proceeding, we comment on several other charm FCNC transitions in the following.

The branching ratio for the purely leptonic decay $D^0 \to ll$, eq. (C.61), receives no perturbative contribution in the SM, as C_{10} is vanishing therein. However, a non-zero branching ratio in the SM is given by off-shell photons at the loop level. It is found to be $\sim \mathcal{O}(10^{-13})$ [58, 170, 171], and experimentally constrained as $2.7 \times 10^{-5}\,\mathcal{B}(D^0 \to \gamma\gamma) < 2.3 \times 10^{-11}$ at CL=90%, where $\mathcal{B}(D^0 \to \gamma\gamma) = 8.4 \times 10^{-7}$ is taken from the measurement [172]. The current experimental limits are $\mathcal{B}(D^0 \to e^+e^-) < 7.9 \times 10^{-8}$ and $\mathcal{B}(D^0 \to \mu^+\mu^-) < 6.2 \times 10^{-9}$ at CL=90% [21]. Mixing effects of the D^0 have to be taken into account to compare experimental data with theoretical predictions, see e.g. [173] for b decays, which turn out to be negligible due to the small width difference [21]. Finally, note that the diphoton contribution may be overestimated [174].

For the decay $D^{*0} \to l^+l^-$ the SM branching ratio is $\sim 10^{-18}$ [175] due to the small lifetime. At the LHCb the decay $D^{*0} \to \pi^+\pi^-$ induces an irreducible uncertainty due to the $\pi \to \mu$ misidentification rate. We find the $D^{*0} \to \pi^+\pi^-$ total width by means of factorization via [176]

$$\begin{aligned}\Gamma_{D^{*0}\to\pi^+\pi^-} = \frac{G_F^2}{32\pi}\frac{\sqrt{(m_{D^{*0}}^2-(2m_{\pi^+})^2)^2-4m_{\pi^+}^4}^3}{m_{D^{*0}}^3}|V_{cd}^*V_{ud}||a_1(\pi^+\pi^-)|^2 f_\pi^2 \\ \times (A_0^{(D^*\to\pi)})^2(m_{\pi^+}^2)\,,\end{aligned} \tag{3.58}$$

where we fix the coefficient $|a_1(\pi^+\pi^-)|$ from

$$\mathcal{B}_{D^0\to\pi^+\pi^-} = \frac{1}{\Gamma_{D^0}}\frac{G_F^2}{32\pi}\frac{(m_{D^0}^2-m_{\pi^+}^2)^2\sqrt{(m_{D^0}^2-(2m_{\pi^+})^2)^2-4m_{\pi^+}^4}}{m_{D^0}^3}|V_{cd}^*V_{ud}||a_1(\pi^+\pi^-)|^2 \times f_\pi^2 f_0^2(m_{\pi^+}^2)\,, \tag{3.59}$$

and the measured $\mathcal{B}(D^0\to\pi^+\pi^-)\simeq 1.4\times10^{-3}$ [21]. Furthermore, we approximate the form factor $A_0^{(D^*\to\pi)}\simeq A_0^{(D\to\rho)}$, see appendix D, yielding $\mathcal{B}_{D^{*0}\to\pi^+\pi^-}\sim 5\times10^{-11}$ for $\Gamma_{D^{*0}}\simeq 6\times10^{-5}\,\text{GeV}$. We find that the background is larger than the SM prediction for the $D^{*0}\to l^+l^-$ branching ratio.

The SM contribution to the dineutrino decays $D\to P\nu_L\bar\nu_L$ is negligible [58], if we restrict $q^2>(m_\tau^2-m_{\pi^+}^2)(m_{D^+}^2-m_\tau^2)/m_\tau^2\simeq 0.34\,\text{GeV}^2$ to cut the resonant $D\to\tau(\to\pi\nu)\nu$ mode [177]. This holds also for different neutrinos in the final state.

The LFV decays $D\to Pll'$ and $D^0\to ll'$ are vanishing in the SM, also including Majorana neutrinos, and do not emerge from resonant decays. Furthermore, angular distributions in LFV decays vanish in the SM.

Several charm FCNC transitions were studied in the literature. These contain the decays $D^0\to V(\to l^+l^-)\gamma$ [48], $B_c\to B_u^*\gamma$ [178] and $D^0\to\pi^+\pi^-\gamma$ [148]. For the latter a non-vanishing C_7' is generated at leading order in $\frac{\Lambda_{\text{QCD}}}{m_c}$ by means of a soft and a hard pion, see [179] for b decays.

One possible extension of the previous sections would be a study on $D\to Vll$ decays. They were studied in [58, 69, 110], including BSM physics. We do not agree with [69] on the perturbative contribution to the SM branching ratios, see the discussion around eq. (2.22). In [58, 110] it was found to be negligible. We estimate that they are in the same range as for $D\to Pll$ decays. The smaller phase space in $D\to Vll$ decays reduces the high q^2 range, where the contribution to the branching ratio is small. Nevertheless, the branching ratios are dominated by non-perturbative effects. They are approximated in [58] by $D\to PV(\to ll)$ decays, and are taken from chiral theory in [69, 110]. The lineshapes at low q^2 are not in agreement, see also [58]. The strongest experimental limit is obtained for $D^0\to\rho^0\mu^+\mu^-$, i.e. $\mathcal{B}(D^0\to\rho^0\mu^+\mu^-)<2.2\times10^{-5}$ at CL=90% [21]. Compared to the decay into a pseudoscalar meson, $D\to Vll$ decays give rise to additional observables. Kinematic endpoint relations, where non-factorisable terms vanish, see [143] for b decays, offer additional information. A dedicated analysis may be done elsewhere.

The decay $D\to Vll$ is a resonant mode for $D\to PPll$ decays, which were studied in [180, 181]. Note that the phase space for $D^0\to PPll$ decays is larger than the corresponding one for the decay into a vector meson. Experimentally the most stringent constraints are obtained for non-resonant $D^0\to\pi^+\pi^-\mu^+\mu^-$ as $\mathcal{B}(D^0\to\pi^+\pi^-\mu^+\mu^-)<5.5\times10^{-7}$ at CL=90% [21]. Including resonances, the $D^0\to\pi^+\pi^-\mu^+\mu^-$ branching ratios $\sim\mathcal{O}(10^{-10}-10^{-9})$ [180] and $\sim 10^{-7}$ [181] were found. The latter reference

also predicts $\mathcal{B}(D^0 \to K^-\pi^+\mu^+\mu^-)$, which in agreement with the measurement of [182]. Moreover, the SM Dalitz plot is given in [181], as well as an angular analysis in the context of BSM physics. In [180] an angular asymmetry, which is odd under time reversal, $\sim 10^{-2}$, the time-dependent direct CP asymmetry $\sim \mathcal{O}(10^{-4})$, and the time-dependent indirect CP asymmetry $\sim \mathcal{O}(10^{-5})$ were found in the SM, as well as studied in the context of BSM physics. The kinematic endpoint relations for the non-resonant mode are inherited by and smearing the resonant vector mode relations, due to different endpoints, see e.g. [183] for b decays.

A further possible extension of the previous sections would be a study on $\Lambda_c \to pll$ decays. The strongest experimental limit is obtained for $\Lambda_c \to pee$, i.e. $\mathcal{B}(\Lambda_c \to pee) < 5.5 \times 10^{-6}$ at CL=90% [21]. The SM branching ratios due to perturbative contributions were found to be $\sim \mathcal{O}(10^{-14})$ in [184] and [185], where the latter reference also studies BSM physics. This result should be taken with care: A reference for the SM Wilson coefficients is not given in [184] and [185] employs the Wilson coefficients from [59], see the clarification around eq. (2.22). Both references employ the form factors as calculated in [184] (and references therein) by use of QCD LCSR. However, the form factors do not agree with the QCD LCSR calculations performed by [186, 187], also noted in [186, 188]. We estimate that the perturbative contribution to the branching ratios is similar to the one for $D \to Pll$ decays, however, non-perturbative effects are dominating. Due to the baryons involved in $\Lambda_c \to pll$ decays additional (angular) observables can be constructed. A dedicated analysis may be done elsewhere. The radiative decay $\Lambda_c \to p\gamma$ will be studied in section 4.5.

4. Probing the standard model and physics beyond

In the previous chapters we have calculated the SM contributions to observables within an effective theory. The same framework, in particular the definitions given at the beginning of chapter 3, is used to study BSM effects in this chapter, based on [1] and [3]. Keep in mind that a Wilson coefficient C does not necessarily relate to the SM in the current chapter as opposed to the previous ones. Wilson coefficients reflect the high energy physics, whereas the SM is the low energy theory. At the BSM scale, which is around or above the EW scale, the BSM theory is matched onto the SM. Mainly two approaches are used. In the top-down approach, a UV complete BSM theory, realized at a certain scale, is evolved down to the EW scale, matched onto the SM, and thereafter evolved to the scale where physics are probed. As traces of concrete BSM models are presently missing, we utilize the bottom-up approach, where classes of models are directly probed at low energies. A UV completion can be built once the BSM direction shows up. In a general approach, BSM effects will be studied model-independently in section 4.1 by analyzing the Wilson coefficients. Effects from models which were considered in the literature will be summarized in section 4.2. We will mostly be concerned with LQ models introduced in section 4.2.1. Their effects in the decays $D \to Pll$, $D \to V\gamma$ and $\Lambda_c \to p\gamma$ will be studied in sections 4.3, 4.4 and 4.5, respectively. For the latter two we also utilize SUSY models.

4.1. Model-independent analysis

For the model-independent analysis of this section we constrain the Wilson coefficients by experimental data and we correlate different observables. The Wilson coefficients in BSM scenarios do not exhibit a q^2 dependence. We have seen in the previous chapter that the perturbative SM Wilson coefficients are small with respect to the current experimental data. In view of satisfying them by BSM physics we neglect the perturbative SM Wilson coefficients. Still, non-perturbative corrections may be sizable and should be taken into account.

For the $D^+ \to \pi^+\mu^+\mu^-$ branching ratio in the range $\sqrt{q^2} \geq 1.25\,\text{GeV}$ resonant decays can presently be neglected in view of the experimental data, see figure 3.5. Thus, the Wilson coefficients are constrained as

$$\begin{aligned}10^8 \times \mathcal{B}(D^+ \to \pi^+\mu^+\mu^-) \simeq\ & 5.9|C_7|^2 + 2.3|C_9^{(\mu)}|^2 + 2.4|C_{10}^{(\mu)}|^2 + 10.7|C_S^{(\mu)}|^2 \\ & + 10.9|C_P^{(\mu)}|^2 + 2.8|C_T^{(\mu)}|^2 + 2.6|C_{T5}^{(\mu)}|^2 \\ & + 7.4\,\text{Re}[C_7^* C_9^{(\mu)}] + 2.2\text{Re}[C_7^* C_T^{(\mu)}] \\ & + 1.6\,\text{Re}[C_9^{(\mu)}(C_T^{(\mu)})^*] + 3.2\,\text{Re}[C_{10}^{(\mu)}(C_P^{(\mu)})^*]\,. \end{aligned} \tag{4.1}$$

Here $\mathcal{B}(D^+ \to \pi^+\mu^+\mu^-) < 2.0 \times 10^{-8}$ at CL=90% [136], the primed Wilson coefficients are additive and the lepton flavor dependence is labeled. It is possible to obtain similar constraints for low and full q^2 ranges, see [1]. The experimental data for the full q^2 range assume a model dependent phase space interpolation of the low and high q^2 ranges, where the intermediate range is dominated by resonances, which are subtracted from the data. For constraints from the low q^2 range the SM contribution, perturbative and resonant, should be taken into account as well. For electrons the experimental limit is $B(D^+ \to \pi^+e^+e^-) < 1.1 \times 10^{-6}$ at CL=90% [21] for the full q^2 range. This limit is above the low and high q^2 SM predictions and assuming the experimental limit to be satisfied by BSM physics, one obtains

$$\begin{aligned}10^6 \times \mathcal{B}(D^+ \to \pi^+e^+e^-) \simeq\ & 0.28|C_7|^2 + 0.10|C_9^{(e)}|^2 + 0.10|C_{10}^{(e)}|^2 + 0.17|C_S^{(e)}|^2 \\ & + 0.17|C_P^{(e)}|^2 + 0.06|C_T^{(e)}|^2 + 0.06|C_{T5}^{(e)}|^2 + 0.33\,\text{Re}[C_7^* C_9^{(e)}] \\ & + 0.0005\,\text{Re}[C_7^* C_T^{(e)}] + 0.0003\,\text{Re}[C_9^{(e)}(C_T^{(e)})^*] \\ & + 0.0004\,\text{Re}[C_{10}^{(e)}(C_P^{(e)})^*]\,, \end{aligned} \tag{4.2}$$

where the primed Wilson coefficients are additive.

In addition, from $\mathcal{B}(D^0 \to \mu^+\mu^-) < 6.2 \times 10^{-9}$ at CL=90% [21] one obtains

$$\begin{aligned}10^6 \times B(D \to \mu^+\mu^-) \simeq\ & 1.0|C_S^{(\mu)} - C_S^{\prime(\mu)}|^2 \\ & + 1.0|C_P^{(\mu)} - C_P^{\prime(\mu)} + 0.1(C_{10}^{(\mu)} - C_{10}^{\prime(\mu)})|^2\,. \end{aligned} \tag{4.3}$$

Satisfying the experimental limit, the SM contribution can be neglected. Furthermore, $\mathcal{B}(D^0 \to e^+e^-) < 7.9 \times 10^{-8}$ at CL=90% [21] gives

$$\begin{aligned}10^6 \times B(D \to e^+e^-) \simeq\ & 1.0|C_S^{(e)} - C_S^{\prime(e)}|^2 \\ & + 1.0|C_P^{(e)} - C_P^{\prime(e)} + 0.0004(C_{10}^{(e)} - C_{10}^{\prime(e)})|^2\,. \end{aligned} \tag{4.4}$$

To summarize, similar model-independent constraints on the Wilson coefficients are obtained from different observables. The constraints on individual BSM Wilson coefficients δC read

$$|\delta C_i^{(\prime)(\mu)}| \lesssim 1\,, \quad |\delta C_{S,P}^{(\prime)(\mu)}| \lesssim 0.1\,, \tag{4.5}$$

$$|\delta C_{9,10}^{(\prime)(e)}| \lesssim 4\,, \quad |\delta C_{T,T5}^{(\prime)(e)}| \lesssim 5\,, \quad |\delta(C_7 C_9^{(\prime)(e)})| \lesssim 2\,, \quad |\delta C_{S,P}^{(\prime)(e)}| \lesssim 0.3\,. \tag{4.6}$$

Additional limits for electron Wilson coefficients are above 10, which we do not take into account in view of weakly induced tree level or loop BSM contributions $\sim g^2/\Lambda^2$ or $\sim g^2/(16\pi^2\Lambda^2)$, respectively, implying a too low BSM scale Λ below 1 TeV or the EW scale. On the other hand, the muon limits imply that $\Lambda \sim \mathcal{O}(10\,\text{TeV})$ are probed for tree level induced BSM contributions with order one couplings. This scale is competitive with the one in reach of b physics, i.e. $\Lambda \sim 36\,\text{TeV}$ [189]. Charm physics allow to probe $\Lambda \sim \mathcal{O}(100\,\text{TeV})$ for an experimental sensitivity on asymmetries $\sim \mathcal{O}(0.1\%)$ that is in the reach of LHCb [139] and where SM contributions may become relevant.

From the constraints given by eqs. (4.5, 4.6) one can obtain upper limits for the angular observables in $D^+ \to \pi^+ ll$ decays,

$$\begin{aligned} &|A_{FB}(D^+ \to \pi^+\mu^+\mu^-)| \lesssim 0.6\,, && |A_{FB}(D^+ \to \pi^+ ee)| \lesssim 0.8\,, \\ &F_H(D^+ \to \pi^+\mu^+\mu^-) \lesssim 1.5\,, && F_H(D^+ \to \pi^+ ee) \lesssim 1.6\,. \end{aligned} \tag{4.7}$$

Here resonances are taken into account in the normalization and the numerator and denominator in eqs. (C.54, C.57) were separately integrated over $\sqrt{q^2} \geq 1.25\,\text{GeV}$. The SM contributions are negligible with respect to the limits. Furthermore, we find $\mathcal{B}_{D^{*0}\to\mu^+\mu^-} \lesssim 2\times10^{-14}$ and $\mathcal{B}_{D^{*0}\to e^+e^-} \lesssim 3\times10^{-13}$, which are below the background estimated in section 3.4.

In the following, we constrain the LFV Wilson coefficients $K_i = K_i^{(e\mu,\mu e)}$. Recall that the associated operators are defined as given at the beginning of chapter 3 by the replacements $\bar{l}\Gamma l \to (\bar{e}\Gamma\mu, \bar{\mu}\Gamma e)$ for Dirac matrices Γ. One obtains, with additive primed Wilson coefficients,

$$\begin{aligned} 10^6 \times \mathcal{B}(D^+ \to \pi^+ e^\pm \mu^\mp) \simeq\ & 0.10|K_9|^2 + 0.10|K_{10}|^2 + 0.17|K_S|^2 + 0.17|K_P|^2 \\ & + 0.06|K_T|^2 + 0.06|K_{T5}|^2 \pm 0.04\,\text{Re}[K_9 K_S^*] \pm 0.04\text{Re}[K_{10} K_{T5}^*] \\ & + 0.04\,\text{Re}[K_9 K_T^*] + 0.04\,\text{Re}[K_{10}^{(\mu)} K_P^*] \end{aligned} \tag{4.8}$$

for $B(D^+ \to \pi^+ e^+\mu^-) < 2.9\times10^{-6}$, and $B(D^+ \to \pi^+ e^-\mu^+) < 3.6\times10^{-6}$ at 90% CL [21]. Furthermore, for $\mathcal{B}(D^0 \to (e^+\mu^- + e^-\mu^+)) < 1.3\times10^{-8}$ at 90% CL [25] one obtains

$$\begin{aligned} 10^6 \times \mathcal{B}(D^0 \to e^\pm \mu^\mp) \simeq\ & 1.1|K_S - K_S' \pm 0.002(K_9 - K_9')|^2 \\ & + 1.1|K_P - K_P' + 0.002(K_{10} - K_{10}|^2\,. \end{aligned} \tag{4.9}$$

Barring cancellations and considering again only limits less than 10 it follows that

$$|K_{9,10}^{(\prime)}| \lesssim 6\,, \quad |K_{S,P}^{(\prime)}| \lesssim 0.4\,, \quad |K_{T,T5}^{(\prime)}| \lesssim 7\,. \tag{4.10}$$

These constraints are weaker than the ones from dielectron modes, hence sizable effects in angular observables from LFV decays are possible.

From $\mathcal{B}(D^0 \to \rho^0\gamma) = (1.77 \pm 0.30 \pm 0.07) \times 10^{-5}$ [24] one obtains constraints on the coefficients as

$$|A_7^{(\prime)}\,,\ \delta A_7^{(\prime)}| \lesssim 0.5\,. \tag{4.11}$$

Recall that $A_7^{(\prime)}$ contains the SM Wilson coefficient and corrections to it, obtained in section 3.3.1. Indeed, the SM contribution is competitive with the allowed BSM coefficients. Corrections from BSM physics are denoted by $\delta A_7^{(\prime)}$. These constraints are similar to the ones from eq. (4.1). If the branching ratio of $D^0 \to \rho^0\gamma$ is dominated by BSM physics, $\mathcal{B}_{D^0\to\omega\gamma}/\mathcal{B}_{D^0\to\rho^0\gamma} \simeq 1$ follows, the same as in the SM, see table 3.4. This ratio may be different from one for finite non dominant BSM effects. Similar observations were made in [190]. For the charged modes we do not give such relations as they come with larger uncertainties. The constraints from the decay $D^0 \to \rho^0\gamma$ prohibit that branching ratios of $D^+ \to \rho^+\gamma$ and $D_s \to K^{*+}\gamma$ are dominated by BSM physics.

The experimental data on the CP asymmetry, $A_{CP}(D^0 \to \rho^0\gamma) = (0.056 \pm 0.152 \pm 0.006)$ [24], do not give limits on the imaginary part of the coefficients smaller than one. For sizable phases the CP asymmetry $\sim 8\,\mathrm{Im}[\delta C_7]$, which for $\delta C_7'$ is suppressed by a smaller SM contribution, and because different chiralities do not interfere in the branching ratio. In particular, CP asymmetries $\lesssim \mathcal{O}(0.1)$ are also possible for $D^0 \to \omega\gamma$, $D^+ \to \rho^+\gamma$ and $D_s \to K^{*+}\gamma$. Solely the relative signs of the CP asymmetries are correlated, allowing sizable CP asymmetries in only some of the modes. To estimate the impact of future data we work out projected constraints for a 16 times reduced statistical uncertainty in the measurements of [24] keeping the central values, i.e. $A_{CP}^{(\mathrm{proj})} = 0.056 \pm 0.038$, and $\mathcal{B}^{(\mathrm{proj})}(D^0 \to \rho^0\gamma) = (1.77 \pm 0.10) \times 10^{-5}$, where we add uncertainties in quadrature. The statistical uncertainties of the branching ratio and CP asymmetry scale as $1/\sqrt{N}$ and $\sqrt{1 - A_{CP}^2}/\sqrt{N}$, respectively, for N events. A non-vanishing CP asymmetry would be due to BSM physics. The projected constraints on the BSM coefficients are shown in figure 4.1. The SM contributions are obtained from the QCD based approach and from the resonant model, described in section 3.3. The projected constraints are $0.2 \lesssim |\delta A_7^{(\prime)}| \lesssim 0.3$, and $|\mathrm{Im}[\delta A_7^{(\prime)}]| \gtrsim \mathcal{O}(0.001)$ for the QCD based approach, and for the resonant model $0.1 \lesssim |\delta A_7^{(\prime)}| \lesssim 0.4$, $|\mathrm{Im}[\delta A_7]| \gtrsim \mathcal{O}(0.001)$, and $|\mathrm{Im}[\delta A_7']| \gtrsim \mathcal{O}(0.0001)$.

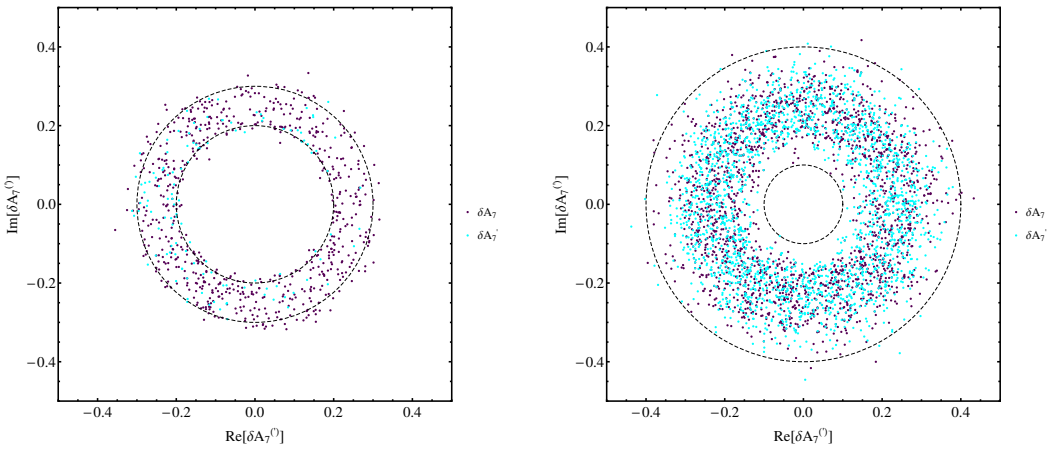

Figure 4.1.: Projected constraints on the BSM coefficients $(\mathrm{Re}[\delta A_7], \mathrm{Im}[\delta A_7])$ (purple) and $(\mathrm{Re}[\delta A_7'], \mathrm{Im}[\delta A_7'])$ (cyan) if $A_{CP}^{(\mathrm{proj})} = 0.056 \pm 0.038$, and $\mathcal{B}^{(\mathrm{proj})}(D^0 \to \rho^0\gamma) = (1.77 \pm 0.10) \times 10^{-5}$, see text. The dashed circles show $|\delta A_7^{(\prime)}| = 0.1, 0.4$ (left plot) and $|\delta A_7^{(\prime)}| = 0.2, 0.3$ (right plot). The left and right plots are obtained for the QCD based approach and the resonant model, respectively, which are described in section 3.3 and for which uncertainties are including.

In section 3.3.1 effects from the chromomagnetic operator are discussed. They do not give limits smaller than one, yet. On the other hand, the CP asymmetry constrains the imaginary part. From LCSR [191]

$$A_{CP}\big|_{\langle Q_8^{(\prime)}\rangle} \sim -\text{Im}\left[2C_8 + \frac{1}{2}C_8'\right] \tag{4.12}$$

yields $|\text{Im}[\delta C_8^{(\prime)}]| \lesssim \mathcal{O}(0.1)$. Recall that the chromomagnetic Wilson coefficients are negligible in the SM. Note that eq. (4.12) is obtained for $V^0 \in \{\rho^0, \omega\}$ and an analogue expression for charged modes can be found in [191]. Furthermore, an orthogonal constraint can be obtained from [191, 192]

$$\Delta A_{CP} = (A_{CP}(K^+K^-) - A_{CP}(\pi^+\pi^-)) \sim -2\text{Im}[C_8 - C_8'] \sin\delta_{KK-\pi\pi}\,. \tag{4.13}$$

The measured difference of the CP asymmetries is $\Delta A_{CP} = -0.00134 \pm 0.00070$ [97], but $\delta_{KK-\pi\pi}$, the strong phase difference between K^+K^- and $\pi^+\pi^-$, is presently not available.

The constraints are obtained at a scale around the charm quark mass. To make contact with a high energy scale, i.e. 1 TeV for simplicity in the following, we employ the RGE. At one loop QCD $C_{9,10}(\mu \sim 1\,\text{TeV}) = C_{9,10}(\mu \sim \mu_c)$, $C_{S,P}(\mu \sim 1\,\text{TeV}) \simeq 0.5\, C_{S,P}(\mu \sim \mu_c)$ and $C_{T,T5}(\mu \sim 1\,\text{TeV}) \simeq 1.3\, C_{T,T5}(\mu \sim \mu_c)$. Hence, the only correlations between these Wilson coefficients are given within a specific BSM scenario. In particular, the running is an order one effect. This is not the case for the magnetic Wilson coefficients, which mix according to

$$C_7^{(\prime)}(\mu_c) = a_7\, C_7^{(\prime)}(M) + \frac{16}{3}(a_7 - a_8) C_8^{(\prime)}(M)\,, \qquad C_8^{(\prime)}(\mu_c) = a_8\, C_8^{(\prime)}(M)\,, \tag{4.14}$$

where M is a high energy scale, and

$$\begin{aligned} a_7 &= \left(\frac{\alpha_s(M)}{\alpha_s(\mu_t)}\right)^{16/21} \left(\frac{\alpha_s(\mu_t)}{\alpha_s(\mu_b)}\right)^{16/23} \left(\frac{\alpha_s(\mu_b)}{\alpha_s(\mu_c)}\right)^{16/25}\,, \\ a_8 &= \left(\frac{\alpha_s(M)}{\alpha_s(\mu_t)}\right)^{14/21} \left(\frac{\alpha_s(\mu_t)}{\alpha_s(\mu_b)}\right)^{14/23} \left(\frac{\alpha_s(\mu_b)}{\alpha_s(\mu_c)}\right)^{14/25}\,. \end{aligned} \tag{4.15}$$

Including chromomagnetic effects, as described in section 3.3.1, and ignoring contributions to the SM Wilson coefficients one obtains at μ_c

$$\delta A_7^{(\prime)}\big|_{\langle Q_8^{(\prime)}\rangle} \simeq 0.38\, \delta C_7^{(\prime)}(1\,\text{TeV}) - (0.31 + 0.07i)\, \delta C_8^{(\prime)}(1\,\text{TeV})\,. \tag{4.16}$$

Furthermore, including effects from the four quark operators, see section 2.6, we find [3]

$$\begin{aligned} \delta A_7^{(\prime)}\big|_{\langle P_{3-6}^{(\prime)}\rangle} \simeq\ & (0.3 - 0.1i)\, \delta C_3^{(\prime)}(1\,\text{TeV}) + (0.7 + 0.1i)\, \delta C_4^{(\prime)}(1\,\text{TeV}) \\ & + (-3.5 - 1.9i)\, \delta C_5^{(\prime)}(1\,\text{TeV}) + (-0.6 + 1.1i)\, \delta C_6^{(\prime)}(1\,\text{TeV})\,, \end{aligned} \tag{4.17}$$

model [reference(s)]	$\mathcal{B}$	A_{CP}	A_{FB}
little Higgs model [59, 110]	$\lesssim \mathcal{B}_{\text{SM}}$	$\lesssim \mathcal{O}(10^{-3})$	$\lesssim \mathcal{O}(5 \times 10^{-3})$
minimal SUSY SM [58, 60, 70, 127]	$\lesssim \mathcal{B}_{\text{exp}}$	$\lesssim \mathcal{O}(10^{-3})$	$\lesssim \mathcal{O}(10^{-1})$
two Higgs doublet model [70, 129, 193]	$\lesssim \mathcal{B}_{\text{SM}}$	–	–
unparticle [193]	$\lesssim \mathcal{B}_{\text{SM}}$	–	–
up vector-like quark singlet [127]	$\lesssim \mathcal{B}_{\text{SM}}$	–	$\lesssim 10^{-3}$
warped extra dimension [194, 195]	$\lesssim \mathcal{B}_{\text{SM}}$	$\lesssim \mathcal{O}(10^{-2})$	$\lesssim \mathcal{O}(5 \times 10^{-2})$
weak vector triplet [129]	$\lesssim \mathcal{B}_{\text{SM}}$	–	–
Z' boson [129, 193, 196]	$\lesssim \mathcal{B}_{\text{SM}}$	–	–

Table 4.1.: Models beyond the SM generating semileptonic decays. The predictions were found for inclusive and exclusive sample modes.

where SM contributions are negligible. Note that the imaginary parts in eq. (4.17) are CP even and that the running and mixing also hold for the Wilson coefficients K_i.

The model-independent constraints obtained in the current section will be confronted with specific models in the next sections.

4.2. Models extending the standard model

Extensions of the SM respect the SM gauge group at low energies. At high energies further symmetries may be present along with additional interactions and particles. The latter can be gauged if they follow from a spontaneously broken gauge symmetry.

Several models which extend the SM and generate semileptonic decays were studied in the literature. We summarize them in table 4.1 and list predictions for observables if available. They include a sample of exclusive and inclusive modes but can be seen as generic here from what we have learnt in chapter 3. From these models only the minimal SUSY SM can give branching ratios above the SM, and close to the experimental limits. The predictions for the CP asymmetry and the forward-backward asymmetry differ from model to model. In most cases these observables can be larger than the SM contributions. Furthermore, the A_{FB}^{CP} is predicted to be $\lesssim \mathcal{O}(10^{-1})$ in the little Higgs model and warped extra dimension give $\lesssim \mathcal{O}(10^{2})$, while in the SM $\sim \mathcal{O}(10^{-5})$.

Additionally, left-right symmetric models and a vector-like quark were studied in the context of inclusive radiative decays in [166]. While the branching ratio was found to be below the SM, deviations from the SM are possible in the photon polarization. Moreover, charm FCNC induced $D^0 \to ll$ decays were studied for BSM scenarios in [58, 60, 129, 171, 195, 197].

Up to this point we have not considered LQ models, which were studied in [128, 129, 196] for the models S_1, S_2 and $\tilde{V}_1$ In the following sections we will give a comprehensive study on LQ models.

4.2.1. Leptoquark models

As a bottom-up approach we assume the existence of renormalizable up-type quark-lepton-boson couplings extending the SM gauge group, that is colored scalar and vector LQs which are $SU(2)_L$ singlets, doublets and triplets [198]. A recent review of LQ models is given in [199], to which we also refer for embeddings into larger symmetry groups, see also [200] (and references therein) for UV completions. Models involving LQs are of recent interest as they can account for several SM anomalies, see, e.g., [144, 200–206]. Note that the measured $R(D) = \mathcal{B}(D \to \tau\nu)/\mathcal{B}(D \to (e,\mu)\nu)$ may not constitute an anomaly in the SM [207] and $R(D)$ may be correlated to leptonic decays of vectors [208]. Furthermore, neutrino masses and mixing can be generated within LQ models [209–211].

The LQ models relevant for $c \to ul^{(\prime)}l$ transitions, that is $S_{1,2,3}$, and $\tilde{V}_{1,2}$, $V_{2,3}$, their couplings, weak hypercharges Y_w, and electric charges along with the induced effective vertices are listed in table 4.2. The latter are obtained by integrating out the LQs and employing Fierz identities, provided in appendix F. The effective $c \to u(l')^+l^-$ vertices for the $SU(2)_L$ triplets follow from the completeness relation for the Pauli matrices, $\vec{\tau}_{\alpha\beta} \cdot \vec{\tau}_{\mu\nu} = (2\delta_{\alpha\mu}\delta_{\beta\nu} - \delta_{\alpha\beta}\delta_{\mu\nu})$. Charge conjugation of quark fields $\bar{q}^C = -q^T C^{-1}$, $q^C = C\bar{q}^T$ yields $q \leftrightarrow q'$, and an additional minus sign in the vector and tensor effective vertices with respect to the non-conjugated fields, see, e.g., [212]. Note that a minus sign is present in the propagator of the vector LQs, which was omitted in [1]. For non-gauge vector LQs with momentum k, and mass M additional terms $\sim k^\mu k^\nu/M^2$ emerge in the propagator. In tree diagrams, e.g. the ones for the effective vertices, these terms are negligible. Note that the models $S_{1,2}$ each contain two couplings denoted by the lepton chirality.

$\subset \mathcal{L}_{LQ}$	$[Y_w^{(LQ)}\ (q_{LQ})]$	effective vertices
$\left(\lambda_{S_1 L}\bar{\mathbf{Q}}_L^C i\tau_2 \mathbf{L}_L + \lambda_{S_1 R} q_R^C l_R\right) S_1^\dagger$	$[-\frac{1}{3}\ (-\frac{1}{3})]$	$\frac{\lambda_{S_1 R}^{(q'l')}\left(\lambda_{S_1 R}^{(ql)}\right)^*}{2M_{S_1}^2}\left(\bar{q}_R\gamma_\mu q'_R\right)\left(\bar{l}_R\gamma^\mu l'_R\right)$
		$\frac{\lambda_{S_1 L}^{(q'l')}\left(\lambda_{S_1 L}^{(ql)}\right)^*}{2M_{S_1}^2}\left(\bar{q}_L\gamma_\mu q'_L\right)\left(\bar{l}_L\gamma^\mu l'_L\right)$
		$-\frac{\lambda_{S_1 R}^{(q'l')}\left(\lambda_{S_1 L}^{(ql)}\right)^*}{2M_{S_1}^2}\left(\bar{q}_L q'_R\right)\left(\bar{l}_L l'_R\right)$

		$-\frac{\lambda_{S_1L}^{(q'l')}\left(\lambda_{S_1R}^{(ql)}\right)^*}{2M_{S_1}^2}\left(\bar{q}_R q'_L\right)\left(\bar{l}_R l'_L\right)$
		$\frac{\lambda_{S_1R}^{(q'l')}\left(\lambda_{S_1L}^{(ql)}\right)^*}{8M_{S_1}^2}\left(\bar{q}\sigma_{\mu\nu}q'\right)\left(\bar{l}_L\sigma^{\mu\nu}l'_R\right)$
		$\frac{\lambda_{S_1L}^{(q'l')}\left(\lambda_{S_1R}^{(ql)}\right)^*}{8M_{S_1}^2}\left(\bar{q}\sigma_{\mu\nu}q'\right)\left(\bar{l}_R\sigma^{\mu\nu}l'_L\right)$
$\left(\lambda_{S_2L}\bar{q}_R\mathbf{L}_L+\lambda_{S_2R}\bar{\mathbf{Q}}_L i\tau_2 l_R\right)S_2^\dagger$	$[-\frac{7}{6}\ (-\frac{2}{3},-\frac{5}{3})]$	$-\frac{\lambda_{S_2R}^{(ql')}\left(\lambda_{S_2R}^{(q'l)}\right)^*}{2M_{S_2}^2}\left(\bar{q}_L\gamma_\mu q'_L\right)\left(\bar{l}_R\gamma^\mu l'_R\right)$
		$-\frac{\lambda_{S_2L}^{(ql')}\left(\lambda_{S_2L}^{(q'l)}\right)^*}{2M_{S_2}^2}\left(\bar{q}_R\gamma_\mu q'_R\right)\left(\bar{l}_L\gamma^\mu l'_L\right)$
		$-\frac{\lambda_{S_2R}^{(ql')}\left(\lambda_{S_2L}^{(q'l)}\right)^*}{2M_{S_2}^2}\left(\bar{q}_L q'_R\right)\left(\bar{l}_L l'_R\right)$
		$-\frac{\lambda_{S_2L}^{(ql')}\left(\lambda_{S_2R}^{(q'l)}\right)^*}{2M_{S_2}^2}\left(\bar{q}_R q'_L\right)\left(\bar{l}_R l'_L\right)$
		$-\frac{\lambda_{S_2R}^{(ql')}\left(\lambda_{S_2L}^{(q'l)}\right)^*}{8M_{S_2}^2}\left(\bar{q}\sigma_{\mu\nu}q'\right)\left(\bar{l}_L\sigma^{\mu\nu}l'_R\right)$
		$-\frac{\lambda_{S_2L}^{(ql')}\left(\lambda_{S_2R}^{(q'l)}\right)^*}{8M_{S_2}^2}\left(\bar{q}\sigma_{\mu\nu}q'\right)\left(\bar{l}_R\sigma^{\mu\nu}l'_L\right)$
$\left(\lambda_{S_3}\bar{\mathbf{Q}}_L^C i\tau_2\vec{\tau}\mathbf{L}_L\right)\cdot\vec{S_3}^\dagger$	$[-\frac{1}{3}\ (\frac{2}{3},-\frac{1}{3},-\frac{4}{3})]$	$\frac{\lambda_{S_3}^{(q'l')}\left(\lambda_{S_3}^{(ql)}\right)^*}{2M_{S_3}^2}\left(\bar{q}_L\gamma_\mu q'_L\right)\left(\bar{l}_L\gamma^\mu l'_L\right)$
$\lambda_{\tilde{V}_1}\bar{q}_R\gamma_\mu l_R\left(\tilde{V}_1^\mu\right)^\dagger$	$[-\frac{5}{3}\ (-\frac{5}{3})]$	$-\frac{\lambda_{\tilde{V}_1}^{(ql')}\left(\lambda_{\tilde{V}_1}^{(q'l)}\right)^*}{M_{\tilde{V}_1}^2}\left(\bar{q}_R\gamma_\mu q'_R\right)\left(\bar{l}_R\gamma^\mu l'_R\right)$
$\lambda_{V_2}\bar{\mathbf{Q}}_L^C\gamma_\mu l_R\left(V_2^\mu\right)^\dagger$	$[-\frac{5}{6}\ (-\frac{1}{3},-\frac{4}{3})]$	$\frac{\lambda_{V_2}^{(q'l')}\left(\lambda_{V_2}^{(ql)}\right)^*}{M_{V_2}^2}\left(\bar{q}_L\gamma_\mu q'_L\right)\left(\bar{l}_R\gamma^\mu l'_R\right)$
$\lambda_{\tilde{V}_2}\bar{q}_R^C\gamma_\mu\mathbf{L}_L\left(\tilde{V}_2^\mu\right)^\dagger$	$[\frac{1}{6}\ (\frac{2}{3},-\frac{1}{3})]$	$\frac{\lambda_{\tilde{V}_2}^{(q'l')}\left(\lambda_{\tilde{V}_2}^{(ql)}\right)^*}{M_{\tilde{V}_2}^2}\left(\bar{q}_R\gamma_\mu q'_R\right)\left(\bar{l}_L\gamma^\mu l'_L\right)$
$\lambda_{V_3}\bar{\mathbf{Q}}_L\gamma_\mu\vec{\tau}\mathbf{L}_L\cdot\left(\vec{V_3}^\mu\right)^\dagger$	$[-\frac{2}{3}\ (\frac{1}{3},-\frac{2}{3},-\frac{5}{3})]$	$-\frac{2\lambda_{V_3}^{(ql')}\left(\lambda_{V_3}^{(q'l)}\right)^*}{M_{V_3}^2}\left(\bar{q}_L\gamma_\mu q'_L\right)\left(\bar{l}_L\gamma^\mu l'_L\right)$

Table 4.2.: Part of the Lagrangian defining the LQ interactions with the SM fermions. Here $q_R, q'_R \in \{u_R, c_R\}$, $l_R, l'_R \in \{e_R, \mu_R\}$ and $\mathbf{Q}$, $\mathbf{L}$ are $SU(2)_L$ doublets, see table 2.1 for the SM fermion charges. In case of a single coupling λ we do not write the lepton chirality. The weak hypercharge is defined as $Y_w = (q - T_3)$, where T_3 is the third component of the weak isospin.

Additional couplings and effective vertices, involving neutrinos and down-type quarks, are given in [213]. The effective vertices of table 4.2 agree with and extend the ones obtained in [213–216] but differ from the ones given in [128] by a relative sign for the tensor vertices, and by a factor 1/2 from the vector vertices of [129].

Note that $\tilde{V}_2$ only couples up-type quarks and charged leptons. Down-type quark bilinears obey a different structure and do not induce, e.g., pseudoscalar nor (pseudo-)tensor effective vertices. However, the entire set of effective vertices can be generated via weakly mixing states of equal quantum numbers in the broken EW phase due to LQ-Higgs couplings [217]. These can further induce mass splitting, neutrinoless double beta decay [218], a Majorana mass matrix [219] and stabilize the EW vacuum [220].

Spontaneous breaking of the EW symmetry induces unitary matrices which modify the couplings to quark and lepton doublets. Thus, quark and charged lepton flavors mix. Note that a mixing of neutrino flavors is irrelevant since they are summed in decay rates, and due to the unitarity. We neglect mixing effects for simplicity, yet they provide the link for a full flavor analysis.

Baryon number and lepton number are each conserved in the interactions as we neglect possible diquark couplings so that the proton is stable at tree level. Note that for S_3 a possible quark bilinear coupling is absent due to its antisymmetry in flavor space [221]. Furthermore, one can employ unitary transformations to suppress the LO vector LQ contributions to proton decay [222] (and references therein). However, mixed trilinear renormalized operators [223] can induce proton decay [221]. Proton decay inducing non-renormalizable dimension five operators in an $SU(2)_L$ singlet scalar LQ model are absent if an additional Z_3 gauge symmetry is assumed [216].

We add that LQ couplings to SM gauge bosons are given in [224, 225], and for anomalous couplings in [226]. A UV complete LQ model should not induce anomalies, see e.g. [227, 228].

The LQ masses are constrained by oblique parameters [215], yielding a small range for mass differences in an $SU(2)_L$ multiplet. We take LQ masses to be degenerate. Collider experiments obtain $M_S \gtrsim 1.730\,\text{TeV}$ and $M_S \gtrsim 1.165\,\text{TeV}$ at 95% CL for couplings to electrons and muons, respectively, assuming the branching ratio into a charged lepton and a quark is 100% [229, 230] (and [231]). These bounds are relaxed for smaller branching ratios, i.e. taking into account other final states, and are obtained via direct pair production which depends on the mass only. On the other hand, direct single production

of scalar LQs depends on the mass and the couplings. The relative number of direct single to pair produced scalar LQs is large/small for small/large couplings and masses [232]. Measurements for vector LQs rely on assumptions of the anomalous LQ-gluon couplings [233]. As a reference LQ mass we take $M = 1\,\text{TeV}$. Furthermore, we consider perturbative LQ couplings, $\lambda \lesssim 1$. Note that the total widths $\Gamma_S = 1/(16\pi)\,\lambda_S^2 m_S$ and $\Gamma_V = 1/(24\pi)\,\lambda_V^2 m_V$ [198] provide complementary information on masses and couplings, once the total widths are measured.

The tree level LQ induced Wilson coefficients read

$$
\begin{aligned}
\delta_{LQ} C_{9,10} &= \frac{\sqrt{2}\pi}{G_F \alpha_e} k_{9,10} \frac{\lambda_i^I \left(\lambda_i^J\right)^*}{M^2}\,, \\
\delta_{LQ} C'_{9,10} &= \frac{\sqrt{2}\pi}{G_F \alpha_e} k'_{9,10} \frac{\lambda_j^I \left(\lambda_j^J\right)^*}{M^2}\,, \\
\delta_{LQ} C_S = \delta_{LQ} C_P &= \frac{\sqrt{2}\pi}{G_F \alpha_e} k_{S,P} \frac{\lambda_R^I \left(\lambda_L^J\right)^*}{M^2}\,, \\
\delta_{LQ} C'_S = -\delta_{LQ} C'_P &= \frac{\sqrt{2}\pi}{G_F \alpha_e} k'_{S,P} \frac{\lambda_L^I \left(\lambda_R^J\right)^*}{M^2}\,, \\
\delta_{LQ} C_T &= \frac{\sqrt{2}\pi}{G_F \alpha_e} k_T \left(\frac{\lambda_i^I \left(\lambda_j^J\right)^*}{M^2} + \frac{\lambda_j^I \left(\lambda_i^J\right)^*}{M^2} \right)\,, \\
\delta_{LQ} C_{T5} &= \frac{\sqrt{2}\pi}{G_F \alpha_e} k_{T5} \left(\frac{\lambda_i^I \left(\lambda_j^J\right)^*}{M^2} - \frac{\lambda_j^I \left(\lambda_i^J\right)^*}{M^2} \right)\,,
\end{aligned}
\tag{4.18}
$$

where the coefficients $k^{(\prime)}$ are given in table 4.3.

The Wilson coefficients $C_7^{(\prime)}$ are generically induced at loop level. We calculate the corresponding contributions from LQs in RG-improved perturbation theory. Within LQ models $\delta_{LQ} C_{1-8}^{(\prime)}(M_{LQ}) = 0$ due to light leptons in the loop, however, Wilson coefficients $C_V^{(l)}(M_{LQ})$, and, schematically, $C_S^{(l)}(M_{LQ}) = \lambda_R \lambda_L / M_S^2$ are induced at tree level. Here the scalar and vector operators are $O_V^{(l)} = (\bar{u}_L \gamma_\mu l_L)(\bar{l}_L \gamma^\mu c_L)$ and $O_S^{(l)} = (\bar{u}_L l_R)(\bar{l}_L c_R)$ respectively, with $C_i^{(l)} O_i^{(l)} \subset \mathcal{L}$ as well as analogue contributions from chirality-flipped operators. At one loop QCD $C_V^{(l)}(\mu_c) = C_V^{(l)}(M_{LQ})$ and $C_S^{(l)}(\mu) = (\frac{\alpha_s(M_{LQ})}{\alpha_s(\mu)})^{8/(2\beta_0)}\, C_S^{(l)}(M_{LQ})$, where threshold effects from $\beta_0 = 11 - \frac{2}{3} n_f$ arise. At the scale $\mu = m_\tau$ the τ lepton is integrated out. Since numerically $m_\tau \simeq \sqrt{2} m_c \sim \mu_c$ we include its one loop contribution in the matrix element $\langle Q_{V,S}^{(l)} \rangle$, see figure 4.2.

LQ	$I\,,J$	$i\,,j$	k_9	k_{10}	k'_9	k'_{10}	$k_{S,P}$	$k'_{S,P}$	k_T	k_{T5}
S_1	$(cl)\,,(ul)$	$L\,,R$	$1/4$	$-1/4$	$1/4$	$1/4$	$-1/4$	$-1/4$	$-1/8$	$-1/8$
S_2	$(ul)\,,(cl)$	$R\,,L$	$-1/4$	$-1/4$	$-1/4$	$1/4$	$-1/4$	$-1/4$	$-1/8$	$-1/8$
S_3	$(cl)\,,(ul)$	$L\,,-$	$1/4$	$-1/4$	0	0	0	0	0	0
$\tilde{V}_1$	$(ul)\,,(cl)$	$-\,,R$	0	0	$-1/2$	$-1/2$	0	0	0	0
V_2	$(cl)\,,(ul)$	$R\,,-$	$1/2$	$1/2$	0	0	0	0	0	0
$\tilde{V}_2$	$(cl)\,,(ul)$	$-\,,L$	0	0	$1/2$	$-1/2$	0	0	0	0
V_3	$(ul)\,,(cl)$	$L\,,-$	-1	1	0	0	0	0	0	0

Table 4.3.: Coefficients for eq. (4.18).

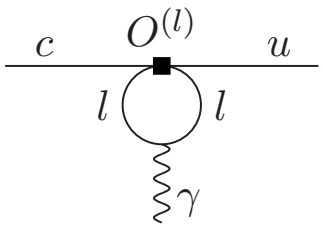

Figure 4.2.: One loop diagram inducing $c \to u\gamma$ transitions within LQ models. The box denotes an operator insertion, see text.

The coefficients from $\langle O_V^{(l)(\prime)}\rangle$ are found to be zero to all orders in α_s. The contributions from $\langle O_S^{(l)(\prime)}\rangle$ are non-zero,

$$\delta_S A_7^{(\prime)}(\mu_c) = \frac{1}{2\sqrt{2}G_F}\frac{-q_l m_l}{2m_c}\left(1+\ln\frac{\mu_c^2}{m_l^2}\right) \times \left(\frac{\alpha_s(M_S)}{\alpha_s(\mu_t)}\right)^{12/21}\left(\frac{\alpha_s(\mu_t)}{\alpha_s(\mu_b)}\right)^{12/23}\left(\frac{\alpha_s(\mu_b)}{\alpha_s(\mu_c)}\right)^{12/25}\frac{\nu^{(\prime)}}{M_S^2}\,, \tag{4.19}$$

where q_l is the charge of the lepton, and the LQ couplings $\nu^{(\prime)}$ are given in table 4.4. Numerically, one obtains $|\delta_{S_{1,2}} A_7^{(\prime)}(\mu_c)| \simeq 0.01|\lambda_R\lambda_L^*|\,(\frac{\text{TeV}}{M_S})^2$ for $l=\tau$. Note that $\delta_{LQ}A_8^{(\prime)}(\mu_c)$ are additionally α_e suppressed.

The matrix elements $\langle O_V^{(l)(\prime)}\rangle$ are non-zero at two loop, where the corresponding diagrams can be read off from figure 2.5 with the gluons replaced by a photons. As it turns out, we can adopt the calculation of section 2.6.1 with modifications of the perturbative coupling. Therefore, only diagrams with a photon exchange between the external up-type quark lines and internal LQs contribute, yielding an overall factor $\frac{2}{3}q_l\frac{3}{4}$, where the last factor compensates the $SU(3)_C$ group invariant C_F. We find for $l=\tau$

$$|\delta_V A_7^{(\prime)}(\mu_c)| \simeq (0.00004, 0.00006, 0.00009)\,|\kappa^{(\prime)}|\left(\frac{1\,\text{TeV}}{M_V}\right)^2\,, \tag{4.20}$$

where $(\tilde{V}_1, \{V_2, \tilde{V}_2\}, V_3)$ is distinguished due to different lepton charges. For V_3 an additional factor 2 from the completeness relation for Pauli matrices emerges. These two loop contributions are newly obtained with respect to [3], and allow to estimate effects from $V_{2,3}$ which vanish otherwise. The couplings $\kappa^{(\prime)}$ are given in table 4.4. The induced coefficients from vector LQs are small due to the loop suppression $\sim \alpha_e/(4\pi)$.

Nevertheless, coefficients for scalar LQs with equal chirality couplings fall short. Thus, we employ the fixed order one loop calculation [234] to obtain the matrix elements in the full SM plus (gauge vector) LQ theory. The coefficients are

$$\begin{aligned}\delta_{\langle S\rangle} A_7^{(\prime)} &= -\frac{1}{2\sqrt{2}G_F}\frac{\kappa^{(\prime)}}{M_S^2}\left(q_l k_1 + q_S \bar{k}_1\right)\,,\\ \delta_{\langle V\rangle} A_7^{(\prime)} &= -\frac{1}{2\sqrt{2}G_F}\frac{\kappa^{(\prime)}}{M_S^2}(q_l y_1 + q_V \bar{y}_1)\,,\end{aligned} \tag{4.21}$$

where

$$k_1 = \frac{1}{12}\,,\quad \bar{k}_1 = \frac{1}{24}\,,\qquad y_1 = \frac{-1}{3}\,,\quad \bar{y}_1 = 1\,, \tag{4.22}$$

and the couplings are given in table 4.4. Here light fermion masses are neglected to avoid spurious large logarithms, which are resummed in the RG-improved perturbation theory. Indeed, the logarithm in the fixed order calculation is resummed by eq. (4.19) [3].

LQ	κ	κ'	ν	ν'
S_1	$\lambda_R^{(cl)}(\lambda_R^{(ul)})^*$	$\lambda_L^{(cl)}(\lambda_L^{(ul)})^*$	$\lambda_L^{(cl)}(\lambda_R^{(ul)})^*$	$\lambda_R^{(cl)}(\lambda_L^{(ul)})^*$
S_2	$(\lambda_R^{(cl)})^*\lambda_R^{(ul)}$	$(\lambda_L^{(cl)})^*\lambda_L^{(ul)}$	$(\lambda_L^{(cl)})^*\lambda_R^{(ul)}$	$(\lambda_R^{(cl)})^*\lambda_L^{(ul)}$
S_3	–	$\lambda^{(cl)}(\lambda^{(ul)})^*$	–	–
$\tilde{V}_1$	$(\lambda^{(cl)})^*\lambda^{(ul)}$	–	–	–
V_2	$\lambda^{(cl)}(\lambda^{(ul)})^*$	–	–	–
$\tilde{V}_2$	–	$\lambda^{(cl)}(\lambda^{(ul)})^*$	–	–
V_3	–	$(\lambda^{(cl)})^*\lambda^{(ul)}$	–	–

Table 4.4.: Couplings for eqs. (4.19), (4.20) and (4.21).

The numerical coefficients are given in table 4.5. Note that different contributions cancel for $V_{2,3}$, thus no $A_7^{(\prime)}$ are induced in these models from the fixed order calculation. In the subsequent analysis we combine both approaches, as otherwise we would miss important contributions in each of them.

In appendix G we work out constraints on LQ couplings from various observables relevant for charm FCNC transitions. The constraints are calculated at fixed order for simplicity, hence RGE effects for the lepton Wilson coefficients given by eq. (4.18) are neglected. Assuming perturbativity of the couplings and gauge vector LQs, the constraints due to the experimental data, see appendix A, are collected in appendix G.1, updating and extending the tables given in [1].

To summarize, LQ constraints are basically compatible with all considered observables. In general, products of couplings are constrained $\sim \mathcal{O}(10^{-3} - 10^{-1})$, thus no definite conclusion on a single coupling can be drawn. Only bounds from kaon decays, electric moments, semileptonic and LFV decays are stronger. Whereas the former, in particular $K^+ \to \pi^+\bar{\nu}\nu$ decays, constrain products of quark doublets with equal chirality couplings, i.e. S_1L, S_2R, S_3, and $V_{2,3}$, the other ones constrain products of couplings with different chiralities in $S_{1,2}$ models. Note that the products of couplings relevant for charm FCNC transitions are directly bounded only by rare charm decays, yielding similar constraints, see section 4.1. To further accommodate constraints from other decays and study correlations between observables we employ flavor patterns in the next section.

LQ	$\delta_{\langle LQ\rangle} A_7$	$\delta_{\langle LQ\rangle} A_7'$
S_1	$-0.003\,\lambda_R^{(cl)}(\lambda_R^{(ul)})^*$	$-0.003\,\lambda_L^{(cl)}(\lambda_L^{(ul)})^*$
S_2	$0.005\,(\lambda_R^{(cl)})^*\lambda_R^{(ul)}$	$0.006\,(\lambda_L^{(cl)})^*\lambda_L^{(ul)}$
S_3	0	$-0.002\,\lambda^{(cl)}(\lambda^{(ul)})^*$
$\tilde{V}_1$	$0.04\,(\lambda^{(cl)})^*\lambda^{(ul)}$	0
V_2	0	0
$\tilde{V}_2$	0	$-0.02\,\lambda^{(cl)}(\lambda^{(ul)})^*$
V_3	0	0

Table 4.5.: The LQ induced coefficients from the fixed order calculation for $M = 1\,\text{TeV}$. For $M \to 10\,\text{TeV}$ the effective coupling $\lambda^{(cl)}\lambda^{(ul)}/(M = 1\,\text{TeV})^2 \to 0.9\,\lambda^{(cl)}\lambda^{(ul)}/(M = 10\,\text{TeV})^2$.

LQ	(ee)	$(e\mu)$, (μe)	$(\mu\mu)$
$S_1 L$	$\lesssim 4 \times 10^{-3}$	$\lesssim 4 \times 10^{-3}$	$\lesssim 4 \times 10^{-3}$
$S_2 R$, V_2	$\lesssim 3 \times 10^{-2}$	$\lesssim 2 \times 10^{-4}$	$\lesssim 4 \times 10^{-3}$
S_3	$\lesssim 4 \times 10^{-3}$	$\lesssim 1 \times 10^{-4}$	$\lesssim 2 \times 10^{-3}$
V_3	$\lesssim 4 \times 10^{-3}$	$\lesssim 2 \times 10^{-4}$	$\lesssim 4 \times 10^{-3}$

Table 4.6.: Limits on LQ induced $c \to u l^{(\prime)} l$ Wilson coefficients $|C_{9,10}^{(\prime)}|$ and $|K_{9,10}^{(\prime)}|$ due to kaon decays. Here $M = 1\,\text{TeV}$.

4.3. Probes with rare semileptonic D decays

The strongest limits on tree level induced Wilson coefficients are listed in tables 4.6 and 4.7. Additionally, from the electric dipole moments one finds $\text{Im}[C_{S,P,T,T5}^{(e)}] \lesssim 4 \times 10^{-9}$ and $\text{Im}[C_{S,P,T,T5}^{(\mu)}] \lesssim 4 \times 10^{-6}$.

As already mentioned we employ flavor patterns to enhance the predictivity. We define the following classes of LQ couplings, inspired by [235], that is Frogatt-Nielsen $U(1)$ [236] and A_4 symmetries [237], for quarks (rows) and leptons (columns), respectively: (i) a

LQ	$(ee)(\mu\mu)$, $(e\mu)(\mu e)$
S_1	$\lesssim 2 \times 10^{-7}$
S_2	$\lesssim 8 \times 10^{-8}$
S_3, $\tilde{V}_1$, V_2, $\tilde{V}_2$, V_3	$\lesssim 6 \times 10^{-8}$
$S_1\vert_{LR}$, $S_2\vert_{LR}$	$\lesssim 2 \times 10^{-10}$

Table 4.7.: Limits on the products of two $c \to ul^{(\prime)}l$ Wilson coefficients $|C_i^{(e)(\prime)} C_i^{(\mu)(\prime)}|$ and $|K_i^{(e\mu)(\prime)} K_i^{(\mu e)(\prime)}|$ due to $\mu - e$ conversion and $\mu \to e\gamma$ decays. Here $M = 1\,\text{TeV}$. The label LR denotes products of couplings with different chiralities, i.e. for (pseudo-)scalar and (pseudo-)tensor Wilson coefficients.

hierarchical flavor pattern, (ii) a single flavor lepton pattern, where couplings to electron are negligible, and (iii) a skewed pattern, where $\lambda^{(u\mu)}$ and $\lambda^{(ce)}$ are negligible, that is

$$\lambda_i \sim \begin{pmatrix} \rho_d\kappa & \rho_d & \rho_d \\ \rho\kappa & \rho & \rho \\ \kappa & 1 & 1 \end{pmatrix}, \quad \lambda_{ii} \sim \begin{pmatrix} 0 & * & 0 \\ 0 & * & 0 \\ 0 & * & 0 \end{pmatrix}, \quad \lambda_{iii} \sim \begin{pmatrix} * & 0 & 0 \\ 0 & * & 0 \\ 0 & * & 0 \end{pmatrix}. \tag{4.23}$$

The binary textures involving "*" reflect a discrete non-abelian symmetry, i.e. A_4. The patterns (i) and (ii) have been obtained for quarks coupling to lepton doublets by means of the A_4 symmetry [1]. Further justification for the (sub-)patterns employed here is given in [213].

For the patterns (ii) and (iii) we further distinguish subclasses: (1) represents $S_{1,2}$, and $\tilde{V}_{1,2}$ and a second subclass (2) with S_3, and $V_{2,3}$ is not affected by bounds from kaon decays. For pattern (i) we exemplary study $\kappa \sim 1$, for which table 4.7 implies that all Wilson coefficients are similar. If κ is small, the pattern (i) effectively reduces to pattern (ii).

The electron Wilson coefficients are zero for patterns (ii) and (iii). The muon Wilson coefficients in class (ii.1) are constrained by $D^+ \to \pi^+\mu^+\mu^-$ and $D^0 \to \mu^+\mu^-$ decays and the constraints for class (ii.2) are given in table 4.6. For pattern (iii) the muon Wilson coefficients are zero in any case.

The LFV Wilson coefficients are zero for the pattern (ii). For the pattern (iii) either, for $q_{LQ} = -1/3$, $\mathcal{B}(D^0 \to \mu^- e^+)$ and $\mathcal{B}(\bar{D}^0 \to \mu^+ e^-)$ vanish or, for $q_{LQ} = 5/3$, $\mathcal{B}(D^0 \to \mu^+ e^-)$ and $\mathcal{B}(\bar{D}^0 \to \mu^- e^+)$ vanish as well as analogously for $D^+ \to \pi^+ e^\pm \mu^\mp$ decays. In class (iii.1) the LFV Wilson coefficients are constrained by $D^+ \to \pi^+ e^\pm \mu^\mp$ and $D^0 \to e^\pm \mu^\mp$ decays giving $\lesssim \mathcal{O}(10)$ and the constraints for class (iii.2) are given in table 4.6.

Exemplary, the decay distribution for $D^+ \to \pi^+\mu^+\mu^-$ at high q^2 including LQs of the class (ii.2) is shown in figure 4.3. In agreement with the model-independent observations the LQ induced branching ratio at high q^2 can be larger than the SM predictions and close the experimental limit.

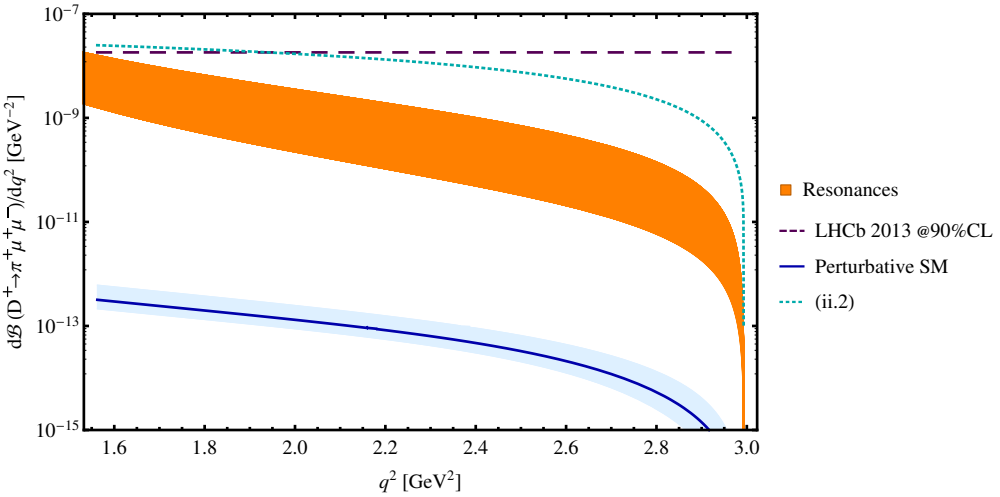

Figure 4.3.: Branching ratio of $D^+ \to \pi^+\mu^+\mu^-$ at high q^2. The orange band shows the resonant modes and the dashed purple line represents the 90% CL experimental upper limit [136]. The solid blue curve and lighter band are the perturbative SM prediction at $\mu_c = m_c$ and its μ_c uncertainty, respectively. Additionally, the dotted cyan curve is for LQ models of the class (ii.2), see text.

	$\mathcal{B}_{D^+\to\pi^+\mu^+\mu^-}$	$\mathcal{B}_{D^0\to\mu^+\mu^-}$	$\mathcal{B}_{D^+\to\pi^+e\mu}$	$\mathcal{B}_{D^0\to e\mu}$	$\mathcal{B}_{D^+\to\pi^+\nu\bar{\nu}}$
(i)	SM-like	SM-like	$\lesssim 2\times10^{-13}$	$\lesssim 7\times10^{-15}$	$\lesssim 3\times10^{-13}$
(ii.1)	$\lesssim 7/2\times10^{-8}$	$\lesssim 3\times10^{-9}$	0	0	$\lesssim 8\times10^{-8}$
(ii.2)	SM-like	$\lesssim 4\times10^{-13}$	0	0	$\lesssim 4\times10^{-12}$
(iii.1)	SM-like	SM-like	$\lesssim 2\times10^{-6}$	$\lesssim 1\times10^{-8}$	$\lesssim 2\times10^{-6}$
(iii.2)	SM-like	SM-like	$\lesssim 8\times10^{-15}$	$\lesssim 2\times10^{-16}$	$\lesssim 9\times10^{-15}$
exp.	$< 7.3/2.6\times10^{-8}$	$< 6.2\times10^{-6}$	$\lesssim 3\times10^{-6}$	$< 1.3\times10^{-8}$	–

Table 4.8.: Integrated branching ratios on the full/high q^2 range for different cases of LQ couplings. The experimental limits at 90% CL are taken from [21, 136], where $\mathcal{B}(D^0\to e\mu)=\mathcal{B}(D^0\to(e^+\mu^-+e^-\mu^+))$, and from [25] for $\mathcal{B}(D^+\to\pi^+e^+\mu^-)<2.9\times10^{-6}$, and $\mathcal{B}(D^+\to\pi^+e^-\mu^+)<3.6\times10^{-6}$, see text for the LFV decays in LQ models.

The integrated branching ratios for rare semileptonic D decays are provided in table 4.8. We observe that different classes give distinguishable predictions. The pattern (i) allows for limited effects. For each mode the induced branching ratios can be above the SM predictions and, apart from $\mathcal{B}(D^0\to\mu^+\mu^-)$, close to the experimental limits. Only $\mathcal{B}_{D^+\to\pi^+e^+e^-}$ and $\mathcal{B}_{D^0\to e^+e^-}$ are SM-like in any case. Note that these results are optimistic in contrast to the statement of [193]. The dineutrino mode can be induced via $S_{2,3}$, $\tilde{V}_2$, and V_3. Therefore, we sum the lepton flavors and remind the experimental cut due to resonant $D\to\tau(\to\pi\nu)\nu$ decays, see section 3.4. Recall that $\mathcal{B}_{D^0\to\mu^+\mu^-}\sim\mathcal{O}(10^{-13})$ in the SM. Note that one may distinguish between different LQ models by the q^2-shape of the observables which are different for the various induced Wilson coefficients, see appendix C and table 4.3. Furthermore, note that the lepton charge asymmetry for $D\to Pe^\pm\mu^\mp$ and $D^0\to e^\pm\mu^\mp$ may be non-zero due to different couplings but also due to different signs in the distributions, see eqs. (C.63) and (C.69), respectively.

We have already identified the resonance catalyzed CP asymmetry as an approximate SM null test in section 3.2.3. The $D^+\to\pi^+\mu^+\mu^-$ CP asymmetry for the pattern (ii) is shown in figure 4.4. We observe that the CP asymmetry can be sizable for large imaginary Wilson coefficients. Nevertheless, also small Wilson coefficients, as in the class (ii.2), which comes with an interface to b physics, can be probed if sizable phases are present. In particular, a non-vanishing CP asymmetry can arise around the ϕ resonance, independent of strong phases. For the pattern (i) the CP asymmetry is $\lesssim 0.003$ on the ϕ resonance, and $\lesssim 0.03$ at high q^2.

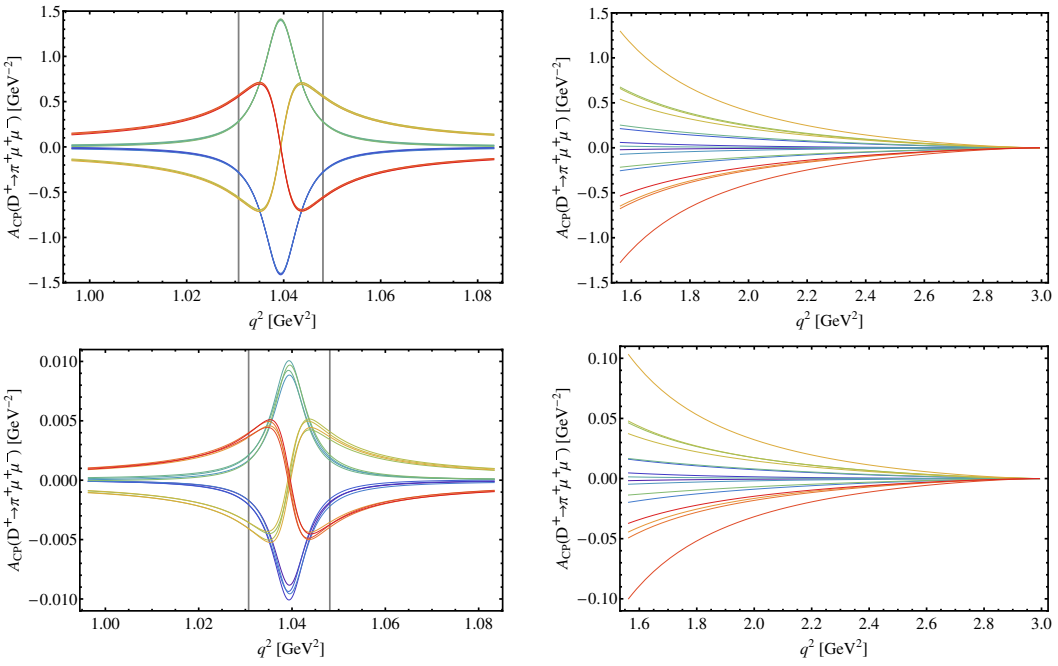

Figure 4.4.: Direct CP asymmetry for $D^+ \to \pi^+\mu^+\mu^-$ normalized to the decay rate that is integrated over $[q^2_{\rm min} = (m_\phi - 5\Gamma_\phi)^2,\ q^2_{\rm max} = (m_\phi + 5\Gamma_\phi)^2]$ (left plots) and $[q^2_{\rm min} = 1.25^2\,{\rm GeV}^2,\ q^2_{\rm max} = (m_{D^+} - m_{\pi^+})^2]$ (right plots) for the classes (ii.1) (upper plots) and (ii.2) (lower plots), see text. From yellow (upper curves above ϕ) to red (lower curves above ϕ) each bunch represents $\delta_\phi = \pi/2, \pi, 0, 3/2\pi$, where a further splitting follows from $\delta_\rho \in \{0, \pi/2, \pi, 3\pi/2\}$. The vertical lines in the left plots indicate $(m_\phi \pm \Gamma_\phi)^2$.

Finally, also decays involving τ leptons at tree level can be probed via $D^0 \to \tau^\pm e^\mp$ decays. From eq. (C.69) one obtains the branching ratio as

$$\begin{aligned}\mathcal{B}_{D^0\to\tau^\pm e^\mp} \simeq 5\times 10^{-9}\big(&|1.3(K_S^{(\tau e/e\tau)} - K_S^{\prime(\tau e/e\tau)}) \mp (K_9^{(\tau e/e\tau)} - K_9^{\prime(\tau e/e\tau)})|^2 \\ &+ |1.3(K_P^{(\tau e/e\tau)} - K_P^{\prime(\tau e/e\tau)}) + K_{10}^{(\tau e/e\tau)} - K_{10}^{\prime(\tau e/e\tau)}|^2\big)\,. \end{aligned} \tag{4.24}$$

The strongest constraints emerge from $SU(2)_L$ relations, yielding $|K_{9,10}^{(\tau e,e\tau)}| \lesssim 4\times 10^{-3}$ ($\mathcal{B}(K^+\to\pi^+\bar\nu\nu)$), $|K_{9,10}^{\prime(\tau e,e\tau)}| \lesssim 0.2$ ($\mathcal{B}(\tau\to eK)$) and $|K_{S,P}^{(\prime)(\tau e,e\tau)}| \lesssim 7\times 10^{-3}$ ($\mathcal{B}(K^+\to \bar e\nu)$), which are obtained from [238]. Thus, the pattern (i) gives $\mathcal{B}(D^0\to\tau^\pm e^\mp) \lesssim 7\times 10^{-15}$, which is zero for the patterns (ii) and (iii). No experimental data is currently available.

A pattern to bypass the constraints the $SU(2)_L$ relations and to obtain sizable branching ratios is, inspired by [235],

$$\lambda_{iv} \sim \begin{pmatrix} 0 & 0 & * \\ * & 0 & 0 \\ * & 0 & 0 \end{pmatrix}. \tag{4.25}$$

This pattern yields SM-like $c\to u l^+ l^-$ induced decays, where $l\in\{e,\mu\}$, and vanishing $c\to u e^\pm\mu^\mp$ induced modes, whereas $c\to u\nu\bar\nu$ induced branching ratios can be sizable.

4.4. Probes with rare radiative D decays

Firstly, we extend the analysis of the previous section by considering $D\to V\gamma$ decays in LQ models, thus probing the magnetic operators. In a further step we also obtain predictions in SUSY models. Presently it is not clear if the experimental data on the branching ratio of $D^0\to\rho^0\gamma$ exhibit a discrepancy with the SM due to uncertainties of non-perturbative contributions. In view of future data we give predictions for the branching ratios. Possible signals from BSM physics can be cleaner revealed in CP asymmetries, where the SM contribution is negligible at the current state of precision.

In contrast to the tree level induced operators discussed in the previous sections radiative decays are only induced at loop level. In particular, the τ lepton directly contributes. From the constraints listed in appendix G and the coefficients found in section 4.2.1 one obtains for e,μ leptons $|\delta_{\langle\tilde V_1\rangle}A_7|_{e,\mu} \lesssim 0.002$, $|\delta_{\langle\tilde V_2\rangle}A_7'|_{e,\mu} \lesssim 0.002$, and $|\delta_{\langle S_{1,2,3}\rangle}A_7^{(\prime)}|_{e,\mu} \lesssim \mathcal{O}(10^{-5})$. Effects from $V_{2,3}$ are negligible in any case. The constraints for τ leptons are generically softer, e.g. assuming smaller couplings to electrons and muons, we obtain $|\delta_{S_{1,2}}|_\tau \lesssim \mathcal{O}(0.001)$, $|\delta_{\langle\tilde V_1\rangle}A_7|_\tau \lesssim 0.04$ and $|\delta_{\langle\tilde V_2\rangle}A_7'|_\tau \lesssim 0.02$. Here we further assumed phases to evade the constraints from $D^0-\bar D^0$ mass difference, which would otherwise yield $|\delta_{\langle S_1L,S_2L,S_2R\rangle}A_7^{(\prime)}|_\tau \lesssim \mathcal{O}(10^{-4})$. Only for S_1L and S_3 bounds on the τ couplings are stronger, yielding $|\delta_{\langle S_1L,S_3\rangle}A_7'|_\tau \lesssim \mathcal{O}(10^{-6})$. The impact from four

quark operators, as given by eq. (4.17), is negligible in the RG-improved perturbation theory due to double insertions of the operator $O^{(l)}$, see section 4.2.1.

We conclude that in LQ models the $c \to u\gamma$ induced branching ratios and the photon polarization are SM-like. However, $S_{1,2}$, and $\tilde{V}_2$ may induce CP asymmetries $\sim \mathcal{O}(0.01)$ which are SM-like for S_3, and $V_{1,2}$. The largest CP asymmetries $\sim \mathcal{O}(0.1)$ are possible for $\tilde{V}_1$.

A characteristic of LQ models is that magnetic operators are induced via a heavy and a light particle, i.e. the LQ and a SM lepton, in the loop. In particular, a helicity flip requires a mass insertion of participating particles, i.e. the lepton mass. Another class of BSM models constitute two heavy particles in the loop, hence a mass suppression is generically avoided. As an example we study SUSY models within the mass insertion approximation (MIA) [239]. In particular, we only consider leading gluino contribution, but note that charginos and neutralinos are negligible in, e.g., the minimal SUSY SM [240].

The induced Wilson coefficients at the BSM scale can be obtained from [239] as

$$
\begin{aligned}
\delta_{\rm MIA} C_3^{(\prime)}(M) &= -\frac{1}{8\sqrt{2}G_F}\frac{\alpha_s^2}{m_{\tilde{q}}^2}(\delta_{12}^u)_{LL(RR)}\left(B_1 - \frac{1}{2}B_2 - \frac{1}{9}P_1 - P_2\right), \\
\delta_{\rm MIA} C_4^{(\prime)}(M) &= -\frac{1}{8\sqrt{2}G_F}\frac{\alpha_s^2}{m_{\tilde{q}}^2}(\delta_{12}^u)_{LL(RR)}\left(-\frac{5}{3}B_1 + \frac{5}{6}B_2 + \frac{5}{27}P_1 + \frac{5}{3}P_2\right), \\
\delta_{\rm MIA} C_5^{(\prime)}(M) &= -\frac{1}{8\sqrt{2}G_F}\frac{\alpha_s^2}{m_{\tilde{q}}^2}(\delta_{12}^u)_{LL(RR)}\left(\frac{8}{3}B_1 - \frac{26}{3}B_2 - \frac{10}{9}P_1 - 10P_2\right), \\
\delta_{\rm MIA} C_6^{(\prime)}(M) &= -\frac{1}{8\sqrt{2}G_F}\frac{\alpha_s^2}{m_{\tilde{q}}^2}(\delta_{12}^u)_{LL(RR)}\left(-\frac{184}{9}B_1 + \frac{58}{9}B_2 + \frac{50}{27}P_1 + \frac{50}{3}P_2\right), \\
\delta_{\rm MIA} C_7^{(\prime)}(M) &= -\frac{2}{3\sqrt{2}G_F}\frac{\alpha_s\pi}{m_{\tilde{q}}^2}\left((\delta_{12}^u)_{LL(RR)}\,\frac{8}{3}M_3 + (\delta_{12}^u)_{LR(RL)}\,\frac{m_{\tilde{g}}}{m_c}\frac{8}{3}M_1\right), \\
\delta_{\rm MIA} C_8^{(\prime)}(M) &= -\frac{1}{\sqrt{2}G_F}\frac{\alpha_s\pi}{m_{\tilde{q}}^2}\left((\delta_{12}^u)_{LL(RR)}\,\left(-\frac{1}{3}M_3 - 3M_4\right)\right. \\
&\qquad \left. + (\delta_{12}^u)_{LR(RL)}\,\frac{m_{\tilde{g}}}{m_c}\left(-\frac{1}{3}M_1 - 3M_2\right)\right),
\end{aligned}
\tag{4.26}
$$

where

$$
\begin{aligned}
B_1 &= \frac{1+4x-5x^2+4x\ln x+2x^2\ln x}{8(1-x)^4}\,, & B_1(x=1) &= \frac{1}{48}\,,\\
B_2 &= x\frac{5-4x-x^2+2\ln x+4x\ln x}{2(1-x)^4}\,, & B_2(x=1) &= -\frac{1}{12}\,,\\
P_1 &= \frac{1-6x+18x^2-10x^3-3x^4+12x^3\ln x}{18(x-1)^5}\,, & P_1(x=1) &= -\frac{1}{30}\,,\\
P_2 &= \frac{7-18x+9x^2+2x^3+3\ln x-9x^2\ln x}{9(x-1)^5}\,, & P_2(x=1) &= \frac{1}{30}\,,\\
M_1 &= 4B_1\,,\\
M_2 &= -xB_2\,,\\
M_3 &= \frac{-1+9x+9x^2-17x^3+18x^2\ln x+6x^3\ln x}{12(x-1)^5}\,, & M_3(x=1) &= \frac{1}{40}\,,\\
M_4 &= \frac{-1-9x+9x^2+x^3-6x\ln x-6x^2\ln x}{6(x-1)^5}\,, & M_4(x=1) &= \frac{1}{60}\,.
\end{aligned}
\tag{4.27}
$$

Here $m_{\tilde{q}}$ is the average squark mass, where the individual masses are assumed to be approximately degenerate, and $m_{\tilde{g}}$ is the gluino mass. Furthermore, $x = m_{\tilde{g}}^2/m_{\tilde{q}}^2$ and $M \sim m_{\tilde{g},\tilde{q}}$.

The mass insertions δ^u_{12} are constrained by data on the $D^0 - \bar{D}^0$ mass difference, see appendix A. We consider the two cases ($m_{\tilde{g}}^{(i)} = 1\,\text{TeV}$, $m_{\tilde{q}}^{(i)} = 2\,\text{TeV}$) and ($m_{\tilde{g}}^{(ii)} = 2\,\text{TeV}$, $m_{\tilde{q}}^{(ii)} = 1\,\text{TeV}$) to obtain via [239]

$$
\begin{aligned}
&\sqrt{\left|\text{Re}(\delta^{u(i)}_{12})^2_{LL,RR}\right|} \lesssim 0.05\,, \quad \sqrt{\left|\text{Re}(\delta^{u(i)}_{12})^2_{LR,RL}\right|} \lesssim 0.07\,,\\
&\sqrt{\left|\text{Re}\left[(\delta^{u(i)}_{12})_{LL}(\delta^{u(i)}_{12})_{RR}\right]\right|} \lesssim 0.02\,,
\end{aligned}
\tag{4.28}
$$

$$
\begin{aligned}
&\sqrt{\left|\text{Re}(\delta^{u(ii)}_{12})^2_{LL,RR}\right|} \lesssim 0.2\,, \quad \sqrt{\left|\text{Re}(\delta^{u(ii)}_{12})^2_{LR,RL}\right|} \lesssim 0.02\,,\\
&\sqrt{\left|\text{Re}\left[(\delta^{u(ii)}_{12})_{LL}(\delta^{u(ii)}_{12})_{RR}\right]\right|} \lesssim 0.02\,.
\end{aligned}
\tag{4.29}
$$

These constraints yield $|\delta^{(i),(ii)}_{\text{MIA}} C^{(\prime)}_{3-6}(M)| \lesssim 10^{-5}$, negligible. On the oder hand, as $\delta_{\text{MIA}} C^{(\prime)}_{7,8}(M) \sim (\delta^u_{12})_{LR,RL}\frac{m_{\tilde{g}}}{m_c}$ one finds $|\delta^{(i)}_{\text{MIA}} A^{(\prime)}_7| \lesssim 0.2$ and $|\delta^{(ii)}_{\text{MIA}} A^{(\prime)}_7| \lesssim 0.3$. We add that $|\delta_{\text{MIA}} A^{(\prime)}_7/\delta_{\text{MIA}} A^{(\prime)}_8| \in [0.75, 5.46]$, where the lower and upper limits are for $x \gtrsim 10$ and $x \lesssim 0.01$, respectively.

Moreover, [241] found $\sqrt{\left|\text{Im}(\delta^{u(ii)}_{12})^2_{LR,RL}\right|} \lesssim 0.0025$ at 95% CL for $m_{\tilde{q}} = m_{\tilde{g}} = 1\,\text{TeV}$. This limit is based on the parameters $|q/p| \in [0.981, 1.058]$ and $\phi[^\circ] \in [-1.8, 0.6]$ at 95%

CL [242], which are presently relaxed as $|q/p| \in [0.77, 1.12]$ and $\phi(^\circ) \in [-30.2, 10.6]$ at 95% CL [97]. Furthermore, constraints from ϵ'/ϵ and chargino loops are model-dependent, e.g. [243], yet not stronger than corresponding bounds from $D^0 - \bar{D}^0$ mixing.

Thus, the constraints found for $\delta_{\rm MIA} A_7^{(\prime)}$ are similar to the model-independent bounds of section 4.1, and the limits on $\delta A_8^{(\prime)}$ are satisfied. We conclude that generic SUSY models may show up in $c \to u\gamma$ induced branching ratios and CP asymmetries, being above the SM predictions and close to the experimental limits. Moreover, a photon polarization $P_\gamma \in [-1, 1]$ may be induced. Indeed, in a specific SUSY model the experimental data on $\mathcal{B}(D^0 \to \rho^0\gamma)$ may already constrain parameters. Furthermore, keep in mind that additional constraints may have to be taken into account, e.g. for the minimal SUSY SM with SUSY breaking [240].

4.5. Probes with $\Lambda_c \to p\gamma$

In this section we discuss possibilities to discover BSM physics in $\Lambda_c \to p\gamma$ decays. A calculation of the SM contribution may be done elsewhere, but it is most likely dominated by non-perturbative physics. Nevertheless, we estimate the branching ratio on general grounds. The expressions for the branching ratio of the decay $\Lambda_c \to p\gamma$ is the same as for $D^0 \to \rho^0\gamma$ decays, see e.g. [244] and eq. (3.39). Thus, we write

$$\mathcal{B}_{\Lambda_c \to p\gamma} = r(\Lambda_c \to p\gamma / D^0 \to \rho^0\gamma)\, \mathcal{B}(D^0 \to \rho^0\gamma) \sim \mathcal{O}(10^{-5})\,, \tag{4.30}$$

where $\mathcal{B}(D^0 \to \rho^0\gamma)$ is given by experimental data. Here infer the ratio of the two modes for common decay mechanisms as follows: WA gives $r(\Lambda_c \to p\gamma / D^0 \to \rho^0\gamma) \sim \sqrt{2}$ due to color counting, which is even larger for radiative D decays, see section 3.3.1. Considering the amplitude $A^{\rm III, \Lambda_c \to p\gamma}$ [245] suggests $r(\Lambda_c \to p\gamma / D^0 \to \rho^0\gamma) \sim 1$ for resonant decays. Finally, perturbative contributions, including BSM dynamics, yield $r(\Lambda_c \to p\gamma / D^0 \to \rho^0\gamma) \simeq \sqrt{2} f_\perp / T \sim 1$. Here, the form factor $f_\perp = f_\perp^T(0) = f_\perp^{T5}(0)$ is defined as in [246], and it is calculated within QCD LCSR [186] [187], a covariant confined quark model [247] and a relativistic quark model [188]. The estimate given by eq. (4.30) is in agreement with $\mathcal{B}(\Lambda_c \to p\gamma) = 2.2 \times 10^{-5}$ found in the constituent quark model [248]. We only utilize the branching ratio to infer experimental sensitivities. Ultimately, the branching ratio has to be measured, e.g. at the forthcoming Belle II, where the cross section $\sigma(e^+e^- \to \bar{c}c) \simeq 1.3\,\text{nb}$ and a luminosity $L \simeq 5\,\text{ab}^{-1}$ within one year [249] indicate a number of $N = [10^4, 10^5]$ decays.

For the remainder of the current section we focus on an observable which, not accessible in rare D decays, is induced by the spin of the decaying charmed particle, i.e. the Λ_c baryon, once the particle is produced polarized. Following [244], an angular asymmetry can be defined in the Λ_c rest frame by the angle between the Λ_c spin and the proton

momentum, that is the forward-backward asymmetry of the photon momentum relative to the Λ_c boost, normalized to the total width by

$$A^\gamma = -\frac{P_{\Lambda_c}}{2}\frac{1-|r|^2}{1+|r|^2}\,, \tag{4.31}$$

where $r = A_7'/A_7$.

Here the longitudinal polarization of the Λ_c, P_{Λ_c}, is presently not measured. Nonetheless, it can be parametrized in terms of the polarization of the charm quark, P_c, as [250–252]

$$\frac{P_{\Lambda_c}}{P_c} \simeq \frac{1+A(0.07+0.46\omega_1)}{1+A}\,, \tag{4.32}$$

where $A \simeq 1.1$ is extrapolated [251] from a measurement by the E791 collaboration [253], and $\omega_1 = 0.71 \pm 0.13$ is measured by the CLEO collaboration [254], yielding $P_{\Lambda_c}/P_c \simeq 0.68 \pm 0.03$. Furthermore, the parameters A and ω_1 are measurable at Atlas, BaBar, Belle, CMS and LHCb [251]. Note that P_{Λ_c}/P_c is approximately scale independent and it can be related to fragmentation functions [251] (and references therein). At the Z pole, where $P_c^{(Z)} \simeq -0.65$ [255], one obtains

$$P_{\Lambda_c}^{(Z)} \simeq -0.44 \pm 0.02\,. \tag{4.33}$$

Note that $P < 0$ by means of a left-handed polarization. In Z decays (0.0305 ± 0.0045) $c\bar{c}$ are produced via gluon splitting [21], hence this depolarization effect is negligible. In principle, one can also include a depolarization due to $\Lambda_{c1}^{(\prime)}$ decaying strongly into Λ_c, which induces additional parameters B and $\tilde{\omega}_1$, [256, 257]. However, no experimental data are available, thus we neglect its contribution. The Λ_c polarization is directly measurable, e.g. via $\Lambda_c \to \Lambda(\to p\pi)l\nu$ decays, where $\mathcal{B}(\Lambda_c \to \Lambda(\to p\pi)e\nu_e) = 0.023$ [21] and, in particular, at Atlas, CMS, and LHCb via $pp \to t(\to bW^+(\to c\bar{s}))\bar{t}(\to \bar{b}W^-(\to l^-\bar{\nu}))$ [251] and $pp \to W^-c$ [252] production with $P_c^{(W^-)} \simeq -0.97$ [255]. Note that eq. (4.33) indicates a sizable, non-zero, polarization that, ultimately, needs to be measured.

The observable A^γ can be extracted in the laboratory frame for a boost $\vec{\beta} = \vec{p}_{\Lambda_c}/E_{\Lambda_c}$, where $\vec{p}$ and E denote is the three momentum and energy, respectively, by

$$\langle q_\parallel \rangle_{|\vec{\beta}|} = \gamma E_\gamma^* \left(\left|\vec{\beta}\right| + \frac{2}{3}A^\gamma \right)\,. \tag{4.34}$$

Here $\langle q_\parallel \rangle_{|\vec{\beta}|}$ is the average longitudinal momentum of the photon in the laboratory frame relative to the boost axis, $\gamma = 1/\sqrt{1-|\vec{\beta}|^2}$, and $E_\gamma^* = (m_{\Lambda_c}^2 - m_p^2)/(2m_{\Lambda_c}) \simeq 0.95\,\mathrm{GeV}$ is the photon energy in the Λ_c rest frame. The statistical uncertainty is given by

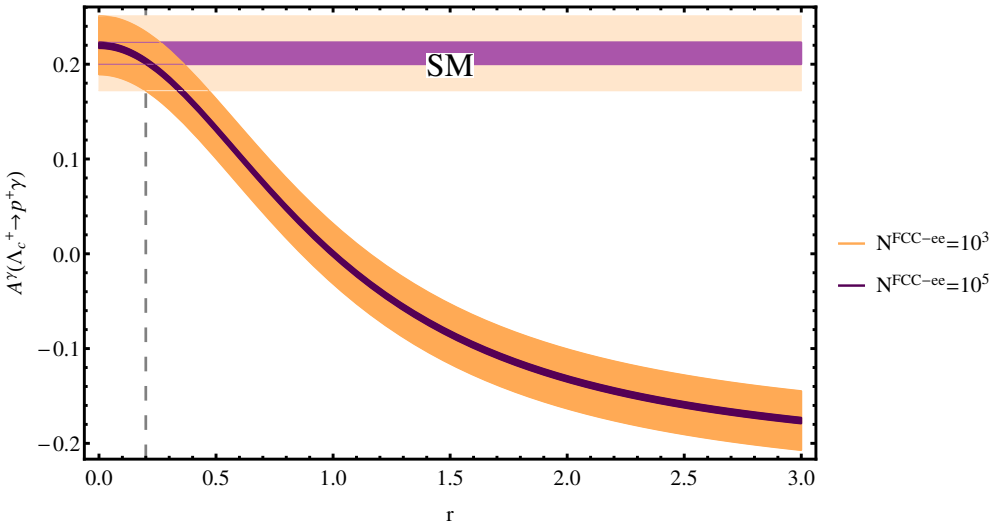

Figure 4.5.: Angular asymmetry of $\Lambda_c \to p\gamma$ as a function of $r = A_7'/A_7$ taking $P_{\Lambda_c} = -0.44$. It approaches $P_{\Lambda_c}/2$ as $r \to \infty$. The bands represent the statistical uncertainties for 10^3 (orange curved band) and 10^5 decays (purple curved band). Within the SM and LQ models $A^\gamma(r \lesssim 0.2)$, which are represented by the lighter horizontal bands and the dashed vertical line. For SUSY models $A^\gamma(|r| \lesssim \mathcal{O}(1))$ covers the shown range.

$\delta A^\gamma = \sqrt{1-(A^\gamma)^2}/\sqrt{N}$ for N decays of $\Lambda_c \to p\gamma$. To estimate the latter we neglect reconstruction efficiencies to find

$$N = N(c\bar{c})\, f(c \to \Lambda_c)\, \mathcal{B}_{\Lambda_c \to p\gamma} \sim N(c\bar{c}) \times 10^{-6}\,, \tag{4.35}$$

where $f(c \to \Lambda_c) \simeq 0.06$ [258] is the fragmentation function, which is insensitive to the production process, and $N(c\bar{c})$ denotes the number of produced $c\bar{c}$. At a future e^+e^- collider operating at the Z pole, i.e. an FCC-ee with $N(Z) \sim 10^{12}$ within one year [259] and $\mathcal{B}(Z \to c\bar{c}) \simeq 0.12$ [21]. Thus, it would allow for sizable statistics to measure the branching ratio of $\Lambda_c \to p\gamma$, the polarization P_{Λ_c} as well as the angular asymmetry A^γ.

The above considerations suggest to measure A^γ, hence testing the handedness of the $c \to u\gamma$ current and models beyond the SM. The angular asymmetry is shown in figure 4.5, where $P_{\Lambda_c} = -0.44$ is assumed. From the analysis of section 3.3 we infer $r \lesssim 0.2$ for SM-like scenarios, and $A_7^{(\prime)} \sim \delta C_7^{(\prime)}$ for large BSM effects. We observe that A^γ is a complementary observable to search for right-handed currents and to distinguish between different models. In particular, $A^\gamma > 0$ in the SM. On the other side, SUSY models, see section 4.4, may induce significant deviations, including a flip of the sign, which is observable already for $N = 10^3$.

5. Conclusion and outlook

This thesis comprises a study of FCNC transitions of charm quarks. Chapters 2 and 3 are dedicated to the calculation of Wilson coefficients in the framework of the effective weak Lagrangian and predictions for observables within the SM, respectively. The chapters are summarized in sections 2.9 and 3.4. The main observations are:

- The SM Wilson coefficients are known to (partly) NNLL order, where the missing pieces of NNLO are negligible in phenomenological applications.
- A longstanding inconsistency in the treatment of light quarks within the effective theory, which affects the Wilson coefficients to a considerable extent is resolved.
- A novel calculation of two loop matrix elements is presented, which yields the dominant perturbative contribution in phenomenological applications. However, a breakdown of the perturbation theory for $c \to u$ transitions cannot be deduced, as lower order contributions are more strongly GIM suppressed. Nonetheless, sizable perturbative corrections are indicated.
- Whereas the perturbative calculation is state-of-the-art, the branching ratios for $c \to u\gamma$ and $c \to ull$ induced decays are dominated by non-perturbative effects, which are presently not known from first principles and accompanied with sizable uncertainties.
- On the other hand, angular observables and asymmetries that are (approximate) null tests of the SM, including the non-perturbative uncertainties, can be constructed. This observation is characteristic for rare charm decays due to the structure of the Wilson coefficients and the CKM matrix, e.g. the GIM mechanism.

In view of the BSM potential, see chapter 4, the modes and observables considered are competitive and complementary to each other as well as b physics, while being sensitive to different types of BSM physics, see section 4.1. To mention the main issues: Basically any sizable BSM effect is visible in the decay $D^+ \to \pi^+\mu^+\mu^-$ at high q^2. Smaller effects may be observed in CP asymmetries once sizable BSM phases are present. Presently, any signal in angular observables, dineutrino and LFV modes can be assigned to BSM physics. LQ models, see section 4.2.1, are an instructive example where sizable BSM effects close to the experimental reach are possible. Nonetheless, the different LQ models can be distinguished by experimental data, see sections 4.3 and 4.4. Further correlations

with, e.g., kaon and b physics, see section 4.3, may add valuable information to reveal the source of the present SM anomalies in b decays as well as, ultimately, to identify the origin of flavor. SUSY models constitute a second example with similar signatures as LQ models, see section 4.2. Nevertheless, both models are distinguishable in radiative decays, where SUSY models can induce larger deviations from the SM, see sections 4.4 and 4.5.

To conclude this thesis, we comment on the present status and on future prospects of rare charm decays, which uniquely probe the up-type sector. The current available methods and techniques for calculating SM contributions seem to be exhausted. Nevertheless, a few improvements as noted in this thesis are possible. Further ones include, e.g., the identification of additional observables and lattice calculations. SM predictions are generically vague due to our deficiency of understanding QCD, where theoretical ideas are welcome. Nonetheless, striking observations of BSM physics are possible and assisted by various hadronic and BSM models. Further models, including flavor patterns on the BSM side, may be studied. Irrespective of the potential for BSM searches, charm physics are also important probes of QCD. We emphasize that experimental searches in all modes and observables are desirable, as they allow to improve the theoretical understanding, to detect different types of BSM physics and, once revealed, to identify its underlying model. Despite the experimental effort only one charm FCNC induced mode, i.e. $D^0 \to \rho^0\gamma$, was recently observed. Nevertheless, other modes, e.g. $D^+ \to \pi^+\mu^+\mu^-$, are planned to be measured and call for imminent detection. It is desirable to include rare charm decays, e.g. $\Lambda_c \to p\gamma$, in (future) experimental programs. In this respect theoretical studies on, e.g., $D \to Vll$, $D \to PPll$ and $\Lambda_c \to pll$ decays will support experimental searches.

A. Parameters

As a rule at hand, we give parameters within 68% CL in the Bayesian/Frequentist language. We neglect uncertainties if their numerical effect is negligible. Their distributions are taken to be uniform. If uncertainties σ_i are added, we take them as uncorrelated and add them in quadrature, i.e. $\sigma = \sqrt{\sum \sigma_i^2}$. Upper limits are given at 90% CL or 95% CL as stated, which multiplied with 0.60 or 0.51, respectively, yield limits at 68% CL.

The parameters used for the calculation of the SM Wilson coefficients, see chapter 2, are given by [21]

$$\begin{aligned}
&m_t(m_t) = (160^{+5}_{-4})\,\text{GeV}\,,\\
&m_Z = 91.19\,\text{GeV}\,,\\
&m_W = 80.4\,\text{GeV}\,,\\
&m_b(m_b) = (4.18^{+0.04}_{-0.03})\,\text{GeV}\,,\\
&m_c(m_c) = (1.27 \pm 0.03)\,\text{GeV}\,,\\
&m_s(2\,\text{GeV}) = (0.096^{+0.008}_{-0.004})\,\text{GeV}\,,\\
&\alpha_s(m_Z) = 0.1182 \pm 0.0012\,,\\
&\alpha_e = 7.297\,352\,57 \times 10^{-3}\,,\\
&\sin^2\theta_w(m_Z) = 0.2313\,,\\
&G_F = 1.166\,379 \times 10^{-5}\,\text{GeV}^{-2}\,,
\end{aligned} \tag{A.1}$$

where $m(\mu)$ denotes a $\overline{\text{MS}}$ mass. The NNLO QCD running and decoupling at flavor thresholds is taken from [260].

The CKM matrix as obtained by the UTfit collaboration [45] via a Bayesian fit reads

$$\begin{aligned}
V_{ud} &= 0.974\,31 \pm 0.000\,15\,,\\
V_{us} &= 0.225\,12 \pm 0.000\,67\,,\\
V_{ub} &= (0.003\,65 \pm 0.000\,12)\exp[i(-65.88 \pm 1.88)^\circ]\,,\\
V_{cd} &= (-0.224\,97 \pm 0.000\,67)\exp[i(0.0352 \pm 0.0010)^\circ]\,,\\
V_{cs} &= (0.973\,44 \pm 0.000\,15)\exp[i(-0.001\,877 \pm 0.000\,055)^\circ]\,,\\
V_{cb} &= 0.042\,55 \pm 0.000\,69\,.
\end{aligned} \tag{A.2}$$

For a Frequentist fit, see the CKMfitter group [261].

In the calculation of the inclusive branching ratios we use inclusive semileptonic branching ratios as a normalization, see section 3.1. The inclusive $c \to d$ induced branching ratios for massless leptons are obtained from a sum of the corresponding exclusive modes [21],

$$\begin{aligned}
\mathcal{B}(D^+ \to X_d e\nu) &= \mathcal{B}(D^+ \to \pi^0 e^+\nu) + \mathcal{B}(D^+ \to \rho^0 e^+\nu) + \mathcal{B}(D^+ \to \omega e^+\nu) \\
&\quad + \mathcal{B}(D^+ \to \eta e^+\nu) + \mathcal{B}(D^+ \to \eta' e^+\nu) = 0.00928^{+0.00035}_{-0.00029}\,, \\
\mathcal{B}(D^0 \to X_d e\nu) &= \mathcal{B}(D^0 \to \pi^- e^+\nu) + \mathcal{B}(D^0 \to \rho^- e^+\nu) = 0.004\,68 \pm 0.000\,16\,, \\
\mathcal{B}(D_s \to X_d e\nu) &= \mathcal{B}(D_s \to K^0 e^+\nu) + \mathcal{B}(D_s \to K^{*0} - e^+\nu) \\
&= 0.0057 \pm 0.0010\,.
\end{aligned} \tag{A.3}$$

Due to missing experimental information we take for muons [21]

$$\begin{aligned}
\mathcal{B}(D^+ \to X\mu^+) &= 0.176 \pm 0.032\,, \\
\mathcal{B}(D^0 \to X\mu^+) &= 0.067 \pm 0.006\,,
\end{aligned} \tag{A.4}$$

as approximations of the corresponding $c \to (d, s)$ induced semileptonic modes. The approximation $\mathcal{B}(D \to X\mu^+\nu_\mu) = \mathcal{B}(D \to X\mu^+)$ is justified as the branching ratios of the leptonic modes $\sim \mathcal{O}(10^{-4})$ [21]. Since no corresponding branching ratio for D_s is measured we assume $\mathcal{B}(D_s \to X\mu^+\nu_\mu) \simeq \mathcal{B}(D_s \to Xe^+)$, where [21]

$$\mathcal{B}(D_s \to Xe^+) = 0.065 \pm 0.004\,. \tag{A.5}$$

Comparing the measured muonic modes given by eq. (A.4) with $\mathcal{B}(D^+ \to Xe^+) = 0.1607 \pm 0.0030$, and $\mathcal{B}(D^0 \to Xe^+) = 0.0649 \pm 0.0011$ [21] suggests that the approximation for the $D_s \to X\mu^+\nu_\mu$ branching ratio, eq. (A.5), yields a slightly smaller branching ratio.

Further used particle masses and total widths, where $\Gamma = \hbar/\tau$, are [21]

$$
\begin{aligned}
&m_{\Lambda_c^+} = 2.286\,\mathrm{GeV}\,, && \\
&m_{D_s^*} = 2.112\,\mathrm{GeV}\,, && \\
&m_{D^{*+}} = 2.0103\,\mathrm{GeV}\,, && \\
&m_{D^{*0}} = 2.0069\,\mathrm{GeV}\,, && \\
&m_{D_s} = 1.968\,\mathrm{GeV}\,, && \tau_{D_s} = (500 \pm 7) \times 10^{-15}\,\mathrm{s}\,, \\
&m_{D^+} = 1.8696\,\mathrm{GeV}\,, && \tau_{D^+} = (1040 \pm 7) \times 10^{-15}\,\mathrm{s}\,, \\
&m_{D^0} = 1.8648\,\mathrm{GeV}\,, && \tau_{D^0} = (410.1 \pm 1.5) \times 10^{-15}\,\mathrm{s}\,, \\
&m_{\tau} = 1.777\,\mathrm{GeV}\,, && \tau_{\tau} = (290.3 \pm 0.5) \times 10^{-15}\,\mathrm{s}\,, \\
&m_{\phi} = 1.0195\,\mathrm{GeV}\,, && \Gamma_{\phi} = (4.2660 \pm 0.0311) \times 10^{-3}\,\mathrm{GeV}\,, \\
&m_{\eta'} = 0.9578\,\mathrm{GeV}\,, && \Gamma_{\eta'} = (1.97 \pm 0.09) \times 10^{-4}\,\mathrm{GeV}\,, \\
&m_{p} = 0.938\,272\,08\,\mathrm{GeV}\,, && \\
&m_{K^{*0}} = 0.896\,\mathrm{GeV}\,, && \Gamma_{K^{*0}} = (0.0474 \pm 0.0006)\,\mathrm{GeV}\,, \\
&m_{K^{*+}} = 0.892\,\mathrm{GeV}\,, && \Gamma_{K^{*+}} = (0.0508 \pm 0.0009)\,\mathrm{GeV}\,, \\
&m_{\omega} = 0.783\,\mathrm{GeV}\,, && \Gamma_{\omega} = (8.49 \pm 0.08) \times 10^{-3}\,\mathrm{GeV}\,, \\
&m_{\rho} = 0.775\,\mathrm{GeV}\,, && \Gamma_{\rho} = (0.1491 \pm 0.0008)\,\mathrm{GeV}\,, \\
&m_{\eta} = 0.5479\,\mathrm{GeV}\,, && \Gamma_{\eta} = (1.31 \pm 0.05) \times 10^{-6}\,\mathrm{GeV}\,, \\
&m_{K^0} = 0.4976\,\mathrm{GeV}\,, && \\
&m_{K^+} = 0.4937\,\mathrm{GeV}\,, && \tau_{K^+} = (1.2380 \pm 0.0020) \times 10^{-8}\,\mathrm{s}\,, \\
&m_{\pi^+} = 0.139\,570\,\mathrm{GeV}\,, && \tau_{\pi^+} = (2.6033 \pm 0.0005) \times 10^{-8}\,\mathrm{s}\,, \\
&m_{\pi^0} = 0.134\,977\,\mathrm{GeV}\,, && \tau_{\pi^0} = (8.52 \pm 0.18) \times 10^{-17}\,\mathrm{s}\,, \\
&m_{\mu} = 0.105\,658\,37\,\mathrm{GeV}\,, && \tau_{\mu} = (2.196\,981\,1 \pm 0.000\,002\,2) \times 10^{-6}\,\mathrm{s}\,, \\
&m_{e} = 0.000\,510\,998\,95\,\mathrm{GeV}\,. &&
\end{aligned}
\tag{A.6}
$$

For resonant decays, see section 3.2.2 and appendix E, we use the branching ratios [21]

$$
\begin{aligned}
&\mathcal{B}(D^{*+} \to D^+\pi^0) = 0.307 \pm 0.005\,, \quad \mathcal{B}(D^{*+} \to D^+\gamma) = 0.016 \pm 0.004\,, \\
&\Gamma(D^{*0} \to D^0\pi^0)/\Gamma(D^{*0} \to D^0\gamma) = 1.85 \pm 0.07\,, \\
&\mathcal{B}(D^+ \to \pi^+\eta') = (4.84 \pm 0.31) \times 10^{-3}\,, \\
&\mathcal{B}(D^+ \to \pi^+\rho) = (8.4 \pm 1.5) \times 10^{-4}\,, \\
&\mathcal{B}(D^+ \to \pi^+\eta) = (3.66 \pm 0.22) \times 10^{-3}\,, \\
&\mathcal{B}(\phi \to \mu\mu) = (2.87 \pm 0.19) \times 10^{-4}\,, \\
&\mathcal{B}(\eta' \to \gamma\gamma) = (2.21 \pm 0.08) \times 10^{-2}\,,
\end{aligned}
$$

$$\begin{aligned}
&\mathcal{B}(K^{*0} \to K^0\gamma) = (2.46 \pm 0.21) \times 10^{-3}\,,\\
&\mathcal{B}(K^{*+} \to K^+\gamma) = (9.9 \pm 0.9) \times 10^{-4}\,,\\
&\mathcal{B}(\omega \to \mu\mu) = (9.0 \pm 3.1) \times 10^{-5}\,,\\
&\mathcal{B}(\omega \to \pi^0\gamma) = 0.0828 \pm 0.0028\,,\\
&\mathcal{B}(\rho \to \mu\mu) = (4.55 \pm 0.28) \times 10^{-5}\,,\\
&\mathcal{B}(\rho^0 \to \pi^0\gamma) = (6.0 \pm 0.8) \times 10^{-4}\,, \quad \mathcal{B}(\rho^+ \to \pi^+\gamma) = (4.5 \pm 0.5) \times 10^{-4}\,,\\
&\mathcal{B}(\eta \to \mu\mu) = (5.8 \pm 0.8) \times 10^{-6}\,,
\end{aligned} \tag{A.7}$$

and observed by the BESIII collaboration [262]

$$\mathcal{B}(D^+ \to \omega\pi^+) = (2.79 \pm 0.57 \pm 0.16) \times 10^{-4}\,. \tag{A.8}$$

The decay constants are given by the FLAG [263]

$$\begin{aligned}
f_{D_s} &= (0.248\,83 \pm 0.001\,27)\,\text{GeV}\,,\\
f_D &= (0.212\,15 \pm 0.001\,45)\,\text{GeV}\,,\\
f_K &= (0.1556 \pm 0.0004)\,\text{GeV}\,,\\
f_\pi &= (0.1302 \pm 0.0014)\,\text{GeV}\,,
\end{aligned} \tag{A.9}$$

and by [152, 264] (and references therein)

$$\begin{aligned}
&f_\phi = (0.233 \pm 0.004)\,\text{GeV}\,,\\
&f_{K^*} = (0.204 \pm 0.007)\,\text{GeV}\,, && f_{K^*}^\perp = (0.163 \pm 0.008)\,\text{GeV}\,,\\
&f_\rho = (0.213 \pm 0.005)\,\text{GeV}\,, && f_\rho^\perp = (0.160 \pm 0.011)\,\text{GeV}\,,\\
&f_{\rho^0}^{(d)} = (0.2097 \pm 0.0003)\,\text{GeV}\,,\\
&f_\omega = (0.197 \pm 0.008)\,\text{GeV}\,, && f_\omega^\perp = (0.139 \pm 0.018)\,\text{GeV}\,,\\
&f_\omega^{(d)} = (0.2013 \pm 0.0008)\,\text{GeV}\,,
\end{aligned} \tag{A.10}$$

where the label d indicates the quark content. Here $\mu = 1\,\text{GeV}$ for the transverse decay constants, for which the running can be taken from, e.g., [150].

In the following, we list the experimental data utilized to constrain the LQ couplings in appendix G. We update the nuclear weak charge of Cs [21, 265, 266]

$$\Delta Q_w(\text{Cs}) = 0.69 \pm 0.44\,, \tag{A.11}$$

where $\Delta Q_w = Q_w^{\text{exp}} - Q_w^{\text{SM}}$. We obtain the ratio of leptonic pion decays as

$$\Delta R_{e/\mu} = (-2.5 \pm 2.3) \times 10^{-7}\,, \tag{A.12}$$

where the experimental data $R^{\rm exp}_{e/\mu} = \frac{\Gamma(\pi^+\to(e^+\nu_e+e^+\nu_e\gamma))}{\Gamma(\pi^+\to(\mu^+\nu_\mu+\mu^+\nu_\mu\gamma))} = (1.2327 \pm 0.0023) \times 10^{-4}$ [21], and the SM prediction $R^{\rm SM}_{e/\mu} = (1.2352 \pm 0.0001) \times 10^{-4}$ [267]. The anomalous magnetic moment of the electron is found to be [268]

$$\Delta a(e) = (-0.91 \pm 0.82) \times 10^{-12} \tag{A.13}$$

and the electric dipole moment of Hg is [269]

$$|d(\mathrm{Hg})| < 7.4 \times 10^{-30}\, e\,\mathrm{cm}\,. \tag{A.14}$$

Note that this constraint on Hg implies a slightly stronger model-dependent limit on the neutron magnetic moment, i.e. $d(n) < 1.6 \times 10^{-26}\, e\,\mathrm{cm}$ [269], as compared to the direct bound given in eq. (A.18). The parity odd triple correlation coefficient in Li beta decay is [270]

$$R(\mathrm{Li}) = (0.9 \pm 2.2) \times 10^{-3}\,. \tag{A.15}$$

Other observables are taken from [21], reading

$$\begin{aligned}
&D(n) = (-1.2 \pm 2.0) \times 10^{-4}\,,\\
&R(n) = 0.004 \pm 0.013\,,\\
&\Delta a(\mu) = (288 \pm 80) \times 10^{-11}\,,\\
&d(\mu) = (-0.1 \pm 0.9) \times 10^{-19}\, e\,\mathrm{cm}\,,\\
&|m_{D_1^0} - m_{D_2^0}| = (0.95^{+0.41}_{-0.44}) \times 10^{10}\,\hbar\,\mathrm{s}^{-1}\,,\\
&(\Gamma_{D_1^0} - \Gamma_{D_2^0})/\Gamma_{D^0} = (1.29^{+0.14}_{-0.18}) \times 10^{-2}\,,\\
&\mathcal{B}(D^+ \to \mu^+\nu_\mu) = (3.74 \pm 0.17) \times 10^{-4}\,,\\
&\mathcal{B}(D_s \to \mu^+\nu_\mu) = (5.56 \pm 0.25) \times 10^{-3}\,,\\
&\mathcal{B}(K^+ \to \mu^+\nu_\mu) = (63.56 \pm 0.11) \times 10^{-2}\,,\\
&\Gamma(Z \to \mu^+\mu^-)/\Gamma(Z \to e^+e^-) = 1.0009 \pm 0.0028\,,\\
&\Gamma(Z \to (u\bar{u} + c\bar{c})/2)/\Gamma(Z \to \mathrm{hadrons}) = 0.166 \pm 0.009\,,\\
&\Gamma(Z \to c\bar{c})/\Gamma(Z \to \mathrm{hadrons}) = 0.1721 \pm 0.0030\,, \quad \Gamma^{\rm SM}_{Z\to c\bar{c}}/\Gamma(Z \to \mathrm{hadrons}) = 0.1723\,,\\
&\mathcal{B}(D_s \to \tau^+\nu_\tau) = (5.55 \pm 0.24) \times 10^{-2}\,,\\
&\mathcal{B}(K^+ \to e^+\nu_e) = (1.582 \pm 0.007) \times 10^{-5}\,,\\
&\mathcal{B}(\tau^- \to \pi^+\nu_\tau) = (10.82 \pm 0.05) \times 10^{-2}\,,\\
&\mathcal{B}(\tau^- \to K^+\nu_\tau) = (6.96 \pm 0.10) \times 10^{-2}\,,
\end{aligned} \tag{A.16}$$

where

$$\Gamma(Z \to \mathrm{hadrons}) = 1.74\,\mathrm{GeV}\,. \tag{A.17}$$

Additionally, at CL=90% [21]

$$
\begin{aligned}
&d(n) < 0.30 \times 10^{-25}\, e\,\mathrm{cm}\,,\\
&d(e) < 0.87 \times 10^{-28}\, e\,\mathrm{cm}\,,\\
&\mathcal{B}(D^+ \to e^+\nu_e) < 8.8 \times 10^{-6}\,,\\
&\mathcal{B}(D_s \to e^+\nu_e) < 8.3 \times 10^{-5}\,,\\
&\mathcal{B}(\pi^+ \to \mu^+\nu_e) < 8.0 \times 10^{-3}\,,\\
&\mathcal{B}(K^+ \to \mu^+\nu_e) < 4 \times 10^{-3}\,,\\
&\mathcal{B}(\mu^- \to e^-e^+e^-) < 1.0 \times 10^{-12}\,,\\
&\mathcal{B}(Z \to (e^+\mu^- + e^-\mu^+)) < 7.5 \times 10^{-6}\ @\mathrm{CL} = 95\%\,,\\
&\mathcal{B}(D^+ \to \tau^+\nu_\tau) < 1.2 \times 10^{-3}\,,\\
&\mathcal{B}(\tau^- \to e^-\gamma) < 3.3 \times 10^{-8}\,,\\
&\mathcal{B}(\tau^- \to \mu^-\gamma) < 4.4 \times 10^{-8}\,,\\
&\mathcal{B}(\tau^- \to e^-e^+e^-) < 2.7 \times 10^{-8}\,,\\
&\mathcal{B}(\tau^- \to \mu^-\mu^+\mu^-) < 2.1 \times 10^{-8}\,,\\
&\Gamma(\mu^-\mathrm{Ti} \to e^-\mathrm{Ti})/\Gamma_{\mathrm{capture}}(\mu^-\mathrm{Ti}) < 4.3 \times 10^{-12}\,,\\
&\Gamma(\mu^-\mathrm{Au} \to e^-\mathrm{Au})/\Gamma_{\mathrm{capture}}(\mu^-\mathrm{Au}) < 7 \times 10^{-13}\,,
\end{aligned}
\tag{A.18}
$$

where [271]

$$
\Gamma_{\mathrm{capture}}(\mu^-\mathrm{Ti}) = 2.59 \times 10^6\,\mathrm{s}^{-1}\,, \qquad \Gamma_{\mathrm{capture}}(\mu^-\mathrm{Au}) = 13.07 \times 10^6\,\mathrm{s}^{-1}\,. \tag{A.19}
$$

Furthermore, we use the experimental limit obtained by the MEG collaboration [272]

$$
\mathcal{B}(\mu^+ \to e^+\gamma) < 4.2 \times 10^{-13}\,. \tag{A.20}
$$

Future searches for LFV decays will improve the limits by a few order of magnitude. The MEG-II experiment [273] will test $\mathcal{B}(\mu \to e\gamma)$ to $\mathcal{O}(10^{-14})$, whereas the Mu3e experiment [274] will reach $\mathcal{O}(10^{-16})$ for $\mathcal{B}(\mu \to eee)$. For the $\mu \to e\gamma$ and $\mu \to eee$ experiments the SM background from the transitions $\mu \to e\nu\bar{\nu}\gamma$ [275] and $\mu \to e(e^+e^-)\nu\bar{\nu}$ via internal conversion [276], respectively, may become important. The COMET experiment [277], the DeMee experiment [278] and the Mu2e experiment [279] will probe $\mu - e$ conversion to $\mathcal{O}(10^{17})$.

Finally, we collect experimental data involving charm FCNC transitions at CL=90% [21],

$$\begin{aligned}
&\mathcal{B}(D^+ \to \pi^+ e^+ e^-) < 0.3 \times 10^{-6}\,, && \mathcal{B}(D^+ \to \pi^+ \mu^+ \mu^-) < 7.3 \times 10^{-8}\,,\\
&\mathcal{B}(D^0 \to \pi^0 e^+ e^-) < 4.5 \times 10^{-5}\,, && \mathcal{B}(D^0 \to \pi^0 \mu^+ \mu^-) < 1.8 \times 10^{-4}\,,\\
&\mathcal{B}(D^0 \to \eta e^+ e^-) < 1.1 \times 10^{-4}\,, && \mathcal{B}(D^0 \to \eta \mu^+ \mu^-) < 5.3 \times 10^{-4}\,,\\
&\mathcal{B}(D_s \to K^+ e^+ e^-) < 3.7 \times 10^{-6}\,, && \mathcal{B}(D_s \to\ K^+ \mu^+ \mu^-) < 2.1 \times 10^{-5}\,,\\
&\mathcal{B}(D^0 \to e^+ e^-) < 7.9 \times 10^{-8}\,, && \mathcal{B}(D^0 \to \mu^+ \mu^-) < 6.2 \times 10^{-9}\,,\\
&\mathcal{B}(D^+ \to \pi^+ e^+ \mu^-) < 2.9 \times 10^{-6}\,, && \mathcal{B}(D^+ \to \pi^+ e^- \mu^+) < 3.6 \times 10^{-6}\,,\\
&\mathcal{B}(D^0 \to \pi^0 (e^+ \mu^- + e^- \mu^+)) < 8.6 \times 10^{-5}\,, &&\\
&\mathcal{B}(D_s \to K^+ e^+ \mu^-) < 1.4 \times 10^{-5}\,, && \mathcal{B}(D_s \to K^+ e^- \mu^+) < 9.7 \times 10^{-6}\,,\\
&\mathcal{B}(D^0 \to (e^+ \mu^- + e^- \mu^+)) < 1.3 \times 10^{-8}\,, &&\\
&\mathcal{B}(D^0 \to \omega\gamma) < 2.4 \times 10^{-4}\,, &&
\end{aligned} \tag{A.21}$$

where $B(D^0 \to (e^+\mu^- + e^-\mu^+))$ was obtained by the LHCb collaboration [25], $\mathcal{B}(D^+ \to \pi^+ e^+ e^-)$ was found by BESIII collaboration [138] (preliminary), and the $\sqrt{q^2}$-binned branching ratios of the LHCb collaboration [136] read

$$\begin{aligned}
&\mathcal{B}(D^+ \to \pi^+ \mu^+ \mu^-)_{[0.250,0.525]} < 2.0 \times 10^{-8}\,,\\
&\mathcal{B}(D^+ \to \pi^+ \mu^+ \mu^-)_{[1.250,2.000]} < 2.6 \times 10^{-8}\,.
\end{aligned} \tag{A.22}$$

Additionally, the Belle collaboration measured [24]

$$\mathcal{B}(D^0 \to \rho^0\gamma) = (1.77 \pm 0.30 \pm 0.07) \times 10^{-5}\,, \quad A_{CP} = 0.056 \pm 0.152 \pm 0.006\,. \tag{A.23}$$

Recall that $\mathcal{B}(D^+ \to \pi^+\mu^+\mu^-)$ on the full q^2 range assumes a model dependent phase space interpolation of the low and high q^2 ranges, neglecting resonant interferences, and that the CP asymmetry is mostly direct. The LHCb experiment will probe branching ratios for $D^+ \to \pi^+\mu^+\mu^-$, $D_s \to K^+\mu^+\mu^-$, $D^0 \to \mu^+\mu^-$ and $D^0 \to e\mu$ at the levels of $\mathcal{O}(10^{-9})$, $\mathcal{O}(10^{-8})$, $\mathcal{O}(10^{-10})$ and $\mathcal{O}(10^{-9})$, respectively, as well as asymmetries $\mathcal{O}(0.1\%)$ for $D^+ \to \pi^+\mu^+\mu^-$ [139]. In [193] the future sensitivity of the BESIII experiment is estimated as $\mathcal{O}(10^{-7}) - \mathcal{O}(10^{-6})$ for $D_s \to K^+e^+e^-$ and $D_s \to K^+e\mu$ branching ratios.

B. Renormalization group equation

The RGE for Wilson coefficients C at a scale μ reads

$$\mu \frac{\mathrm{d}}{\mathrm{d}\mu} C(\mu) = \gamma^T C(\mu)\,, \tag{B.1}$$

where γ is the ADM. In appendix B.1 we derive the solution of the RGE to next-to-next-to-next-to leading order (NNNLO). The corresponding ADM to NNLO as well as the known parts at NNNLO are provided in appendix B.2.

B.1. Solution of the renormalization group equation

The RGE, eq. (B.1), encodes the mixing and running of the Wilson coefficients. The evolution of the latter from an initial scale μ_0 is given by

$$C(\mu) = U(\mu, \mu_0) C(\mu_0)\,, \tag{B.2}$$

where the evolution matrix U is the formal solution of the RGE, eq. (B.1). It reads

$$U(\mu, \mu_0) = T_g \exp\left[\int_{g(\mu_0)}^{g(\mu)} \mathrm{d}g \frac{\gamma^T(g)}{\beta(g)}\right], \qquad U(\mu_0, \mu_0) = 1\,, \tag{B.3}$$

where T_g operates as an ordering in powers of g, from left to right, and $\beta(g) = \frac{\partial g}{\partial \ln \mu}$ with

$$\beta = -g \sum_{i=0}^{\infty} \left(\frac{g^2}{16\pi^2}\right) \beta_i\,. \tag{B.4}$$

In case of QCD [67]

$$\begin{aligned}
\beta_0(n_f) &= 11 - \frac{2}{3} n_f\,,\\
\beta_1(n_f) &= 102 - \frac{38}{3} n_f\,,\\
\beta_2(n_f) &= \frac{2857}{2} - \frac{5033}{18} n_f + \frac{325}{54} n_f^2\,,\\
\beta_3(n_f) &= \frac{149753}{6} + 3564\zeta(3) - \left(\frac{1078361}{162} + \frac{6508}{27}\zeta(3)\right) n_f\\
&\quad + \left(\frac{50065}{162} + \frac{6472}{81}\zeta(3)\right) n_f^2 + \frac{1093}{729} n_f^3\,,
\end{aligned} \tag{B.5}$$

where ζ is the Riemann zeta function, and n_f denotes the number of flavors.

The ADM is expanded as

$$\gamma = \sum_{i=0}^{\infty} \left(\frac{g^2}{16\pi^2}\right)^{i+1} \gamma^{(i)}\,, \tag{B.6}$$

where $\gamma^{(0,1,2)}$ and known parts of $\gamma^{(3)}$ are given in appendix B.2.

In the current appendix we work out the solution U as an expansion in the QCD coupling $\alpha_s = g_s^2/(4\pi)$ to $\mathcal{O}(\alpha_s^3)$. This extends the $\mathcal{O}(\alpha_s^2)$ expansion in [2, 55]. In particular, an alternative representation with respect to [2] is provided here. Throughout this thesis we employ the $\mathcal{O}(\alpha_s^2)$ solution. As the ADM for the mixing into the dipole operators is available at NNNLO, from four loop calculations, we give the solution of the evolution matrix to this order and provide the Wilson coefficients at NNNLL order in section 2.9.

The expansion of the solution is conveniently written as

$$U(\mu,\mu_0) = K(\mu) U^{(0)}(\mu,\mu_0) K^{-1}(\mu_0) \tag{B.7}$$

with

$$\begin{aligned}
K(\mu) &= 1 + \frac{\alpha_s(\mu)}{4\pi} J^{(1)} + \left(\frac{\alpha_s(\mu)}{4\pi}\right)^2 J^{(2)} + \left(\frac{\alpha_s(\mu)}{4\pi}\right)^3 J^{(3)}\,,\\
K^{-1}(\mu_0) &= 1 - \frac{\alpha_s(\mu_0)}{4\pi} J^{(1)} - \left(\frac{\alpha_s(\mu_0)}{4\pi}\right)^2 \left(J^{(2)} - \left(J^{(1)}\right)^2\right)\\
&\quad - \left(\frac{\alpha_s(\mu_0)}{4\pi}\right)^3 \left(J^{(3)} - 2J^{(1)}J^{(2)} + \left(J^{(1)}\right)^3\right)\,,\\
U^{(0)}(\mu,\mu_0) &= V \,\mathrm{diag}\left[\left(\frac{\alpha_s(\mu_0)}{\alpha_s(\mu)}\right)^{a_i}\right] V^{-1}\,,
\end{aligned} \tag{B.8}$$

where

$$\left(V^{-1}\left(\gamma^{(0)}\right)^T V\right)_{ij} = 2\beta_0 a_i \delta_{ij}\,. \tag{B.9}$$

Thus, the RGE yields a differential equation in g_s [55],

$$\partial_{g_s} K(g_s) + \frac{1}{g_s}\left[\frac{\left(\gamma^{(0)}\right)^T}{\beta_0}, K(g_s)\right] = \left(\frac{\left(\gamma^{(0)}\right)^T}{\beta(g_s)} + \frac{1}{g_s}\frac{\left(\gamma^{(0)}\right)^T}{\beta_0}\right) K(g_s)\,. \tag{B.10}$$

Its solutions, at respective order in α_s, read

$$
\begin{aligned}
J^{(1)} + \left[\frac{\left(\gamma^{(0)}\right)^T}{2\beta_0}, J^{(1)}\right] &= \frac{\beta_1}{2\beta_0^2}\left(\gamma^{(0)}\right)^T - \frac{1}{2\beta_0}\left(\gamma^{(1)}\right)^T ,\\
J^{(2)} + \left[\frac{\left(\gamma^{(0)}\right)^T}{4\beta_0}, J^{(2)}\right] &= \left(\frac{\beta_2}{4\beta_0^2} - \frac{\beta_1^2}{4\beta_0^3}\right)\left(\gamma^{(0)}\right)^T + \frac{\beta_1}{4\beta_0^2}\left(\gamma^{(1)}\right)^T - \frac{1}{4\beta_0}\left(\gamma^{(2)}\right)^T\\
&\quad + \left(\frac{\beta_1}{4\beta_0^2}\left(\gamma^{(0)}\right)^T - \frac{1}{4\beta_0}\left(\gamma^{(1)}\right)^T\right) J^{(1)} ,\\
J^{(3)} + \left[\frac{\left(\gamma^{(0)}\right)^T}{6\beta_0}, J^{(3)}\right] &= \left(\frac{\beta_3}{6\beta_0^2} - \frac{\beta_1\beta_2}{3\beta_0^3} + \frac{\beta_1^3}{6\beta_0^4}\right)\left(\gamma^{(0)}\right)^T + \left(\frac{\beta_2}{6\beta_0^2} - \frac{\beta_1^2}{6\beta_0^3}\right)\left(\gamma^{(1)}\right)^T\\
&\quad + \frac{\beta_1}{6\beta_0^2}\left(\gamma^{(2)}\right)^T - \frac{1}{6\beta_0}\left(\gamma^{(3)}\right)^T\\
&\quad + \left(\left(\frac{\beta_2}{6\beta_0^2} - \frac{\beta_1^2}{6\beta_0^3}\right)\left(\gamma^{(0)}\right)^T + \frac{\beta_1}{6\beta_0^2}\left(\gamma^{(1)}\right)^T - \frac{1}{6\beta_0}\left(\gamma^{(2)}\right)^T\right) J^{(1)}\\
&\quad + \left(\frac{\beta_1}{6\beta_0^2}\left(\gamma^{(0)}\right)^T - \frac{1}{6\beta_0}\left(\gamma^{(1)}\right)^T\right) J^{(2)} .
\end{aligned}
\tag{B.11}
$$

Defining

$$
J^{(i)} = V S^{(i)} V^{-1} , \qquad\qquad G^{(i)} = V^{-1}\left(\gamma^{(i)}\right)^T V , \tag{B.12}
$$

the matrix kernels obey the relations

$$
S_{ij}^{(1)} = \frac{\beta_1}{\beta_0} a_i \delta_{ij} - \frac{G_{ij}^{(1)}}{2\beta_0(1 + a_i - a_j)} , \tag{B.13}
$$

$$
S_{ij}^{(2)} = \left(\frac{\beta_2}{2\beta_0} - \frac{\beta_1^2}{2\beta_0^2}\right) a_i \delta_{ij} + \sum_k \frac{2\beta_1 a_i \delta_{ik} - G_{ik}^{(1)}}{2\beta_0(2 + a_i - a_j)} S_{kj}^{(1)} + \frac{\beta_1 G_{ij}^{(1)} - \beta_0 G_{ij}^{(2)}}{2\beta_0^2(2 + a_i - a_j)} , \tag{B.14}
$$

$$
\begin{aligned}
S_{ij}^{(3)} &= \left(\frac{\beta_3}{3\beta_0} - \frac{2\beta_1\beta_2}{3\beta_0^2} + \frac{\beta_1^3}{3\beta_0^3}\right) a_i \delta_{ij} + \sum_k \frac{2\left(\beta_0\beta_2 - \beta_1^2\right) a_i \delta_{ik} + \beta_1 G_{ik}^{(1)} - \beta_0 G_{ik}^{(2)}}{2\beta_0^2(3 + a_i - a_j)} S_{kj}^{(1)}\\
&\quad + \sum_k \frac{2\beta_1 a_i \delta_{ik} - G_{ik}^{(1)}}{2\beta_0(3 + a_i - a_j)} S_{kj}^{(2)} + \frac{\left(\beta_0\beta_2 - \beta_1^2\right) G_{ij}^{(1)} + \beta_0\beta_1 G_{ij}^{(2)} - \beta_0^2 G_{ij}^{(3)}}{2\beta_0^3(3 + a_i - a_j)} .
\end{aligned}
\tag{B.15}
$$

The evolution matrices $U^{(0,1)}$ can already be read off from the above equations, cutting the higher order terms. For $U^{(2,3)}$ we simplify the matrix kernels $S^{(2,3)}$ at first. Therefore, one obtains

$$G_{ij}^{(1)} = 2\beta_1 a_i \delta_{ij} - 2\beta_0 (1 + a_i - a_j) S_{ij}^{(1)} \,, \tag{B.16}$$

$$S_{ij}^{(2)} = \frac{\beta_2}{2\beta_0} a_i \delta_{ij} + \sum_k \frac{1 + a_i - a_k}{2 + a_i - a_j} \left(S_{ik}^{(1)} S_{kj}^{(1)} - \frac{\beta_1}{\beta_0} S_{ij}^{(1)} \delta_{jk} \right) - \frac{G_{ij}^{(2)}}{2\beta_0 (2 + a_i - a_j)} \,, \tag{B.17}$$

giving

$$\begin{aligned} G_{ij}^{(2)} &= 2\beta_2 a_i \delta_{ij} - 2\beta_0 (2 + a_i - a_j) S_{ij}^{(2)} \\ &\quad + \sum_k 2(1 + a_i - a_k) \left(\beta_0 S_{ik}^{(1)} S_{kj}^{(1)} - \beta_1 S_{ij}^{(1)} \delta_{jk} \right) . \end{aligned} \tag{B.18}$$

Finally, we find

$$\begin{aligned} S_{ij}^{(3)} &= \frac{\beta_3}{3\beta_0} a_i \delta_{ij} - \sum_{k,l} \frac{1 + a_i - a_l}{3 + a_i - a_j} \\ &\quad \times \left(S_{ik}^{(1)} S_{kl}^{(1)} S_{lj}^{(1)} - \frac{\beta_1}{\beta_0} S_{ik}^{(1)} S_{kj}^{(1)} \delta_{kl} - S_{ik}^{(1)} S_{kj}^{(2)} \delta_{kl} + \frac{\beta_2}{\beta_0} S_{ij}^{(1)} \delta_{jk} \delta_{kl} \right) \\ &\quad + \sum_k \frac{2 + a_i - a_k}{3 + a_i - a_j} \left(S_{ik}^{(2)} S_{kj}^{(1)} - \frac{\beta_1}{\beta_0} S_{ij}^{(2)} \delta_{jk} \right) - \frac{G_{ij}^{(3)}}{2\beta_0 (3 + a_i - a_j)} \,. \end{aligned} \tag{B.19}$$

Note that the eigenvalues given by eq. (B.9) obtained for the running $\mu_W \to \mu_b$ and $\mu_b \to \mu_c$, for the ADM given in the next appendix, do not give rise to singularities of the matrix kernels of eqs. (B.13, B.17, B.19). Finally, to complement the discussion about light quark masses in section 2.3, we add that the RGE needs to be modified for non-vanishing light quark masses, that is within a mass-dependent renormalization scheme, see e.g. [280].

B.2. Anomalous dimension matrix

On the following pages we provide the ADM for the operators defined in section 2.2 and which is utilized for the solution of the RGE as derived in the previous appendix. The ADM at NNLO QCD can partly be extracted from [51, 55, 281, 282]. The missing parts are given in [2] in the basis for effective Wilson coefficients, thus we provide complementary information here. The ADM for the mixing of the penguin operators into the dipole operators at NNNLO QCD can be found in [282].

In the following, $q_u = 2/3$ and $q_d = -1/3$ denote the up- and down-type quark charges, respectively, in units of the proton charge. Furthermore, $\bar{q} = n_u\, q_u + n_d\, q_d$, where n_i

depend on the range of the evolution, i.e. $n_f = 5$, $n_u = 2$ and $n_d = 3$ for $\mu_b \leq \mu \leq \mu_W$, and $n_f = 4$, $n_u = 2$ and $n_d = 2$ for $\mu_c \leq \mu \leq \mu_b$. With appropriate changes of these parameters the ADM relevant in b decays can be regained. We use the expansion of the ADM given by eq. (B.6) and we decompose the ADM in block as

$$\gamma = \begin{pmatrix} (\gamma_{1,2})_{2\times2} & (\gamma_{3-6})_{2\times4} & (\gamma_{7,8})_{2\times2} & (\gamma_9)_{2\times1} & 0_{2\times1} \\ 0_{4\times2} & (\gamma_{3-6})_{4\times4} & (\gamma_{7,8})_{4\times2} & (\gamma_9)_{4\times1} & 0_{4\times1} \\ 0_{2\times2} & 0_{2\times4} & (\gamma_{7,8})_{2\times2} & 0_{2\times1} & 0_{2\times1} \\ 0_{1\times2} & 0_{1\times4} & 0_{1\times2} & (\gamma_9)_{1\times1} & 0_{1\times1} \\ 0_{1\times2} & 0_{1\times4} & 0_{1\times2} & 0_{1\times1} & (\gamma_{10})_{1\times1} \end{pmatrix}, \tag{B.20}$$

where the labels represent the corresponding columns, and the dimension of the matrices are indicated. With the decomposition into blocks the evaluation of subsets of Wilson coefficients is readily obtained, e.g. for $C_{1,2}(\mu_W)$. Terms $\propto \beta_i(n_f)$ emerge due to the factor α_s in the definitions of the corresponding operators, i.e. for P_{7-10}.

Specifically,

$$(\gamma_9^{(i)})_{1\times1} = (\gamma_{10}^{(i)})_{1\times1} = -2\beta_i(n_f)\,. \tag{B.21}$$

The other blocks are given as unified matrices for the respective columns, where we omit the zeros in eq. (B.20). The LO ADM reads

$$\gamma_{1,2}^{(0)} = \begin{pmatrix} -4 & \frac{8}{3} \\ 12 & 0 \end{pmatrix}, \tag{B.22}$$

$$\gamma_{3-6}^{(0)} = \begin{pmatrix} 0 & -\frac{2}{9} & 0 & 0 \\ 0 & \frac{4}{3} & 0 & 0 \\ 0 & -\frac{52}{3} & 0 & 2 \\ -\frac{40}{9} & -\frac{160}{9} + \frac{4}{3}n_f & \frac{4}{9} & \frac{5}{6} \\ 0 & -\frac{256}{3} & 0 & 20 \\ -\frac{256}{9} & -\frac{544}{9} + \frac{40}{3}n_f & \frac{40}{9} & -\frac{2}{3} \end{pmatrix}, \tag{B.23}$$

$$\gamma_{7,8}^{(0)} = \begin{pmatrix} 0 & 0 \\ 0 & 0 \\ 0 & 0 \\ 0 & 0 \\ 0 & 0 \\ 0 & 0 \\ \frac{32}{3} - 2\beta_0(n_f) & 0 \\ \frac{32}{3} q_u & \frac{28}{3} - 2\beta_0(n_f) \end{pmatrix}, \tag{B.24}$$

$$\gamma_9^{(0)} = \begin{pmatrix} -\frac{16}{9} q_d \\ -\frac{4}{3} q_d \\ -8\bar{q} - \frac{8}{3} q_u \\ -\frac{32}{9} q_u \\ -80\bar{q} - \frac{128}{3} q_u \\ -\frac{512}{9} q_u \end{pmatrix}. \tag{B.25}$$

Note that the LO ADM is independent of specific renormalization schemes as long as it is a mass independent renormalization scheme, as used in this thesis. The NLO ADM is given by

$$\gamma_{1,2}^{(1)} = \begin{pmatrix} -\frac{145}{3} + \frac{16}{9} n_f & -26 + \frac{40}{27} n_f \\ -45 + \frac{20}{3} n_f & -\frac{28}{3} \end{pmatrix}, \tag{B.26}$$

$$\gamma_{3-6}^{(1)} = \begin{pmatrix} -\frac{1412}{243} & -\frac{1369}{243} & \frac{134}{243} & -\frac{35}{162} \\ -\frac{416}{81} & \frac{1280}{81} & \frac{56}{81} & \frac{35}{27} \\ -\frac{4468}{81} & -\frac{29129}{81} - \frac{52}{9} n_f & \frac{400}{81} & \frac{3493}{108} - \frac{2}{9} n_f \\ -\frac{13678}{243} + \frac{368}{81} n_f & -\frac{79409}{243} + \frac{1334}{81} n_f & \frac{509}{486} - \frac{8}{81} n_f & \frac{13499}{648} - \frac{5}{27} n_f \\ -\frac{244480}{81} - \frac{160}{9} n_f & -\frac{29648}{81} - \frac{2200}{9} n_f & \frac{23116}{81} + \frac{16}{9} n_f & \frac{3886}{27} + \frac{148}{9} n_f \\ \frac{77600}{243} - \frac{1264}{81} n_f & -\frac{28808}{243} + \frac{164}{81} n_f & -\frac{20324}{243} + \frac{400}{81} n_f & -\frac{21211}{162} + \frac{622}{27} n_f \end{pmatrix}, \tag{B.27}$$

$$\gamma^{(1)}_{7,8} = \begin{pmatrix} -\frac{4}{3}q_d + \frac{16}{81}q_u & \frac{167}{162} \\ 8q_d - \frac{32}{27}q_u & \frac{76}{27} \\ -\frac{64}{27}q_u & \frac{368}{27} \\ \left(\frac{680}{81} - \frac{32}{27}n_f\right) q_u & -\frac{427}{81} - \frac{37}{54}n_f \\ \frac{6464}{27}q_u & \frac{8192}{27} + 36n_f \\ 48\bar{q} + \left(\frac{20096}{81} - \frac{320}{27}n_f\right) q_u & -\frac{6040}{81} + \frac{220}{27}n_f \\ \frac{1936}{9} - \frac{224}{27}n_f - 2\beta_1(n_f) & 0 \\ \left(\frac{368}{3} - \frac{224}{27}n_f\right) q_u & \frac{1456}{9} - \frac{61}{27}n_f - 2\beta_1(n_f) \end{pmatrix}, \tag{B.28}$$

$$\gamma^{(1)}_{9} = \begin{pmatrix} -\frac{136}{27}q_d - \frac{176}{243}q_u \\ \frac{128}{9}q_d + \frac{352}{81}q_u \\ -32\bar{q} + \frac{4160}{81}q_u \\ \frac{64}{3}\bar{q} + \left(-\frac{784}{243} + \frac{544}{81}n_f\right) q_u \\ -320\bar{q} + \frac{58112}{81}q_u \\ \frac{608}{3}\bar{q} + \left(\frac{22784}{243} + \frac{4288}{81}n_f\right) q_u \end{pmatrix}. \tag{B.29}$$

For each column, the NNLO ADM reads

$$\gamma^{(2)}_{1} = \begin{pmatrix} -\frac{1927}{2} + \frac{257}{9}n_f + \frac{40}{9}n_f^2 + \left(224 + \frac{160}{3}n_f\right)\zeta_3 \\ \frac{307}{2} + \frac{361}{3}n_f - \frac{20}{3}n_f^2 - (1344 + 160n_f)\,\zeta_3 \end{pmatrix}, \tag{B.30}$$

$$\gamma^{(2)}_{2} = \begin{pmatrix} \frac{475}{9} + \frac{362}{27}n_f - \frac{40}{27}n_f^2 - \left(\frac{896}{3} + \frac{320}{9}n_f\right)\zeta_3 \\ \frac{1298}{3} - \frac{76}{3}n_f - 224\zeta_3 \end{pmatrix}, \tag{B.31}$$

$$\gamma_3^{(2)} = \begin{pmatrix} \frac{269107}{13122} - \frac{2288}{729}n_f - \frac{1360}{81}\zeta_3 \\ \frac{69797}{2187} + \frac{904}{243}n_f + \frac{2720}{27}\zeta_3 \\ -\frac{4203068}{2187} + \frac{14012}{243}n_f - \frac{608}{27}\zeta_3 \\ -\frac{5875184}{6561} + \frac{217892}{2187}n_f + \frac{472}{81}n_f^2 + \left(\frac{27520}{81} + \frac{1360}{9}n_f\right)\zeta_3 \\ -\frac{194951552}{2187} + \frac{358672}{81}n_f - \frac{2144}{81}n_f^2 + \frac{87040}{27}\zeta_3 \\ \frac{162733912}{6561} - \frac{2535466}{2187}n_f + \frac{17920}{243}n_f^2 + \left(\frac{174208}{81} + \frac{12160}{9}n_f\right)\zeta_3 \end{pmatrix}, \tag{B.32}$$

$$\gamma_4^{(2)} = \begin{pmatrix} -\frac{2425817}{13122} + \frac{30815}{4374}n_f - \frac{776}{81}\zeta_3 \\ \frac{1457549}{8748} - \frac{22067}{729}n_f - \frac{2768}{27}\zeta_3 \\ -\frac{18422762}{2187} + \frac{888605}{2916}n_f + \frac{272}{27}f^2 + \left(\frac{39824}{27} + 160n_f\right)\zeta_3 \\ -\frac{70274587}{13122} + \frac{8860733}{17496}n_f - \frac{4010}{729}n_f^2 + \left(\frac{16592}{81} + \frac{2512}{27}n_f\right)\zeta_3 \\ -\frac{130500332}{2187} - \frac{2949616}{729}n_f + \frac{3088}{27}n_f^2 + \left(\frac{238016}{27} + 640n_f\right)\zeta_3 \\ \frac{13286236}{6561} - \frac{1826023}{4374}n_f - \frac{159548}{729}n_f^2 - \left(\frac{24832}{81} + \frac{9440}{27}n_f\right)\zeta_3 \end{pmatrix}, \tag{B.33}$$

$$\gamma_5^{(2)} = \begin{pmatrix} -\frac{343783}{52488} + \frac{392}{729}n_f + \frac{124}{81}\zeta_3 \\ -\frac{37889}{8748} - \frac{28}{243}n_f - \frac{248}{27}\zeta_3 \\ \frac{674281}{4374} - \frac{1352}{243}n_f - \frac{496}{27}\zeta_3 \\ \frac{2951809}{52488} - \frac{31175}{8748}n_f - \frac{52}{81}n_f^2 - \left(\frac{3154}{81} + \frac{136}{9}n_f\right)\zeta_3 \\ \frac{14732222}{2187} - \frac{27428}{81}n_f + \frac{272}{81}n_f^2 - \frac{13984}{27}\zeta_3 \\ -\frac{22191107}{13122} + \frac{395783}{4374}n_f - \frac{1720}{243}n_f^2 - \left(\frac{33832}{81} + \frac{1360}{9}n_f\right)\zeta_3 \end{pmatrix}, \tag{B.34}$$

$$\gamma_6^{(2)} = \begin{pmatrix} -\frac{37573}{69984} + \frac{35}{972}n_f + \frac{100}{27}\zeta_3 \\ \frac{366919}{11664} - \frac{35}{162}n_f - \frac{110}{9}\zeta_3 \\ \frac{9284531}{11664} - \frac{2798}{81}n_f - \frac{26}{27}n_f^2 - \left(\frac{1921}{9} + 20n_f\right)\zeta_3 \\ \frac{3227801}{8748} - \frac{105293}{11664}n_f - \frac{65}{54}n_f^2 - \left(-\frac{200}{27} + \frac{220}{9}n_f\right)\zeta_3 \\ \frac{16521659}{2916} + \frac{8081}{54}n_f - \frac{316}{27}n_f^2 - \left(\frac{22420}{9} + 200n_f\right)\zeta_3 \\ -\frac{32043361}{8748} + \frac{3353393}{5832}n_f - \frac{533}{81}n_f^2 - \left(-\frac{9248}{27} + \frac{1120}{9}n_f\right)\zeta_3 \end{pmatrix}, \tag{B.35}$$

$$\gamma_7^{(2)} = \begin{pmatrix} -\left(\frac{374}{27} - \frac{2}{27}n_f\right) q_d - \left(\frac{6742}{729} - \frac{64}{729}n_f\right) q_u \\ \left(\frac{136}{9} - \frac{4}{9}n_f\right) q_d - \left(\frac{13300}{243} + \frac{128}{243}n_f\right) q_u \\ -\frac{112}{3}\bar{q} - \left(\frac{119456}{243} - \frac{3632}{243}n_f\right) q_u \\ -\frac{140}{9}\bar{q} + \left(\frac{202990}{729} - \frac{5548}{729}n_f - \frac{32}{243}n_f^2\right) q_u \\ -\frac{3136}{3}\bar{q} - \left(\frac{530240}{81} + \frac{46912}{243}n_f\right) q_u \\ -\left(\frac{1136}{9} + \frac{56}{3}n_f\right)\bar{q} + \left(\frac{1112344}{243} - \frac{327424}{729}n_f - \frac{896}{243}n_f^2\right) q_u \\ \frac{307448}{81} - \frac{23776}{81}n_f - \frac{352}{81}n_f^2 - \left(\frac{1856}{27} + \frac{1280}{9}n_f\right)\zeta_3 - 2\beta_2(n_f) \\ -\frac{1600}{27}\bar{q} + \left(\frac{159872}{81} - \frac{17108}{81}n_f - \frac{352}{81}n_f^2\right) q_u + \left(\frac{640}{9}\bar{q} - \left(\frac{1856}{27} + \frac{1280}{9}n_f\right) q_u\right)\zeta_3 \end{pmatrix}, \tag{B.36}$$

$$\gamma_8^{(2)} = \begin{pmatrix} \frac{25759}{5832} + \frac{431}{5832}n_f \\ \frac{9733}{486} - \frac{917}{972}n_f \\ \frac{82873}{243} - \frac{3361}{243}n_f \\ -\frac{570773}{2916} - \frac{40091}{5832}n_f - \frac{253}{486}n_f^2 \\ \frac{838684}{81} + \frac{129074}{243}n_f - 14n_f^2 \\ -\frac{923522}{243} - \frac{13247}{1458}n_f - \frac{6031}{486}n_f^2 \\ 0 \\ \frac{268807}{81} - \frac{4343}{27}n_f - \frac{461}{81}n_f^2 - \left(\frac{28624}{27} + \frac{1312}{9}n_f\right)\zeta_3 - 2\beta_2(n_f) \end{pmatrix}, \tag{B.37}$$

and for each component,

$$
\begin{aligned}
(\gamma_9^{(2)})_1 &= \frac{536}{27}\bar{q} - \left(\frac{14999}{81} - \frac{3152}{243}n_f\right) q_d - \left(\frac{72560}{6561} + \frac{1120}{2187}n_f\right) q_u \\
&\quad + \left(\frac{352}{9}q_d - \frac{640}{81}q_u\right)\zeta_3\,, \\
(\gamma_9^{(2)})_2 &= \frac{224}{9}\bar{q} + \left(\frac{820}{27} - \frac{184}{81}n_f\right) q_d + \left(\frac{333688}{2187} + \frac{2240}{729}n_f\right) q_u \\
&\quad + \left(-\frac{128}{3}q_d + \frac{1280}{27}q_u\right)\zeta_3\,, \\
(\gamma_9^{(2)})_3 &= -\left(\frac{2636}{9} - \frac{176}{9}f\right)\bar{q} + \left(\frac{1524104}{2187} - \frac{44048}{729}n_f\right) q_u + \left(128\bar{q} + \frac{256}{27}q_u\right)\zeta_3\,, \\
(\gamma_9^{(2)})_4 &= \left(\frac{1201}{27} - \frac{32}{9}n_f\right)\bar{q} + \left(-\frac{1535926}{6561} + \frac{159620}{2187}n_f + \frac{608}{729}n_f^2\right) q_u \\
&\quad + \left(\frac{160}{3}\bar{q} + \left(\frac{5056}{81} + \frac{1280}{27}n_f\right) q_u\right)\zeta_3\,, \\
(\gamma_9^{(2)})_5 &= \left(\frac{46552}{9} + \frac{2912}{9}n_f\right)\bar{q} + \left(\frac{31433600}{2187} + \frac{15904}{729}n_f\right) q_u + \left(1280\bar{q} + \frac{4096}{27}q_u\right)\zeta_3\,, \\
(\gamma_9^{(2)})_6 &= -\left(\frac{47624}{27} - \frac{1312}{27}n_f\right)\bar{q} + \left(-\frac{48510784}{6561} + \frac{3516560}{2187}n_f + \frac{15872}{729}n_f^2\right) q_u \\
&\quad + \left(-\frac{512}{3}\bar{q} + \left(\frac{80896}{81} + \frac{12800}{27}n_f\right) q_u\right)\zeta_3\,.
\end{aligned}
\tag{B.38}
$$

Additionally, at NNNLO the ADM encoding the mixing of P_{1-6} into $P_{7,8}$ is given by [282],

$$
\begin{aligned}
(\gamma_7^{(3)})_1 &= \frac{3695}{486}\bar{q} + \left(-\frac{9731}{162} + \frac{11045}{729}n_f + \frac{316}{729}n_f^2\right) q_d - \left(\frac{23465621}{354294} + \frac{185708}{59049}n_f\right. \\
&\quad \left. + \frac{560}{6561}n_f^2\right) q_u + \left(-\frac{100}{27}\bar{q} + \left(\frac{25508}{81} - \frac{64}{81}n_f\right) q_d - \left(\frac{106088}{2187} + \frac{728}{243}n_f\right) q_u\right)\zeta_3\,, \\
(\gamma_7^{(3)})_2 &= -\frac{3695}{81}\bar{q} + \left(\frac{55748}{27} - \frac{33970}{243}n_f - \frac{632}{243}n_f^2\right) q_d - \left(\frac{43958455}{59049} - \frac{637744}{19683}n_f\right. \\
&\quad \left. - \frac{1120}{2187}n_f^2\right) q_u + \left(\frac{200}{9}\bar{q} - \left(\frac{51232}{27} + \frac{1024}{27}n_f\right) q_d + \left(\frac{32032}{729} + \frac{1168}{81}n_f\right) q_u\right)\zeta_3\,, \\
(\gamma_7^{(3)})_3 &= \left(\frac{21839}{81} - \frac{8}{27}n_f\right)\bar{q} - \left(\frac{420528560}{59049} - \frac{13527449}{19683}n_f - \frac{1952}{2187}n_f^2\right) q_u \\
&\quad + \left(-\left(\frac{448}{3} + \frac{64}{9}n_f\right)\bar{q} - \left(\frac{609136}{729} - \frac{4784}{81}n_f\right) q_u\right)\zeta_3\,,
\end{aligned}
$$

$$
\begin{aligned}
(\gamma_7^{(3)})_4 &= \left(-\frac{40393}{972}+\frac{305}{27}n_f\right)\bar{q}+\left(\frac{1566264949}{177147}-\frac{43414337}{59049}n_f+\frac{570520}{19683}n_f^2\right.\\
&\quad\left.+\frac{1184}{2187}n_f^3\right)q_u+\left(\left(\frac{2710}{27}-\frac{200}{27}n_f\right)\bar{q}+\left(\frac{1677680}{2187}+\frac{65320}{729}n_f+\frac{1280}{81}n_f^2\right)q_u\right)\\
&\quad\times\zeta_3\,,\\
(\gamma_7^{(3)})_5 &= -\left(\frac{765694}{81}-\frac{10672}{27}n_f\right)\bar{q}-\left(\frac{8910264032}{59049}-\frac{49924856}{19683}n_f+\frac{14944}{243}n_f^2\right)q_u\\
&\quad+\left(-\left(\frac{12080}{9}+\frac{640}{9}n_f\right)\bar{q}-\left(\frac{80487616}{729}-\frac{109792}{81}n_f+\frac{128}{9}n_f^2\right)q_u\right)\zeta_3\,,\\
(\gamma_7^{(3)})_6 &= \left(\frac{3998201}{243}-\frac{130538}{81}n_f-\frac{592}{81}n_f^2\right)\bar{q}+\left(\frac{27503551444}{177147}-\frac{979809110}{59049}n_f\right.\\
&\quad\left.+\frac{9016384}{19683}n_f^2+\frac{11456}{2187}n_f^3\right)q_u+\left(-\left(\frac{332152}{27}+\frac{1136}{27}n_f\right)\bar{q}\right.\\
&\quad\left.-\left(\frac{16723168}{2187}+\frac{1296896}{729}n_f-\frac{12320}{81}n_f^2\right)q_u\right)\zeta_3\,,
\end{aligned}
\tag{B.39}
$$

and

$$
\begin{aligned}
(\gamma_8^{(3)})_1 &= -\frac{621789145}{2834352}-\frac{11196403}{472392}n_f-\frac{1955}{6561}n_f^2-\left(\frac{959774}{2187}+\frac{10381}{486}n_f\right)\zeta_3\,,\\
(\gamma_8^{(3)})_2 &= \frac{187044487}{472392}-\frac{6180527}{78732}n_f-\frac{2489}{2187}n_f^2-\left(\frac{588779}{729}+\frac{1679}{81}n_f\right)\zeta_3\,,\\
(\gamma_8^{(3)})_3 &= \frac{2407231267}{236196}-\frac{163003183}{314928}n_f+\frac{27313}{4374}n_f^2-\left(\frac{2425642}{729}+\frac{2020}{81}n_f+\frac{20}{9}n_f^2\right)\zeta_3\,,\\
(\gamma_8^{(3)})_4 &= -\frac{7940239169}{2834352}+\frac{227708063}{1889568}n_f+\frac{2176469}{157464}n_f^2+\frac{505}{4374}n_f^3\\
&\quad+\left(\frac{3787892}{2187}+\frac{208123}{729}n_f+\frac{920}{81}n_f^2\right)\zeta_3\,,\\
(\gamma_8^{(3)})_5 &= \frac{16262270803}{59049}-\frac{84893785}{19683}n_f-\frac{273358}{243}n_f^2-\frac{148}{27}n_f^3\\
&\quad-\left(\frac{84597232}{729}+\frac{1166876}{81}n_f+\frac{5080}{9}n_f^2\right)\zeta_3\,,\\
(\gamma_8^{(3)})_6 &= -\frac{82670094587}{708588}+\frac{3364425683}{472392}n_f-\frac{31543895}{78732}n_f^2-\frac{3988}{2187}n_f^3\\
&\quad+\left(-\frac{37712140}{2187}+\frac{542128}{729}n_f+\frac{350}{81}n_f^2\right)\zeta_3\,.
\end{aligned}
\tag{B.40}
$$

C. Distributions and observables

In the following appendices several distributions and observables used throughout the thesis are provided. Only the ones for radiative decays are given in the main text, see sections 3.1.1, 3.3 and 4.5. For the definition of the Lagrangian, see the beginning of chapter 3.

C.1. Inclusive $D \to X_u ll$ decays

The inclusive q^2 distribution, where $q^\mu = (p_c - p_u)^\mu = (p_+ + p_-)^\mu$, for $c \to ull$ induced decays, as studied in section 3.1, can be obtained to leading order in the HQE [283, 284] as

$$\begin{aligned}\frac{\mathrm{d}\Gamma_{c\to ull}}{\mathrm{d}q^2} = \frac{G_F^2\alpha_e^2 m_c^3}{768\pi^5}\left(1-\frac{q^2}{m_c^2}\right)^2\sqrt{1-\frac{(2m_l)^2}{q^2}}\Bigg[\left(1+2\frac{q^2}{m_c^2}-2\frac{m_l^2}{m_c^2}\left(1-\frac{m_c^2}{q^2}\right)\right)\\ \times\left(|C_9|^2+|C_{10}|^2\right)+\left(1+2\frac{m_l^2}{q^2}\right)\left(4\left(2\frac{m_c^2}{q^2}+1\right)|C_7|^2+12\mathrm{Re}\left[C_7C_9^*\right]\right)\\ +6\frac{m_l^2}{m_c^2}\left(|C_9|^2-|C_{10}|^2\right)\Bigg],\end{aligned} \tag{C.1}$$

where $(2m_l)^2 \leq q^2 \leq m_c^2$, and the up quark mass is neglected.

The distribution stemming from additional operators, beyond the SM ones, can be found in [283, 284]. The $c \to (d,s)l\nu_l$ distribution for massless leptons can be recovered for $C_9 = -C_{10} = 1/2$, $C_7 = 0$ and $\alpha_e/(4\pi) \to -V^*_{c(d,s)}$.

Corrections to the matrix elements of the operators $Q_{7,9,10}$ at NLO QCD can be incorporated following [79] (and references therein). They can compactly be absorbed in the Wilson coefficients as

$$C_i \to C_i\left(1+\frac{\alpha_s}{\pi}\sigma_i(q^2/m_c^2)\right), \quad \mathrm{Re}[C_iC_j^*] \to \mathrm{Re}[C_iC_j^*]\left(1+\frac{\alpha_s}{\pi}\tau_{ij}^{(1)}(q^2/m_c^2)\right). \tag{C.2}$$

Here

$$\begin{aligned}\sigma_7(\rho) &= -\frac{4}{3}\mathrm{Li}_2[\rho]-\frac{2}{3}\ln\rho\ln[1-\rho]-\frac{2}{9}\pi^2-\ln[1-\rho]-\frac{2}{9}(1-\rho)\ln[1-\rho]+\frac{1}{6}\\ &\quad-\frac{4}{3}\ln\frac{\mu_c^2}{m_c^2},\\ \sigma_9(\rho) &= -\frac{4}{3}\mathrm{Li}_2[\rho]-\frac{2}{3}\ln\rho\ln[1-\rho]-\frac{2}{9}\pi^2-\ln[1-\rho]-\frac{2}{9}(1-\rho)\ln[1-\rho]+\frac{3}{2},\end{aligned} \tag{C.3}$$

where $\sigma_{10} = \sigma_9$ due to parity invariance of QCD. Furthermore, for massless leptons

$$\begin{aligned}
\tau_{77}^{(1)}(\rho) &= -\frac{2}{9(2+\rho)}\left(2(1-\rho)^2\ln[1-\rho] + \frac{6\rho(2-2\rho-\rho^2)}{(1-\rho)^2}\ln\rho + \frac{11-7\rho-10\rho^2}{1-\rho}\right), \\
\tau_{99}^{(1)}(\rho) &= -\frac{4}{9(1+2\rho)}\left(2(1-\rho)^2\ln[1-\rho] + \frac{3\rho(1+\rho)(1-2\rho)}{(1-\rho)^2}\ln\rho + \frac{3(1-3\rho^2}{1-\rho}\right), \\
\tau_{79}^{(1)}(\rho) &= -\frac{4(1-\rho)^2}{9\rho}\ln[1-\rho] - \frac{4\rho(3-2\rho)}{9(1-\rho)^2}\ln\rho - \frac{2(5-3\rho)}{9(1-\rho)},
\end{aligned} \tag{C.4}$$

where $\tau_{10\,10} = \tau_{99}$, and

$$\begin{aligned}
\tau_{710}^{(1)}(\rho) &= -\frac{5}{2} + \frac{1}{3(1-3\rho)} - \frac{\rho(6-7\rho)\ln\rho}{3(1-\rho)^2} - \frac{(3-7\rho+4\rho^2)\ln[1-\rho]}{9\rho} + \frac{1}{18(1-\rho)^2} \\
&\quad\times\big[24\left(1+13\rho-4\rho^2\right)\mathrm{Li}_2[\sqrt{\rho}] + 12\left(1-17\rho+6\rho^2\right)\mathrm{Li}_2[\rho] + 6\rho(6-7\rho)\ln\rho \\
&\quad + 24(1-\rho)^2\ln\rho\ln[1-\rho] + 12\left(-13+16\rho-3\rho^2\right)\left(\ln[1-\sqrt{\rho}] - \ln[1-\rho]\right) \\
&\quad + 39 - 2\pi^2 + 252\rho - 26\pi^2\rho + 21\rho^2 + 8\pi^2\rho^2 - 180\sqrt{\rho} - 132\rho\sqrt{\rho}\big], \\
\tau_{910}^{(1)}(\rho) &= -\frac{5}{2} + \frac{1}{3(1-\rho)} - \frac{\rho(6-7\rho)\ln\rho}{3(1-\rho)^2} - \frac{2(3-5\rho+2\rho^2)\ln[1-\rho]}{9\rho} - \frac{1}{18(1-\rho)^2} \\
&\quad\times\big[48\rho(-5+2\rho)\mathrm{Li}_2[\sqrt{\rho}] + 24\left(-1+7\rho-3\rho^2\right)\mathrm{Li}_2[\rho] + 6\rho(-6+7\rho)\ln\rho \\
&\quad - 24(1-\rho)^2\ln\rho\ln[1-\rho] + 24\left(5-7\rho+2\rho^2\right)\left(\ln[1-\sqrt{\rho}] - \ln[1-\rho]\right) \\
&\quad - 21 - 156\rho + 20\pi^2\rho + 9\rho^2 - 8\pi^2\rho^2 + 120\sqrt{\rho} + 48\rho\sqrt{\rho}\big].
\end{aligned} \tag{C.5}$$

The logarithm in σ_7 stems from infrared singularities. We neglect finite bremsstrahlung corrections not related to matrix elements of $Q_{7,9,10} \otimes Q_{7,9,10}$. They are estimated to be at the percent level in b decays [285]. The NNLO QCD correction, normalized to the tree level matrix element, can be obtained from [286], yielding

$$|C_9|^2|_{\alpha_s^2} = |C_9|^2\left(\frac{\alpha_s}{\pi}\right)^2\tau_{99}^{(2)}(q^2/m_c^2). \tag{C.6}$$

Here

$$\begin{aligned}
\tau_{99}^{(2)}(\rho) &= \frac{1}{(1-\rho)^2(1+2\rho)}\bigg[\frac{2}{3}\left(2.854 - 0.665\rho - 0.109\rho^2 - 8.572\rho^3 + 5.561\rho^4 + 0.931\rho^5\right) \\
&\quad\times f_l + \frac{2}{3}\big(-0.063615 + 0.098146\rho + 0.144642\rho^2 - 0.307331\rho^3 + 0.107417\rho^4 \\
&\quad + 0.020707\rho^5\big) f_h + \frac{16}{9}\big(3.575 - 2.867\rho + 2.241\rho^2 - 12.027\rho^3 + 11.564\rho^4 \\
&\quad - 2.489\rho^5\big) + 4\big(-8.151 + 2.990\rho - 3.537\rho^2 + 36.561\rho^3 - 42.275\rho^4 + 23.899\rho^5 \\
&\quad - 9.494\rho^6\big)\bigg],
\end{aligned} \tag{C.7}$$

where $f_l = 3$ and $f_h = 1$ denote the numbers of light and heavy flavors, respectively. This approximative expression is exact within less than one percent compared to the analytic function for any value of ρ.

As in the case of radiative decays we normalize the distribution with respect the semileptonic decay width to reduce parametric uncertainties. For massless leptons, to leading order in the HQE, and NNLO in QCD it is [287]

$$\Gamma_{c\to(d,s)l\nu} = \frac{G_F^2 m_c^3}{192\pi^3} \sum_{q\in\{d,s\}} |V_{cq}|^2 \Bigg(X_0(m_q/m_c) + \frac{\alpha_s}{\pi} X_1(m_q/m_c) + \left(\frac{\alpha_s}{\pi}\right)^2 X_2(m_q/m_c) \Bigg) . \tag{C.8}$$

Here

$$\begin{aligned} X_0(\rho) &= 1 - 8\rho^2 - 24\rho^4 \ln\rho + 8\rho^6 - \rho^8 \,, \\ X_1(\rho) &= \frac{4}{3}\Bigg(\frac{25}{8} - \frac{\pi^2}{2} - (34 + 24\ln\rho)\rho^2 + 16\pi^2\rho^3 - \left(\frac{273}{2} - 36\ln\rho + 72\ln\rho^2 + 8\pi^2\right)\rho^4 \\ &\quad + 16\pi^2\rho^5 - \left(\frac{526}{9} - \frac{152}{3}\ln\rho\right)\rho^6 \Bigg) + \mathcal{O}\left(\rho^7\right) \,, \end{aligned} \tag{C.9}$$

and

$$\begin{aligned} X_2(\rho) = \frac{2}{3}\Bigg[&- \frac{1009}{288} + \frac{8}{3}\zeta_3 + \frac{77}{216}\pi^2 + \left(\frac{118}{3} - \frac{4}{3}\pi^2 + \frac{52}{3}\ln\rho - 8\ln^2\rho\right)\rho^2 + \left(\frac{64}{3}\ln 2 \right. \\ &\left. - \frac{112}{9} + \frac{32}{3}\ln\rho\right)\pi^2\rho^3 + \left(76\zeta_3 - \frac{5}{3}\pi^2 - 33 + 52\ln^2\rho + \left(39 - \frac{16}{3}\pi^2\right)\ln\rho \right. \\ &\left. - 32\ln^3\rho\right)\rho^4 + \left(\frac{64}{3}\ln 2 - \frac{1216}{45} + \frac{32}{3}\ln\rho\right)\pi^2\rho^5 + \left(\frac{344}{27} + \frac{28}{27}\pi^2 - \frac{1564}{27}\ln\rho \right. \\ &\left. + 24\ln^2\rho\right)\rho^6 + \frac{40}{21}\pi^2\rho^7\Bigg] f_l + \frac{2}{3}\Bigg[\frac{16987}{576} - \frac{64}{3}\zeta_3 - \frac{85}{216}\pi^2 + \left(\frac{8}{3}\pi^2 - \frac{1198}{45}\right)\rho^2 \\ &+ \left(\frac{156901877}{2116800} - \frac{11}{18}\pi^2 - 64\zeta_3 - \left(\frac{186689}{2520} - \frac{20}{3}\pi^2\right)\ln\rho\right)\rho^4 + \left(\frac{189825233}{7144200} \right. \\ &\left. - \frac{52}{27}\pi^2 - \frac{181627}{14175}\ln\rho + \frac{16}{5}\ln^2\rho\right)\rho^6 + \left(\frac{629309}{1403325} - \frac{4}{3}\zeta_3 + \frac{19}{72}\pi^2 - \left(\frac{4741}{9072} \right.\right. \\ &\left.\left. + \frac{1}{9}\pi^2\right)\ln\rho\right)\rho^8\Bigg] f_h + \left(\frac{16}{9} - 2\right)\Bigg[\frac{11047}{2592} - \frac{223}{36}\zeta_3 - \frac{515}{81}\pi^2 + \frac{53}{6}\pi^2\ln 2 + \frac{67}{720}\pi^4 \\ &+ \left(\frac{497}{108}\pi^2 - \frac{2089}{8} + 86\zeta_3 - 8\pi^2\ln 2 + \frac{121}{540}\pi^4 - 105\ln\rho - 36\ln^2\rho\right)\rho^2 + \left(\frac{752}{9} \right. \\ &\left. - \frac{112}{3}\pi\right)\pi^2\rho^3 + \Bigg[\frac{16586}{27} - \frac{1139}{24}\pi^2 - \frac{795}{2}\zeta_3 + \frac{415}{3}\pi^2\zeta_3 + 13\pi^2\ln 2 - 96\mathrm{Li}_4\frac{1}{2} \end{aligned}$$

$$
\begin{aligned}
&- 8\pi^2 \ln^2 2 - 4\ln^4 2 - 144\ln^3\rho - \left(\frac{19459}{18} + \frac{71}{3}\pi^2 - 246\zeta_3 + 60\pi^2\ln 2 - \frac{40}{3}\pi^4\right) \\
&\times \ln\rho - \frac{349}{72}\pi^4 + \left(99 + 4\pi^2\right)\ln^2\rho + 935\zeta_5\Big]\rho^4 + \left(\frac{67448}{675} - \frac{776}{15}\pi + 160\ln\rho\right)\pi^2\rho^5 \\
&+ \left(\frac{4859}{12}\zeta_3 - \frac{1732}{9} - \frac{14921}{216}\pi^2 + \frac{89}{6}\pi^2\ln 2 - \frac{10}{3}\pi^4 + \left(\frac{1862}{9} - \frac{34}{3}\pi^2\right)\ln^2\rho\right. \\
&\left. - \left(\frac{3635}{18} + 136\zeta_3 - \frac{833}{18}\pi^2\right)\ln\rho\right)\rho^6 + \left(\frac{86}{7}\pi - \frac{469304}{11025} + \frac{1376}{45}\ln\rho\right)\pi^2\rho^7\Big] + 4 \\
&\times \left[\frac{19669}{1152} - \frac{70}{27}\pi^2 + \frac{7}{60}\pi^4 - \frac{101}{12}\zeta_3 + \left(\frac{11}{18}\pi^4 - \frac{1813}{8} - \frac{19}{6}\pi^2 - \frac{685}{6}\ln\rho + 4\ln^2\rho\right)\right. \\
&\times \rho^2 + \left(\frac{2044}{9} - \frac{1136}{3}\ln 2 - \frac{124}{3}\ln\rho\right)\pi^2\rho^3 + \Big[\frac{8947}{32} - \frac{103}{12}\pi^2 + \frac{2}{45}\pi^4 + 200\zeta_5 \\
&- \frac{705}{2}\zeta_3 + \frac{100}{3}\pi^2\zeta_3 + \left(84\zeta_3 - \frac{1049}{2} - \frac{161}{6}\pi^2 + \frac{10}{3}\pi^4\right)\ln\rho + \left(7\pi^2 - \frac{271}{2}\right)\ln^2\rho \\
&+ 16\ln^3\rho\Big]\rho^4 + \left(\frac{58024}{225} - \frac{1136}{3}\ln 2 - \frac{292}{15}\ln\rho\right)\pi^2\rho^5 + \left(\frac{269297}{1296} + \frac{2303}{216}\pi^2\right. \\
&- \frac{1}{2}\pi^4 - 24\zeta_3 + \left(12\zeta_3 - \frac{2441}{72} - \frac{17}{3}\pi^2\right)\ln\rho + \left(\frac{229}{9} + \pi^2\right)\ln^2\rho\Big)\rho^6 - \Big(\frac{242554}{33075} \\
&\left. + \frac{256}{315}\ln\rho\right)\pi^2\rho^7\Big] + \delta_{qd}X_{2,s}^{(d)}(m_s/m_c) + \delta_{qs}X_{2,s}^{(s)}(\rho) + \mathcal{O}\left(\rho^8\right) \qquad \text{(C.10)}
\end{aligned}
$$

with

$$
\begin{aligned}
X_{2,s}^{(d)}(\rho) = \frac{2}{3}\Big[&- \frac{1009}{288} + \frac{8}{3}\zeta_3 + \frac{77}{216}\pi^2 - \frac{5}{4}\pi^2\rho + \left(21 + \frac{8}{3}\pi^2\right)\rho^2 + \Big(\frac{64}{3}\ln 2 - \frac{95}{36} \\
&+ \frac{32}{3}\ln\rho\Big)\pi^2\rho^3 + \left(48\zeta_3 - \frac{4375}{36} - \frac{25}{6}\pi^2 + \left(\frac{365}{6} + 6\pi^2\right)\ln\rho - 8\ln^2\rho\right)\rho^4 \\
&- \frac{112}{15}\pi^2\rho^5 + \left(\frac{7804}{675} + \frac{64}{27}\pi^2 + \frac{8}{5}\ln\rho - \frac{64}{9}\ln^2\rho\right)\rho^6 - \frac{24}{7}\pi^2\rho^7\Big], \\
X_{2,s}^{(s)}(\rho) = \frac{2}{3}\Big[&- \frac{1009}{288} + \frac{8}{3}\zeta_3 + \frac{77}{216}\pi^2 - \frac{5}{4}\pi^2\rho + \left(\frac{145}{3} + \frac{16}{3}\pi^2 + \frac{52}{3}\ln\rho - 8\ln^2\rho\right)\rho^2 \\
&+ \left(\frac{569}{36} + \frac{64}{3}\ln\rho\right)\pi^2\rho^3 + \Big(196\zeta_3 + \frac{1}{6}\pi^2 - \frac{4483}{36} + 44\ln^2\rho - 32\ln^3\rho + \Big(\frac{599}{6} \\
&+ \frac{74}{3}\pi^2\Big)\ln\rho\Big)\rho^4 + \left(\frac{50}{3}\ln\rho - \frac{172}{9}\right)\pi^2\rho^5 - \Big(\frac{33982}{225} + \frac{232}{27}\pi^2 - \frac{11836}{135}\ln\rho \\
&+ \frac{64}{9}\ln^2\rho\Big)\rho^6 + \left(\frac{44}{3} + 18\ln\rho\right)\pi^2\rho^7\Big]. \qquad \text{(C.11)}
\end{aligned}
$$

With the above expressions the branching ratio is given as

$$\frac{\mathrm{d}\mathcal{B}_{D\to X_u ll}}{\mathrm{d}q^2} = \frac{\mathcal{B}(D\to X_{(d,s)}l\nu)}{\Gamma_{c\to(d,s)l\nu}}\frac{\mathrm{d}\Gamma_{c\to ull}}{\mathrm{d}q^2}\,, \tag{C.12}$$

where $\mathcal{B}(D\to X_{(d,s)}l\nu)$ is taken from measurements, see appendix A.

Next, we include the leading power corrections. For massless leptons they can be adopted from [103, 288],

$$\begin{aligned}\delta_{1/m_c^2}\frac{\mathrm{d}\mathcal{B}_{D\to X_u ll}}{\mathrm{d}q^2} = \frac{3\lambda_2}{2m_c^2}\frac{\mathcal{B}(D\to X_{(d,s)}l\nu)}{\Gamma_{c\to(d,s)l\nu}}\Bigg[\frac{G_F^2\alpha_e^2 m_c^3}{768\pi^5}\Bigg[\left(1-15\left(\frac{q^2}{m_c^2}\right)^2+10\left(\frac{q^2}{m_c^2}\right)^3\right)\\ \times\left(|C_9|^2+|C_{10}|^2\right)-4\left(6\frac{m_c^2}{q^2}+3-5\left(\frac{q^2}{m_c^2}\right)^2\right)|C_7|^2-4\Bigg(5+6\frac{q^2}{m_c^2}\\ -7\left(\frac{q^2}{m_c^2}\right)^2\Bigg)\mathrm{Re}[C_7C_9^*]\Bigg]+\frac{g(m_q^2/m_c^2)}{X_0(m_q^2/m_c^2)}\frac{\mathrm{d}\Gamma_{c\to ull}}{\mathrm{d}q^2}\Bigg]\,.\end{aligned} \tag{C.13}$$

Here $\delta_{1/m_c^2}\Gamma_{c\to(d,s)l\nu} = (\frac{\lambda_1}{2m_c^2}-\frac{3\lambda_2}{2m_c^2}\frac{g(m_q^2/m_c^2}{X_0(m_q^2/m_c^2)})\Gamma_{c\to(d,s)l\nu}$ is included and for a heavy charm quark h_v with velocity v

$$\lambda_2 = \frac{1}{6}\frac{\langle D|\bar{h}_v g\sigma_{\mu\nu}G^{\mu\nu}h_v|D\rangle}{2m_D} = \frac{(m_D^*)^2-m_D^2}{4}\,, \tag{C.14}$$

$$g(\rho) = 3-8\rho+24\rho^2-24\rho^3+5\rho^4+12\rho^2\ln\rho\,. \tag{C.15}$$

The normalization to the semileptonic decay width reduces uncertainties due to power corrections. In fact, $\frac{\Lambda_{\mathrm{QCD}}}{m_c}$ corrections and the multiplicative kinetic matrix element $\lambda_1 = \langle D|\bar{h}_v(iD)^2h_v|D\rangle/(2m_D)$ are canceled due to the normalization. In principle, one can include $(\frac{\Lambda_{\mathrm{QCD}}}{m_c})^3$ corrections, analogue to [79]. However, these corrections give rise to additional matrix elements.

For the phenomenological analysis, the above expressions will be expanded consistently to $\mathcal{O}(\alpha_s/(4\pi))^2$, including the expansion of the Wilson coefficients. Furthermore, as the above expressions are given for zero lepton masses, $m_l = 0$ will be used in eq. (C.1). To

estimate the effect of non-vanishing lepton masses, a non-zero mass can be retained by replacing eq. (C.4) with

$$\begin{aligned}
\tau_{77}^{(1)}(\rho) &\to \tau_{77}^{(1)}(\rho)\frac{1}{\sqrt{1-\frac{(2m_l)^2}{q^2}}}\,,\\
\tau_{99}^{(1,2)}(\rho) &\to \tau_{99}^{(1,2)}(\rho)\frac{1+2\rho}{\left(1+2\rho+4\frac{m_l^2}{q^2}\rho+2\frac{m_l^2}{q^2}\right)\sqrt{1-\frac{(2m_l)^2}{q^2}}}\,,\\
\tau_{10\,10}^{(1)}(\rho) &\to \tau_{10\,10}^{(1)}(\rho)\frac{1+2\rho}{\left(1+2\rho-8\frac{m_l^2}{q^2}\rho+2\frac{m_l^2}{q^2}\right)\sqrt{1-\frac{(2m_l)^2}{q^2}}}\,,\\
\tau_{79}^{(1)}(\rho) &\to \tau_{79}^{(1)}(\rho)\frac{1}{\sqrt{1-\frac{(2m_l)^2}{q^2}}}\,.
\end{aligned} \tag{C.16}$$

We still neglect lepton masses in terms $\sim \mathcal{O}((\frac{\Lambda_{\rm QCD}}{m_c})^2)$.

The lepton forward-backward asymmetry, normalized to $c \to (d,s)l\nu$ decays, can be obtained from [283]. For massless leptons is given by

$$\begin{aligned}
A_{FB} = &\frac{\mathcal{B}(D\to X_{(d,s)}l\nu)}{\Gamma_{c\to(d,s)l\nu}}\frac{G_F^2\alpha_e^2 m_c^3}{768\pi^5}(-3)\left(1-\frac{q^2}{m_c^2}\right)^2\\
&\times\left(\frac{q^2}{m_c^2}\mathrm{Re}[C_9C_{10}^*]+2\mathrm{Re}[C_7C_{10}^*]\right)\,.
\end{aligned} \tag{C.17}$$

The leading power corrections can be adopted from [103], reading

$$\begin{aligned}
\delta_{1/m_c^2}\frac{\mathrm{d}A_{FB}}{\mathrm{d}q^2} = \frac{3\lambda_2}{2m_c^2}\Bigg[&\frac{\mathcal{B}(D\to X_{(d,s)}l\nu)}{\Gamma_{c\to(d,s)l\nu}}\frac{G_F^2\alpha_e^2 m_c^3}{768\pi^5}\left(\frac{q^2}{m_c^2}\left(9+14\frac{q^2}{m_c^2}-15\left(\frac{q^2}{m_c^2}\right)^2\right)\right.\\
&\left.\times\,\mathrm{Re}[C_9C_{10}^*]+2\left(7+10\frac{q^2}{m_c^2}-9\left(\frac{q^2}{m_c^2}\right)^2\right)\mathrm{Re}[C_7C_{10}^*]\right)\\
&+\frac{g(m_q^2/m_c^2)}{X_0(m_q^2/m_c^2)}\frac{\mathrm{d}A_{FB}}{\mathrm{d}q^2}\Bigg]+\frac{4\lambda_1}{3m_c^2}\frac{\frac{q^2}{m_c^2}}{\left(1-\frac{q^2}{m_c^2}\right)^2}\frac{\mathrm{d}A_{FB}}{\mathrm{d}q^2}\,.
\end{aligned} \tag{C.18}$$

Here we neglect finite bremsstrahlung corrections not related to $Q_{7,9,10}\otimes Q_{7,9,10}$, which constitute less than one percent in b decays [289]. The energy asymmetry turned out to be an equivalent observable [288].

The lepton left-right asymmetry, normalized to $c \to (d,s) l\nu$ decays, can be obtained by the replacements $C_9 \to C_9^{L/R} = (C_9 \mp C_{10})/2$, $C_{10} \to C_{10}^{L/R} = (C_{10} \mp C_9)/2$ and $|C_7|^2 \to |C_7|^2/2$ in eq. (C.1). We obtain for massless leptons

$$A_{LR} = \frac{\mathcal{B}(D \to X_{(d,s)} l\nu)}{\Gamma_{c\to(d,s)l\nu}} \frac{G_F^2 \alpha_e^2 m_c^3}{768\pi^5} \left(1 - \frac{q^2}{m_c^2}\right)^2 \times \left(-2\left(1 + 2\frac{q^2}{m_c^2}\right) \mathrm{Re}[C_9 C_{10}^*] - 12\mathrm{Re}[C_7 C_{10}^*]\right) . \tag{C.19}$$

The leading power corrections are given in [103] as

$$\begin{aligned}\delta_{1/m_c^2} \frac{\mathrm{d}A_{LR}}{\mathrm{d}q^2} = \frac{3\lambda_2}{2m_c^2}\Bigg[& \frac{\mathcal{B}(D \to X_{(d,s)} l\nu)}{\Gamma_{c\to(d,s)l\nu}} \frac{G_F^2 \alpha_e^2 m_c^3}{768\pi^5} \Bigg(-2\left(1 - 15\left(\frac{q^2}{m_c^2}\right)^2 + 10\left(\frac{q^2}{m_c^2}\right)^3\right) \\ & \times \mathrm{Re}[C_9 C_{10}^*] + 4\left(5 + 6\frac{q^2}{m_c^2} - 7\left(\frac{q^2}{m_c^2}\right)^2\right) \mathrm{Re}[C_7 C_{10}^*]\Bigg) \\ & + \frac{g(m_q^2/m_c^2)}{X_0(m_q^2/m_c^2)} \frac{\mathrm{d}A_{LR}}{\mathrm{d}q^2}\Bigg] . \end{aligned} \tag{C.20}$$

Here finite bremsstrahlung corrections not related to $Q_{7,9,10} \otimes Q_{7,9,10}$ vanish.

The lepton longitudinal and normal polarization asymmetries of $l^\pm$ are obtained from [284]. They are given as

$$\begin{aligned}\frac{\mathrm{d}P_L^\pm}{\mathrm{d}q^2} = & \pm m_c^4 u(q^2) \sqrt{1 - \frac{4m_l^2}{q^2}} \\ & \times \mathrm{Re}\left[8\left(1 - \frac{q^2}{m_c^2}\right) C_7 C_{10}^* + \left(1 - \frac{q^4}{m_c^4} - \frac{u^2(q^2)}{3m_c^4(1 - 4m_l^2/q^2)}\right) C_9 C_{10}^*\right] \end{aligned} \tag{C.21}$$

and

$$\frac{\mathrm{d}P_N^\pm}{\mathrm{d}q^2} = \pm 2\pi \frac{m_l m_c^2}{\sqrt{q^2}} u^2(q^2)\, \mathrm{Im}\left[C_7 C_{10}^*\right] . \tag{C.22}$$

The defining angle is the one between the momentum of the charm quark and the momentum of the negatively charged lepton in the dilepton center of mass frame and

$$u(q^2) = (m_c^2 - q^2)^2 \sqrt{1 - \frac{4m_l^2}{q^2}} . \tag{C.23}$$

We neglect electromagnetic interactions between the leptons. The distribution due to additional operators can also be obtained from [284].

The lepton transverse polarization asymmetries of $l^\pm$ are given by [284] as

$$\frac{\mathrm{d}P_T^\pm}{\mathrm{d}q^2} = -\frac{\pi}{2}\frac{m_l m_c^2}{\sqrt{q^2}(1-4m_l^2/q^2)}u^2(q^2) \times \left(16\frac{m_c^2}{q^2}|C_7|^2 + \mathrm{Re}[4C_7C_9^* \mp 2C_7C_{10}^* - C_9C_{10}^*]\right). \tag{C.24}$$

C.2. The decay $D \to Pll$

In this appendix we derive the distribution for the decay of a pseudoscalar into a lighter pseudoscalar and a lepton pair, i.e. for $D \to Pll$, which is analyzed in section 3.2 and chapter 4. Along we introduce form factors and observables.

In the D meson rest frame, the distribution can be written as

$$\begin{aligned}\mathrm{d}\Gamma &= \frac{1}{2m_D}\langle|\mathcal{A}|^2\rangle\frac{\mathrm{d}^3p_P}{(2\pi)^3 2E_P}\frac{\mathrm{d}^3p_+}{(2\pi)^3 2E_+}\frac{\mathrm{d}^3p_-}{(2\pi)^3 2E_-}(2\pi)^4\delta(p_D - p_P - p_+ - p_-) \\ &= \frac{\langle|\mathcal{A}|^2\rangle}{2m_D(2\pi)^5}\mathrm{d}PS\,,\end{aligned} \tag{C.25}$$

where we separate the amplitude $\mathcal{A}$, and the factorized phase space

$$\mathrm{d}PS = \mathrm{d}q^2\delta(p_D - q - p_P)\frac{\mathrm{d}^3q}{2E_q}\frac{\mathrm{d}^3p_P}{2E_P}\delta(q - p_+ - p_-)\frac{\mathrm{d}^3p_+}{2E_+}\frac{\mathrm{d}^3p_-}{2E_-}\,. \tag{C.26}$$

Firstly, we work out the phase space.

Keeping in mind that an integration is performed, we can write

$$\frac{\mathrm{d}^3p_+}{2E_+} \to \mathrm{d}^4p_+\delta(p_+^2 - m_+^2) \tag{C.27}$$

which is implicitly multiplied by $\theta(p_+^0)$. It follows that, again by means of integration,

$$\delta(q - p_+ - p_-)\frac{\mathrm{d}^3p_+}{2E_+} \to \frac{\delta(\cos\phi - \cos\phi^*)}{2|q||p_-|}\,, \qquad \cos\phi^* = \frac{2E_qE_- - q^2}{2|p_q||p_-|}\,, \tag{C.28}$$

where ϕ is the angle between the momenta q and p_-. We obtain

$$\frac{\mathrm{d}^3p_-}{2E_-} = \pi|p_-|\,\mathrm{d}E_-\,\mathrm{d}\cos\phi\,. \tag{C.29}$$

Analogously,

$$\delta(p_D - q - p_P)\frac{\mathrm{d}^3p_P}{2E_P} \to \frac{\delta(E_q - E_q^*)}{2m_D}\,, \qquad E_q^* = \frac{m_D^2 - m_P^2 + q^2}{2m_D} \tag{C.30}$$

give

$$\frac{\mathrm{d}^3 q}{2E_q} = 2\pi |q| \, \mathrm{d}E_q \,. \tag{C.31}$$

Combining these expression we can write the phase space as

$$\mathrm{d}PS = \frac{\pi^2}{2m_D} \mathrm{d}q^2 \mathrm{d}E_- \,. \tag{C.32}$$

We define [290]

$$u = (p_D - p_-)^2 - (p_D - p_+)^2 = -u(q^2)\cos\theta \,, \tag{C.33}$$

where θ is the angle between the momentum of the positively charged lepton and the D meson in the dilepton center of mass frame. With this definition we obtain

$$-u(q^2) \leq u \leq u(q^2) \,, \qquad\qquad u(q^2) = \sqrt{\lambda(m_D^2, m_P^2, q^2)}\beta_l \,, \tag{C.34}$$

where

$$\lambda(a,b,c) = a^2 + b^2 + c^2 - 2ab - 2ac - 2bc \,, \qquad\qquad \beta_l = \sqrt{1 - 4\frac{m_l^2}{q^2}} \,. \tag{C.35}$$

It follows that, in the D meson rest frame,

$$\mathrm{d}E_- = -\frac{1}{4m_D} \mathrm{d}u \,. \tag{C.36}$$

The pseudoscalar distribution is thus given as

$$\frac{\mathrm{d}^2\Gamma}{\mathrm{d}q^2 \mathrm{d}u} = \frac{\langle |\mathcal{A}|^2 \rangle}{512\pi^3 m_D^3} \,. \tag{C.37}$$

To calculate the amplitude we restrict ourselves, at first, to the SM operator basis, see the beginning of chapter 3. We factorize the leptonic and hadronic currents in the amplitude as

$$\begin{aligned} i\mathcal{A}|_{\mathrm{SM}} &= \langle llP | \mathcal{H}_{\mathrm{eff}}^{\mathrm{weak}} |_{\mathrm{SM}} | D \rangle \\ &= -\frac{2G_F}{\sqrt{2}} \frac{\alpha_e}{4\pi} \Bigg(C_7 \frac{m_c}{e} \left[-\frac{2eiq_\nu}{q^2} \bar{l}(p_+)\gamma_\mu l(p_-) \right] \langle P | j^{\mu\nu} | D \rangle \\ &\quad + C_9 \left[\bar{l}(p_+)\gamma_\mu l(p_-) \right] \langle P | j^\mu | D \rangle + C_{10} \left[\bar{l}(p_+)\gamma^\mu\gamma_5 l(p_-) \right] \langle P | j^\mu | D \rangle \Bigg) \,, \end{aligned} \tag{C.38}$$

where the currents are defined by

$$\langle P|j^\mu|D\rangle = \langle P|\bar{u}\gamma^\mu(1-\gamma_5)c|D\rangle\,, \qquad \langle P|j^{\mu\nu}|D\rangle = \langle P|\bar{u}\sigma^{\mu\nu}(1+\gamma_5)c|D\rangle\,. \tag{C.39}$$

Note that the vector current in eq. (C.39) is conserved, which implies that its anomalous dimension is zero. Furthermore, the hadronic axialvector current vanishes as the D meson is parity odd.

Concerning the hadronic matrix elements we utilize the Lorentz structure and parity invariance of QCD to parametrize them in terms of the form factors $f_{+,0,T}$ as

$$\langle P(p_P)|\bar{u}\gamma^\mu c|D(p_D)\rangle = f_+(q^2)\left(p^\mu - \frac{m_D^2-m_P^2}{q^2}q^\mu\right) + f_0(q^2)\frac{m_D^2-m_P^2}{q^2}q^\mu\,, \tag{C.40}$$

$$\langle P(p_P)|\bar{u}\sigma^{\mu\nu}(1\pm\gamma_5)c|D(p_D)\rangle = if_T(q^2)(p^\mu q^\nu - q^\mu p^\nu \pm i\epsilon^{\mu\nu\rho\sigma}p_\rho q_\sigma)\,. \tag{C.41}$$

Here $q^\mu = (p_D - p_P)^\mu = (p_+ + p_-)^\mu$ and $p^\mu = (p_D + p_P)^\mu$.

The amplitude follows as

$$-i\mathcal{A}|_{\rm SM} = \frac{G_F\alpha_e}{2\sqrt{2}\pi}\bar{l}\left(c_\mu^V\gamma^\mu + c_\mu^A\gamma^\mu\gamma_5\right)l\,, \tag{C.42}$$

where

$$\begin{aligned} c_\mu^V &= (C_9 f_+ + 2C_7 m_c f_T)\left(p_\mu - \frac{m_D^2-m_P^2}{q^2}q_\mu\right) + C_9 f_0\frac{m_D^2-m_P^2}{q^2}q_\mu\,,\\ c_\mu^A &= C_{10}f_+\left(p_\mu - \frac{m_D^2-m_P^2}{q^2}q_\mu\right) + C_{10}f_0\frac{m_D^2-m_P^2}{q^2}q_\mu\,. \end{aligned} \tag{C.43}$$

We sum over the spin of the leptons to find for $\Gamma^\mu \in \{\gamma^\mu, \gamma^\mu\gamma_5\}$

$$\begin{aligned} \left(\frac{G_F^2\alpha_e^2}{8\pi^2}\right)^{-1}\langle|\mathcal{A}|_{\rm SM}|^2\rangle &= \sum_{i,j=V,A} c_\mu^i\left(c^j\right)_\nu^* \mathrm{Tr}\left[\Gamma_i^\mu\left(\not{p}_+ - m_l\right)\Gamma_j^\nu\left(\not{p}_- + m_l\right)\right]\\ &= -4\left(\left|c^V\right|^2 - \left|c^A\right|^2\right)m_l^2 - 4\left(\left|c^V\right|^2 + \left|c^A\right|^2\right)(p_+\cdot p_-)\\ &\quad + 8\mathrm{Re}\left[c_\mu^V\left(c^V\right)_\nu^* + c_\mu^A\left(c^A\right)_\nu^*\right]p_+^\mu p_-^\nu\,, \end{aligned} \tag{C.44}$$

where $\left(c^V\right)^\rho\left(c^{A*}\right)^\sigma\epsilon_{\rho\sigma\mu\nu}p_+^\mu p_-^\nu = 0$, hence the pseudotensor current vanishes. Writing the scalar products as $p_+\cdot p_- = q^2/2 - m_l^2$, $q\cdot p_\pm = q^2/2$, $p^2 = 2m_D^2 + 2m_P^2 - q^2$, and $p\cdot p_\pm = (m_D^2 - m_P^2 \pm u)/2$, finally, we obtain the SM differential distribution

$$\begin{aligned} \left(\frac{G_F^2\alpha_e^2}{2048\pi^5 m_D^3}\right)^{-1}\frac{\mathrm{d}^2\Gamma|_{\rm SM}}{\mathrm{d}q^2\mathrm{d}u} &= \Big(\left(|C_9|^2 + |C_{10}|^2\right)|f_+|^2 + 4|C_7|^2|f_T|^2 m_c^2\\ &\quad + 4\mathrm{Re}\left[C_7 C_9^* f_T f_+\right]m_c\Big)\left(\lambda(m_D^2, m_P^2, q^2) - u^2\right) + |C_{10}|^2\\ &\quad \times\left(-|f_+|^2\lambda(m_D^2, m_P^2, q^2) + |f_0|^2\left(m_D^2 - m_P^2\right)^2\right)\frac{4m_l^2}{q^2}\,, \end{aligned} \tag{C.45}$$

in agreement with the result in [290]. Here the form factors are taken to be real.

Next we include all dimension six operators. The required matrix elements are related to the ones defined by eqs. (C.40, C.41) by the EOM, yielding

$$\langle P(p_P)|\bar{u}c|D(p_D)\rangle = \frac{q_\mu}{m_c-m_u}\langle P(p_P)|\bar{u}\gamma^\mu c|D(p_D)\rangle = f_0\frac{m_D^2-m_P^2}{m_c-m_u}\,, \tag{C.46}$$

where hadronic pseudoscalar currents vanish by parity arguments. Writing

$$\begin{aligned} c^S &= (C_S+C_S')f_0\frac{m_D^2-m_P^2}{m_c-m_u}\,, & c^P &= (C_P+C_P')f_0\frac{m_D^2-m_P^2}{m_c-m_u}\,,\\ c^T_{\mu\nu} &= C_T f_T(p_\mu q_\nu - q_\mu p_\nu)\,, & c^{T5}_{\mu\nu} &= C_{T5} f_T(p_\mu q_\nu - q_\mu p_\nu) \end{aligned} \tag{C.47}$$

the amplitude reads

$$-i\mathcal{A} = \frac{G_F\alpha_e}{2\sqrt{2}\pi}\bar{l}\left(... + c^S + c^P\gamma_5 + c^T_{\mu\nu}\gamma^{\mu\nu} + c^{T5}_{\mu\nu}\gamma^{\mu\nu}\gamma_5\right) l\,, \tag{C.48}$$

where the ellipses represent the SM amplitude (C.42). Calculating the traces, we obtain for $\Gamma \in \{..., 1, \gamma_5, \sigma^{\mu\nu}, \sigma^{\mu\nu}\gamma_5\}$ and $\overline{\Gamma} \in \{..., 1, -\gamma_5, \sigma^{\mu\nu}, -\sigma^{\mu\nu}\gamma_5\}$

$$\begin{aligned} \left(\frac{G_F^2\alpha_e^2}{8\pi^2}\right)^{-1}\langle|\mathcal{A}|^2\rangle &= \sum_{i,j} c^i c^{j*}\mathrm{Tr}\left[\Gamma_i\left(\not{p}_+ - m_l\right)\overline{\Gamma}_j\left(\not{p}_- + m_l\right)\right]\\ &= ... + 4\left|c^S\right|^2(p_+\cdot p_- - m_l^2) + 4\left|c^P\right|^2(p_+\cdot p_- + m_l^2)\\ &+ 8\mathrm{Re}\left[c^S\left(c^V\right)^*_\mu\right]\left(p_+^\mu - p_-^\mu\right)m_l + 8\mathrm{Re}\left[c^P\left(c^A\right)^*_\mu\right]\left(p_+^\mu + p_-^\mu\right)m_l\\ &+ 8\mathrm{Re}\left[c^S\left(c^T\right)^*_{\mu\nu} + c^P\left(c^{T5*}\right)_{\mu\nu}\right]\left(p_+^\mu p_-^\nu - p_-^\mu p_+^\nu\right)\\ &+ 8\mathrm{Re}\left[c^V_\mu\left(c^T\right)^*_{\nu\rho}\right]\left(g^{\mu\rho}\left(p_+^\nu + p_-^\nu\right) - g^{\mu\nu}\left(p_+^\rho + p_-^\rho\right)\right)m_l\\ &+ 8\mathrm{Re}\left[c^A_\mu\left(c^{T5}\right)^*_{\nu\rho}\right]\left(g^{\mu\rho}\left(p_+^\nu - p_-^\nu\right) - g^{\mu\nu}\left(p_+^\rho - p_-^\rho\right)\right)m_l\\ &+ 4\left(c^T_{\mu\nu}\left(c^T\right)^*_{\rho\sigma} + c^{T5}_{\mu\nu}\left(c^{T5}\right)^*_{\rho\sigma}\right)\left(g^{\mu\rho}\left(g^{\nu\sigma}p_+\cdot p_- - p_+^\nu p_-^\sigma + p_+^\sigma p_-^\nu\right)\right.\\ &- g^{\mu\sigma}\left(g^{\nu\rho}p_+\cdot p_- - p_+^\nu p_-^\rho + p_+^\rho p_-^\nu\right) + g^{\nu\rho}\left(p_+^\mu p_-^\sigma + p_+^\sigma p_-^\mu\right)\\ &\left.- g^{\nu\sigma}\left(p_+^\mu p_-^\rho + p_+^\rho p_-^\mu\right)\right)\\ &- 4\left(c^T_{\mu\nu}\left(c^T\right)^*_{\rho\sigma} - c^{T5}_{\mu\nu}\left(c^{T5}\right)^*_{\rho\sigma}\right)(g^{\mu\rho}g^{\nu\sigma} - g^{\mu\sigma}g^{\nu\rho})m_l^2 \end{aligned} \tag{C.49}$$

since

$$\begin{aligned} 0 &= c^P\left(c^T\right)^{*\mu\nu}\epsilon_{\mu\nu\rho\sigma}p_+^\rho p_-^\sigma = c^S\left(c^{T5}\right)^{*\mu\nu}\epsilon_{\mu\nu\rho\sigma}p_+^\rho p_-^\sigma = \left(c^A\right)^\mu\left(c^T\right)^{*\nu\rho}\epsilon_{\mu\nu\rho\sigma}\left(p_+^\sigma + p_-^\sigma\right)\\ &= \left(c^V\right)^\mu\left(c^{T5}\right)^{*\nu\rho}\epsilon_{\mu\nu\rho\sigma}\left(p_+^\sigma - p_-^\sigma\right)\,. \end{aligned} \tag{C.50}$$

Finally, the full differential distribution follows as

$$\begin{aligned}\left(\frac{G_F^2\alpha_e^2}{2048\pi^5 m_D^3}\right)^{-1}\frac{\mathrm{d}\Gamma^2}{\mathrm{d}q^2\mathrm{d}u} = &\ldots + \left(|C_S|^2\left(q^2-4m_l^2\right)+|C_P|^2q^2\right)|f_0|^2\frac{\left(m_D^2-m_P^2\right)^2}{(m_c-m_u)^2}\\ &+8\mathrm{Re}\left[C_T^*\left(C_9f_+ + 2C_7f_Tm_c\right)f_T\right]\lambda(m_D^2,m_P^2,q^2)m_l\\ &+4\mathrm{Re}\left[C_{10}C_P^*\right]|f_0|^2\frac{\left(m_D^2-m_P^2\right)^2}{m_c-m_u}m_l\\ &+16|C_T|^2|f_T|^2\lambda(m_D^2,m_P^2,q^2)m_l^2\\ &+4\mathrm{Re}\left[\left(C_SC_T^*+C_PC_{T5}^*\right)f_Tf_0\right]\frac{m_D^2-m_P^2}{m_c-m_u}q^2u\\ &+4\mathrm{Re}\left[C_S^*\left(C_9f_+ + 2C_7m_cf_T\right)f_0\right]\frac{m_D^2-m_P^2}{m_c-m_u}m_lu\\ &+8\mathrm{Re}\left[C_{10}C_{T5}^*f_Tf_0\right]\left(m_D^2-m_P^2\right)m_lu\\ &+4\left(|C_T|^2+|C_{T5}|^2\right)|f_T|^2q^2u^2\,, \end{aligned}\tag{C.51}$$

where the ellipsis represent the SM distribution of eq. (C.45)- Here and in the following, for simplicity, $C_7m_c \to (C_7m_c + C_7'm_u)$, and $C_{9,10,S,P} \to (C_{9,10,S,P} + C'_{9,10,S,P})$ since hadronic axialvector currents vanish. With appropriate changes in the definitions of f_T and θ, the distribution is agreement with the result in [96]. Lepton dependence can be implemented by the replacements $C_i \to C_i^{(l)}$, where $i \neq 7$. The CP conjugated distribution is given by the replacements $V_{cq}^*V_{uq} \to V_{cq}V_{uq}^*$ and $u \to -u$. We use $m_u = 0$ in the following.

Integrating u gives the q^2 spectrum

$$\begin{aligned}\frac{\mathrm{d}\Gamma}{\mathrm{d}q^2} = &\frac{G_F^2\alpha_e^2}{1024\pi^5 m_D^3}\left(\frac{2}{3}\left(\left(|C_9|^2+|C_{10}|^2\right)f_+^2 + 4|C_7|^2f_T^2m_c^2 + 4\mathrm{Re}[C_7C_9^*]f_Tf_+m_c\right)\right.\\ &\times\lambda(m_D^2,m_P^2,q^2)\left(1+\frac{2m_l^2}{q^2}\right)+|C_{10}|^2\left(-f_+^2\lambda(m_D^2,m_P^2,q^2)+f_0^2\left(m_D^2-m_P^2\right)^2\right)\frac{4m_l^2}{q^2}\\ &+\left(|C_S|^2\left(q^2-4m_l^2\right)+|C_P|^2q^2\right)f_0^2\frac{\left(m_D^2-m_P^2\right)^2}{m_c^2}\\ &+\frac{4}{3}\left(|C_T|^2+|C_{T5}|^2\right)f_T^2q^2\lambda(m_D^2,m_P^2,q^2)\left(1-\frac{4m_l^2}{q^2}\right)\\ &+8\mathrm{Re}[(C_9f_+ + 2C_7f_Tm_c)C_T^*]f_T\lambda(m_D^2,m_P^2,q^2)m_l\\ &+4\mathrm{Re}[C_{10}C_P^*]f_0^2\frac{\left(m_D^2-m_P^2\right)^2}{m_c}m_l\\ &\left.+16|C_T|^2f_T^2\lambda(m_D^2,m_P^2,q^2)m_l^2\right)\sqrt{\lambda(m_D^2,m_P^2,q^2)\left(1-\frac{4m_l^2}{q^2}\right)}\,, \end{aligned}\tag{C.52}$$

in agreement with the result in [1], for appropriate changes in the definitions of f_T and θ.

The differential lepton forward-backward asymmetry is defined as the asymmetry between the forward minus backward flying l^+ in the dilepton center of mass frame relative to the recoiling P, i.e.

$$\frac{\mathrm{d}A_{FB}}{\mathrm{d}q^2} \propto \int_{-u(q^2)}^{0} \mathrm{d}u \frac{\mathrm{d}^2\Gamma}{\mathrm{d}q^2\mathrm{d}u} - \int_{0}^{u(q^2)} \mathrm{d}u \frac{\mathrm{d}^2\Gamma}{\mathrm{d}q^2\mathrm{d}u} \,. \tag{C.53}$$

Here and in the following, the proportionality holds up to the normalization, which will be specified wherever needed. We obtain for $D^+ \to P^+ll$

$$\begin{aligned}\frac{\mathrm{d}A_{FB}}{\mathrm{d}q^2} \propto \frac{G_F^2\alpha_e^2}{2048\pi^5 m_D^3}\Bigg[-4\Bigg[&\mathrm{Re}\left[\left(C_S C_T^* + C_P C_{T5}^*\right) f_T f_0\right] \frac{m_D^2 - m_P^2}{m_c} q^2 \\ &+ \mathrm{Re}\left[C_S^* \left(C_9 f_+ + 2C_7 f_T m_c\right) f_0\right] \frac{m_D^2 - m_P^2}{m_c} m_l \\ &+ 2\mathrm{Re}\left[C_{10} C_{T5}^* f_T f_0\right] \left(m_D^2 - m_P^2\right) m_l \Bigg] \lambda(m_D^2, m_P^2, q^2) \left(1 - \frac{4m_l^2}{q^2}\right) \Bigg] \,. \end{aligned} \tag{C.54}$$

Under CP conjugation the forward-backward asymmetry changes its sign.

A combined observable is the lepton forward-backward CP asymmetry defined as

$$\frac{\mathrm{d}A_{FB}^{CP}}{\mathrm{d}q^2} \propto A_{FB}^{D^+ \to P^+ll} + A_{FB}^{D^- \to P^-ll} \,. \tag{C.55}$$

The "flat" term is defined as

$$F_H \propto \sum_{i=0}^{1} \int \mathrm{d}q^2 \left.\frac{\mathrm{d}^2\Gamma}{\mathrm{d}q^2 \mathrm{d}\cos\theta}\right|_{\cos^{2i}\theta} \,. \tag{C.56}$$

In the approximation of vanishing lepton masses we obtain

$$\begin{aligned} F_H \propto \frac{G_F^2\alpha_e^2}{2048\pi^5 m_D^3}\Bigg(&\left(|C_S|^2 + |C_P|^2\right) |f_0|^2 \frac{\left(m_D^2 - m_P^2\right)^2}{m_c^2} q^2 \sqrt{\lambda(m_D^2, m_P^2, q^2)} \\ &+ 4\left(|C_T|^2 + |C_{T5}|^2\right) |f_T|^2 q^2 \sqrt{\lambda(m_D^2, m_P^2, q^2)}^3 \Bigg) + \mathcal{O}(m_l) \,. \end{aligned} \tag{C.57}$$

Note that the lepton flavor ratio $\mathcal{B}_{D\to P\mu^+\mu^-}/\mathcal{B}_{D\to Pe^+e^-}$ and the flat term F_H are related [96]. The lepton flavor ratio restricted to the SM operator basis at high q^2 follows from kinematics as

$$\begin{aligned}\left.\frac{\mathcal{B}_{D\to P\mu^+\mu^-}}{\mathcal{B}_{D\to Pe^+e^-}}\right|_{\rm SM} - 1 = \frac{8}{3}\frac{m_\mu^2}{q^2}\Bigg[&|C_{10}|^2\left(-|f_+|^2\lambda(m_D^2,m_P^2,q^2)+|f_0|^2\left(m_D^2-m_P^2\right)^2\right)\\ &\times\lambda^{1/2}(m_D^2,m_P^2,q^2)\Bigg]\\ \Bigg/\Bigg[&\left(\left(|C_9|^2+|C_{10}|^2\right)|f_+|^2+4|C_7|^2|f_T|^2\frac{m_c^2}{}+4{\rm Re}\left[C_7C_9^*f_Tf_+\right]m_c\right)\\ &\times\lambda^{3/2}(m_D^2,m_P^2,q^2)\Bigg]+\mathcal{O}\left(\left(\frac{m_\mu^2}{q^2}\right)^2\right).\end{aligned} \tag{C.58}$$

We use a zero electron mass and will integrate the numerator and the denominator separately.

The resonant catalyzed CP asymmetry is [1]

$$\begin{aligned}\frac{{\rm d}A_{CP}}{{\rm d}q^2} &= \frac{{\rm d}\mathcal{B}_{D^+\to P^+ll}}{{\rm d}q^2} - \frac{{\rm d}\mathcal{B}_{D^-\to P^-ll}}{{\rm d}q^2}\\ &= -\frac{1}{\Gamma_D}\frac{G_F^2\alpha_e^2}{384\pi^5 m_D^3}\sqrt{\lambda^3(m_D^2,m_P^2,q^2)\left(1-4\frac{m_l^2}{q^2}\right)}\left(1+2\frac{m_l^2}{q^2}\right)\\ &\times\Bigg({\rm Im}[V_{cd}^*V_{ud}(V_{cs}V_{us}^*)]{\rm Im}[c_dc_s^*]+{\rm Im}[V_{cd}^*V_{ud}(\delta C_9+\delta C_9')^*]{\rm Im}[c_d]f_+\\ &+{\rm Im}[V_{cs}^*V_{us}(\delta C_9+\delta C_9')^*]{\rm Im}[c_s]f_+\Bigg),\end{aligned} \tag{C.59}$$

where

$$c_d = \frac{4\pi}{\alpha_s}2C_7^{{\rm eff}(d)}f_Tm_c + C_9^\rho\frac{f_+}{V_{cd}^*V_{ud}}, \qquad c_s = \frac{4\pi}{\alpha_s}2C_7^{{\rm eff}(s)}f_Tm_c + C_9^\phi\frac{f_+}{V_{cs}^*V_{us}}, \tag{C.60}$$

and $(\delta C_9+\delta C_9')$ correspond to possible BSM contributions. The SM contribution $C_9^{\rm eff}$ is omitted to avoid double counting. Compared with [126] effects of the ρ resonance and $\delta C_9^{(\prime)}$ are included. In turn [126] considers BSM effects due to C_7.

C.3. Exclusive (semi-)leptonic decays

Here we provide distributions and observables of other exclusive (semi-)leptonic decays for section 3.4.

The branching ratio for $D^0 \to l^+ l^-$ reads [96]

$$\mathcal{B}_{D^0\to l^+l^-} = \frac{G_F^2 \alpha_e^2 m_{D^0}^5 f_{D^0}^2}{64\pi^3 \Gamma_{D^0}} \sqrt{1-\frac{4m_l^2}{m_{D^0}^2}} \times \left(\left(1-\frac{4m_l^2}{m_{D^0}^2}\right) \left|\frac{C_S - C_S'}{m_c+m_u}\right|^2 + \left|\frac{C_P - C_P'}{m_c+m_u} + \frac{2m_l}{m_{D^0}^2}(C_{10}-C_{10}')\right|^2 \right) . \quad \text{(C.61)}$$

Here the only non-perturbative parameter is the decay constant f_D.

For $D^{*0} \to l^+ l^-$ the total width can be written as [175]

$$\Gamma = \frac{\alpha_e^2 G_F^2}{96\pi^3} m_{D^{*0}}^3 f_{D^{*0}}^2 \left(\left| C_9 + 2\frac{m_c}{m_{D^{*0}}} \frac{f_{D^{*0}}^T}{f_{D^{*0}}} C_7 \right|^2 + |C_{10}|^2 \right) , \quad \text{(C.62)}$$

where the lepton and up quark masses are neglected. We use $\Gamma_{D^{*0}} \simeq 6 \times 10^{-5}\,\text{GeV}$, $f_{D^{*0}}^T \simeq f_{D^{*0}}$ and $f_{D^{*0}} \simeq 0.242\,\text{GeV}$ [175].

The distribution for the dineutrino decay $D \to P\nu_L\bar{\nu}_L$ is obtained from eq. (C.45) by the replacements $m_l \to 0$, $C_7 \to 0$ and $C_{10} = -C_9$. Note that the amplitude factorizes on the full q^2 range as neutrinos do not couple strongly nor electromagnetically. Furthermore, neutrino flavors are summed as they are not detectable in experiments.

We obtain the distribution for $D \to Pe\mu$ analogue to the one for $D \to Pll$, see the previous appendix. The starting point is eq. (C.37). We neglect the electron mass and write the scalar products as $p_+ \cdot p_- = q^2/2 - (m_+^2 + m_-^2)/2$, $q \cdot p_\pm = q^2/2 \pm (m_+ - m_-)/2$, and $p \cdot p_\pm = (m_D^2 - m_P^2 \pm u)/2 - (m_+^2 - m_-^2)/2 \pm (m_+^2 - m_-^2)/2$. It follows that the differential distribution is given by

$$\begin{aligned}
\left(\frac{G_F^2\alpha_e^2}{2048\pi^5 m_D^3}\right)^{-1} \frac{\mathrm{d}^2\Gamma_{D^+\to P^+ e^\pm \mu^\mp}}{\mathrm{d}q^2 \mathrm{d}u} &= \left(|K_9|^2 + |K_{10}|^2\right) |f_+|^2 \left(\lambda(m_D^2, m_P^2, q^2) - u^2\right) \\
&+ \left(|K_S|^2 + |K_P|^2\right) |f_0|^2 \frac{\left(m_D^2 - m_P^2\right)^2}{(m_c - m_u)^2} q^2 \\
&+ 4\left(|K_T|^2 + |K_{T5}|^2\right) |f_T|^2 q^2 u^2 \\
&+ 4\mathrm{Re}\left[\left(K_S K_T^* + K_P K_{T5}^*\right) f_T f_0\right] \frac{m_D^2 - m_P^2}{m_c - m_u} q^2 u \\
&+ 2\mathrm{Re}\left[\pm K_9 K_S^* + K_{10} K_P^*\right] |f_0|^2 \frac{\left(m_D^2 - m_P^2\right)^2}{m_c - m_u} m_\mu \\
&+ 4\mathrm{Re}\left[\left(K_9 K_T^* \pm K_{10} K_{T5}^*\right) f_T f_+\right] \lambda(m_D^2, m_P^2, q^2) m_\mu \\
&+ 2\mathrm{Re}\left[\left(K_9 K_S^* \pm K_{10} K_P^*\right) f_0 f_+\right] \frac{m_D^2 - m_P^2}{m_c - m_u} m_\mu u \\
&+ 4\mathrm{Re}\left[\left(\pm K_9 K_T^* + K_{10} K_{T5}^*\right) f_T f_0\right] \left(m_D^2 - m_P^2\right) m_\mu u \\
&+ \mathcal{O}\left(m_\mu^2\right) , \qquad \text{(C.63)}
\end{aligned}$$

where $K_i = K_i^{(e\mu,\mu e)}$ are the Wilson coefficients of the operators obtained from the ones defined at the beginning of chapter 3 by the replacements $\bar{l}\Gamma l \to (\bar{e}\Gamma\mu, \bar{\mu}\Gamma e)$ for Dirac matrices Γ. Here $m_\mu^2 \leq q^2 \leq (m_D - m_P)^2$. We obtain

$$u \in [m_+^2 - m_-^2 + 2(E_p(E_+ - E_-) \mp |p_P|(|p_+| + |p_-|))] \,, \tag{C.64}$$

and in the dilepton center-of-mass frame, due to momentum conservation,

$$q^2 = \left(\sqrt{m_D^2 + |p_P|^2} - \sqrt{m_P^2 + |p_P|^2}\right)^2 . \tag{C.65}$$

It follows that

$$|p_P|^2 = \frac{1}{4q^2}\lambda(m_D^2, m_P^2, q^2) \,, \qquad E_P^2 = \frac{1}{4q^2}\left(m_D^2 - m_P^2 - q^2\right)^2 , \tag{C.66}$$

and, analogously,

$$|p_\pm|^2 = \frac{1}{4q^2}\lambda(m_+^2, m_-^2, q^2) \,, \qquad E_\pm^2 = \frac{1}{4q^2}\left(m_\pm^2 - m_\mp^2 + q^2\right)^2 . \tag{C.67}$$

Combining the above equations one obtains

$$\begin{aligned} u &\geq \left(m_D^2 - m_P^2\right)\frac{m_+^2 - m_-^2}{q^2} - \sqrt{\lambda(m_D^2, m_P^2, q^2)}\left(1 - \frac{m_+^2 + m_-^2}{q^2}\right) , \\ u &\leq \left(m_D^2 - m_P^2\right)\frac{m_+^2 - m_-^2}{q^2} + \sqrt{\lambda(m_D^2, m_P^2, q^2)}\left(1 - \frac{m_+^2 + m_-^2}{q^2}\right) , \end{aligned} \tag{C.68}$$

that is $u(q^2) = \sqrt{\lambda(m_D^2, m_P^2, q^2)} + \mathcal{O}(m_\mu^2)$. Note that the hadronic matrix elements are the same as for $D \to Pll$ decays, and no Wilson coefficient K_7 analogue to the one for the operator Q_7 is present, as the photon does not couple to different lepton flavors. Furthermore one can define angular observables, e.g. the forward-backward asymmetry and flat term, as for $D \to Pll$ decays.

Finally, the branching ratio for $D^0 \to \mu^\pm e^\mp$ is obtained as [1]

$$\begin{aligned} \mathcal{B}(D^0 \to \mu^\pm e^\mp) = \frac{G_F^2 \alpha_e^2 m_{D^0}^5 f_{D^0}^2}{64\pi^3 \Gamma_{D^0}} \left(1 - \frac{m_\mu^2}{m_{D^0}^2}\right)^2 \Bigg(\left| \frac{K_S - K_S'}{m_c} \mp \frac{m_\mu}{m_{D^0}^2}(K_9 - K_9') \right|^2 \\ + \left| \frac{K_P - K_P'}{m_c} + \frac{m_\mu}{m_{D^0}^2}(K_{10} - K_{10}') \right|^2 \Bigg) , \end{aligned} \tag{C.69}$$

where the electron and up quark masses are neglected.

D. Form factors for $D \to V$ transitions

For $D \to V\gamma$ decays, see sections 3.3 and 4.4, only a few form factor at certain q^2 are needed. Compared to transitions into a pseudoscalar meson less information on $D \to V$ form factors are available. To draw a consistent picture and to obtain reliable form factors including uncertainties we consider the full set of form factors for any q^2 in the current appendix. Moreover, they may be of use in view of a future work on $D \to Vll$ decays.

The form factors V, $A_{1,2,0}$, and $T_{1,2,3}$ are defined by

$$\begin{aligned}
\langle V(p_V,\epsilon^\nu)|\bar{u}\gamma_\mu(1-\gamma_5)c|D(p_D)\rangle &= -2\epsilon_{\mu\nu_1\nu_2\nu_3}(\epsilon^*)^{\nu_1}p_D^{\nu_2}q^{\nu_3}\frac{V}{m_D+m_V} \\
&\quad + i\left(q_\mu\frac{\epsilon^*\cdot q}{q^2}-\epsilon^*_\mu\right)(m_D+m_V)A_1 \\
&\quad - i\left(q_\mu\frac{m_D^2-m_V^2}{q^2}-(p_D+p_V)_\mu\right)\frac{\epsilon^*\cdot q}{m_D+m_V}A_2 \\
&\quad - iq_\mu(\epsilon^*\cdot q)\frac{2m_V}{q^2}A_0\,, \qquad \text{(D.1)} \\
\langle V(p_V,\epsilon^\nu)|\bar{u}\sigma_{\mu\nu_1}q^{\nu_1}(1+\gamma_5)c|D(p_D)\rangle &= -i2\epsilon_{\mu\nu_1\nu_2\nu_3}(\epsilon^*)^{\nu_1}p_D^{\nu_2}q^{\nu_3}T_1 \\
&\quad - \left((p_D+p_V)_\mu(\epsilon^*\cdot q)-\epsilon^*_\mu\left(m_D^2-m_V^2\right)\right)T_2 \\
&\quad + \left(q_\mu-(p_D+p_V)_\mu\frac{q^2}{m_D^2-m_V^2}\right)(\epsilon^*\cdot q)T_3\,, \qquad \text{(D.2)}
\end{aligned}$$

where $\epsilon_{0123}=1$, and $q^\mu=(p_D-p_V)^\mu$. For a neutrally charged V meson the form factors are multiplied by the isospin factor of the $u\bar{u}$ content in V, e.g. $1/\sqrt{2}$ for $V\in\{\rho^0,\omega\}$.

For perturbative $D\to V\gamma$ decays only one form factor $T_1(0)=T_2(0)$, which follows from the EOM, is needed. Furthermore, $2m_VA_0(0)=((m_D+m_V)A_1(0)-(m_D-m_V)A_2(0))$. Note that $\langle V|\bar{u}c|D\rangle=0$ and $\langle V|\bar{u}\gamma_5c|D\rangle=2m_V/(m_c+m_u)\,(\epsilon^*\cdot q)A_0$.

In the following, we compile available measurements and calculations of the form factors for $D_{(s)}\to(\rho,\omega,K^*)$ transitions. For the transition $D\to\rho$ the CLEO collaboration measured [291], adding uncertainties in quadrature,

$$\begin{aligned}
&V(0)=0.84^{+0.10}_{-0.11}\,, \quad A_1(0)=0.56^{+0.02}_{-0.03}\,, \quad A_2(0)=0.47\pm0.07\,, \\
&\frac{V(0)}{A_1(0)}=1.48\pm0.16\,, \quad \frac{A_2(0)}{A_1(0)}=0.83\pm0.12\,. \qquad \text{(D.3)}
\end{aligned}$$

These values are consistent with lattice computations [292] (and references therein) yielding

$$\begin{aligned} V(0) &= 1.1 \pm 0.2 \; (0.71^{+0.10}_{-0.12})\,, & A_1(0) &= 0.65 \pm 0.07 \; (0.60 \pm 0.06)\,, \\ A_2(0) &= 0.55 \pm 0.10 \; (0.61^{+0.12}_{-0.14})\,, & A_0(0) &= 0.70^{+0.05}_{-0.12} \; (0.59 \pm 0.06)\,. \end{aligned} \tag{D.4}$$

Here, in parenthesis the preliminary results of [293] are given, where we have doubled the uncertainties to account for systematic ones. Note that the form factors from lattice computations slightly differ from each other.

For the transition $D \to \omega$ the BESIII collaboration measured [294]

$$\frac{V(0)}{A_1(0)} = 1.24 \pm 0.11\,, \qquad \frac{A_2(0)}{A_1(0)} = 1.06 \pm 0.16\,, \tag{D.5}$$

where uncertainties are added in quadrature. A comparison with eq. (D.3) does not show a sensitivity to the spectator quark. Within the LEET $V(0) = A_1(0)(m_D + m_V)^2/(m_D^2 + m_V^2)$ [295], hence from eqs. (D.3, D.5) a $1/m_D$ uncertainty of $\sim 35\%$ can be inferred.

For the transition $D_s \to K^*$ no measurement or lattice computation is available. However, employing spectator invariance one can relate the form factors of $D_s \to K^*$ to $D \to (\rho, \omega)$ form factors. A measurement of the $D \to K^*$ form factor at $q^2 = 0$ [296] yields $A_1(0)$, $A_1(0)/V(0)$ and $A_2(0)/V(0)$ consistent with $SU(3)$ flavor symmetry. In [296] also form factors in the helicity basis were measured, which allows for a model independent form factor extraction, once current uncertainties are reduced.

To complement the information on the form factors from experiments and lattice computations we include QCD LCSR calculations as well as model dependent calculations in the following.

Within QCD LCSR the form factors are parametrized as [297]

$$F(q^2) = \frac{F(0)}{1 - a_F \, q^2/m_D^2 + b_F (q^2/m_D^2)^2}\,. \tag{D.6}$$

The corresponding parameters are for $D \to \rho$

$$\begin{aligned} V(0) &= 0.801^{+0.044}_{-0.036}\,, & a_V &= 0.78^{+0.24}_{-0.20}\,, & b_V &= 2.61^{+0.29}_{-0.04}\,, \\ A_1(0) &= 0.599^{+0.035}_{-0.030}\,, & a_{A_1} &= 0.44^{+0.10}_{-0.06}\,, & b_{A_1} &= 0.58^{+0.23}_{-0.04}\,, \\ A_2(0) &= 0.372^{+0.026}_{-0.031}\,, & a_{A_2} &= 1.64^{+0.10}_{-0.16}\,, & b_{A_2} &= 0.56^{+0.04}_{-0.28}\,, \\ A_3(0) &= -0.719^{+0.055}_{-0.066}\,, & a_{A_3} &= 1.05 \pm 0.15\,, & b_{A_3} &= 1.77^{+0.20}_{-0.11}\,, \end{aligned} \tag{D.7}$$

for $D \to \omega$

$$\begin{aligned} V(0) &= 0.742^{+0.041}_{-0.034}\,, & a_V &= 0.79^{+0.22}_{-0.20}\,, & b_V &= 2.52^{+0.28}_{-0.13}\,, \\ A_1(0) &= 0.556^{+0.033}_{-0.028}\,, & a_{A_1} &= 0.45^{+0.09}_{-0.05}\,, & b_{A_1} &= 0.54^{+0.17}_{-0.10}\,, \\ A_2(0) &= 0.333^{+0.026}_{-0.030}\,, & a_{A_2} &= 1.67^{+0.09}_{-0.15}\,, & b_{A_2} &= 0.44^{+0.05}_{-0.29}\,, \\ A_3(0) &= -0.657^{+0.053}_{-0.065}\,, & a_{A_3} &= 1.07^{+0.17}_{-0.14}\,, & b_{A_3} &= 1.77^{+0.14}_{-0.07} \end{aligned} \tag{D.8}$$

and for $D_s \to K^*$

$$\begin{aligned}
&V(0) = 0.771 \pm 0.049\,, && a_V = 1.08 \pm 0.02\,, && b_V = 0.13^{+0.03}_{-0.02}\,,\\
&A_1(0) = 0.589^{+0.040}_{-0.042}\,, && a_{A_1} = 0.56 \pm 0.02\,, && b_{A_1} = -0.12^{+0.03}_{-0.02}\,,\\
&A_2(0) = 0.315^{+0.024}_{-0.018}\,, && a_{A_2} = 0.15^{+0.22}_{-0.14}\,, && b_{A_2} = 0.24^{+0.83}_{-0.94}\,,\\
&A_3(0) = -0.675^{+0.027}_{-0.037}\,, && a_{A_3} = 0.48^{+0.13}_{-0.11}\,, && b_{A_3} = -0.14^{+0.18}_{-0.17}\,.
\end{aligned} \tag{D.9}$$

Here the form factor A_0 is obtained via $A_0 = ((m_D + m_V)A_1 - (m_D - m_V)A_2 - \frac{q^2}{m_D+m_V}A_3)/(2m_V)$. For weak annihilation modes we also need

$$A_1(0)^{(D\to K^*)} = 0.571^{+0.020}_{-0.022}\,, \quad a_{A_1^{(D\to K^*)}} = 0.65^{+0.10}_{-0.06}\,, \quad b_{A_1^{(D\to K^*)}} = 0.66^{+0.21}_{-0.18}\,, \tag{D.10}$$

$$A_1(0)^{(D_s\to \phi)} = 0.569^{+0.046}_{-0.049}\,, \quad a_{A_1^{(D_s\to \phi)}} = 0.84^{+0.06}_{-0.05}\,, \quad b_{A_1^{(D_s\to \phi)}} = 0.16 \pm 0.01\,. \tag{D.11}$$

Note that LCSR calculations are valid only at low q^2. The results for $A_2(0)$ are lower than the measurements and lattice computations.

The same parametrization, eq. (D.6), is utilized in the covariant light front quark model (CLFQM) [298]. The parameters are for $D \to \rho$

$$\begin{aligned}
&V(0) = 0.88^{+0.01}_{-0.02}\,, && a_V = 1.23 \pm 0.01\,, && b_V = 0.40^{+0.04}_{-0.03}\,,\\
&A_0(0) = 0.69 \pm 0.01\,, && a_{A_0} = 1.08^{+0.01}_{-0.02}\,, && b_{A_0} = 0.45 \pm 0.03\,,\\
&A_1(0) = 0.60^{+0.00}_{-0.01}\,, && a_{A_1} = 0.46 \pm 0.02\,, && b_{A_1} = 0.01 \pm 0.00\,,\\
&A_2(0) = 0.47 \pm 0.00\,, && a_{A_2} = 0.89 \pm 0.02\,, && b_{A_2} = 0.23 \pm 0.03\,,
\end{aligned} \tag{D.12}$$

for $D \to \omega$

$$\begin{aligned}
&V(0) = 0.85^{+0.01}_{-0.02}\,, && a_V = 1.24 \pm 0.01\,, && b_V = 0.45 \pm 0.04\,,\\
&A_0(0) = 0.64 \pm 0.01\,, && a_{A_0} = 1.08^{+0.01}_{-0.02}\,, && b_{A_0} = 0.50 \pm 0.04\,,\\
&A_1(0) = 0.58^{+0.00}_{-0.01}\,, && a_{A_1} = 0.49 \pm 0.02\,, && b_{A_1} = 0.02^{+0.01}_{-0.00}\,,\\
&A_2(0) = 0.49 \pm 0.00\,, && a_{A_2} = 0.95 \pm 0.01\,, && b_{A_2} = 0.28 \pm 0.02
\end{aligned} \tag{D.13}$$

and for $D_s \to K^*$

$$\begin{aligned}
&V(0) = 0.87 \pm 0.01\,, && a_V = 1.13^{+0.00}_{-0.01}\,, && b_V = 0.69^{+0.06}_{-0.04}\,,\\
&A_0(0) = 0.61 \pm 0.01\,, && a_{A_0} = 0.90^{+0.02}_{-0.01}\,, && b_{A_0} = 0.87 \pm 0.05\,,\\
&A_1(0) = 0.56 \pm 0.01\,, && a_{A_1} = 0.59 \pm 0.01\,, && b_{A_1} = 0.08 \pm 0.01\,,\\
&A_2(0) = 0.46 \pm 0.00\,, && a_{A_2} = 0.90 \pm 0.01\,, && b_{A_2} = 0.43 \pm 0.03\,.
\end{aligned} \tag{D.14}$$

For weak annihilation modes the needed parameters are given as

$$A_1(0)^{(D\to K^*)} = 0.72 \pm 0.01\,, \quad a_{A_1^{(D\to K^*)}} = 0.45 \pm 0.02\,,$$
$$b_{A_1^{(D\to K^*)}} = 0.01 \pm 0.00\,, \tag{D.15}$$
$$A_1(0)^{(D_s\to\phi)} = 0.69 \pm 0.00\,, \quad a_{A_1^{(D_s\to\phi)}} = 0.56 \pm 0.03\,,$$
$$b_{A_1^{(D_s\to\phi)}} = 0.07 \pm 0.01\,. \tag{D.16}$$

Here we add uncertainties in quadrature.

In the constituent quark model (CQM) the form factors are parametrized as [299]

$$F(q^2) = \frac{\tilde{F}(0)}{1 - \sigma_1\, q^2/M^2 + \sigma_2\, q^4/M^4}\,, \tag{D.17}$$

where $\tilde{F}(0) = F(0)/(1 - q^2/M^2)$ for $F \in \{V, A_0, T_1\}$, else $\tilde{F}(0) = F(0)$, and $M = m_D$ for A_0, else $M = m_{D^*}$. Here the parameters are for $D \to \rho$

$$\begin{aligned}
&V(0) = 0.90\,, && \sigma_1 = 0.46\,, && \sigma_2 = 0\,,\\
&A_0(0) = 0.66\,, && \sigma_1 = 0.36\,, && \sigma_2 = 0\,,\\
&A_1(0) = 0.59\,, && \sigma_1 = 0.50\,, && \sigma_2 = 0\,,\\
&A_2(0) = 0.49\,, && \sigma_1 = 0.89\,, && \sigma_2 = 0\,,\\
&T_1(0) = 0.66\,, && \sigma_1 = 0.44\,, && \sigma_2 = 0\,,\\
&T_2(0) = 0.66\,, && \sigma_1 = 0.38\,, && \sigma_2 = 0.50\,,\\
&T_3(0) = 0.31\,, && \sigma_1 = 1.10\,, && \sigma_2 = 0.17
\end{aligned} \tag{D.18}$$

and for $D_s \to K^*$

$$\begin{aligned}
&V(0) = 0.90\,, && \sigma_1 = 0.46\,, && \sigma_2 = 0\,,\\
&A_0(0) = 0.66\,, && \sigma_1 = 0.36\,, && \sigma_2 = 0\,,\\
&A_1(0) = 0.59\,, && \sigma_1 = 0.50\,, && \sigma_2 = 0\,,\\
&A_2(0) = 0.49\,, && \sigma_1 = 0.89\,, && \sigma_2 = 0\,,\\
&T_1(0) = 0.66\,, && \sigma_1 = 0.44\,, && \sigma_2 = 0\,,\\
&T_2(0) = 0.66\,, && \sigma_1 = 0.38\,, && \sigma_2 = 0.50\,,\\
&T_3(0) = 0.31\,, && \sigma_1 = 1.10\,, && \sigma_2 = 0.17\,.
\end{aligned} \tag{D.19}$$

Furthermore, [300] gives the form factors based on chiral theory. The $D \to (\rho, \omega)$ form factors at $q^2 = 0$, however, differ from measurements and lattice computations. The same observation is made for the $D \to \pi$ form factors given in [300].

In the heavy quark limit the tensor form factors T_i are related to the vector form factor V, and axialvector form factors A_i as [297]

$$\begin{aligned}
T_1 &= \frac{m_D^2 - m_V^2 + q^2}{2m_D(m_D + m_V)} V + \frac{m_D + m_V}{2m_D} A_1 \,, \\
T_2 &= \frac{\lambda(m_D^2, m_V^2, q^2)}{2m_D(m_D - m_V)(m_D + m_V)^2} V + \frac{m_D^2 - m_V^2 + q^2}{2m_D(m_D - m_V)} A_1 \,, \\
T_3 &= \frac{m_D^2 + 3m_V^2 - q^2}{2m_D(m_D + m_V)} V + \frac{m_V(m_D^2 - m_V^2)}{m_D q^2} A_0 - \frac{(m_D + m_V)(m_D^2 - m_V^2 + q^2)}{2m_D q^2} A_1 \\
&\quad + \frac{(m_D - m_V)(m_D^2 - m_V^2 + q^2)}{2m_D q^2} A_2 \,.
\end{aligned} \tag{D.20}$$

In different models it is shown that the heavy quark relations hold on the full q^2 range approximatively $\geq 70\%$ [297] (and references therein). For $q^2 = 0$ the heavy quark relations read [118]

$$T_1(0) = T_2(0) = V(0) \frac{m_D}{m_D + m_V} \,, \qquad T_3(0) = V(0) \frac{m_D^2 + 3m_V^2}{2m_D(m_D + m_V)} \,. \tag{D.21}$$

Perturbative corrections can be obtained form [118]. At high q^2, the relations to leading order in heavy quark limit and $\mathcal{O}(\alpha_s^2)$ are [114]

$$\begin{aligned}
&T_1(q^2 \sim m_D^2) = V(q^2 \sim m_D^2) \,, \quad T_2(q^2 \sim m_D^2) = A_1(q^2 \sim m_D^2) \,, \\
&T_3(q^2 \sim m_D^2) = A_2(q^2 \sim m_D^2) \frac{q^2}{m_D^2} \,.
\end{aligned} \tag{D.22}$$

The form factors from the CQM, the CLFQM, LCSR and the heavy quark relations, eq. (D.20), are shown in figure D.1. We deduce that the uncertainties for the form factors are sizable, and that further experimental data are needed. However, with the compilation of available information we can set a range for the uncertainties, see the blue band in the plots which is used for the form factor A_1 in section 3.3. In particular, with respect to the CQM form factors, we infer the model and spectator quark sensitivity for $D \to (\rho, \omega)$ form factors to be within the range of $\sigma(V, A_{0,2}) \sim 20\%$, $\sigma A_1 \sim 10\%$ and $\sigma T_{1,2,3} \sim 25\%$. These ranges cover the form factors from measurements, lattice computations, LCSR, and the CLFQM. The uncertainties of the tensor form factors T_i follow from the heavy quark relations. For $D_s \to K^*$ form factors we infer $\sigma(V, A_0) \sim 25\%$, $\sigma A_1 \sim (10 - 20)\%$ (low q^2 to large q^2), $\sigma A_2 \sim 35\%$ and $\sigma T_{1,2,3} \sim 30\%$. Here we assume spectator quark invariance for $A_{0,2}$, which is consistent with observations from V and A_1. The heavy quark relations differ by $\sim 15\%$ for T_1, $\lesssim 35\%$ (low q^2 to large q^2) for T_2 and $\lesssim 55\%$ for T_3 within the CQM. Similar differences are found in b physics [301].

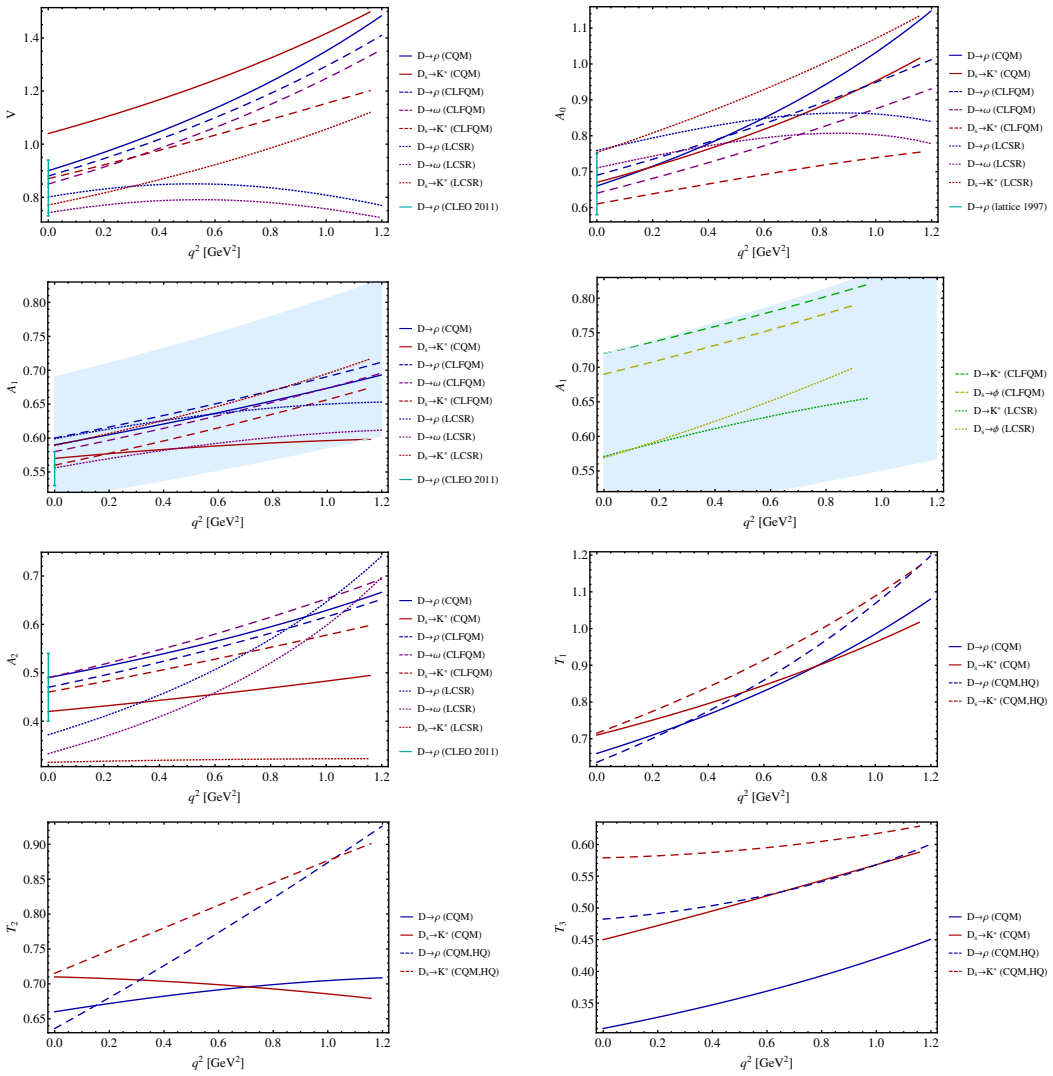

Figure D.1.: The form factors for $D \to V$ transitions from the CQM (solid curves), the CLFQM (dashed curves) and LCSR (dotted curves). For T_i we additionally provide predictions from the heavy quark relations (HQ), eq. (D.20). The blue, purple, orange, cyan and yellow curves are for $D \to \rho$, $D \to \omega$, $D_s \to K^*$, $D \to K^*$ and $D_s \to \phi$, respectively. The error bars depict the measurements or lattice computation [291, 292]. We cut at the kinematical endpoint. The blue band represents the form factor used in section 3.3.

E. Resonant decays in $D \to V\gamma$

In this appendix the amplitudes of the resonance model from [146, 147], employed in section 3.3, are collected. The amplitudes of [146, 147] are rewritten to account for additionally measured parameters and typing errors.

The PC and PV amplitudes are defined as [146, 147]

$$A_{\mathrm{PC/PV}} = \sqrt{\alpha_e 2\pi} G_F V_{cq}^* V_{uq'} \left(A^{\mathrm{I}}_{\mathrm{PC/PV}} + A^{\mathrm{II}}_{\mathrm{PC/PV}} + A^{\mathrm{III}}_{\mathrm{PC/PV}} \right) , \tag{E.1}$$

where $V_{cq}^* V_{uq'}$ are the CKM elements of the weak $D \to V$ transition. With [302] the amplitudes are rewritten as

$$\begin{aligned}
|A^{\mathrm{I},V^0}_{\mathrm{PC}}| &= -\frac{m_{D^{*0}}^{7/2} \left(m_{D^{*0}}^2 - (m_{D^0} + m_{\pi^0})^2\right)^{\frac{3}{4}} \left(m_{D^{*0}}^2 - (m_{D^0} - m_{\pi^0})^2\right)^{\frac{3}{4}} m_{V^0}}{\sqrt{2\pi\alpha_e} m_{D^0}^{3/2} \left(m_{D^{*0}}^2 - m_{D^0}^2\right)^{\frac{3}{2}} (m_{D^{*0}} + m_{D^0} - m_{\pi^0})(m_{D^{*0}}^2 - m_{V^0}^2)} \\
&\quad \times a_2 f_{V^0} \sqrt{\frac{\Gamma(D^{*0} \to D^0\gamma)}{\Gamma(D^{*0} \to D^0\pi^0)}} f_+(0) , \\
|A^{\mathrm{II},V^0}_{\mathrm{PC}}| &= \frac{2\sqrt{3} m_{D^0}^2}{\sqrt{\alpha_e}(m_{D^0}^2 - m_{\pi^0}^2)} \\
&\quad \times a_2 f_D f_\pi \left(\sqrt{\Gamma(\rho^0 \to \pi^0\gamma)} \frac{m_\rho^{3/2}}{\left(m_\rho^2 - m_{\pi^0}^2\right)^{\frac{3}{2}}} - \sqrt{\Gamma(\omega \to \pi^0\gamma)} \frac{m_\omega^{3/2}}{\left(m_\omega^2 - m_{\pi^0}^2\right)^{\frac{3}{2}}} \right) , \\
|A^{\mathrm{III},V^0}_{\mathrm{PC}}| &= \frac{1}{m_{D^0} + m_{V^0}} a_2 \left(-f_\rho^2 + \frac{1}{3} f_\omega^2 - \frac{V_{cs}^* V_{us}}{V_{cd}^* V_{ud}} \frac{2}{3} f_\phi^2 \right) V^{V^0}(0) , \\
|A^{\mathrm{I},V^0}_{\mathrm{PV}}| &= 0 , \\
|A^{\mathrm{II},V^0}_{\mathrm{PV}}| &= -\frac{1}{\sqrt{2}(m_{D^0}^2 - m_{V^0}^2)} \\
&\quad \times a_2 f_\rho \left(f_\rho A_1^\rho(m_{V^0}^2)(m_{D^0} + m_\rho) + f_\omega A_1^\omega(m_{V^0}^2) \frac{(m_{D^0} + m_\omega) m_\rho}{3 m_\omega} \right) , \\
|A^{\mathrm{III},V^0}_{\mathrm{PV}}| &= \frac{1}{m_{D^0} - m_{V^0}} a_2 \left(-f_\rho^2 + \frac{1}{3} f_\omega^2 - \frac{V_{cs}^* V_{us}}{V_{cd}^* V_{ud}} \frac{2}{3} f_\phi^2 \right) A_1^{V^0}(0)
\end{aligned} \tag{E.2}$$

for $V = V^0 \in \{\rho^0, \omega\}$ and for $V = \rho^+$ they read

$$
\begin{aligned}
|A_{\rm PC}^{{\rm I},\rho^+}| &= \frac{m_{D^{*+}}^{7/2}\left(m_{D^{*+}}^2-(m_{D^+}+m_{\pi^0})^2\right)^{\frac{3}{4}}\left(m_{D^{*+}}^2-(m_{D^+}-m_{\pi^0})^2\right)^{\frac{3}{4}} m_\rho}{\sqrt{\pi\alpha_e}m_{D^+}^{3/2}\left(m_{D^{*+}}^2-m_{D^+}^2\right)^{\frac{3}{2}}(m_{D^{*+}}+m_{D^+}-m_{\pi^+})(m_{D^{*+}}^2-m_\rho^2)} \\
&\quad\times a_1 f_\rho\sqrt{\frac{\Gamma(D^{*+}\to D^+\gamma)}{\Gamma(D^{*+}\to D^+\pi^0)}}f_+(0)\,, \\
|A_{\rm PC}^{{\rm II},\rho^+}| &= \frac{2\sqrt{6}m_{D^+}^2 m_\rho^{3/2}}{\sqrt{\alpha_e}(m_{D^+}^2-m_{\pi^+}^2)\left(m_\rho^2-m_{\pi^+}^2\right)^{\frac{3}{2}}}a_1 f_D f_\pi\sqrt{\Gamma(\rho^+\to\pi^+\gamma)}\,, \\
|A_{\rm PC}^{{\rm III},\rho^+}| &= \frac{1}{m_{D^+}+m_\rho}a_2\left(-f_\rho^2+\frac{1}{3}f_\omega^2-\frac{V_{cs}^*V_{us}}{V_{cd}^*V_{ud}}\frac{2}{3}f_\phi^2\right)V^\rho(0)\,, \\
|A_{\rm PV}^{{\rm I},\rho^+}| &= \frac{2m_\rho}{m_{D^+}^2-m_\rho^2}a_1 f_D f_\rho\,, \\
|A_{\rm PV}^{{\rm II},\rho^+}| &= \frac{1}{m_{D^+}^2-m_\rho^2}a_1 f_\rho\left(f_\rho A_1^\rho(m_\rho^2)(m_{D^+}+m_\rho)-f_\omega A_1^\omega(m_\rho^2)\frac{(m_{D^+}+m_\omega)m_\rho}{3m_\omega}\right)\,, \\
|A_{\rm PV}^{{\rm III},\rho^+}| &= \frac{1}{m_{D^+}-m_\rho}a_2\left(-f_\rho^2+\frac{1}{3}f_\omega^2-\frac{V_{cs}^*V_{us}}{V_{cd}^*V_{ud}}\frac{2}{3}f_\phi^2\right)A_1^\rho(0)\,.
\end{aligned}
\tag{E.3}
$$

Here the coefficients $a_1 = 1.3 \pm 0.1$, $a_2 = -0.55 \pm 0.1$ [167] (and [303]) are obtained by fitting non-leptonic decays. The coefficients effectively include non-factorisable effects [304] and they yield the largest parametric uncertainties. Furthermore, we take $f_V(m_V^2) = f_V(0) = f_V$.

For the decay $D_s \to K^{*+}\gamma$ the amplitudes are

$$
\begin{aligned}
|A_{\rm PC}^{{\rm I},K^{*+}}| &= \frac{4m_{D_s^*}^{3/2}m_{K^{*+}}}{m_{D_s}^{1/2}(m_{D_s^*}^2-m_{K^{*+}}^2)}a_1 f_{D_s}f_{K^*}\left|\lambda'+\lambda\tilde{g}_V\frac{-f_\phi}{3\sqrt{2}m_\phi}\right|\,, \\
|A_{\rm PC}^{{\rm II},K^{*+}}| &= \frac{2\sqrt{6}m_{D_s}^2 m_{K^{*+}}^{3/2}}{\sqrt{\alpha_e}(m_{D_s}^2-m_{K^+}^2)\left(m_{K^{*+}}^2-m_{K^+}^2\right)^{\frac{3}{2}}}a_1 f_{D_s}f_K\sqrt{\Gamma(K^{*+}\to K^+\gamma)}\,, \\
|A_{\rm PC}^{{\rm III},K^{*+}}| &= \frac{1}{m_{D_s}+m_{K^{*+}}}a_2\left(-\frac{V_{cd}^*V_{ud}}{V_{cs}^*V_{us}}\left(-f_\rho^2+\frac{1}{3}f_\omega^2\right)+\frac{2}{3}f_\phi^2\right)V^{K^*}(0)\,, \\
|A_{\rm PV}^{{\rm I},K^{*+}}| &= \frac{2m_{K^{*+}}}{m_{D_s}^2-m_{K^{*+}}^2}a_1 f_{D_s}f_{K^*}\,, \\
|A_{\rm PV}^{{\rm II},K^{*+}}| &= \frac{2(m_{D_s}+m_\phi)m_{K^{*+}}}{3m_\phi(m_{D_s}^2-m_{K^{*+}}^2)}a_1 f_{K^*}f_\phi A_1^{(D_s\to\phi)}(m_{K^{*+}}^2)\,, \\
|A_{\rm PV}^{{\rm III},K^{*+}}| &= \frac{1}{m_{D_s}-m_{K^{*+}}}a_2\left(-\frac{V_{cd}^*V_{ud}}{V_{cs}^*V_{us}}\left(-f_\rho^2+\frac{1}{3}f_\omega^2\right)+\frac{2}{3}f_\phi^2\right)A_1^{K^*}(0)\,.
\end{aligned}
\tag{E.4}
$$

Concerning the amplitude $A_{\rm PC}^{{\rm I},K^{*+}}$, one cannot normalize to $\mathcal{B}(D_s^* \to D_s\pi^0)$ due to its isospin breaking nature [305], which violates the approximation of [146, 147]. Furthermore, $\Gamma_{D_s^*}$, as a normalization, is not measured. However, the combination of parameters $\lambda' + \lambda\tilde{g}_V(-f_\phi)/(3\sqrt{2}m_\phi)$ can be obtained in the framework of [146, 147] by

$$\begin{aligned}\left|\lambda' + \lambda\tilde{g}_V\left(\pm\frac{f_\rho}{2\sqrt{2}m_\rho} + \frac{f_\omega}{6\sqrt{2}m_\omega}\right)\right| &= \frac{m_{D^*}^2\left(m_{D^*}^2 - (m_D + m_{\pi^0})^2\right)^{3/4}}{4\sqrt{\pi\alpha_e}m_D(m_{D^*}^2 - m_D^2)^{3/2}} \\ &\times \frac{\left(m_{D^*}^2 - (m_D - m_{\pi^0})^2\right)^{3/4}}{(m_{D^*} + m_D - m_{\pi^{0/+}})} \\ &\times \frac{f_+(0)}{f_D}\sqrt{\frac{\Gamma(D^{*0/+} \to D^{0/+}\gamma)}{\Gamma(D^{*0/+} \to D^{0/+}\pi^0)}}\,, \end{aligned} \tag{E.5}$$

where the ambiguity in λ' and $\lambda\tilde{g}_V$ is fixed by means of [302]

$$\lambda\tilde{g}_V = \frac{V^V(0)}{f_D}\frac{\sqrt{2}m_{D^*}^2}{(m_D + m_V)(m_{D^*} + m_D - m_V)}\,. \tag{E.6}$$

Compared to [146, 147] we adjust the CKM factors in the penguin amplitudes $A_{\rm PC/PV}^{\rm III}$, allowing for CP violation, and its sign to recover vanishing amplitudes in the $SU(3)$ flavor limit. The strong phases are not fixed within this model, yielding the largest uncertainties.

In the following, we list the amplitudes for the WA modes. They are

$$\begin{aligned}|A_{\rm PC}^{{\rm I},D^0\to\phi\gamma}| &= -\frac{m_{D^{*0}}^{7/2}\left(m_{D^{*0}}^2 - (m_{D^0} + m_{\pi^0})^2\right)^{\frac{3}{4}}\left(m_{D^{*0}}^2 - (m_{D^0} - m_{\pi^0})^2\right)^{\frac{3}{4}}m_\phi}{\sqrt{\pi\alpha_e}m_{D^0}^{3/2}\left(m_{D^{*0}}^2 - m_{D^0}^2\right)^{\frac{3}{2}}(m_{D^{*0}} + m_{D^0} - m_{\pi^0})(m_{D^{*0}}^2 - m_\phi^2)} \\ &\quad\times a_2 f_\phi\sqrt{\frac{\Gamma(D^{*0} \to D^0\gamma)}{\Gamma(D^{*0} \to D^0\pi^0)}}f_+(0)\,, \\ |A_{\rm PC}^{{\rm II},D^0\to\phi\gamma}| &= -\frac{8m_{D^0}^2}{3(m_{D^0}^2 - m_{K^0}^2)m_\phi}a_2 f_D f_\phi |C_{VV\Pi}|\,, \\ |A_{\rm PC}^{{\rm III},D^0\to\phi\gamma}| &= 0\,, \\ |A_{\rm PV}^{{\rm I},D^0\to\phi\gamma}| &= 0\,, \\ |A_{\rm PV}^{{\rm II},D^0\to\phi\gamma}| &= -\frac{m_\phi}{m_{D^0}^2 - m_\phi^2}a_2 f_\phi\left(f_\rho A_1^\rho(m_\phi^2)\frac{m_{D^0} + m_\rho}{m_\rho} + f_\omega A_1^\omega(m_\phi^2)\frac{m_{D^0} + m_\omega}{3m_\omega}\right)\,, \\ |A_{\rm PV}^{{\rm III},D^0\to\phi\gamma}| &= 0\,, \end{aligned} \tag{E.7}$$

where the parameter $|C_{VV\text{II}}| \simeq 0.3$ is determined by

$$|C_{VV\text{II}}| = \frac{\sqrt{6} m_{K^{*0/+}}^{3/2}}{\sqrt{\alpha_e}(m_{K^{*0/+}}^2 - m_{K^{0/+}}^2)^{3/2}} \frac{f_K}{\left| \mp \frac{f_\rho}{m_\rho} + \frac{f_\omega}{3m_\omega} - \frac{2f_\phi}{3m_\phi} \right|} \times \sqrt{\Gamma(K^{*0/+} \to K^{0/+}\gamma)}\,. \tag{E.8}$$

Further amplitudes are

$$\begin{aligned}
|A_{\text{PC}}^{\text{I},D^0\to\bar{K}^{*0}\gamma}| &= -\frac{m_{D^{*0}}^{7/2}\left(m_{D^{*0}}^2 - (m_{D^0}+m_{\pi^0})^2\right)^{\frac{3}{4}}\left(m_{D^{*0}}^2 - (m_{D^0}-m_{\pi^0})^2\right)^{\frac{3}{4}} m_{K^{*0}}}{\sqrt{\pi\alpha_e} m_{D^0}^{3/2}\left(m_{D^{*0}}^2 - m_{D^0}^2\right)^{\frac{3}{2}}(m_{D^{*0}} + m_{D^0} - m_{\pi^0})(m_{D^{*0}}^2 - m_{K^{*0}}^2)} \\
&\quad \times a_2 f_{K^*}\sqrt{\frac{\Gamma(D^{*0}\to D^0\gamma)}{\Gamma(D^{*0}\to D^0\pi^0)}} f_+(0)\,, \\
|A_{\text{PC}}^{\text{II},D^0\to\bar{K}^{*0}\gamma}| &= -\frac{2\sqrt{6} m_{D^0}^2 m_{K^{*0}}^{3/2}}{\sqrt{\alpha_e}(m_{D^0}^2 - m_{K^0}^2)\left(m_{K^{*0}}^2 - m_{K^0}^2\right)^{\frac{3}{2}}} a_2 f_D f_K \sqrt{\Gamma(K^{*0}\to K^0\gamma)}\,, \\
|A_{\text{PC}}^{\text{III},D^0\to K^{*0}\gamma}| &= 0\,, \\
|A_{\text{PV}}^{\text{I},D^0\to\bar{K}^{*0}\gamma}| &= 0\,, \\
|A_{\text{PV}}^{\text{II},D^0\to\bar{K}^{*0}\gamma}| &= -\frac{m_{K^{*0}}}{m_{D^0}^2 - m_{K^{*0}}^2} a_2 f_{K^*} \\
&\quad \times \left(f_\rho A_1^\rho(m_{K^{*0}}^2)\frac{m_{D^0}+m_\rho}{m_\rho} + f_\omega A_1^\omega(m_{K^{*0}}^2)\frac{m_{D^0}+m_\omega}{3m_\omega}\right)\,, \\
|A_{\text{PV}}^{\text{III},D^0\to\bar{K}^{*0}\gamma}| &= 0
\end{aligned} \tag{E.9}$$

as well as $|A_{\text{PC,PV}}^{\text{I,II,III},D^0\to K^{*0}\gamma}| = |\frac{V_{cd}^* V_{us}}{V_{cs}^* V_{ud}}|\,|A_{\text{PC,PV}}^{\text{I,II,III},D^0\to\bar{K}^{*0}\gamma}|$. Furthermore,

$$\begin{aligned}
|A_{\text{PC}}^{\text{I},D^+\to K^{*+}\gamma}| &= \frac{m_{D^{*+}}^{7/2}\left(m_{D^{*+}}^2 - (m_{D^+}+m_{\pi^0})^2\right)^{\frac{3}{4}}\left(m_{D^{*+}}^2 - (m_{D^+}-m_{\pi^0})^2\right)^{\frac{3}{4}} m_{K^{*+}}}{\sqrt{\pi\alpha_e} m_{D^+}^{3/2}\left(m_{D^{*+}}^2 - m_{D^+}^2\right)^{\frac{3}{2}}(m_{D^{*+}} + m_{D^+} - m_{\pi^+})(m_{D^{*+}}^2 - m_{K^{*+}}^2)} \\
&\quad \times a_1 f_{K^*}\sqrt{\frac{\Gamma(D^{*+}\to D^+\gamma)}{\Gamma(D^{*+}\to D^+\pi^0)}} f_+(0)\,, \\
|A_{\text{PC}}^{\text{II},D^+\to K^{*+}\gamma}| &= \frac{2\sqrt{6} m_{D^+}^2 m_{K^{*+}}^{3/2}}{\sqrt{\alpha_e}(m_{D^+}^2 - m_{K^+}^2)\left(m_{K^{*+}}^2 - m_{K^+}^2\right)^{\frac{3}{2}}} a_1 f_D f_K \sqrt{\Gamma(K^*\to K^+\gamma)}\,,
\end{aligned}$$

$$
\begin{aligned}
|A_{\rm PC}^{{\rm III},D^+\to K^{*+}\gamma}| &= 0\,,\\
|A_{\rm PV}^{{\rm I},D^+\to K^{*+}\gamma}| &= \frac{2m_{K^{*+}}}{m_{D^+}^2-m_{K^{*+}}^2}a_1 f_D f_{K^*}\,,\\
|A_{\rm PV}^{{\rm II},D^+\to K^{*+}\gamma}| &= \frac{m_{K^{*+}}}{m_{D^+}^2-m_{K^{*+}}^2}\\
&\quad\times a_1 f_{K^*}\left(f_\rho A_1^\rho(m_{K^{*+}}^2)\frac{m_{D^+}+m_\rho}{m_\rho}-f_\omega A_1^{(D_s\to K^*)}(m_{K^{*+}}^2)\frac{m_{D^+}+m_\omega}{3m_\omega}\right),\\
|A_{\rm PV}^{{\rm III},D^+\to K^{*+}\gamma}| &= 0
\end{aligned}
\tag{E.10}
$$

and

$$
\begin{aligned}
|A_{\rm PC}^{{\rm I},D_s\to\rho^+\gamma}| &= \frac{4m_{D_s^*}^{3/2}m_\rho}{m_{D_s}^{1/2}(m_{D_s^*}^2-m_\rho^2)}a_1 f_{D_s} f_\rho\left|\lambda'+\lambda\tilde{g}_V\frac{-f_\phi}{3\sqrt{2}m_\phi}\right|,\\
|A_{\rm PC}^{{\rm II},D_s\to\rho^+\gamma}| &= \frac{2\sqrt{6}m_{D_s}^2 m_\rho^{3/2}}{\sqrt{\alpha_e}(m_{D_s}^2-m_{\pi^+}^2)\left(m_\rho^2-m_{\pi^+}^2\right)^{\frac{3}{2}}}a_1 f_{D_s} f_\pi\sqrt{\Gamma(\rho^+\to\pi^+\gamma)}\,,\\
|A_{\rm PC}^{{\rm III},D_s\to\rho^+\gamma}| &= 0\,,\\
|A_{\rm PV}^{{\rm I},D_s\to\rho^+\gamma}| &= \frac{2m_\rho}{m_{D_s}^2-m_\rho^2}a_1 f_{D_s} f_\rho\,,\\
|A_{\rm PV}^{{\rm II},D_s\to\rho^+\gamma}| &= \frac{2(m_{D_s}+m_\phi)m_\rho}{3m_\phi(m_{D_s}^2-m_\rho^2)}a_1 f_\rho f_\phi A_1^{(D_s\to\phi)}(m_{K^{*+}}^2)\,,\\
|A_{\rm PV}^{{\rm III},D_s\to\rho^+\gamma}| &= 0\,.
\end{aligned}
\tag{E.11}
$$

F. Chiral Fierz identities

In this appendix we derive chiral Fierz identities, which are employed in section 4.2.1. We follow the notation as given at the beginning of chapter 3. The formalism employed here is based on [306], see also [307].

Defining the chiral basis as

$$\Gamma^A \in \{P_R, P_L, \gamma^\mu P_L, \gamma^\mu P_R, \sigma^{\mu\nu}\} \tag{F.1}$$

its dual basis is given by

$$\Gamma_A \in \{P_R, P_L, \gamma_\mu P_R, \gamma_\mu P_L, \frac{1}{2}\sigma_{\mu\nu}\}\,. \tag{F.2}$$

Here, $P_{R/L} = \frac{1}{2}(1 \pm \gamma_5)$, $\gamma_5 = i\gamma^0\gamma^1\gamma^2\gamma^3$, $\{\gamma^\mu, \gamma^\nu\} = 2g^{\mu\nu}$, $g^{\mu\nu} = \mathrm{diag}(1, -1, -1, -1)$, $\sigma^{\mu\nu} = \frac{i}{2}[\gamma^\mu, \gamma^\nu]$, $\sigma^{\mu\nu}\gamma_5 = \frac{i}{2}\epsilon^{\mu\nu\alpha\beta}\sigma_{\alpha\beta}$ and $\epsilon^{0123} = -\epsilon_{0123} = 1$. The normalization is $\mathrm{Tr}[\Gamma^A\Gamma_B] = 2\delta^A_B$, where $\mu < \nu$. Following [306] we represent pairs of indices, i.e. color indices, by closed parentheses and brackets, that is "()" and "[]".

The completeness relations read

$$\begin{aligned}(\Gamma^A][\Gamma^B) &= -\frac{1}{4}\mathrm{Tr}\left[\Gamma^A\Gamma_D\Gamma^B\Gamma_C\right](\Gamma^C)[\Gamma^D]\,,\\ (\Gamma^A)[\Gamma^B] &= -\frac{1}{4}\mathrm{Tr}\left[\Gamma^A\Gamma_D\Gamma^B\Gamma_C\right](\Gamma^C][\Gamma^D)\,,\end{aligned} \tag{F.3}$$

where the minus sign arises from the anticommutation of fermion fields.

The Lorentz invariant bilinears are written as

$$\begin{aligned}
O_1 &= (P_R][P_R)\,, & O_2 &= (P_R)[P_R]\,,\\
O_3 &= (P_R][P_L)\,, & O_4 &= (P_R)[P_L]\,,\\
O_5 &= (P_L][P_R)\,, & O_6 &= (P_L)[P_R]\,,\\
O_7 &= (P_L][P_L)\,, & O_8 &= (P_L)[P_L]\,,\\
O_9 &= (\gamma^\mu P_R][\gamma_\mu P_R)\,, & O_{10} &= (\gamma^\mu P_R)[\gamma_\mu P_R]\,,\\
O_{11} &= (\gamma^\mu P_R][\gamma_\mu P_L)\,, & O_{12} &= (\gamma^\mu P_R)[\gamma_\mu P_L]\,,\\
O_{13} &= (\gamma^\mu P_L][\gamma_\mu P_R)\,, & O_{14} &= (\gamma^\mu P_L)[\gamma_\mu P_R]\,,\\
O_{15} &= (\gamma^\mu P_L][\gamma_\mu P_L)\,, & O_{16} &= (\gamma^\mu P_L)[\gamma_\mu P_L]\,,\\
O_{17} &= (\sigma^{\mu\nu}][\sigma_{\mu\nu})\,, & O_{18} &= (\sigma^{\mu\nu})[\sigma_{\mu\nu}]\,,\\
O_{19} &= (\sigma^{\mu\nu}][\sigma_{\mu\nu}\gamma_5)\,, & O_{20} &= (\sigma_{\mu\nu})[\sigma_{\mu\nu}\gamma_5]\,.
\end{aligned} \tag{F.4}$$

Here we implicitly sum μ, ν, which is compensated by the replacement $\sigma^{\mu\nu} \to \frac{1}{2}\sigma^{\mu\nu}$.

We find the chiral Fierz identities for fermion fields, labeled by $\mathcal{F}$,

$$
\begin{aligned}
&O_1 \overset{\mathcal{F}}{=} -\frac{1}{2}O_2 - \frac{1}{16}O_{18} - \frac{1}{16}O_{20}\,, && O_2 \overset{\mathcal{F}}{=} -\frac{1}{2}O_1 - \frac{1}{16}O_{17} - \frac{1}{16}O_{19}\,,\\
&O_3 \overset{\mathcal{F}}{=} -\frac{1}{2}O_{14}\,, && O_4 \overset{\mathcal{F}}{=} -\frac{1}{2}O_{13}\,,\\
&O_5 \overset{\mathcal{F}}{=} -\frac{1}{2}O_{12}\,, && O_6 \overset{\mathcal{F}}{=} -\frac{1}{2}O_{11}\,,\\
&O_7 \overset{\mathcal{F}}{=} -\frac{1}{2}O_8 - \frac{1}{16}O_{18} + \frac{1}{16}O_{20}\,, && O_8 \overset{\mathcal{F}}{=} -\frac{1}{2}O_7 - \frac{1}{16}O_{17} + \frac{1}{16}O_{19}\,,\\
&O_9 \overset{\mathcal{F}}{=} O_{10}\,,\\
&O_{15} \overset{\mathcal{F}}{=} O_{16}\,,\\
&O_{17} \overset{\mathcal{F}}{=} -6O_2 - 6O_8 + \frac{1}{2}O_{18}\,, && O_{18} \overset{\mathcal{F}}{=} -6O_1 - 6O_7 + \frac{1}{2}O_{17}\,,\\
&O_{19} \overset{\mathcal{F}}{=} -6O_2 + 6O_8 + \frac{1}{2}O_{20}\,, && O_{20} \overset{\mathcal{F}}{=} -6O_1 + 6O_7 + \frac{1}{2}O_{19}\,.
\end{aligned}
\tag{F.5}
$$

G. Constraints on leptoquark models

This appendix is a compilation of expressions used to calculate constraints on LQ models listed in appendix G.1 and utilized in chapter 4. The parameters and experimental data are listed in appendix A. We constrain gauge vector LQ models only, as non-gauge vector LQs depend on the cutoff characteristic for a certain UV model, see e.g. [214]. Moreover, we do not utilize observables which depend on anomalous couplings, e.g. corrections to the $Z \to ff$ and the W vertex, which can be found in [224]. Note that fermion doublets coupling to LQs are taken into account. In the current appendix we do not neglect light fermion masses if they are needed as regulators. Due to the variety of scales involved we chose the LQ mass as the reference scale and use $m_c(\mu \sim 1\,\mathrm{TeV}) \simeq 0.5\,\mathrm{GeV}$, $m_s(\mu \sim 1\,\mathrm{TeV}) \simeq 0.05\,\mathrm{GeV}$, $m_d(\mu \sim 1\,\mathrm{TeV}) \simeq 0.002\,\mathrm{GeV}$ and $m_u(\mu \sim 1\,\mathrm{TeV}) \simeq 0.001\,\mathrm{GeV}$. However, this choice does not affect ratios of the masses and our issue is to constrain the couplings at leading order.

Utilizing the model-independent limits from section 4.1 and the Wilson coefficients given in eq. (4.18), we obtain constraints due to $c \to ul^{(\prime)}l$ induced decays, i.e. $D \to Pll$, $D \to Pe\mu$, $D^0 \to ll$ and $D^0 \to \mu e$. The Wilson coefficients for the radiative decay $D^0 \to \rho^0\gamma$ are worked out in section 4.2.1. In particular, they also involve couplings to τ leptons. The experimental $D^0 \to \rho^0\gamma$ data on do not give constraints for $|\lambda| \lesssim \frac{M}{\mathrm{TeV}}$.

The $D^0 - \bar{D}^0$ mass difference to second order in the weak interaction is given by [308]

$$\begin{aligned}\Delta m_{D^0} = \frac{1}{m_D}\mathrm{Re}\Bigg[&\left\langle \bar{D}^0 \middle| H^{(|\Delta C|=2)} \middle| D^0 \right\rangle \\ &+ \left\langle \bar{D}^0 \middle| i\int \mathrm{d}^4x\, T\left[\mathcal{H}^{(|\Delta C|=1)}(x)\mathcal{H}^{(|\Delta C|=1)}(0)\right] \middle| D^0 \right\rangle\Bigg],\end{aligned} \tag{G.1}$$

where T indicates time ordering. Here CP violation is neglected, which is consistent with experiments [97]. In the SM $\Delta^{\mathrm{SM}} m_{D^0}/\Gamma_{D^0} \simeq 1.5 \times 10^6\,\hbar\,\mathrm{s}^{-1}$ is found via the OPE and to one loop QCD [308]. This contribution is helicity suppressed and subject to the GIM mechanism, however, larger contribution are possible via higher dimensional operators or non-local contributions [309] (and references therein). We estimate the constraints on LQ models neglecting the SM, which dominates the non-local product of Hamiltonian densities in the second term of eq. (G.1) [308]. On the other hand, the SM contribution

to the local Hamiltonian in the first term of eq. (G.1) is negligible [308]. For vector LQs one obtains [61]

$$\Delta^V m_{D^0} = \frac{2}{3} m_D f_D^2 B_D \frac{m_l^2 \mathrm{Re}\left[\lambda_{V_2}^{(ul)} \left(\lambda_{V_2}^{(cl)}\right)^*\right]^2}{\pi^2 M_{V_2}^4}\,, \tag{G.2}$$

which is multiplied by 3 for V_3 due to additional neutrinos. The matrix elements are, for massless quarks, which imply no helicity flip and since QCD is parity invariant,

$$\langle \bar{D}^0 | (\bar{u}_{L,R}\gamma_\mu c_{L,R})(\bar{u}_{L,R}\gamma^\mu c_{L,R}) | D^0 \rangle = \frac{2}{3} m_D^2 f_D^2 B_D\,. \tag{G.3}$$

For the bag parameter we use [310], adding uncertainties in quadrature,

$$B_{D^0}(\mu = 3\,\mathrm{GeV}) = 0.757 \pm 0.028 \tag{G.4}$$

which is consistent with the one obtained in [311]. Here, e.g., a non-gauge vector LQ would yield eq. (G.2) with the replacement $m_l \to M$ for a cutoff scale M. For scalar LQs [312]

$$H_S^{|\Delta C|=2} = \frac{1}{128\pi^2} \frac{\lambda_{L,R}^{(cl)} \left(\lambda_{L,R}^{(ul)}\right)^* \lambda_{L,R}^{(cl')} \left(\lambda_{L,R}^{(ul')}\right)^*}{M^2} (\bar{u}_{L,R}\gamma_\mu c_{L,R})(\bar{u}_{L,R}\gamma^\mu c_{L,R})\,, \tag{G.5}$$

which is multiplied by 2 for $S_2 L$ and by 5 for S_3. It follows

$$\begin{aligned}\Delta^S m_{D^0} = \frac{m_D f_D^2 B_D}{96\pi^2} \frac{1}{M^2} \mathrm{Re}\Big[&\lambda_L^{(ce)} \left(\lambda_L^{(ue)}\right)^* + \lambda_R^{(ce)} \left(\lambda_R^{(ue)}\right)^* + \lambda_L^{(c\mu)} \left(\lambda_L^{(u\mu)}\right)^* \\ &+ \lambda_R^{(c\mu)} \left(\lambda_R^{(u\mu)}\right)^* + \lambda_L^{(c\tau)} \left(\lambda_L^{(u\tau)}\right)^* + \lambda_R^{(c\tau)} \left(\lambda_R^{(u\tau)}\right)^* \Big]^2 .\end{aligned} \tag{G.6}$$

Note that $\Delta^S m_{D^0}$ scales non-linear in the mass and couplings.

The $D^0 - \bar{D}^0$ lifetime difference follows from double $\Delta C = 1$ insertions as [308]

$$\Delta\Gamma_{D^0} = -\frac{1}{m_D} \mathrm{Im}\left[\left\langle \bar{D}^0 \left| i \int \mathrm{d}^4 x\, T\left[\mathcal{H}^{(|\Delta C|=1)}(x) \mathcal{H}^{(|\Delta C|=1)}(0)\right] \right| D^0 \right\rangle\right], \tag{G.7}$$

where CP violation is neglected. We neglect the SM contribution $\Delta^{\mathrm{SM}}\Gamma_{D^0}/(2\Gamma_{D^0}) \simeq 6 \times 10^{-7}$ which is small due to the GIM mechanism [308] but could be larger via higher dimensional operators or non-local contributions [309] (and references therein). The non-local contribution is obtained from diagrams with light fields, yielding for vector LQs [313]

$$\Delta^V \Gamma_{D^0} = -m_D m_c^2 f_D^2 B_D \frac{\mathrm{Re}\left[\lambda_{V_2}^{(ue)} \left(\lambda_{V_2}^{(ce)}\right)^* + \lambda_{V_2}^{(u\mu)} \left(\lambda_{V_2}^{(c\mu)}\right)^* + \lambda_{V_2}^{(u\tau)} \left(\lambda_{V_2}^{(c\tau)}\right)^*\right]^2}{128\pi M_{V_2}^4}\,, \tag{G.8}$$

multiplied by 3 for V_3 due to additional neutrinos. We obtain $|\Delta^V \Gamma_{D^0}/\Gamma_{D^0}| \lesssim 6 \times 10^{-3}$ for $|\lambda| \lesssim \frac{M}{\text{TeV}}$, thus no constraint. Up to combinatorial factors and additive LQ couplings eq. (G.8) holds also for scalar LQs [314], yielding the same conclusion.

The Lagrangian for atomic parity violation is given by [315]

$$\mathcal{L}_{\text{APV}} = \frac{G_F}{\sqrt{2}} \sum_{q\in\{u,d\}} (C_{1q}\bar{e}\gamma^\mu\gamma_5 e\bar{q}\gamma_\mu q + C_{2q}\bar{e}\gamma^\mu e\bar{q}\gamma_\mu\gamma_5 q) \tag{G.9}$$

from which the nuclear weak charge follows as

$$Q_w(Z,N) = -2((2Z+N)C_{1u} + (2N+Z)C_{1d})\,. \tag{G.10}$$

Here $Z = 55$ and $N = 78$ are the proton and neutron numbers for Cs, respectively. We find via matching

$$\begin{aligned}
&\delta_{\tilde{V}_1} C_{1u} = -\delta_{\tilde{V}_2} C_{1u} = -\frac{1}{2}\delta_{V_3} C_{1u} = -\delta_{V_3} C_{1d} = -\frac{\sqrt{2}}{4G_F}\frac{\left|\lambda_{\tilde{V}}^{(ue)}\right|^2}{M_{\tilde{V}}^2}\,,\\
&\delta_{S_1} C_{1u} = -\delta_{S_2} C_{1u} = \frac{\sqrt{2}}{8G_F}\frac{\left|\lambda_R^{(ue)}\right|^2 - \left|\lambda_L^{(ue)}\right|^2}{M_{S_1}^2}\,, \quad \delta_{S_2} C_{1d} = -\frac{\sqrt{2}}{8G_F}\frac{\left|\lambda_{S_2R}^{(ue)}\right|^2}{M_{S_2}^2}\,,\\
&\delta_{S_3} C_{1u} = \frac{1}{2}\delta_{S_3} C_{1d} = -\frac{\sqrt{2}}{8G_F}\frac{\left|\lambda_{S_3}^{(ue)}\right|^2}{M_{S_3}^2}\,.
\end{aligned} \tag{G.11}$$

We do not match the model V_2 due to an additional d_R quark coupling which is not relevant for charm FCNC transitions.

As mentioned we do not use observables involving the Z boson to constrain vector LQ models. Nonetheless, we consider the shift due to scalar LQs for Z decaying to fermions f, which is [316]

$$\delta_S \Gamma_{Z\to ff} = \frac{\alpha_e m_Z}{3\sin^2\theta\cos^2\theta} g_f \frac{|\lambda_{L,R}^{(ff')}|^2}{16\pi^2}\frac{m_Z^2}{3M^2}\left(\left(-\frac{11}{6} - \ln\frac{m_{f'}^2}{M^2}\right) g_{f'} + \frac{1}{3}g\right) \tag{G.12}$$

with

$$g_f = T_3^{(f)} - q_f \sin^2\theta_w\,, \qquad g = T_3^{(e)} - q_e\sin^2\theta_w\,, \tag{G.13}$$

where we neglect terms $\sim \lambda_L\lambda_R$. Here T_3 and q denote the third component of the weak hypercharge and the electric charge, respectively, see tables 4.2 and 2.1 for the LQ and SM fermion charges. The eq. (G.12) is multiplied by 3 if the conjugate f' is a quark, i.e. the fermion f is a lepton, due to color and by 2 if the conjugate f' is a down-type quark for S_3. In the SM the ratios of up-type quarks and leptons are $\Gamma^{\text{SM}}_{Z\to ff}/\Gamma^{\text{SM}}_{Z\to f'f'} = 1$ and

measurements yield $\Gamma(Z \to ((uu + cc)/2))/\Gamma(Z \to cc) = 0.96 \pm 0.06$, see appendix A. One obtains $|\delta_S \Gamma_{Z\to ff}| \lesssim 6 \times 10^{-5}$ for $|\lambda| \lesssim \frac{M}{\text{TeV}}$, yielding no constraint.

Further, the LFV decay of a Z boson induced by scalar LQs is [317]

$$\delta_S \mathcal{B}_{Z\to e\mu} = \frac{\alpha_e m_Z}{6\Gamma_Z}\left(\left|F^Z_{1L}\right|^2 + \left|F^Z_{1R}\right|^2 + \frac{1}{2m_Z^2}\left(\left|F^Z_{2LR}\right|^2 + \left|F^Z_{2RL}\right|^2\right)\right), \tag{G.14}$$

where

$$\begin{aligned}
F^Z_{1L,1R} = {} & \frac{3}{16\pi^2}\frac{1}{M^2}\left(\lambda^{(qe)}_{L,R}\left(\lambda^{(q\mu)}_{L,R}\right)^*\left(\frac{-1}{18}g + \left(\frac{4}{9} - \frac{2}{3}\ln\frac{m_q^2}{M^2}\right)g_{L,R}\right) - \frac{m_q}{-m_\mu^2}\right. \\
& \left.\times\left(-m_\mu\lambda^{(qe)}_{L,R}\left(\lambda^{(q\mu)}_{R,L}\right)^*\right)\left(-\frac{3}{4} - \ln\frac{m_q^2}{M^2}\right)(g_{R,L} - g_{L,R})\right)\frac{-1}{\sin\theta_w\cos\theta_w}, \\
F^Z_{2LR,2RL} = {} & \frac{3}{16\pi^2}\frac{1}{M^2}\left(m_q\lambda^{(qe)}_{R,L}\left(\lambda^{(q\mu)}_{L,R}\right)^*\left(-\frac{3}{4} - \ln\frac{m_q^2}{M^2}\right)(g_{L,R} + g_{R,L})\right. \\
& + m_\mu\lambda^{(qe)}_{R,L}\left(\lambda^{(q\mu)}_{R,L}\right)^*\frac{1}{6}g_{R,L} \\
& \left. - \left(m_\mu\lambda^{(qe)}_{R,L}\left(\lambda^{(q\mu)}_{R,L}\right)^*\frac{1}{12} + m_q\lambda^{(qe)}_{R,L}\left(\lambda^{(q\mu)}_{L,R}\right)^*\frac{1}{2}\right)g\right)\frac{-1}{\sin\theta_w\cos\theta_w}.
\end{aligned} \tag{G.15}$$

Here

$$g_{L,R} = T_3^{(q_L,q_R)} - q_q\sin^2\theta_w, \qquad g = T_3^{(e)} - q_e\sin^2\theta_w \tag{G.16}$$

and for S_2 the interchange $g_L \leftrightarrow g_R$. LFV decays are zero in the SM and for $|\lambda| \lesssim \frac{M}{\text{TeV}}$ we find no constraint as $|\delta_{LQ}\mathcal{B}_{Z\to e\mu}| \lesssim 5 \times 10^{-13}$.

The anomalous magnetic moments receive a contribution from vector LQs as [318]

$$\Delta^V a_l = -\frac{3m_l^2}{16\pi^2}\frac{|\lambda^{(ql)}|^2}{M^2}\left(\frac{2}{3}q_q + \frac{5}{6}q_e\right), \tag{G.17}$$

times 2 for up-type quarks in the model V_3. We obtain $|\Delta^V a_e| \lesssim 2 \times 10^{-14}$ and $|\Delta^V a_\mu| \lesssim 6 \times 10^{-10}$ for $|\lambda| \lesssim \frac{M}{\text{TeV}}$, giving no constraints. For scalar LQs the corresponding expression is given by [319]

$$\begin{aligned}
\Delta^S a_l = {} & -\frac{3m_l}{16\pi^2}\frac{1}{M^2}\left(m_l\left(\left|\lambda^{(ql)}_L\right|^2 + \left|\lambda^{(ql)}_R\right|^2\right)\left(\frac{1}{3}q_q - \frac{1}{6}q_e\right)\right. \\
& \left. + m_q\,\mathrm{Re}\left[\lambda^{(ql)}_L\left(\lambda^{(ql)}_R\right)^*\right]\left(\left(-3 - 2\ln\frac{m_q^2}{M^2}\right)q_q - q_e\right)\right)
\end{aligned} \tag{G.18}$$

which agrees with the result in [317], when $F_1 \leftrightarrow F_2$ therein.

Couplings involving different chiralities are present in scalar LQ models only. Consequently only scalar LQs contribute to the CP violating fermion electric dipole moments, which is [319]

$$\delta_S d_f = \frac{e}{32\pi^2}\frac{1}{M^2} m_{f'} \mathrm{Im}\left[\lambda_L^{(ff')}\left(\lambda_R^{(ff')}\right)^*\right]\left(\left(-3-2\ln\frac{m_{f'}^2}{M^2}\right)q_{f'}-q_e\right). \tag{G.19}$$

If the conjugate f' is a quark, i.e. the fermion f is a lepton, eq. (G.19) is multiplied by 3 due to color. To compare with experiments the factor $\frac{\hbar c}{m_f}$m needs to be taken into account. The SM lepton electric dipole moment is negligible, $d_e^{\mathrm{SM}} \leq 10^{-38}\, e\,\mathrm{cm}$ [320], as small as the neutron electric dipole moment, $d_n^{\mathrm{SM}} \sim (-\mathcal{O}(10^{-34})\, e\,\mathrm{cm})$ [321], given by its quark content as $d_n = 4/3 d_d - 1/3 d_u$. No constraint is obtained for $|\mathrm{Im}[\lambda_L^{(c\mu)}(\lambda_R^{(c\mu)})^*]|$ from the muon electric dipole moment. For the Hg electric dipole moment the corresponding expression reads [269] (and references therein)

$$|\delta_S d_{\mathrm{Hg}}| = \frac{4.89\times 10^{-20}\, e\,\mathrm{cm}}{8\sqrt{2}G_F}\frac{\left|\mathrm{Im}\left[\lambda_L^{(qe)}(\lambda_R^{(qe)})^*\right]\right|}{M^2} \tag{G.20}$$

which is negligible in the SM. Here the matching of the nuclear onto the quark theory is neglected.

The amplitude for LFV radiative muon decay in vector LQ models is defined as [214]

$$\mathcal{A}^{\mu_1}_{\mu\to e\gamma} = i\bar{e}\left(\frac{\sigma^{\mu_1\mu_2}q_{\mu_2}}{m_\mu}\left(F^V + F^A\gamma_5\right)\right)\mu\,, \tag{G.21}$$

yielding the branching ratio

$$\delta_V \mathcal{B}_{\mu\to e\gamma} = \frac{1}{\Gamma_\mu}\frac{m_\mu}{8\pi}\left(\left|F^V\right|^2 + \left|F^A\right|^2\right). \tag{G.22}$$

Here

$$\left|F^{V,A}\right| = \sqrt{\alpha_e 4\pi}\frac{\left|\lambda^{(q\mu)}\left(\lambda^{(qe)}\right)^*\right|}{32\pi^2}\frac{m_\mu^2}{M^2}\left(q_q 2 + q_e\frac{5}{2}\right), \tag{G.23}$$

times 2 for up-type quarks in the model V_3. We add that F^V comes with a minus sign. For scalar LQs the corresponding amplitude reads [317]

$$\mathcal{A}_{\mu\to e\gamma} = \sqrt{\alpha_e 4\pi}\,\bar{e}\left(F^\gamma_{2RL}P_L + F^\gamma_{2LR}P_R\right)(i\sigma_{\mu_1\mu_2}q^{\mu_1})\mu\left(\epsilon_\gamma^{\mu_2}\right)^* \tag{G.24}$$

with the polarization ϵ. The branching ratio is obtained as

$$\delta_S \mathcal{B}_{\mu\to e\gamma} = \frac{\alpha_e}{4\Gamma_\mu} m_\mu^5\left(\left|F^\gamma_{2LR}\right|^2 + \left|F^\gamma_{2RL}\right|^2\right), \tag{G.25}$$

where, see the comment after eq. (G.18),

$$F^{\gamma}_{2LR,2RL} = \frac{3}{16\pi^2}\frac{1}{M^2}\left(\lambda^{(q\mu)}_{L,R}\left(\lambda^{(qe)}_{L,R}\right)^*\left(\frac{1}{6}q_q - \frac{1}{12}q_e\right)\right.$$
$$\left. - \frac{m_q}{m_\mu}\lambda^{(q\mu)}_{R,L}\left(\lambda^{(qe)}_{L,R}\right)^*\left(\left(-\frac{3}{2} - \ln\frac{m_q^2}{M^2}\right)q_q - \frac{1}{2}q_e\right)\right). \tag{G.26}$$

Note that one can include effect due to the renormalization group for $\mu \to e\gamma$ decay, $\mu - e$ conversion and $\mu \to eee$ decay, as in [322] (and references therein). The latter two observables are considered in the following, without renormalization group effects.

The Lagrangian for LFV coherent $\mu - e$ conversion is defined as [323]

$$\mathcal{L}_{\mu-e} = (C_{DR}m_\mu\bar{e}_L\sigma^{\mu_1\mu_2}\mu_L + C_{DL}m_\mu\bar{e}_R\sigma^{\mu_1\mu_2}\mu_R)F_{\mu_1\mu_2}$$
$$+ (C_{VR}\bar{e}_R\gamma^{\mu_1}\mu_R + C_{VL}\bar{e}_L\gamma^{\mu_1}\mu_L)\bar{u}\gamma_{\mu_1}u + (C_{SR}\bar{e}_L\mu_R + C_{SL}\bar{e}_R\mu_L)\bar{u}u\,. \tag{G.27}$$

The conversion rate follows as [323]

$$\Gamma_{\text{conversion}} = 4m_\mu^5\left|\frac{1}{4}C_{DR}D + C_{SL}G_S^{(u,p)}S^{(p)} + C_{SL}G_S^{(u,n)}S^{(n)} + 2C_{VR}V^{(p)} + C_{VR}V^{(n)}\right|^2$$
$$+ 4m_\mu^5\left|\frac{1}{4}C_{DL}D + C_{SR}G_S^{(u,p)}S^{(p)} + C_{SR}G_S^{(u,n)}S^{(n)} + 2C_{VL}V^{(p)}\right.$$
$$\left. + C_{VL}V^{(n)}\right|^2 \tag{G.28}$$

which is normalized to the capture rate, and multiplied by $1/\hbar$ to allows for a comparison with experiments. Here the nucleon form factors

$$G_S^{(u,p)} = 5.1\,, \quad G_S^{(u,n)} = 4.3\,, \tag{G.29}$$

and the overlap integrals of muons and electrons weighted by proton and neutron densities for Ti and Au

$$D_{\text{Ti}} = 0.0864\,, \quad S^{(p)}_{\text{Ti}} = 0.0368\,, \quad S^{(n)}_{\text{Ti}} = 0.0435\,, \quad V^{(p)}_{\text{Ti}} = 0.0396\,, \quad V^{(n)}_{\text{Ti}} = 0.0468\,,$$
$$D_{\text{Au}} = 0.189\,, \quad S^{(p)}_{\text{Au}} = 0.0614\,, \quad S^{(n)}_{\text{Au}} = 0.0918\,, \quad V^{(p)}_{\text{Au}} = 0.0974\,,$$
$$V^{(n)}_{\text{Au}} = 0.146\,. \tag{G.30}$$

Matching the coefficients we obtain

$$\delta_{\tilde{V}_1}C_{VR} = \delta_{V_2}C_{VR} = \delta_{\tilde{V}_2}C_{VL} = \frac{1}{2}\delta_{V_3}C_{VL} = -\frac{\lambda^{(u\mu)}\left(\lambda^{(ue)}\right)^*}{2M^2}\,,$$
$$\delta_S C_{VR} = -\frac{\lambda^{(u\mu)}_R\left(\lambda^{(ue)}_R\right)^*}{4M^2}\,, \quad \delta_S C_{VL} = -\frac{\lambda^{(u\mu)}_L\left(\lambda^{(ue)}_L\right)^*}{4M^2}\,,$$
$$\delta_S C_{SR} = -\frac{\lambda^{(u\mu)}_R\left(\lambda^{(uE)}_L\right)^*}{4M^2}\,, \quad \delta_S C_{SL} = -\frac{\lambda^{(u\mu)}_L\left(\lambda^{(ue)}_R\right)^*}{4M^2}\,, \tag{G.31}$$

and with eqs. (G.23) and (G.26) for $F^{V,A}$ and F^{γ}, respectively,

$$\begin{aligned}
\delta_{\tilde{V}_1/V_2} C_{DR,DL} &= -\frac{1}{4m_\mu^2\sqrt{\alpha_e 4\pi}}\left(\left|F^V\right| \pm \left|F^A\right|\right) , \\
\delta_{\tilde{V}_2/V_3} C_{DR,DL} &= -\frac{1}{4m_\mu^2\sqrt{\alpha_e 4\pi}}\left(\left|F^V\right| \mp \left|F^A\right|\right) , \\
\delta_S C_{DR,DL} &= \frac{1}{2m_\mu} F^{\gamma}_{2RL,2LR} ,
\end{aligned} \tag{G.32}$$

times 2 for up-type quarks in the model V_3. Note that the definition of the overlap integral D contains an factor of the electromagnetic coupling. We neglect loop suppressed gluonic interactions, for which the form factor can be related to the scalar form factors by a sum rule [324], and model dependent uncertainties [323, 324]. In principle, one can include incoherent $\mu - e$ conversion as in [325]. The strongest constraints are presently obtained from Au.

The branching ratio for LFV leptonic muon decay induced by vector LQs as obtained in [326] reads

$$\delta_V \mathcal{B}_{\mu\to eee} = \frac{3\alpha_e^2}{8\pi^2} q_q^2 \ln^2\frac{m_q^2}{M^2} \frac{|\lambda^{(q\mu)}\lambda^{(qe)}|^2}{G_F^2 M^4} , \tag{G.33}$$

times 4 for up-type quarks in the model V_3. Terms $\sim q_e$, m_f^2/M^2 suppressed box diagrams, and m_f^2/m_Z^2 suppressed Z diagrams are neglected. For scalar LQs the corresponding branching ratio is given as [327]

$$\begin{aligned}
\delta_S \mathcal{B}_{\mu\to eee} = \frac{\alpha_e^2 m_\mu^5}{32\pi\Gamma_\mu}\Bigg(& |T_{1L}|^2 + |T_{1R}|^2 + \frac{2}{3}\left(|T_{2L}|^2 + |T_{2R}|^2\right)\left(8\ln\frac{m_\mu}{2m_e} - 11\right) \\
& - 4\mathrm{Re}[T_{1L}T_{2R}^* + T_{2L}T_{1R}^*] \\
& + \frac{1}{3}\left(2\left(|Z_L g_{Ll}|^2 + |Z_R g_{Rl}|^2\right) + |Z_L g_{Rl}|^2 + |Z_R g_{Ll}|^2\right) \\
& + \frac{1}{6}\left(|B_{1L}|^2 + |B_{1R}|^2\right) + \frac{1}{3}\left(|B_{2L}|^2 + |B_{2R}|^2\right) \\
& + \frac{2}{3}\mathrm{Re}[T_{1L}B_{1L}^* + T_{1L}B_{2L}^* + T_{1R}B_{1R}^* + T_{1R}B_{2R}^*] \\
& - \frac{4}{3}\mathrm{Re}[T_{2R}B_{1L}^* + T_{2L}B_{1R}^* + T_{2L}B_{2R}^* + T_{2R}B_{2L}^*] \\
& + \frac{2}{3}\mathrm{Re}[B_{1L}Z_L^* g_{Ll} + B_{1R}Z_R^* g_{Rl} + B_{2L}Z_L^* g_{Rl} + B_{2R}Z_R^* g_{Ll}] \\
& + \frac{2}{3}\mathrm{Re}[2(T_{1L}Z_L^* g_{Ll} + T_{1R}Z_R^* g_{Rl}) + T_{1L}Z_L^* g_{Rl} + T_{1R}Z_R^* g_{Ll}] \\
& + \frac{2}{3}\mathrm{Re}[-4(T_{2R}Z_L^* g_{Ll} + T_{2L}Z_R^* g_{Rl}) - 2(T_{2L}Z_R^* g_{Ll} + T_{2R}Z_L^* g_{Rl})]\Bigg) .
\end{aligned} \tag{G.34}$$

Here we correct $Z_{L,R}$, i.e.

$$
\begin{aligned}
T_{1L,1R} &= -\frac{3}{16\pi^2}\frac{1}{M^2}\lambda^{(q\mu)}_{L,R}\left(\lambda^{(qe)}_{L,R}\right)^*\left(\left(\frac{4}{9}+\frac{1}{3}\ln\frac{m_q^2}{M^2}\right)q_q+\frac{-1}{18}q_e\right),\\
T_{2L,2R} &= \frac{3}{16\pi^2}\frac{1}{M^2}\Bigg(-\left(\lambda^{(q\mu)}_{R,L}\left(\lambda^{(qe)}_{R,L}\right)^*\frac{1}{6}+\frac{m_q}{m_\mu}\lambda^{(q\mu)}_{R,L}\left(\lambda^{(qe)}_{L,R}\right)^*\left(-\frac{3}{2}-\ln\frac{m_q^2}{M^2}\right)\right)q_q\\
&\quad+\left(\lambda^{(q\mu)}_{R,L}\left(\lambda^{(qe)}_{R,L}\right)^*\frac{1}{12}+\frac{m_q}{m_\mu}\lambda^{(q\mu)}_{R,L}\left(\lambda^{(qe)}_{L,R}\right)^*\frac{1}{2}\right)q_e\Bigg),\\
Z_{L,R} &= -\frac{3}{16\pi^2}\frac{1}{M^2}\lambda^{(q\mu)}_{L,R}\left(\lambda^{(qe)}_{L,R}\right)^*\frac{1}{m_Z^2\sin^2\theta_w\cos^2\theta_w}\\
&\quad\times\left(m_\mu^2\frac{3}{8}2g_{Lq,Rq}-m_q^2\left(1+\ln\frac{m_q^2}{M^2}\right)g_{Rq,Lq}+m_\mu^2\frac{3}{8}2(-g)\right),\\
B_{1L,1R} &= \frac{3}{32\pi^2}\lambda^{(q\mu)}_{L,R}\left(\lambda^{(qe)}_{L,R}\right)^*\left|\lambda^{(q'e)}_{L,R}\right|^2\frac{-1}{M^2},\\
B_{2L,2R} &= \frac{3}{64\pi^2}\lambda^{(q\mu)}_{L,R}\left(\lambda^{(qe)}_{L,R}\right)^*\left|\lambda^{(q'e)}_{R,L}\right|^2\frac{-1}{M^2}.
\end{aligned}
\tag{G.35}
$$

Furthermore,

$$
g_{Lf,Rf} = T_3^{(f_L,f_R)} - q_f\sin^2\theta_w\,, \qquad g = T_3^{(e)} - q_e\sin^2\theta_w \tag{G.36}
$$

and for S_2 the interchange $g_L \leftrightarrow g_R$. We add that $\mu^- e^- \to e^- e^-$ in muonic atoms may be used to constrain LQ models [328] once the decay measured, e.g. in the COMET Phase-I experiment [329].

From the Lagrangian for $P \to l\nu$ decays [330]

$$
\begin{aligned}
\mathcal{L}_{Pl\nu} &= C_{VLL}(\bar{q}'_L\gamma^\mu q_L)(\bar{\nu}_L\gamma_\mu l_L) + C_{VRL}(\bar{q}'_R\gamma^\mu q_R)(\bar{\nu}_L\gamma_\mu l_L)\\
&\quad + C_{SRR}(\bar{q}'_L q_R)(\bar{\nu}_L l_R) + C_{SLR}(\bar{q}'_R q_L)(\bar{\nu}_L l_R)
\end{aligned}
\tag{G.37}
$$

the total width follows as

$$
\Gamma_{P\to l\nu} = \frac{f_P^2\left(m_P^2-m_l^2\right)^2}{64\pi m_P^3}\left|m_l(C_{VRL}-C_{VLL})+\frac{m_P^2}{m_q+m_{q'}}(C_{SLR}-C_{SRR})\right|^2. \tag{G.38}
$$

In the SM $C_{VLL} = -4G_F/\sqrt{2}\,V_{qq'}$, where q and q' denote the quark content of P. Matching the coefficients in LQ models gives

$$\begin{aligned}
\delta_{V_3} C_{VLL} &= \frac{\lambda_{V_3}^{(q'l)} \left(\lambda_{V_3}^{(q\nu)}\right)^*}{M_{V_3}^2}\,, \\
\delta_{S_1} C_{VLL} &= -\frac{1}{2}\frac{\lambda_{S_1 L}^{(ql)} \left(\lambda_{S_1 L}^{(q'\nu)}\right)^*}{M_{S_1}^2}\,, \quad \delta_{S_1} C_{SRR} = \frac{1}{2}\frac{\lambda_{S_1 R}^{(ql)} \left(\lambda_{S_1 L}^{(q'\nu)}\right)^*}{M_{S_1}^2}\,, \\
\delta_{S_2} C_{SRR} &= \frac{1}{2}\frac{\lambda_{S_2 R}^{(q'l)} \left(\lambda_{S_2 L}^{(q\nu)}\right)^*}{M_{S_2}^2}\,, \quad \delta_{S_3} C_{VLL} = \frac{1}{2}\frac{\lambda_{S_3}^{(ql)} \left(\lambda_{S_3}^{(q'\nu)}\right)^*}{M_{S_3}^2}\,.
\end{aligned} \tag{G.39}$$

We do not match V_2 due to an additional d_L quark coupling. Note that a corrections to W vertex via left-handed couplings due to scalar LQs can be neglected for vanishing fermion masses [225]. Varying the decay constants one obtains no constraints from the decays $D^+ \to e^+\nu_e$ and $D_s \to e^+\nu_e$, i.e. $\delta_{V_3}\mathcal{B}_{D^+\to e^+\nu_e} \lesssim 2\times 10^{-8}$ and $\delta_{V_3}\mathcal{B}_{D_s\to e^+\nu_e} \lesssim 2\times 10^{-7}$ for $|\lambda| \lesssim \frac{M}{\text{TeV}}$, as well as no constraint due to the decay $D_s^+ \to \mu^+\nu_\mu$. The total width for the decay $l \to P\nu$ is given as $\Gamma_{l\to P\nu} = m_P^3/(2m_l^3)\,\Gamma_{P\to l\nu}$ with eq. (G.38). Here only $l = \tau$ is kinematically allowed.

We do not employ constraints from $D \to Kl\nu_l$ decays to avoid correlations with form factors, which are extracted from $D \to Pl\nu_l$ decays and used for other constraints. Ignoring this, we would obtain from the distribution given in [137] the vector LQ induced shift $|\delta_{V_3}\Gamma_{D\to Kl\nu_l}| = \Gamma^{\text{SM}}_{D\to Kl\nu_l}\frac{1}{\sqrt{2}G_F V_{cs}}|\lambda_{V_3}^{(cl)}\lambda_{V_3}^{(cl)}|^2/M^2 \simeq 0.063\,\Gamma^{\text{SM}}_{D\to Kl\nu_l}|\lambda_{V_3}^{(cl)}(\lambda_{V_3}^{(cl)})|^2(\frac{\text{TeV}}{M})^2$, to be multiplied by 1/4 for scalar LQs. Here we neglect lepton masses, and (pseudo-)scalar and (pseudo-)tensor operators, for which contributions to the distribution can be found in [137]. The measured ratio $\Gamma(D^+ \to \bar{K}^0\mu^+\nu_\mu)/\Gamma(D^+ \to \bar{K}^0 e^+ e_\mu) = 0.988 \pm 0.033$ [331] is satisfied for perturbative couplings.

For the ratio of leptonic pions decays, $R_{e/\mu} = \Gamma_{\pi\to e\nu_e}/\Gamma_{\pi\to\mu\nu_\mu}$, the interference between the SM and LQ models is found as

$$\begin{aligned}
\delta_{LQ} R_{e/\mu} = R^{\text{SM}}_{e/\mu}\frac{1}{\sqrt{2}G_F V_{ud}}\text{Re}\Bigg[&\left(C_{VRL}^{(l=e)} - C_{VLL}^{(l=e)}\right) - \left(C_{VRL}^{(l=\mu)} - C_{VLL}^{(l=\mu)}\right) \\
&+ \frac{m_\pi^2}{m_u + m_d}\left(\frac{C_{SLR}^{(l=e)} - C_{SRR}^{(l=e)}}{m_e} - \frac{C_{SLR}^{(l=\mu)} - C_{SRR}^{(l=\mu)}}{m_\mu}\right)\Bigg]\,,
\end{aligned} \tag{G.40}$$

where the matching coefficients are given by eq. (G.39). Note that the irreducible experimental background from $\pi \to l\nu_l\gamma$ decays due to higher dimensional operators or bremsstrahlung cancels in the ratio.

Analogously, we obtain constraints from the decays $K^+ \to e^+\nu_e$ and $K^+ \to \mu^+\nu_\mu$ as well as the LFV decays $\pi^+ \to \mu^+\nu_e$ and $K^+ \to \mu^+\nu_e$. Due to the decay $\pi^+ \to \mu^+\nu_e$

no constraints are obtained for vector LQs. The decays $\pi^0 \to (\mu, e)e$ do not give any constraints due to the small lifetime and mass of the pion. Further LFV quarkonium decays [332] do not give constraints for $|\lambda| \lesssim \frac{M}{\text{TeV}}$, yet.

The CKM parameter V_{ud} can be extracted from quark beta decay normalized to muon decay. The LQ induced shift is

$$\frac{\Delta^{LQ} V_{ud}}{V_{ud}} = \frac{\sqrt{2}}{4G_F} C_{VLL}^{(ue)} \,. \tag{G.41}$$

Here the matching coefficients are given by eq. (G.39).

Further constraints can be obtained from nuclear beta decay. The defining Lagrangian for $N_i \to N_f e \bar{\nu}_e$ decays is [333]

$$\begin{aligned}\mathcal{L}_\beta = {} & (\bar{N}_f \gamma^{\mu_1} N_i)(C_V \bar{e}\gamma_{\mu_1}\nu_e - C'_V \bar{e}\gamma_{\mu_1}\gamma_5\nu_e) - (\bar{N}_f \gamma^{\mu_1}\gamma_5 N_i)(C_A \bar{e}\gamma_{\mu_1}\nu_e - C'_A \bar{e}\gamma_{\mu_1}\gamma_5\nu_e) \\ & + (\bar{N}_f N_i)(C_S \bar{e}\nu_e - C'_S \bar{e}\gamma_5\nu_e) \\ & + \frac{1}{2}(\bar{N}_f \sigma^{\mu_1\mu_2} N_i)(C_T \bar{e}\sigma_{\mu_1\mu_2}\nu_e - C'_T \bar{e}\sigma_{\mu_1\mu_2}\gamma_5\nu_e) \,. \end{aligned} \tag{G.42}$$

In the SM $C_V = C'_V = G_F V_{ud}$ and $C_A = C'_A$, where a pseudoscalar coupling is absent for non-relativistic nucleons. For neutron beta decay the parity-even triple correlation coefficient is given by [334]

$$D_n = \frac{1}{1+3|\lambda_n|^2}\left(-\frac{\text{Im}[C_V C_A^* + C'_V (C'_A)^*]}{|C_V|^2} + \frac{\text{Im}[C_S C_T^* + C'_S (C'_T)^*]}{|C_V|^2}\right) , \tag{G.43}$$

where $\lambda = C_A/C_V$, which is negligible in the SM, and $\lambda_n = -1.27$ [21]. The parity-odd triple correlation coefficient is [335]

$$R_N = -0.436\, G_F V_{ud}\, \text{Im}\left[\frac{C_S + C'_S}{C_V + C'_V}\right] + 0.670\, G_F V_{ud}\, \text{Im}\left[\frac{C_T + C'_T}{C_A + C'_A}\right] \tag{G.44}$$

with vanishing scalar coefficients for Li beta decay, $\lambda_{\rm Li} \simeq \lambda_n$ [270] and we neglect the beta decay asymmetry coefficient term, which is around a permille for neutrons. Both triple correlation coefficients are time reversal violating. A matching gives

$$\begin{aligned}
\delta_{V_3} C_V = \delta_{V_3} C'_V = \delta_{V_3} C_A = \delta_{V_3} C'_A &= -\frac{1}{4} \frac{\lambda_{V_3}^{(q_f \nu_e)} \left(\lambda_{V_3}^{(q_i e)}\right)^*}{M_{V_3}^2} \,, \\
\delta_{S_1} C_V = \delta_{S_1} C'_V = \delta_{S_1} C_A = \delta_{S_1} C'_A &= \frac{1}{8} \frac{\lambda_{S_1 L}^{(q_i \nu_e)} \left(\lambda_{S_1 L}^{(q_f e)}\right)^*}{M_{S_1}^2} \,, \\
\delta_{S_1} C_S = \delta_{S_1} C'_S = -\delta_{S_1} C_T = -\delta_{S_1} C'_T &= -\frac{1}{8} \frac{\lambda_{S_1 L}^{(q_i \nu_e)} \left(\lambda_{S_1 R}^{(q_f e)}\right)^*}{M_{S_1}^2} \,, \\
\delta_{S_2} C_S = \delta_{S_2} C'_S = \delta_{S_2} C_T = \delta_{S_2} C'_T &= -\frac{1}{8} \frac{\lambda_{S_2 L}^{(q_f \nu_e)} \left(\lambda_{S_2 R}^{(q_i e)}\right)^*}{M_{S_2}^2} \,, \\
\delta_{S_3} C_V = \delta_{S_3} C'_V = \delta_{S_3} C_A = \delta_{S_3} C'_A &= -\frac{1}{8} \frac{\lambda_{S_3}^{(q_i \nu_e)} \left(\lambda_{S_3}^{(q_f e)}\right)^*}{M_{S_3}^2} \,. \qquad \text{(G.45)}
\end{aligned}$$

One obtains $|\delta_{V_3} D_n| \lesssim 2 \times 10^{-8}$, $|\delta_{S_{1,3}} D_n| \lesssim 9 \times 10^{-9}$, $|\delta_{S_1,S_2} R_n| \lesssim 2 \times 10^{-7}$, and $|\delta_{S_1,S_2} R_{\rm Li}| \lesssim 7 \times 10^{-8}$ for $|\lambda| \lesssim \frac{M}{\rm TeV}$ as well as $|\delta_{S_2} D_n| = 0$, yielding no constraints.

Further nuclear beta decay parameters yield at 68% CL [336, 337]

$$\begin{aligned}
&1 - 2\frac{|C_S|^2 + |C'_S|^2}{|C_V|^2 + |C'_V|^2} + 2 \times 0.21 \times 14\alpha_e \,\mathrm{Im}\frac{C_S + C'_S}{C_V + C'_V} \\
&\quad + 2 \times 0.1913 \sqrt{1 - (14\alpha_e)^2}\,\mathrm{Re}\frac{C_S + C'_S}{C_V + C'_V} = 0.9989 \pm 0.0064 \,, \qquad \text{(G.46)} \\
&1 + 2\frac{m_e}{0.0033\,\mathrm{GeV}} \sqrt{1 - (19\alpha_e)^2}\,\mathrm{Re}\frac{C_S + C'_S}{C_V + C'_V} = 0.9981^{+0.0044}_{-0.0048} \qquad \text{(G.47)}
\end{aligned}$$

from which we obtain, respectively, $-0.0075 < 0.0042\,\mathrm{Re}[\lambda_R^{(ue)} (\lambda_L^{(ue)})^*] (\frac{\rm TeV}{M})^2 \leq 0.0053$ and $-0.0023 < 0.0034\,\mathrm{Re}[\lambda_R^{(ue)} (\lambda_L^{(ue)})^*] (\frac{\rm TeV}{M})^2 \leq 0.0063$. Here we add uncertainties in quadrature. Additionally, a fit gives at 90% CL [338]

$$\begin{aligned}
-0.14 \times 10^{-2} < \frac{C_T + C'_T}{C_A} < 1.4 \times 10^{-2} \,, \qquad \text{(G.48)} \\
-0.16 < \frac{C_T - C'_T}{C_A} < 0.16 \,, \qquad \text{(G.49)}
\end{aligned}$$

that is $-0.8 < \lambda_{S_1 R}^{(ue)} (\lambda_{S_1 L}^{(ue)})^* (\frac{\rm TeV}{M})^2 < 0.08$ and $-0.08 < \lambda_{S_2 R}^{(ue)} (\lambda_{S_2 L}^{(ue)})^* (\frac{\rm TeV}{M})^2 < 0.8$, respectively, employing λ_n. Note that [338] varies C_S, C'_S and fixes C_T, C'_T, yet primed and

unprimed Wilson coefficients are related in LQ models, see eq. (G.45), which is consistent with eq. (G.47).

Following [339] we deduce that no constraints for vector LQs are found from neutrino trident production. Finally, from model dependent contact interactions [340] we find no constraints as $M/|\lambda_V^{(ql)}| = \Lambda/\sqrt{4\pi} \gtrsim 4.0\,\text{TeV}$, which is multiplied by $\sqrt{2}$ for V_3, and $M/|\lambda_S^{(ql)}| = \frac{1}{\sqrt{2}}\frac{\Lambda}{\sqrt{4\pi}} \gtrsim 2.8\,\text{TeV}$.

G.1. Tables

The constraints from the previous appendix are compiled in tables G.1, G.2 and G.3 for the scalar $S_{1,2}$, S_3 and gauge vector LQs, respectively.

No constraints are found due to the decay $D^0 \to \rho^0\gamma$, $D^0 - \bar{D}^0$ lifetime difference, $\pi^0 \to ee$ decay, LFV quarkonium decays, triple correlation coefficients from nuclear beta decay nor contact interactions. Furthermore, $Z \to ff'$ decays in case of scalar LQs and the decays $D^+ \to e^+\nu_e$, $D_s \to e^+\nu_e$, $D_s^+ \to \mu^+\nu_\mu$, and $\pi^+ \to \mu^+\nu_e$, nuclear beta decay parameters, and neutrino trident production in case of vector LQs do not give constraints.

Additional constraints on quark doublets from kaon and $\tau \to \pi l$ decays [238] are collected in table G.4. Furthermore, we find $|\lambda_{SL}^{(u\mu)}(\lambda_{SR}^{(u\tau)})^*| \lesssim 3 \times 10^{-1}$, which is obtained from $\mathcal{B}(\tau^- \to \pi^0\mu^-)/\mathcal{B}(\tau^- \to \pi^-\nu_\tau)$ times $m_s m_\tau/m_{\pi^0}^2 \simeq 49$. Note that the constraint from $K_L \to \mu\mu$ decays in [235] should be multiplied by $\sqrt{10}$.

couplings/mass	constraint	observable
$\lvert\lambda_{S_1L}^{(ue)}\rvert$	$\sim [0.00, 0.09]$	V_{ud}
$\lambda_{S_1L}^{(ue)}(\lambda_{S_1R}^{(ue)})^*$	$\sim [-0.8, 0.08]$	nuclear beta decay
$\lambda_{S_2L}^{(ue)}(\lambda_{S_2R}^{(ue)})^*$	$\sim [-0.08, 0.8]$	
$\lvert\text{Im}[\lambda_L^{(qe)}(\lambda_R^{(qe)})^*]\rvert$	$\lesssim 2 \times 10^{-8}$	$d(\text{Hg})$
$\lvert\lambda_L^{(ue)}(\lambda_R^{(u\mu)})^*\rvert$	$\lesssim 9 \times 10^{-2}$	$\pi^+ \to \mu^+\nu_e$
$\lvert\lambda_{S_1L,S_2R}^{(ue)}(\lambda_{S_1R,S_2L}^{(ce)})^*\rvert$	$\lesssim 0.04$	$D^+ \to e^+\nu_e$
$\lvert\lambda_{\{L,R\}}^{(ue)}(\lambda_{\{L,R\}}^{(ce)})^*\rvert$	$\lesssim 1 \times 10^{-1}$	$D^+ \to \pi^+e^+e^-$
$\lvert\lambda_{\{L,R\}}^{(ue)}(\lambda_{\{L,R\}}^{(c\mu)})^*\rvert$	$\lesssim 2 \times 10^{-1}$	$D^+ \to \pi^+e^+\mu^-$
$\lvert\lambda_{\{L,R\}}^{(u\mu)}(\lambda_{\{L,R\}}^{(ce)})^*\rvert$	$\lesssim 2 \times 10^{-1}$	$D^+ \to \pi^+e^-\mu^+$
$\lvert\lambda_{\{L,R\}}^{(u\mu)}(\lambda_{\{L,R\}}^{(c\mu)})^*\rvert$	$\lesssim 2 \times 10^{-2}$	$D^+ \to \pi^+\mu^+\mu^-$
$\lvert\text{Im}[\lambda_L^{(u\mu)}(\lambda_R^{(u\mu)})^*]\rvert$	$\lesssim 3 \times 10^{-7}$	$d(n)$

$\mathrm{Re}[\lambda_R^{(u\tau)}(\lambda_L^{(u\tau)})^*]$	$\sim [0.00, 0.09]$	$\tau^- \to \pi^- \nu_\tau$
$\mathrm{Re}[\lambda_{S_1L}^{(u\tau)}(\lambda_{S_1L}^{(c\tau)})^*]$	$\sim [-0.2, 0.2]$	$\tau^- \to K^- \nu_\tau$
$\mathrm{Re}[\lambda_R^{(u\tau)}(\lambda_L^{(c\tau)})^*]$	$\sim [-0.07, 0.04]$	
$\lvert\mathrm{Im}[\lambda_R^{(u\tau)}(\lambda_L^{(c\tau)})^*]\rvert$	$\sim [0.0, 0.7]$	
$\lvert\mathrm{Re}[\lambda_R^{(u\tau)}(\lambda_L^{(c\tau)})^*]\rvert$	$\lesssim 0.3$	$D^+ \to \tau^+ \nu_\tau$
$\lvert\lambda_{S_1L,S_2R}^{(ce)}(\lambda_{S_1R,S_2L}^{(ce)})^*\rvert$	$\lesssim 0.1$	$D_s \to e^+ \nu_e$
$\lvert\mathrm{Im}[\lambda_L^{(ce)}(\lambda_R^{(ce)})^*]\rvert$	$\lesssim 2 \times 10^{-11}$	$d(e)$
$\mathrm{Re}[\lambda_{S_1L}^{(ce)}(\lambda_{S_1R}^{(ce)})^*]$	$\sim [-0.01, 0.00]$	Δa_e
$\mathrm{Re}[\lambda_{S_2L}^{(ce)}(\lambda_{S_2R}^{(ce)})^*]$	$\sim [0.00, 0.01]$	
$\mathrm{Re}[\lambda_{S_1L}^{(c\mu)}(\lambda_{S_1R}^{(c\mu)})^*]$	$\sim [0.1, 0.2]$	Δa_μ
$\mathrm{Re}[\lambda_{S_2L}^{(c\mu)}(\lambda_{S_2R}^{(c\mu)})^*]$	$\sim [-0.2, -0.1]$	
$\mathrm{Re}[\lambda_{S_1L,S_2R}^{(c\mu)}(\lambda_{S_1R,S_2L}^{(c\mu)})^*]$	$\sim [-0.02, 0.08]$	$D_s \to \mu^+ \nu_\mu$
$\lvert\mathrm{Im}[\lambda_{S_1L,S_2R}^{(c\mu)}(\lambda_{S_1R,S_2L}^{(c\mu)})^*]\rvert$	$\lesssim 0.4$	
$\mathrm{Re}[\lambda_R^{(c\tau)}(\lambda_L^{(c\tau)})^*]$	$\sim [-1, 0.09]$	$D_s \to \tau^+ \nu_\tau$
$(-\lvert\lambda_{S_1L}^{(ue)}\rvert^2 + \lvert\lambda_{S_1R}^{(ue)}\rvert^2)^{1/2}$	~ 0.0	$Q_w\,(\mathrm{Cs})$
$(-\lvert\lambda_{S_2L}^{(ue)}\rvert^2 + 2\lvert\lambda_{S_2R}^{(ue)}\rvert^2)^{1/2}$	$\sim [0.2, 0.4]$	
$\mathrm{Re}[(\lambda_L^{(ue)}(\lambda_R^{(ue)})^* - 0.009\,\lambda_L^{(u\mu)}(\lambda_R^{(u\mu)})^*$		$R_{e/\mu}$
$\quad +0.0001\,(-\lvert\lambda_{S_1L}^{(ue)}\rvert^2 + \lvert\lambda_{S_1L}^{(u\mu)}\rvert^2))]$	$\sim [0.00000, 0.00001]$	
$\mathrm{Re}[\lambda_{S_1L,S_2R}^{(ue)}(\lambda_{S_1R,S_2L}^{(ce)})^* - 0.001\,\lambda_{S_1L}^{(ue)}(\lambda_{S_1L}^{(ce)})^*]$	$\sim [0.00000, 0.00001]$	$K^+ \to e^+ \nu_e$
$\mathrm{Im}[\lambda_{\{L,R\}}^{(ue)}(\lambda_{\{L,R\}}^{(ce)})^*]$	~ 0.0	
$\lvert\mathrm{Re}[\lambda_{L,R}^{(ue)}(\lambda_{L,R}^{(ce)})^* + \lambda_{L,R}^{(u\mu)}(\lambda_{L,R}^{(c\mu)})^* + \lambda_{L,R}^{(u\tau)}(\lambda_{L,R}^{(c\tau)})^*]\rvert$	$\sim [0, 0.02]$	Δm_{D^0}
$\lvert\lambda_L^{(ue)}(\lambda_R^{(ce)})^* \pm \lambda_R^{(ue)}(\lambda_L^{(ce)})^*\rvert$	$\lesssim 1 \times 10^{-2}$	$D^0 \to e^+ e^-$
$\lvert\lambda_{L,R}^{(ue)}(\lambda_{L,R}^{(c\mu)})^* + \lambda_{L,R}^{(u\mu)}(\lambda_{L,R}^{(ce)})^*\rvert$	$\lesssim 1 \times 10^{-1}$	$D^0 \to \mu^\pm e^\mp$
$\lvert\lambda_{L,R}^{(ue)}(\lambda_{R,L}^{(c\mu)})^* + \lambda_{L,R}^{(u\mu)}(\lambda_{R,L}^{(ce)})^*\rvert$	$\lesssim 6 \times 10^{-3}$	
$\lvert\lambda_{S_1L,S_2R}^{(u\mu)}(\lambda_{S_1R,S_2L}^{(ce)})^* - 0.2\,\lambda_{S_1L}^{(u\mu)}(\lambda_{S_1L}^{(ce)})^*\rvert$	$\lesssim 0.002$	$K^+ \to \mu^+ \nu_e$
$\lvert\lambda_L^{(u\mu)}(\lambda_L^{(c\mu)})^* + \lambda_R^{(u\mu)}(\lambda_R^{(c\mu)})^*\rvert$	$\lesssim 6 \times 10^{-2}$	$D^0 \to \mu^+ \mu^-$
$\lvert\lambda_L^{(u\mu)}(\lambda_R^{(c\mu)})^* \pm \lambda_R^{(u\mu)}(\lambda_L^{(c\mu)})^*\rvert$	$\lesssim 4 \times 10^{-3}$	

$\mathrm{Re}[\lambda^{(u\mu)}_{S_1L,S_2R}(\lambda^{(c\mu)}_{S_1R,S_2L})^* - 0.01\,\lambda^{(u\mu)}_{S_1L}(\lambda^{(c\mu)}_{S_1L})^*]$	$\sim [-0.02, 0.00]$	$D^+ \to \mu^+\nu_\mu$
$\mathrm{Im}[\lambda^{(u\mu)}_{\{L,R\}}(\lambda^{(c\mu)}_{\{L,R\}})^*]$	~ 0.0	
$\mathrm{Re}[\lambda^{(u\mu)}_{S_1L,S_2R}(\lambda^{(c\mu)}_{S_1R,S_2L})^* - 0.2\,\lambda^{(u\mu)}_{S_1L}(\lambda^{(c\mu)}_{S_1L})^*]$	$\sim [-0.004, -0.001]$	$K^+ \to \mu^+\nu_\mu$
$\lvert\mathrm{Im}[\lambda^{(u\mu)}_{L}(\lambda^{(c\mu)}_{R})^*]\rvert$	$\sim [0.02, 0.05]$	
$\lvert\lambda^{(qe)}_{S_1L,S_1R}(\lambda^{(q\mu)}_{S_1L,S_1R})^*\rvert$	$\lesssim 1 \times 10^{-3}$	$\mu^+ \to e^+\gamma$
$\lvert\lambda^{(qe)}_{S_2L,S_2R}(\lambda^{(q\mu)}_{S_2L,S_2R})^*\rvert$	$\lesssim 4 \times 10^{-4}$	
$\lvert\lambda^{(ce)}_{L,R}(\lambda^{(c\mu)}_{R,L})^*\rvert$	$\lesssim 2 \times 10^{-6}$	
$\lvert\lambda^{(ue)}_{L,R}(\lambda^{(u\mu)}_{L,R})^*\rvert$	$\lesssim 9 \times 10^{-7}$	$\mu - e\,(\mathrm{Au})$
$\lvert\lambda^{(ue)}_{S_2R}(\lambda^{(u\mu)}_{S_2R})^*\rvert$	$\lesssim 7 \times 10^{-7}$	
$\lvert\lambda^{(ue)}_{L,R}(\lambda^{(u\mu)}_{R,L})^*\rvert$	$\lesssim 4 \times 10^{-7}$	
$\lvert\lambda^{(ce)}_{S_1L,S_1R}(\lambda^{(c\mu)}_{S_1L,S_1R})^*\rvert$	$\lesssim 9 \times 10^{-3}$	
$\lvert\lambda^{(ce)}_{S_2L,S_2R}(\lambda^{(c\mu)}_{S_2L,S_2R})^*\rvert$	$\lesssim 3 \times 10^{-3}$	
$\lvert\lambda^{(ce)}_{L,R}(\lambda^{(c\mu)}_{R,L})^*\rvert$	$\lesssim 1 \times 10^{-5}$	
$\lvert\lambda^{(ue)}_{L,R}(\lambda^{(u\mu)}_{L,R})^*\rvert$	$\lesssim 1 \times 10^{-3}$	$\mu^- \to e^-e^+e^-$
$\lvert\lambda^{(ue)}_{S_2R}(\lambda^{(u\mu)}_{S_2R})^*\rvert$	$\lesssim 3 \times 10^{-3}$	
$\lvert\lambda^{(ue)}_{L,R}(\lambda^{(u\mu)}_{R,L})^*\rvert$	$\lesssim 1 \times 10^{-2}$	
$\lvert\lambda^{(ce)}_{L,R}(\lambda^{(c\mu)}_{L,R})^*\rvert$	$\lesssim 3 \times 10^{-3}$	
$\lvert\lambda^{(ce)}_{S_2R}(\lambda^{(c\mu)}_{S_2R})^*\rvert$	$\lesssim 6 \times 10^{-3}$	
$\lvert\lambda^{(ce)}_{S_1L,S_1R}(\lambda^{(c\mu)}_{S_1R,S_1L})^*\rvert$	$\lesssim 6 \times 10^{-5}$	
$\lvert\lambda^{(ce)}_{S_2L,S_2R}(\lambda^{(c\mu)}_{S_2R,S_2L})^*\rvert$	$\lesssim 5 \times 10^{-5}$	
$\lvert\lambda^{(ql)}_{S_2L,S_2R}(\lambda^{(q\tau)}_{S_2L,S_2R})^*\rvert$	$\lesssim 3 \times 10^{-1}$	$\tau^- \to l^-\gamma$
$\lvert\lambda^{(cl)}_{L,R}(\lambda^{(c\tau)}_{R,L})^*\rvert$	$\lesssim 3 \times 10^{-2}$	
$\lvert\lambda^{(ul)}_{S_1L,S_1R}(\lambda^{(u\tau)}_{S_1L,S_1R})^*\rvert$	$\lesssim 7 \times 10^{-1}$	$\tau^- \to l^-l^+l^-$
$\lvert\lambda^{(ul)}_{S_2L,S_2R}(\lambda^{(u\tau)}_{S_2L,S_2R})^*\rvert$	$\lesssim 6 \times 10^{-1}$	
$\lvert\lambda^{(cl)}_{S_1L,S_1R}(\lambda^{(c\tau)}_{S_1R,S_1L})^*\rvert$	$\lesssim 8 \times 10^{-1}$	
$\lvert\lambda^{(cl)}_{S_2L,S_2R}(\lambda^{(c\tau)}_{S_2R,S_2L})^*\rvert$	$\lesssim 7 \times 10^{-1}$	

Table G.1.: Constraints on scalar $SU(2)$ singlet and doublet LQs scaling as $\frac{\text{TeV}}{M}$ and $\sqrt{\frac{\text{TeV}}{M}}$ for Δm_{D^0}. Here $q \in \{u, c\}$ and $l \in \{e, \mu\}$.

couplings/mass	constraint	observable
$\lvert\lambda^{(ue)}\rvert$	$\sim [0.1, 0.3]$	$Q_w\,(\text{Cs})$
$\lvert\lambda^{(ue)}\rvert$	$\lesssim 9 \times 10^{-2}$	V_{ud}
$\lvert\lambda^{(u\tau)}\rvert$	$\sim [0.0, 0.2]$	$\tau^- \to \pi^- \nu_\tau$
$\lvert\lambda^{(c\tau)}\rvert$	$\sim [0.0, 0.4]$	$D_s \to \tau^+ \nu_\tau$
$\text{Re}[\lambda^{(ue)}(\lambda^{(ce)})^*]$	$\sim [0.0, 0.3]$	$K^+ \to e^+ \nu_e$
$\text{Im}[\lambda^{(ue)}(\lambda^{(ce)})^*]$	~ 0.0	
$\lvert\lambda^{(ue)}(\lambda^{(ce)})^*\rvert$	$\lesssim 1 \times 10^{-1}$	$D^+ \to \pi^+ e^+ e^-$
$\lvert\lambda^{(ue)}(\lambda^{(c\mu)})^*\rvert$	$\lesssim 2 \times 10^{-1}$	$D^+ \to \pi^+ e^+ \mu^-$
$\lvert\lambda^{(u\mu)}(\lambda^{(ce)})^*\rvert$	$\lesssim 3 \times 10^{-1}$	$D^+ \to \pi^+ e^- \mu^+$
$\lvert\lambda^{(u\mu)}(\lambda^{(ce)})^*\rvert$	$\lesssim 0.9$	$K^+ \to \mu^+ \nu_e$
$\lvert\lambda^{(u\mu)}(\lambda^{(c\mu)})^*\rvert$	$\lesssim 1 \times 10^{-2}$	$D^+ \to \pi^+ \mu^+ \mu^-$
$\lvert\lambda^{(u\mu)}(\lambda^{(c\mu)})^*\rvert$	$\lesssim 6 \times 10^{-2}$	$D^0 \to \mu^+ \mu^-$
$\text{Re}[\lambda^{(u\mu)}(\lambda^{(c\mu)})^*]$	$\sim [-0.2, 0.0]$	$K^+ \to \mu^+ \nu_\mu$
$\text{Re}[\lambda^{(u\tau)}(\lambda^{(c\tau)})^*]$	$\sim [-0.2, 0.2]$	$\tau^- \to K^- \nu_\tau$
$(\lvert\lambda^{(ue)}\rvert^2 - \lvert\lambda^{(u\mu)}\rvert^2)^{1/2}$	$\sim [0.0, 0.4]$	$R_{e/\mu}$
$\lvert\lambda^{(ue)}(\lambda^{(u\mu)})^* + \lambda^{(ce)}(\lambda^{(c\mu)})^*\rvert$	$\lesssim 4 \times 10^{-4}$	$\mu^+ \to e^+ \gamma$
$\lvert\text{Re}[\lambda^{(ue)}(\lambda^{(ce)})^* + \lambda^{(u\mu)}(\lambda^{(c\mu)})^* + \lambda^{(u\tau)}(\lambda^{(c\tau)})^*]\rvert$	$\sim [0, 0.007]$	Δm_{D^0}
$\lvert\lambda^{(ue)}(\lambda^{(c\mu)})^* + \lambda^{(u\mu)}(\lambda^{(ce)})^*\rvert$	$\lesssim 1 \times 10^{-1}$	$D^0 \to \mu^\pm e^\mp$
$\lvert\lambda^{(ql)}(\lambda^{(q\tau)})^*\rvert$	$\lesssim 3 \times 10^{-1}$	$\tau^- \to l^- \gamma$
$\lvert\lambda^{(ue)}(\lambda^{(u\mu)})^*\rvert$	$\lesssim 7 \times 10^{-7}$	$\mu - e\,(\text{Au})$
$\lvert\lambda^{(ce)}(\lambda^{(c\mu)})^*\rvert$	$\lesssim 9 \times 10^{-3}$	
$\lvert\lambda^{(ue)}(\lambda^{(u\mu)})^*\rvert$	$\lesssim 1 \times 10^{-2}$	$\mu^- \to e^- e^+ e^-$

$\lvert\lambda^{(ce)}(\lambda^{(c\mu)})^*\rvert$	$\lesssim 6\times10^{-3}$	
$\mathrm{Re}[\lambda^{(ue)}(\lambda^{(ce)})^*]$	$\sim[-1,0]$	$D^+\to\mu^+\nu_\mu$
$\mathrm{Im}[\lambda^{(u\mu)}(\lambda^{(c\mu)})^*]$	~ 0.0	

Table G.2.: Constraints on scalar $SU(2)$ triplet LQs scaling as $\frac{\mathrm{TeV}}{M}$ and $\sqrt{\frac{\mathrm{TeV}}{M}}$ for Δm_{D^0}. Here $q\in\{u,c\}$ and $l\in\{e,\mu\}$.

couplings/mass	constraint	observable
$\lvert\lambda^{(ue)}_{\tilde{V}_1}\rvert$	~ 0.0	Q_w (Cs)
$\lvert\lambda^{(ue)}_{\tilde{V}_2,V_3}\rvert$	$\sim[0.0,0.2]$	
$\lvert\lambda^{(ue)}_{V_3}\rvert$	$\sim[0.00,0.06]$	V_{ud}
$\lvert\lambda^{(u\tau)}_{V_3}\rvert$	$\sim[0.0,0.4]$	$\tau^-\to\pi^-\nu_\tau$
$\lvert\lambda^{(c\tau)}_{V_3}\rvert$	$\sim[0.0,0.2]$	$D_s\to\tau^+\nu_\tau$
$\mathrm{Re}[\lambda^{(ue)}_{V_3}(\lambda^{(ce)}_{V_3})^*]$	$\sim[0.0,0.2]$	$K^+\to e^+\nu_e$
$\lvert\lambda^{(ue)}(\lambda^{(ce)})^*\rvert$	$\lesssim 6\times10^{-2}$	$D^+\to\pi^+e^+e^-$
$\lvert\lambda^{(ue)}(\lambda^{(c\mu)})^*\rvert$	$\lesssim 1\times10^{-1}$	$D^+\to\pi^+e^+\mu^-$
$\lvert\lambda^{(u\mu)}(\lambda^{(ce)})^*\rvert$	$\lesssim 1\times10^{-1}$	$D^+\to\pi^+e^-\mu^+$
$\lvert\lambda^{(u\mu)}_{V_3}(\lambda^{(ce)}_{V_3})^*\rvert$	$\lesssim 5\times10^{-1}$	$K^+\to\mu^+\nu_e$
$\lvert\lambda^{(u\mu)}(\lambda^{(c\mu)})^*\rvert$	$\lesssim 1\times10^{-2}$	$D^+\to\pi^+\mu^+\mu^-$
$\lvert\lambda^{(u\mu)}(\lambda^{(c\mu)})^*\rvert$	$\lesssim 3\times10^{-2}$	$D^0\to\mu^+\mu^-$
$\mathrm{Re}[\lambda^{(u\mu)}_{V_3}(\lambda^{(c\mu)}_{V_3})^*]$	$\sim[-0.5,-0.1]$	$D^+\to\mu^+\nu_\mu$
$\mathrm{Im}[\lambda^{(u\mu)}_{V_3}(\lambda^{(c\mu)}_{V_3})^*]$	~ 0.0	
$\mathrm{Re}[\lambda^{(u\mu)}_{V_3}(\lambda^{(c\mu)}_{V_3})^*]$	$\sim[-0.08,-0.01]$	$K^+\to\mu^+\nu_\mu$
$\mathrm{Im}[\lambda^{(u\mu)}_{V_3}(\lambda^{(c\mu)}_{V_3})^*]$	$\sim[-1,-0.6]$	
$\lvert\mathrm{Re}[\lambda^{(u\tau)}_{V_2}(\lambda^{(c\tau)}_{V_2})^*]\rvert$	$\sim[0,0.8]$	Δm_{D^0}
$\lvert\mathrm{Re}[\lambda^{(u\tau)}_{V_3}(\lambda^{(c\tau)}_{V_3})^*]\rvert$	$\sim[0,0.4]$	
$\mathrm{Re}[\lambda^{(u\tau)}_{V_3}(\lambda^{(c\tau)}_{V_3})^*]$	$\sim[-0.1,0.1]$	$\tau^-\to K^-\nu_\tau$

$\lvert\mathrm{Im}[\lambda^{(u\tau)}_{V_3}(\lambda^{(c\tau)}_{V_3})^*]\rvert$	$\sim [0.0, 0.9]$	
$\lvert\mathrm{Re}[\lambda^{(u\tau)}_{V_3}(\lambda^{(c\tau)}_{V_3})^*]\rvert$	$\lesssim 0.5$	$D^+ \to \tau^+\nu_\tau$
$(\lvert\lambda^{(ue)}_{V_3}\rvert^2 - \lvert\lambda^{(u\mu)}_{V_3}\rvert^2)^{1/2}$	$\sim [0.0, 0.3]$	$R_{e/\mu}$
$\lvert\lambda^{(ue)}(\lambda^{(c\mu)})^* + \lambda^{(u\mu)}(\lambda^{(ce)})^*\rvert$	$\lesssim 9 \times 10^{-2}$	$D^0 \to \mu^\pm e^\mp$
$\lvert\lambda^{(qe)}(\lambda^{(q\mu)})^*\rvert$	$\lesssim 1 \times 10^{-4}$	$\mu^+ \to e^+\gamma$
$\lvert\lambda^{(ue)}(\lambda^{(u\mu)})^*\rvert$	$\lesssim 7 \times 10^{-7}$	$\mu - e\,(\mathrm{Au})$
$\lvert\lambda^{(ce)}_{\tilde{V}_1,\tilde{V}_2}(\lambda^{(c\mu)}_{\tilde{V}_1,\tilde{V}_2})^*\rvert$	$\lesssim 1 \times 10^{-2}$	
$\lvert\lambda^{(ce)}_{V_2}(\lambda^{(c\mu)}_{V_2})^*\rvert$	$\lesssim 6 \times 10^{-3}$	
$\lvert\lambda^{(ce)}_{V_3}(\lambda^{(c\mu)}_{V_3})^*\rvert$	$\lesssim 7 \times 10^{-3}$	
$\lvert\lambda^{(ue)}(\lambda^{(u\mu)})^*\rvert$	$\lesssim 4 \times 10^{-4}$	$\mu^- \to e^-e^+e^-$
$\lvert\lambda^{(ue)}_{V_3}(\lambda^{(u\mu)}_{V_3})^*\rvert$	$\lesssim 2 \times 10^{-4}$	
$\lvert\lambda^{(ce)}_{\tilde{V}_1,\tilde{V}_2}(\lambda^{(c\mu)}_{\tilde{V}_1,\tilde{V}_2})^*\rvert$	$\lesssim 8 \times 10^{-4}$	
$\lvert\lambda^{(ce)}_{V_2}(\lambda^{(c\mu)}_{V_2})^*\rvert$	$\lesssim 6 \times 10^{-4}$	
$\lvert\lambda^{(ce)}_{V_3}(\lambda^{(c\mu)}_{V_3})^*\rvert$	$\lesssim 3 \times 10^{-4}$	
$\lvert\lambda^{(ql)}_{\tilde{V}_1}(\lambda^{(q\tau)}_{\tilde{V}_1})^*\rvert$	$\lesssim 9 \times 10^{-2}$	$\tau^- \to l^-\gamma$
$\lvert\lambda^{(ql)}_{V_2}(\lambda^{(q\tau)}_{V_2})^*\rvert$	$\lesssim 8 \times 10^{-2}$	
$\lvert\lambda^{(ql)}_{\tilde{V}_2}(\lambda^{(q\tau)}_{\tilde{V}_2})^*\rvert$	$\lesssim 1 \times 10^{-1}$	
$\lvert\lambda^{(ql)}_{V_3}(\lambda^{(q\tau)}_{V_3})^*\rvert$	$\lesssim 4 \times 10^{-2}$	
$\lvert\lambda^{(ul)}_{\tilde{V}_1,\tilde{V}_2}(\lambda^{(u\tau)}_{\tilde{V}_1,\tilde{V}_2})^*\rvert$	$\lesssim 7 \times 10^{-2}$	$\tau^- \to l^-l^+l^-$
$\lvert\lambda^{(ul)}_{V_2}(\lambda^{(u\tau)}_{V_2})^*\rvert$	$\lesssim 6 \times 10^{-2}$	
$\lvert\lambda^{(ul)}_{V_3}(\lambda^{(u\tau)}_{V_3})^*\rvert$	$\lesssim 3 \times 10^{-2}$	
$\lvert\lambda^{(cl)}_{\tilde{V}_1,V_2,\tilde{V}_2}(\lambda^{(c\tau)}_{\tilde{V}_1,V_2,\tilde{V}_2})^*\rvert$	$\lesssim 1 \times 10^{-1}$	
$\lvert\lambda^{(cl)}_{V_3}(\lambda^{(c\tau)}_{V_3})^*\rvert$	$\lesssim 6 \times 10^{-2}$	
$\mathrm{Im}[\lambda^{(ue)}_{V_3}(\lambda^{(ce)}_{V_3})^*]$	~ 0.0	

Table G.3.: Constraints on vector LQs scaling as $\frac{\mathrm{TeV}}{M}$. For V_3 unlabeled constraints are multiplied by $1/2$. Here $q \in \{u, c\}$ and $l \in \{e, \mu\}$.

couplings/mass	constraint	observable
$\lvert\lambda^{(ul')}_{S_1L}(\lambda^{(cl'')}_{S_1L})^*\rvert$	$\lesssim 4\times10^{-4}$	$(K^+\to\pi^+\bar\nu\nu)/(K^+\to\pi^0\bar e\nu_e)$
$\lvert\lambda^{(ue)}_{S_2R}(\lambda^{(ce)}_{S_2R})^*\rvert$	$\lesssim 2\times10^{-3}$	$K^0_L\to\bar e e$
$\lvert\lambda^{(u\mu)}_{S_2R}(\lambda^{(ce)}_{S_2R})^*\rvert$	$\lesssim 1\times10^{-5}$	$K^0_L\to\bar e\mu$
$\lvert\lambda^{(u\mu)}_{S_2R}(\lambda^{(c\mu)}_{S_2R})^*\rvert$	$\lesssim 3\times10^{-4}$	$K^0_L\to\bar\mu\mu$
$\lvert\lambda^{(ul')}_{S_3}(\lambda^{(cl'')}_{S_3})^*\rvert$	$\lesssim 4\times10^{-4}$	$(K^+\to\pi^+\bar\nu\nu)/(K^+\to\pi^0\bar e\nu_e)$
$\lvert\lambda^{(ue)}_{S_3}(\lambda^{(c\mu)}_{S_3})^*\rvert,\ \lvert\lambda^{(u\mu)}_{S_3}(\lambda^{(ce)}_{S_3})^*\rvert$	$\lesssim 5\times10^{-6}$	$K^0_L\to\bar e\mu$
$\lvert\lambda^{(u\mu)}_{S_3}(\lambda^{(c\mu)}_{S_3})^*\rvert$	$\lesssim 2\times10^{-4}$	$K^0_L\to\bar\mu\mu$
$\lvert\lambda^{(ue)}_{V_2}(\lambda^{(ce)}_{V_2})^*\rvert$	$\lesssim 1\times10^{-3}$	$K^0_L\to\bar e e$
$\lvert\lambda^{(ue)}_{V_2}(\lambda^{(c\mu)}_{V_2})^*\rvert,\ \lvert\lambda^{(u\mu)}_{V_2}(\lambda^{(ce)}_{V_2})^*\rvert$	$\lesssim 5\times10^{-6}$	$K^0_L\to\bar e\mu$
$\lvert\lambda^{(u\mu)}_{V_2}(\lambda^{(c\mu)}_{V_2})^*\rvert$	$\lesssim 2\times10^{-4}$	$K^0_L\to\bar\mu\mu$
$\lvert\lambda^{(ul')}_{V_3}(\lambda^{(cl'')}_{V_3})^*\rvert$	$\lesssim 8\times10^{-5}$	$(K^+\to\pi^+\bar\nu\nu)/(K^+\to\pi^0\bar e\nu_e)$
$\lvert\lambda^{(ue)}_{V_3}(\lambda^{(c\mu)}_{V_3})^*\rvert,\ \lvert\lambda^{(u\mu)}_{V_3}(\lambda^{(ce)}_{V_3})^*\rvert$	$\lesssim 3\times10^{-6}$	$K^0_L\to\bar e\mu$
$\lvert\lambda^{(u\mu)}_{V_3}(\lambda^{(c\mu)}_{V_3})^*\rvert$	$\lesssim 7\times10^{-5}$	$K^0_L\to\bar\mu\mu$
$\lvert\lambda^{(ue)}_{S_2L,S_2R}(\lambda^{(u\tau)}_{S_2L,S_2R})^*\rvert$	$\lesssim 3\times10^{-2}$	$(\tau^-\to\pi^0e^-)/(\tau^-\to\pi^-\nu_\tau)$
$\lvert\lambda^{(u\mu)}_{S_2L,S_2R}(\lambda^{(u\tau)}_{S_2L,S_2R})^*\rvert$	$\lesssim 5\times10^{-3}$	$(\tau^-\to\pi^0\mu^-)/(\tau^-\to\pi^-\nu_\tau)$
$\lvert\lambda^{(ul)}_{S_2L,S_2R}(\lambda^{(c\tau)}_{S_2L,S_2R})^*\rvert$	$\lesssim 2\times10^{-2}$	$(\tau\to lK)/(\tau\to\nu K)$
$\lvert\lambda^{(ue)}_{S_3}(\lambda^{(u\tau)}_{S_3})^*\rvert$	$\lesssim 2\times10^{-2}$	$(\tau^-\to\pi^0e^-)/(\tau^-\to\pi^-\nu_\tau)$
$\lvert\lambda^{(u\mu)}_{S_3}(\lambda^{(u\tau)}_{S_3})^*\rvert$	$\lesssim 3\times10^{-3}$	$(\tau^-\to\pi^0\mu^-)/(\tau^-\to\pi^-\nu_\tau)$
$\lvert\lambda^{(ue)}_{V_2}(\lambda^{(u\tau)}_{V_2})^*\rvert$	$\lesssim 2\times10^{-2}$	$(\tau^-\to\pi^0e^-)/(\tau^-\to\pi^-\nu_\tau)$
$\lvert\lambda^{(u\mu)}_{V_2}(\lambda^{(u\tau)}_{V_2})^*\rvert$	$\lesssim 3\times10^{-3}$	$(\tau^-\to\pi^0\mu^-)/(\tau^-\to\pi^-\nu_\tau)$
$\lvert\lambda^{(ul)}_{V_2}(\lambda^{(c\tau)}_{V_2})^*\rvert$	$\lesssim 9\times10^{-3}$	$(\tau\to lK)/(\tau\to\nu K)$
$\lvert\lambda^{(ue)}_{V_3}(\lambda^{(u\tau)}_{V_3})^*\rvert$	$\lesssim 7\times10^{-3}$	$(\tau^-\to\pi^0e^-)/(\tau^-\to\pi^-\nu_\tau)$
$\lvert\lambda^{(u\mu)}_{V_3}(\lambda^{(u\tau)}_{V_3})^*\rvert$	$\lesssim 2\times10^{-3}$	$(\tau^-\to\pi^0\mu^-)/(\tau^-\to\pi^-\nu_\tau)$

Table G.4.: Constraints on LQs due to kaon and $\tau\to\pi l$ decays scaling as $\frac{\text{TeV}}{M}$. Here $l\in\{e,\mu\}$ and $l',l''\in\{e,\mu,\tau\}$.

Bibliography

[1] Stefan de Boer and Gudrun Hiller. "Flavor and new physics opportunities with rare charm decays into leptons". In: *Phys. Rev.* D93.7 (2016), p. 074001. DOI: 10.1103/PhysRevD.93.074001. arXiv: 1510.00311 [hep-ph].

[2] Stefan de Boer, Bastian Müller, and Dirk Seidel. "Higher-order Wilson coefficients for $c \to u$ transitions in the standard model". In: *JHEP* 08 (2016), p. 091. DOI: 10.1007/JHEP08(2016)091. arXiv: 1606.05521 [hep-ph].

[3] Stefan de Boer and Gudrun Hiller. "Rare radiative charm decays within the standard model and beyond". In: (2017). arXiv: 1701.06392 [hep-ph].

[4] Stefan de Boer. "Two loop virtual corrections to $b \to (d,s)\ell^+\ell^-$ and $c \to u\ell^+\ell^-$ for arbitrary momentum transfer". In: (2017). arXiv: 1707.00988 [hep-ph].

[5] Stefan de Boer. "Rare Semileptonic Charm Decays". In: *7th International Workshop on Charm Physics (Charm 2015) Detroit, MI, USA, May 18-22, 2015*. 2015. arXiv: 1510.00496 [hep-ph]. URL: http://inspirehep.net/record/1395977/files/arXiv:1510.00496.pdf.

[6] Stefan de Boer. "Opportunities with (semi)leptonic rare charm decays". In: *Proceedings, 51st Rencontres de Moriond on Electroweak Interactions and Unified Theories: La Thuile, Italy, March 12-19, 2016*. 2016, pp. 569–572. arXiv: 1605.03415 [hep-ph]. URL: http://inspirehep.net/record/1457615/files/arXiv:1605.03415.pdf.

[7] Georges Aad et al. "Observation of a new particle in the search for the Standard Model Higgs boson with the ATLAS detector at the LHC". In: *Phys. Lett.* B716 (2012), pp. 1–29. DOI: 10.1016/j.physletb.2012.08.020. arXiv: 1207.7214 [hep-ex].

[8] Serguei Chatrchyan et al. "Observation of a new boson at a mass of 125 GeV with the CMS experiment at the LHC". In: *Phys. Lett.* B716 (2012), pp. 30–61. DOI: 10.1016/j.physletb.2012.08.021. arXiv: 1207.7235 [hep-ex].

[9] Philip W. Anderson. "Plasmons, Gauge Invariance, and Mass". In: *Phys. Rev.* 130 (1963), pp. 439–442. DOI: 10.1103/PhysRev.130.439.

[10] Peter W. Higgs. "Broken Symmetries and the Masses of Gauge Bosons". In: *Phys. Rev. Lett.* 13 (1964), pp. 508–509. DOI: 10.1103/PhysRevLett.13.508.

[11] F. Englert and R. Brout. "Broken Symmetry and the Mass of Gauge Vector Mesons". In: *Phys. Rev. Lett.* 13 (1964), pp. 321–323. DOI: 10.1103/PhysRevLett.13.321.

[12] G. S. Guralnik, C. R. Hagen, and T. W. B. Kibble. "Global Conservation Laws and Massless Particles". In: *Phys. Rev. Lett.* 13 (1964), pp. 585–587. DOI: 10.1103/PhysRevLett.13.585.

[13] J. D. Bjorken and S. L. Glashow. "Elementary Particles and SU(4)". In: *Phys. Lett.* 11 (1964), pp. 255–257. DOI: 10.1016/0031-9163(64)90433-0.

[14] J. J. Aubert et al. "Experimental Observation of a Heavy Particle J". In: *Phys. Rev. Lett.* 33 (1974), pp. 1404–1406. DOI: 10.1103/PhysRevLett.33.1404.

[15] J. E. Augustin et al. "Discovery of a Narrow Resonance in e^+e^- Annihilation". In: *Phys. Rev. Lett.* 33 (1974). [Adv. Exp. Phys.5,141(1976)], pp. 1406–1408. DOI: 10.1103/PhysRevLett.33.1406.

[16] Y. Fukuda et al. "Evidence for oscillation of atmospheric neutrinos". In: *Phys. Rev. Lett.* 81 (1998), pp. 1562–1567. DOI: 10.1103/PhysRevLett.81.1562. arXiv: hep-ex/9807003 [hep-ex].

[17] Q. R. Ahmad et al. "Measurement of the rate of $\nu_e + d \to p + p + e^-$ interactions produced by ^8B solar neutrinos at the Sudbury Neutrino Observatory". In: *Phys. Rev. Lett.* 87 (2001), p. 071301. DOI: 10.1103/PhysRevLett.87.071301. arXiv: nucl-ex/0106015 [nucl-ex].

[18] F. Zwicky. "Die Rotverschiebung von extragalaktischen Nebeln". In: *Helv. Phys. Acta* 6 (1933). [Gen. Rel. Grav.41,207(2009)], pp. 110–127. DOI: 10.1007/s10714-008-0707-4.

[19] A. D. Sakharov. "Violation of CP Invariance, c Asymmetry, and Baryon Asymmetry of the Universe". In: *Pisma Zh. Eksp. Teor. Fiz.* 5 (1967). [Usp. Fiz. Nauk161,61(1991)], pp. 32–35. DOI: 10.1070/PU1991v034n05ABEH002497.

[20] Thomas Blum et al. "The Muon (g-2) Theory Value: Present and Future". In: (2013). arXiv: 1311.2198 [hep-ph].

[21] C. Patrignani et al. "Review of Particle Physics". In: *Chin. Phys.* C40.10 (2016), p. 100001. DOI: 10.1088/1674-1137/40/10/100001.

[22] T. Blake et al. "Round table: Flavour anomalies in b $\to$ sl+l processes". In: *EPJ Web Conf.* 137 (2017), p. 01001. DOI: 10.1051/epjconf/201713701001. arXiv: 1703.10005 [hep-ph].

[23] R. Aaij et al. "Test of lepton universality with $B^0 \to K^{*0}\ell^+\ell^-$ decays". In: (2017). arXiv: 1705.05802 [hep-ex].

[24] A. Abdesselam et al. "Observation of $D^0 \to \rho^0\gamma$ and search for CP violation in radiative charm decays". In: *Phys. Rev. Lett.* 118.5 (2017), p. 051801. DOI: 10.1103/PhysRevLett.118.051801. arXiv: 1603.03257 [hep-ex].

[25] Roel Aaij et al. "Search for the lepton-flavour violating decay $D^0 \to e^{\pm}\mu^{\mp}$". In: *Phys. Lett.* B754 (2016), pp. 167–175. DOI: 10.1016/j.physletb.2016.01.029. arXiv: 1512.00322 [hep-ex].

[26] M. Staric et al. "Evidence for D^0 - $\bar{D}^0$ Mixing". In: *Phys. Rev. Lett.* 98 (2007), p. 211803. DOI: 10.1103/PhysRevLett.98.211803. arXiv: hep-ex/0703036 [hep-ex].

[27] Bernard Aubert et al. "Evidence for $D^0 - \overline{D}^0$ Mixing". In: *Phys. Rev. Lett.* 98 (2007), p. 211802. DOI: 10.1103/PhysRevLett.98.211802. arXiv: hep-ex/0703020 [HEP-EX].

[28] T. Aaltonen et al. "Evidence for $D^0 - \bar{D}^0$ mixing using the CDF II Detector". In: *Phys. Rev. Lett.* 100 (2008), p. 121802. DOI: 10.1103/PhysRevLett.100.121802. arXiv: 0712.1567 [hep-ex].

[29] R Aaij et al. "Measurement of $D^0 - \bar{D}^0$ Mixing Parameters and Search for CP Violation Using $D^0 \to K^+\pi^-$ Decays". In: *Phys. Rev. Lett.* 111.25 (2013), p. 251801. DOI: 10.1103/PhysRevLett.111.251801. arXiv: 1309.6534 [hep-ex].

[30] Richard J. Hill. "Update on semileptonic charm decays". In: *eConf* C070805 (2007), p. 22. DOI: 10.2172/922051. arXiv: 0712.3817 [hep-ph].

[31] J. A. Aguilar-Saavedra. "Top flavor-changing neutral interactions: Theoretical expectations and experimental detection". In: *Acta Phys. Polon.* B35 (2004), pp. 2695–2710. arXiv: hep-ph/0409342 [hep-ph].

[32] Alexander Lenz. "Constraints on a fourth generation of fermions from Higgs Boson searches". In: *Adv. High Energy Phys.* 2013 (2013), p. 910275. DOI: 10.1155/2013/910275.

[33] Kenneth G. Wilson. "Nonlagrangian models of current algebra". In: *Phys. Rev.* 179 (1969), pp. 1499–1512. DOI: 10.1103/PhysRev.179.1499.

[34] Matthias Neubert. "Effective field theory and heavy quark physics". In: *Physics in D >= 4. Proceedings, Theoretical Advanced Study Institute in elementary particle physics, TASI 2004, Boulder, USA, June 6-July 2, 2004*. 2005, pp. 149–194. arXiv: hep-ph/0512222 [hep-ph].

[35] Chen-Ning Yang and Robert L. Mills. "Conservation of Isotopic Spin and Isotopic Gauge Invariance". In: *Phys. Rev.* 96 (1954), pp. 191–195. DOI: 10.1103/PhysRev.96.191.

[36] Gerard 't Hooft and M. J. G. Veltman. "Regularization and Renormalization of Gauge Fields". In: *Nucl. Phys.* B44 (1972), pp. 189–213. DOI: 10.1016/0550-3213(72)90279-9.

[37] H. David Politzer. "Reliable Perturbative Results for Strong Interactions?" In: *Phys. Rev. Lett.* 30 (1973), pp. 1346–1349. DOI: 10.1103/PhysRevLett.30.1346.

[38] David J. Gross and Frank Wilczek. "Ultraviolet Behavior of Nonabelian Gauge Theories". In: *Phys. Rev. Lett.* 30 (1973), pp. 1343–1346. DOI: 10.1103/PhysRevLett.30.1343.

[39] S. L. Glashow. "Partial Symmetries of Weak Interactions". In: *Nucl. Phys.* 22 (1961), pp. 579–588. DOI: 10.1016/0029-5582(61)90469-2.

[40] Steven Weinberg. "A Model of Leptons". In: *Phys. Rev. Lett.* 19 (1967), pp. 1264–1266. DOI: 10.1103/PhysRevLett.19.1264.

[41] Norman Dombey. "Abdus Salam: A Reappraisal. PART I. How to Win the Nobel Prize". In: (2011). arXiv: 1109.1972 [physics.hist-ph].

[42] Nicola Cabibbo. "Unitary Symmetry and Leptonic Decays". In: *Phys. Rev. Lett.* 10 (1963). [,648(1963)], pp. 531–533. DOI: 10.1103/PhysRevLett.10.531.

[43] Makoto Kobayashi and Toshihide Maskawa. "CP Violation in the Renormalizable Theory of Weak Interaction". In: *Prog. Theor. Phys.* 49 (1973), pp. 652–657. DOI: 10.1143/PTP.49.652.

[44] S. L. Glashow, J. Iliopoulos, and L. Maiani. "Weak Interactions with Lepton-Hadron Symmetry". In: *Phys. Rev.* D2 (1970), pp. 1285–1292. DOI: 10.1103/PhysRevD.2.1285.

[45] UTfit Collaboration. http://www.utfit.org/UTfit/.

[46] Lincoln Wolfenstein. "Parametrization of the Kobayashi-Maskawa Matrix". In: *Phys. Rev. Lett.* 51 (1983), p. 1945. DOI: 10.1103/PhysRevLett.51.1945.

[47] Christoph Greub et al. "The c —> u gamma contribution to weak radiative charm decay". In: *Phys. Lett.* B382 (1996), pp. 415–420. DOI: 10.1016/0370-2693(96)00694-6. arXiv: hep-ph/9603417 [hep-ph].

[48] S. Fajfer, P. Singer, and J. Zupan. "The Radiative leptonic decays D0 —> e+ e- gamma, mu+ mu- gamma in the standard model and beyond". In: *Eur. Phys. J.* C27 (2003), pp. 201–218. DOI: 10.1140/epjc/s2002-01090-5. arXiv: hep-ph/0209250 [hep-ph].

[49] John C. Collins. "The Problem of scales: Renormalization and all that". In: *QCD and beyond. Proceedings, Theoretical Advanced Study Institute in Elementary Particle Physics, TASI-95, Boulder, USA, June 4-30, 1995*. 1995, pp. 269–326. arXiv: hep-ph/9510276 [hep-ph].

[50] Konstantin G. Chetyrkin, Mikolaj Misiak, and Manfred Munz. "Weak radiative B meson decay beyond leading logarithms". In: *Phys. Lett.* B400 (1997). [Erratum: Phys. Lett.B425,414(1998)], pp. 206–219. DOI: 10.1016/S0370-2693(97)00324-9. arXiv: hep-ph/9612313 [hep-ph].

[51] Christoph Bobeth, Mikolaj Misiak, and Jorg Urban. "Photonic penguins at two loops and m_t dependence of $BR[B \to X_s l^+ l^-]$". In: *Nucl. Phys.* B574 (2000), pp. 291–330. DOI: 10.1016/S0550-3213(00)00007-9. arXiv: hep-ph/9910220 [hep-ph].

[52] Paolo Gambino, Martin Gorbahn, and Ulrich Haisch. "Anomalous dimension matrix for radiative and rare semileptonic B decays up to three loops". In: *Nucl. Phys.* B673 (2003), pp. 238–262. DOI: 10.1016/j.nuclphysb.2003.09.024. arXiv: hep-ph/0306079 [hep-ph].

[53] B. Grzadkowski et al. "Dimension-Six Terms in the Standard Model Lagrangian". In: *JHEP* 10 (2010), p. 085. DOI: 10.1007/JHEP10(2010)085. arXiv: 1008.4884 [hep-ph].

[54] S. A. Larin. "The Renormalization of the axial anomaly in dimensional regularization". In: *Phys. Lett.* B303 (1993), pp. 113–118. DOI: 10.1016/0370-2693(93)90053-K. arXiv: hep-ph/9302240 [hep-ph].

[55] Martin Gorbahn and Ulrich Haisch. "Effective Hamiltonian for non-leptonic $|\Delta F| = 1$ decays at NNLO in QCD". In: *Nucl. Phys.* B713 (2005), pp. 291–332. DOI: 10.1016/j.nuclphysb.2005.01.047. arXiv: hep-ph/0411071 [hep-ph].

[56] Andrzej J. Buras and Manfred Munz. "Effective Hamiltonian for B —> X(s) e+ e- beyond leading logarithms in the NDR and HV schemes". In: *Phys. Rev.* D52 (1995), pp. 186–195. DOI: 10.1103/PhysRevD.52.186. arXiv: hep-ph/9501281 [hep-ph].

[57] Konstantin G. Chetyrkin, Mikolaj Misiak, and Manfred Munz. "$|\Delta F| = 1$ nonleptonic effective Hamiltonian in a simpler scheme". In: *Nucl. Phys.* B520 (1998), pp. 279–297. DOI: 10.1016/S0550-3213(98)00131-X. arXiv: hep-ph/9711280 [hep-ph].

[58] Gustavo Burdman et al. "Rare charm decays in the standard model and beyond". In: *Phys. Rev.* D66 (2002), p. 014009. DOI: 10.1103/PhysRevD.66.014009. arXiv: hep-ph/0112235 [hep-ph].

[59] Ayan Paul, Ikaros I. Bigi, and Stefan Recksiegel. "On $D \to X_u l^+ l^-$ within the Standard Model and Frameworks like the Littlest Higgs Model with T Parity". In: *Phys. Rev.* D83 (2011), p. 114006. DOI: 10.1103/PhysRevD.83.114006. arXiv: 1101.6053 [hep-ph].

[60] Ru-Min Wang et al. "Decays $D^+_{(s)} \to \pi(K)^+\ell^+\ell^-$ and $D^0 \to \ell^+\ell^-$ in the MSSM with and without R-parity". In: *Int. J. Mod. Phys.* A30.12 (2015), p. 1550063. DOI: 10.1142/S0217751X15500633. arXiv: 1409.0181 [hep-ph].

[61] T. Inami and C. S. Lim. "Effects of Superheavy Quarks and Leptons in Low-Energy Weak Processes k(L) —> mu anti-mu, K+ —> pi+ Neutrino anti-neutrino and K0 <—> anti-K0". In: *Prog. Theor. Phys.* 65 (1981). [Erratum: Prog. Theor. Phys.65,1772(1981)], p. 297. DOI: 10.1143/PTP.65.297.

[62] Q. Ho-Kim and Xuan-Yem Pham. "One loop flavor changing electromagnetic transitions". In: *Phys. Rev.* D61 (2000), p. 013008. DOI: 10.1103/PhysRevD.61.013008. arXiv: hep-ph/9906235 [hep-ph].

[63] K. G. Chetyrkin and F. V. Tkachov. "Integration by Parts: The Algorithm to Calculate beta Functions in 4 Loops". In: *Nucl. Phys.* B192 (1981), pp. 159–204. DOI: 10.1016/0550-3213(81)90199-1.

[64] Andrzej J. Buras et al. "Effective Hamiltonians for $\Delta S = 1$ and $\Delta B = 1$ nonleptonic decays beyond the leading logarithmic approximation". In: *Nucl. Phys.* B370 (1992). [Addendum: Nucl. Phys.B375,501(1992)], pp. 69–104. DOI: 10.1016/0550-3213(92)90345-C.

[65] Andrzej J. Buras et al. "Direct CP violation in K(L) —> pi0 e+ e- beyond leading logarithms". In: *Nucl. Phys.* B423 (1994), pp. 349–383. DOI: 10.1016/0550-3213(94)90138-4. arXiv: hep-ph/9402347 [hep-ph].

[66] Joachim Brod and Martin Gorbahn. "ϵ_K at Next-to-Next-to-Leading Order: The Charm-Top-Quark Contribution". In: *Phys. Rev.* D82 (2010), p. 094026. DOI: 10.1103/PhysRevD.82.094026. arXiv: 1007.0684 [hep-ph].

[67] K. G. Chetyrkin, Johann H. Kuhn, and M. Steinhauser. "RunDec: A Mathematica package for running and decoupling of the strong coupling and quark masses". In: *Comput. Phys. Commun.* 133 (2000), pp. 43–65. DOI: 10.1016/S0010-4655(00)00155-7. arXiv: hep-ph/0004189 [hep-ph].

[68] Mikolaj Misiak. "The $b \to se^+e^-$ and $b \to s\gamma$ decays with next-to-leading logarithmic QCD corrections". In: *Nucl. Phys.* B393 (1993). [Erratum: Nucl. Phys.B439,461(1995)], pp. 23–45. DOI: 10.1016/0550-3213(95)00029-R, 10.1016/0550-3213(93)90235-H.

[69] S. Fajfer, Sasa Prelovsek, and P. Singer. "Resonant and nonresonant contributions to the weak D —> V lepton+ lepton- decays". In: *Phys. Rev.* D58 (1998), p. 094038. DOI: 10.1103/PhysRevD.58.094038. arXiv: hep-ph/9805461 [hep-ph].

[70] S. Fajfer, Sasa Prelovsek, and P. Singer. "Rare charm meson decays D —> P lepton+ lepton- and c —> u lepton+ lepton- in SM and MSSM". In: *Phys. Rev.* D64 (2001), p. 114009. DOI: 10.1103/PhysRevD.64.114009. arXiv: hep-ph/0106333 [hep-ph].

[71] Marco Ciuchini et al. "Scheme independence of the effective Hamiltonian for b —> s gamma and b —> s g decays". In: *Phys. Lett.* B316 (1993), pp. 127–136. DOI: 10.1016/0370-2693(93)90668-8. arXiv: hep-ph/9307364 [hep-ph].

[72] Christoph Greub, Volker Pilipp, and Christof Schupbach. "Analytic calculation of two-loop QCD corrections to $b \to sl^+l^-$ in the high q^2 region". In: *JHEP* 12 (2008), p. 040. DOI: 10.1088/1126-6708/2008/12/040. arXiv: 0810.4077 [hep-ph].

[73] Christoph Greub, Tobias Hurth, and Daniel Wyler. "Virtual O (alpha-s) corrections to the inclusive decay b —> s gamma". In: *Phys. Rev.* D54 (1996), pp. 3350–3364. DOI: 10.1103/PhysRevD.54.3350. arXiv: hep-ph/9603404 [hep-ph].

[74] Andrzej J. Buras et al. "Completing the NLO QCD calculation of anti-B —> X(s gamma)". In: *Nucl. Phys.* B631 (2002), pp. 219–238. DOI: 10.1016/S0550-3213(02)00261-4. arXiv: hep-ph/0203135 [hep-ph].

[75] Guido Bell and Tobias Huber. "Master integrals for the two-loop penguin contribution in non-leptonic B-decays". In: *JHEP* 12 (2014), p. 129. DOI: 10.1007/JHEP12(2014)129. arXiv: 1410.2804 [hep-ph].

[76] Hjalte Frellesvig, Damiano Tommasini, and Christopher Wever. "On the reduction of generalized polylogarithms to Li_n and $\mathrm{Li}_{2,2}$ and on the evaluation thereof". In: *JHEP* 03 (2016), p. 189. DOI: 10.1007/JHEP03(2016)189. arXiv: 1601.02649 [hep-ph].

[77] H. H. Asatryan et al. "Calculation of two loop virtual corrections to $b \to sl^+l^-$ in the standard model". In: *Phys. Rev.* D65 (2002), p. 074004. DOI: 10.1103/PhysRevD.65.074004. arXiv: hep-ph/0109140 [hep-ph].

[78] H. M. Asatrian et al. "Virtual corrections and bremsstrahlung corrections to b —> d l+ l- in the standard model". In: *Phys. Rev.* D69 (2004), p. 074007. DOI: 10.1103/PhysRevD.69.074007. arXiv: hep-ph/0312063 [hep-ph].

[79] A. Ghinculov et al. "The Rare decay $B \to X_s l^+ l^-$ to NNLL precision for arbitrary dilepton invariant mass". In: *Nucl. Phys.* B685 (2004), pp. 351–392. DOI: 10.1016/j.nuclphysb.2004.02.028. arXiv: hep-ph/0312128 [hep-ph].

[80] Dirk Seidel. "Analytic two loop virtual corrections to b —> d l+ l-". In: *Phys. Rev.* D70 (2004), p. 094038. DOI: 10.1103/PhysRevD.70.094038. arXiv: hep-ph/0403185 [hep-ph].

[81] J. Kuipers et al. "FORM version 4.0". In: *Comput. Phys. Commun.* 184 (2013), pp. 1453–1467. DOI: 10.1016/j.cpc.2012.12.028. arXiv: 1203.6543 [cs.SC].

[82] A. von Manteuffel and C. Studerus. "Reduze 2 - Distributed Feynman Integral Reduction". In: (2012). arXiv: 1201.4330 [hep-ph].

[83] S. Laporta. "High precision calculation of multiloop Feynman integrals by difference equations". In: *Int. J. Mod. Phys.* A15 (2000), pp. 5087–5159. DOI: 10.1016/S0217-751X(00)00215-7,10.1142/S0217751X00002157. arXiv: hep-ph/0102033 [hep-ph].

[84] T. Gehrmann and E. Remiddi. "Differential equations for two loop four point functions". In: *Nucl. Phys.* B580 (2000), pp. 485–518. DOI: 10.1016/S0550-3213(00)00223-6. arXiv: hep-ph/9912329 [hep-ph].

[85] R. N. Lee. "Group structure of the integration-by-part identities and its application to the reduction of multiloop integrals". In: *JHEP* 07 (2008), p. 031. DOI: 10.1088/1126-6708/2008/07/031. arXiv: 0804.3008 [hep-ph].

[86] Jens Vollinga and Stefan Weinzierl. "Numerical evaluation of multiple polylogarithms". In: *Comput. Phys. Commun.* 167 (2005), p. 177. DOI: 10.1016/j.cpc.2004.12.009. arXiv: hep-ph/0410259 [hep-ph].

[87] Sebastian Kirchner. "LiSK - A C++ Library for Evaluating Classical Polylogarithms and Li_{22}". In: (2016). arXiv: 1605.09571 [hep-ph].

[88] Tobias Huber et al. "Electromagnetic logarithms in $\bar{B} \to X_s l^+ l^-$". In: *Nucl. Phys.* B740 (2006), pp. 105–137. DOI: 10.1016/j.nuclphysb.2006.01.037. arXiv: hep-ph/0512066 [hep-ph].

[89] Christoph Bobeth et al. "Complete NNLO QCD analysis of anti-B —> X(s) l+ l- and higher order electroweak effects". In: *JHEP* 04 (2004), p. 071. DOI: 10.1088/1126-6708/2004/04/071. arXiv: hep-ph/0312090 [hep-ph].

[90] E. Bagan, J. I. Latorre, and P. Pascual. "Heavy and Heavy to Light Quark Expansions". In: *Z. Phys.* C32 (1986), p. 43. DOI: 10.1007/BF01441349.

[91] Matthias Jamin and Manfred Munz. "Current correlators to all orders in the quark masses". In: *Z. Phys.* C60 (1993), pp. 569–578. DOI: 10.1007/BF01560056. arXiv: hep-ph/9208201 [hep-ph].

[92] Gunnar S. Bali and Antonio Pineda. "Phenomenology of renormalons and the OPE from lattice regularization: the gluon condensate and the heavy quark pole mass". In: *AIP Conf. Proc.* 1701 (2016), p. 030010. DOI: 10.1063/1.4938616. arXiv: 1502.00086 [hep-ph].

[93] Ting-Wai Chiu and Tung-Han Hsieh. "Light quark masses, chiral condensate and quark gluon condensate in quenched lattice QCD with exact chiral symmetry". In: *Nucl. Phys.* B673 (2003), pp. 217–237. DOI: 10.1016/j.nuclphysb.2003.09.035. arXiv: hep-lat/0305016 [hep-lat].

[94] C. McNeile et al. "Direct determination of the strange and light quark condensates from full lattice QCD". In: *Phys. Rev.* D87.3 (2013), p. 034503. DOI: 10.1103/PhysRevD.87.034503. arXiv: 1211.6577 [hep-lat].

[95] C. A. Dominguez, L. A. Hernandez, and K. Schilcher. "Determination of the gluon condensate from data in the charm-quark region". In: *JHEP* 07 (2015), p. 110. DOI: 10.1007/JHEP07(2015)110. arXiv: 1411.4500 [hep-ph].

[96] Christoph Bobeth, Gudrun Hiller, and Giorgi Piranishvili. "Angular distributions of $\bar{B} \to \bar{K}\ell^+\ell^-$ decays". In: *JHEP* 12 (2007), p. 040. DOI: 10.1088/1126-6708/2007/12/040. arXiv: 0709.4174 [hep-ph].

[97] Y. Amhis et al. "Averages of b-hadron, c-hadron, and τ-lepton properties as of summer 2016". In: (2016). arXiv: 1612.07233 [hep-ex].

[98] H. M. Asatrian and C. Greub. "Tree-level contribution to $\bar{B} \to X_d\gamma$ using fragmentation functions". In: *Phys. Rev.* D88.7 (2013), p. 074014. DOI: 10.1103/PhysRevD.88.074014. arXiv: 1305.6464 [hep-ph].

[99] Mikolaj Misiak and Michal Poradzinski. "Completing the Calculation of BLM corrections to $\bar{B} \to X_s\gamma$". In: *Phys. Rev.* D83 (2011), p. 014024. DOI: 10.1103/PhysRevD.83.014024. arXiv: 1009.5685 [hep-ph].

[100] Tobias Hurth and Mikihiko Nakao. "Radiative and Electroweak Penguin Decays of B Mesons". In: *Ann. Rev. Nucl. Part. Sci.* 60 (2010), pp. 645–677. DOI: 10.1146/annurev.nucl.012809.104424. arXiv: 1005.1224 [hep-ph].

[101] Thomas Mannel, Sascha Turczyk, and Nikolai Uraltsev. "Higher Order Power Corrections in Inclusive B Decays". In: *JHEP* 11 (2010), p. 109. DOI: 10.1007/JHEP11(2010)109. arXiv: 1009.4622 [hep-ph].

[102] Seung J. Lee, Matthias Neubert, and Gil Paz. "Enhanced Non-local Power Corrections to the anti-B —> X(s) gamma Decay Rate". In: *Phys. Rev.* D75 (2007), p. 114005. DOI: 10.1103/PhysRevD.75.114005. arXiv: hep-ph/0609224 [hep-ph].

[103] Gerhard Buchalla and Gino Isidori. "Nonperturbative effects in $\bar{B} \to X_s l^+ l^-$ for large dilepton invariant mass". In: *Nucl. Phys.* B525 (1998), pp. 333–349. DOI: 10.1016/S0550-3213(98)00261-2. arXiv: hep-ph/9801456 [hep-ph].

[104] Alexander Lenz and Thomas Rauh. "D-meson lifetimes within the heavy quark expansion". In: *Phys. Rev.* D88 (2013), p. 034004. DOI: 10.1103/PhysRevD.88.034004. arXiv: 1305.3588 [hep-ph].

[105] Alexander Lenz and Markus Bobrowski. "Standard Model Predictions for D^0-oscillations and CP-violation". In: *Int. J. Mod. Phys. Conf. Ser.* 02 (2011), pp. 117–121. DOI: 10.1142/S2010194511000651. arXiv: 1011.5608 [hep-ph].

[106] F. Kruger and L. M. Sehgal. "Lepton polarization in the decays b —> X(s) mu+ mu- and B —> X(s) tau+ tau-". In: *Phys. Lett.* B380 (1996), pp. 199–204. DOI: 10.1016/0370-2693(96)00413-3. arXiv: hep-ph/9603237 [hep-ph].

[107] M. Beneke et al. "Penguins with Charm and Quark-Hadron Duality". In: *Eur. Phys. J.* C61 (2009), pp. 439–449. DOI: 10.1140/epjc/s10052-009-1028-9. arXiv: 0902.4446 [hep-ph].

[108] Ahmed Ali and G. Hiller. "Perturbative QCD corrected and power corrected hadron spectra and spectral moments in the decay B —> X(s) lepton+ lepton-". In: *Phys. Rev.* D58 (1998), p. 074001. DOI: 10.1103/PhysRevD.58.074001. arXiv: hep-ph/9803428 [hep-ph].

[109] Keith S. M. Lee and Frank J. Tackmann. "Nonperturbative m_X cut effects in $B \to X_s l^+ l^-$ observables". In: *Phys. Rev.* D79 (2009), p. 114021. DOI: 10.1103/PhysRevD.79.114021. arXiv: 0812.0001 [hep-ph].

[110] Svjetlana Fajfer and Sasa Prelovsek. "Effects of littlest Higgs model in rare D meson decays". In: *Phys. Rev.* D73 (2006), p. 054026. DOI: 10.1103/PhysRevD.73.054026. arXiv: hep-ph/0511048 [hep-ph].

[111] Svjetlana Fajfer and Sasa Prelovsek. "Search for new physics in rare D decays". In: *Conf. Proc.* C060726 (2006). [,811(2006)], pp. 811–814. arXiv: hep-ph/0610032 [hep-ph].

[112] Howard Georgi. "An Effective Field Theory for Heavy Quarks at Low-energies". In: *Phys. Lett.* B240 (1990), pp. 447–450. DOI: 10.1016/0370-2693(90)91128-X.

[113] Nathan Isgur and Mark B. Wise. "Relationship Between Form-factors in Semileptonic $\bar{B}$ and D Decays and Exclusive Rare $\bar{B}$ Meson Decays". In: *Phys. Rev.* D42 (1990), pp. 2388–2391. DOI: 10.1103/PhysRevD.42.2388.

[114] Benjamin Grinstein and Dan Pirjol. "Exclusive rare $B \to K^* \ell^+ \ell^-$ decays at low recoil: Controlling the long-distance effects". In: *Phys. Rev.* D70 (2004), p. 114005. DOI: 10.1103/PhysRevD.70.114005. arXiv: hep-ph/0404250 [hep-ph].

[115] J. Charles et al. "Heavy to light form-factors in the heavy mass to large energy limit of QCD". In: *Phys. Rev.* D60 (1999), p. 014001. DOI: 10.1103/PhysRevD.60.014001. arXiv: hep-ph/9812358 [hep-ph].

[116] D. Ebert, R. N. Faustov, and V. O. Galkin. "Form-factors of heavy to light B decays at large recoil". In: *Phys. Rev.* D64 (2001), p. 094022. DOI: 10.1103/PhysRevD.64.094022. arXiv: hep-ph/0107065 [hep-ph].

[117] Benjamin Grinstein and Dan Pirjol. "Symmetry breaking corrections to heavy meson form-factor relations". In: *Phys. Lett.* B533 (2002), pp. 8–16. DOI: 10.1016/S0370-2693(02)01601-5. arXiv: hep-ph/0201298 [hep-ph].

[118] M. Beneke and T. Feldmann. "Symmetry breaking corrections to heavy to light B meson form-factors at large recoil". In: *Nucl. Phys.* B592 (2001), pp. 3–34. DOI: 10.1016/S0550-3213(00)00585-X. arXiv: hep-ph/0008255 [hep-ph].

[119] Jonna Koponen. "Lattice results for D/D_s leptonic and semileptonic decays". In: *Proceedings, 6th International Workshop on Charm Physics (Charm 2013): Manchester, UK, August 31-September 4, 2013*. 2013. arXiv: 1311.6931 [hep-lat]. URL: http://inspirehep.net/record/1266442/files/arXiv:1311.6931.pdf.

[120] N. Carrasco et al. "Scalar and vector form factors of $D \to \pi l \nu$ and $D \to K l \nu$ decays with $N_f = 2 + 1 + 1$ Twisted femions". In: *PoS* LATTICE2015 (2016), p. 261. arXiv: 1511.04877 [hep-lat].

[121] V. Lubicz et al. "Hypercubic Effects in semileptonic $D \to \pi$ decays on the lattice". In: *PoS* LATTICE2016 (2016), p. 280. arXiv: 1611.00022 [hep-lat].

[122] C. Glenn Boyd, Benjamin Grinstein, and Richard F. Lebed. "Constraints on form-factors for exclusive semileptonic heavy to light meson decays". In: *Phys. Rev. Lett.* 74 (1995), pp. 4603–4606. DOI: 10.1103/PhysRevLett.74.4603. arXiv: hep-ph/9412324 [hep-ph].

[123] L. G. Landsberg. "Electromagnetic Decays of Light Mesons". In: *Phys. Rept.* 128 (1985), pp. 301–376. DOI: 10.1016/0370-1573(85)90129-2.

[124] Pere Masjuan and Pablo Sanchez-Puertas. "η and η' decays into lepton pairs". In: *JHEP* 08 (2016), p. 108. DOI: 10.1007/JHEP08(2016)108. arXiv: 1512.09292 [hep-ph].

[125] Nguyen Thu Huong, Emi Kou, and Benoit Viaud. "Novel approach to measure the leptonic $\eta() \to \mu^+\mu^-$ decays via charmed meson decays". In: *Phys. Rev.* D94.5 (2016), p. 054040. DOI: 10.1103/PhysRevD.94.054040. arXiv: 1606.08195 [hep-ph].

[126] Svjetlana Fajfer and Nejc Košnik. "Resonance catalyzed CP asymmetries in $D \to P\ell^+\ell^-$". In: *Phys. Rev.* D87.5 (2013), p. 054026. DOI: 10.1103/PhysRevD.87.054026. arXiv: 1208.0759 [hep-ph].

[127] Svjetlana Fajfer, Nejc Kosnik, and Sasa Prelovsek. "Updated constraints on new physics in rare charm decays". In: *Phys. Rev.* D76 (2007), p. 074010. DOI: 10.1103/PhysRevD.76.074010. arXiv: 0706.1133 [hep-ph].

[128] Svjetlana Fajfer and Nejc Kosnik. "Leptoquarks in FCNC charm decays". In: *Phys. Rev.* D79 (2009), p. 017502. DOI: 10.1103/PhysRevD.79.017502. arXiv: 0810.4858 [hep-ph].

[129] Svjetlana Fajfer and Nejc Košnik. "Prospects of discovering new physics in rare charm decays". In: *Eur. Phys. J.* C75.12 (2015), p. 567. DOI: 10.1140/epjc/s10052-015-3801-2. arXiv: 1510.00965 [hep-ph].

[130] M. Bartsch et al. "Precision Flavour Physics with $B \to K \nu \bar{\nu}$ and $B \to K l^+ l^-$". In: *JHEP* 11 (2009), p. 011. DOI: 10.1088/1126-6708/2009/11/011. arXiv: 0909.1512 [hep-ph].

[131] M. Beylich, G. Buchalla, and T. Feldmann. "Theory of $B \to K^{(*)}\ell^+\ell^-$ decays at high q^2: OPE and quark-hadron duality". In: *Eur. Phys. J.* C71 (2011), p. 1635. DOI: 10.1140/epjc/s10052-011-1635-0. arXiv: 1101.5118 [hep-ph].

[132] James Lyon and Roman Zwicky. "Resonances gone topsy turvy - the charm of QCD or new physics in $b \to s\ell^+\ell^-$?" In: (2014). arXiv: 1406.0566 [hep-ph].

[133] Simon Braß, Gudrun Hiller, and Ivan Nisandzic. "Zooming in on $B \to K^*\ell\ell$ decays at low recoil". In: *Eur. Phys. J.* C77.1 (2017), p. 16. DOI: 10.1140/epjc/s10052-016-4576-9. arXiv: 1606.00775 [hep-ph].

[134] M. Beneke, T. Feldmann, and D. Seidel. "Systematic approach to exclusive $B \to Vl^+l^-$, $V\gamma$ decays". In: *Nucl. Phys.* B612 (2001), pp. 25–58. DOI: 10.1016/S0550-3213(01)00366-2. arXiv: hep-ph/0106067 [hep-ph].

[135] Benjamin Grinstein and Dan Pirjol. "Factorization in B -> K pi l+ l- decays". In: *Phys. Rev.* D73 (2006), p. 094027. DOI: 10.1103/PhysRevD.73.094027. arXiv: hep-ph/0505155 [hep-ph].

[136] R Aaij et al. "Search for D+(s) to pi+ mu+ mu- and D+(s) to pi- mu+ mu+ decays". In: *Phys. Lett.* B724 (2013), pp. 203–212. DOI: 10.1016/j.physletb.2013.06.010. arXiv: 1304.6365 [hep-ex].

[137] Yasuhito Sakaki et al. "Testing leptoquark models in $\bar{B} \to D^{(*)}\tau\bar{\nu}$". In: *Phys. Rev.* D88.9 (2013), p. 094012. DOI: 10.1103/PhysRevD.88.094012. arXiv: 1309.0301 [hep-ph].

[138] Vindhyawasini Prasad (On behalf of the BESIII experiment). *Experimental status of rare D decays.* https://indico.tifr.res.in/indico/getFile.py/access?contribId=23&sessionId=11&resId=0&materialId=slides&confId=5095. 2016.

[139] Claudia Vacca. "Measurements of charm rare decays at LHCb". In: *7th International Workshop on Charm Physics (Charm 2015) Detroit, MI, USA, May 18-22, 2015.* 2015. arXiv: 1509.02108 [hep-ex]. URL: http://inspirehep.net/record/1392019/files/arXiv:1509.02108.pdf.

[140] R Aaij et al. "Search for CP violation in D+ -> phi pi+ and Ds+ -> Ks pi+ decays". In: *JHEP* 06 (2013), p. 112. DOI: 10.1007/JHEP06(2013)112. arXiv: 1303.4906 [hep-ex].

[141] John F. Donoghue and Fabrizio Gabbiani. "Reanalysis of the decay K(L) —> pi0 e+ e-". In: *Phys. Rev.* D51 (1995), pp. 2187–2200. DOI: 10.1103/PhysRevD.51.2187. arXiv: hep-ph/9408390 [hep-ph].

[142] Gino Isidori, Christopher Smith, and Rene Unterdorfer. "The Rare decay $K_L \to \pi^0\mu^+\mu^-$ within the SM". In: *Eur. Phys. J.* C36 (2004), pp. 57–66. DOI: 10.1140/epjc/s2004-01879-0. arXiv: hep-ph/0404127 [hep-ph].

[143] Gudrun Hiller and Roman Zwicky. "(A)symmetries of weak decays at and near the kinematic endpoint". In: *JHEP* 03 (2014), p. 042. DOI: 10.1007/JHEP03(2014)042. arXiv: 1312.1923 [hep-ph].

[144] Rodrigo Alonso, Benjamín Grinstein, and Jorge Martin Camalich. "Lepton universality violation and lepton flavor conservation in B-meson decays". In: *JHEP* 10 (2015), p. 184. DOI: 10.1007/JHEP10(2015)184. arXiv: 1505.05164 [hep-ph].

[145] Sheldon L. Glashow, Diego Guadagnoli, and Kenneth Lane. "Lepton Flavor Violation in B Decays?" In: *Phys. Rev. Lett.* 114 (2015), p. 091801. DOI: 10.1103/PhysRevLett.114.091801. arXiv: 1411.0565 [hep-ph].

[146] S. Fajfer and P. Singer. "Long distance c —> u gamma effects in weak radiative decays of D mesons". In: *Phys. Rev.* D56 (1997), pp. 4302–4310. DOI: 10.1103/PhysRevD.56.4302. arXiv: hep-ph/9705327 [hep-ph].

[147] S. Fajfer, Sasa Prelovsek, and P. Singer. "Long distance contributions in D —> V gamma decays". In: *Eur. Phys. J.* C6 (1999), pp. 471–476. DOI: 10.1007/s100520050356,10.1007/s100529800914. arXiv: hep-ph/9801279 [hep-ph].

[148] Gino Isidori and Jernej F. Kamenik. "Shedding light on CP violation in the charm system via D to V gamma decays". In: *Phys. Rev. Lett.* 109 (2012), p. 171801. DOI: 10.1103/PhysRevLett.109.171801. arXiv: 1205.3164 [hep-ph].

[149] Stefan W. Bosch and Gerhard Buchalla. "The Radiative decays $B \to V\gamma$ at next-to-leading order in QCD". In: *Nucl. Phys.* B621 (2002), pp. 459–478. DOI: 10.1016/S0550-3213(01)00580-6. arXiv: hep-ph/0106081 [hep-ph].

[150] Ahmed Ali and A. Y. Parkhomenko. "Branching ratios for B —> K* gamma and B —> rho gamma decays in next-to-leading order in the large energy effective theory". In: *Eur. Phys. J.* C23 (2002), pp. 89–112. DOI: 10.1007/s100520100856. arXiv: hep-ph/0105302 [hep-ph].

[151] M. Beneke, Th. Feldmann, and D. Seidel. "Exclusive radiative and electroweak $b \to d$ and $b \to s$ penguin decays at NLO". In: *Eur. Phys. J.* C41 (2005), pp. 173–188. DOI: 10.1140/epjc/s2005-02181-5. arXiv: hep-ph/0412400 [hep-ph].

[152] Maria Dimou, James Lyon, and Roman Zwicky. "Exclusive Chromomagnetism in heavy-to-light FCNCs". In: *Phys. Rev.* D87.7 (2013), p. 074008. DOI: 10.1103/PhysRevD.87.074008. arXiv: 1212.2242 [hep-ph].

[153] Patricia Ball, Gareth W. Jones, and Roman Zwicky. "$B \to V\gamma$ beyond QCD factorisation". In: *Phys. Rev.* D75 (2007), p. 054004. DOI: 10.1103/PhysRevD.75.054004. arXiv: hep-ph/0612081 [hep-ph].

[154] A. Heller et al. "Search for $B^+ \to \ell^+\nu_\ell$ decays with hadronic tagging using the full Belle data sample". In: *Phys. Rev.* D91.11 (2015), p. 112009. DOI: 10.1103/PhysRevD.91.112009. arXiv: 1504.05831 [hep-ex].

[155] Gregory P. Korchemsky, Dan Pirjol, and Tung-Mow Yan. "Radiative leptonic decays of B mesons in QCD". In: *Phys. Rev.* D61 (2000), p. 114510. DOI: 10.1103/PhysRevD.61.114510. arXiv: hep-ph/9911427 [hep-ph].

[156] Patricia Ball and Emi Kou. "B —> gamma e nu transitions from QCD sum rules on the light cone". In: *JHEP* 04 (2003), p. 029. DOI: 10.1088/1126-6708/2003/04/029. arXiv: hep-ph/0301135 [hep-ph].

[157] Alexander Khodjamirian, Thomas Mannel, and Nils Offen. "B-meson distribution amplitude from the B —> pi form-factor". In: *Phys. Lett.* B620 (2005), pp. 52–60. DOI: 10.1016/j.physletb.2005.06.021. arXiv: hep-ph/0504091 [hep-ph].

[158] Volker Pilipp. "Matching of lambda(B) onto HQET". In: (2007). arXiv: hep-ph/0703180 [hep-ph].

[159] Alexander L. Kagan and Matthias Neubert. "Isospin breaking in $B \to K^*\gamma$ decays". In: *Phys. Lett.* B539 (2002), pp. 227–234. DOI: 10.1016/S0370-2693(02)02100-7. arXiv: hep-ph/0110078 [hep-ph].

[160] Stefan W. Bosch and Gerhard Buchalla. "Constraining the unitarity triangle with B —> V gamma". In: *JHEP* 01 (2005), p. 035. DOI: 10.1088/1126-6708/2005/01/035. arXiv: hep-ph/0408231 [hep-ph].

[161] Benjamin Grinstein and Dan Pirjol. "Long distance effects in B —> V gamma radiative weak decays". In: *Phys. Rev.* D62 (2000), p. 093002. DOI: 10.1103/PhysRevD.62.093002. arXiv: hep-ph/0002216 [hep-ph].

[162] Benjamin Grinstein et al. "The Photon polarization in B —> X gamma in the standard model". In: *Phys. Rev.* D71 (2005), p. 011504. DOI: 10.1103/PhysRevD.71.011504. arXiv: hep-ph/0412019 [hep-ph].

[163] Maria Dimou, James Lyon, and Roman Zwicky. "Heavy-to-light chromomagentic matrix element". In: *5th Chaotic Modeling and Simulation International Conference Athens, Greece, June 12-15, 2012*. 2013. arXiv: 1305.5332 [hep-ph]. URL: http://inspirehep.net/record/1235286/files/arXiv:1305.5332.pdf.

[164] Gustavo Burdman et al. "Radiative weak decays of charm mesons". In: *Phys. Rev.* D52 (1995), pp. 6383–6399. DOI: 10.1103/PhysRevD.52.6383. arXiv: hep-ph/9502329 [hep-ph].

[165] A. Khodjamirian, G. Stoll, and D. Wyler. "Calculation of long distance effects in exclusive weak radiative decays of B meson". In: *Phys. Lett.* B358 (1995), pp. 129–138. DOI: 10.1016/0370-2693(95)00972-N. arXiv: hep-ph/9506242 [hep-ph].

[166] Aritra Biswas, Sanjoy Mandal, and Nita Sinha. "Searching for New physics in Charm Radiative decays". In: (2017). arXiv: 1702.05059 [hep-ph].

[167] Manfred Bauer, B. Stech, and M. Wirbel. "Exclusive Nonleptonic Decays of D, D(s), and B Mesons". In: *Z. Phys.* C34 (1987), p. 103. DOI: 10.1007/BF01561122.

[168] Roel Aaij et al. "Measurement of the difference of time-integrated CP asymmetries in $D^0 \to K^-K^+$ and $D^0 \to \pi^-\pi^+$ decays". In: *Phys. Rev. Lett.* 116.19 (2016), p. 191601. DOI: 10.1103/PhysRevLett.116.191601. arXiv: 1602.03160 [hep-ex].

[169] Bernard Aubert et al. "Measurement of the Branching Fractions of the Radiative Charm Decays D0 —> anti-K*0 gamma and D0 —> phi gamma". In: *Phys. Rev.* D78 (2008), p. 071101. DOI: 10.1103/PhysRevD.78.071101. arXiv: 0808.1838 [hep-ex].

[170] S. Fajfer, P. Singer, and J. Zupan. "The Rare decay D0 —> gamma gamma". In: *Phys. Rev.* D64 (2001), p. 074008. DOI: 10.1103/PhysRevD.64.074008. arXiv: hep-ph/0104236 [hep-ph].

[171] Ayan Paul, Ikaros I. Bigi, and Stefan Recksiegel. "$D^0 - > \gamma\gamma$ and $D^0 - > \mu^+\mu^-$ Rates on an Unlikely Impact of the Littlest Higgs Model with T-Parity". In: *Phys. Rev.* D82 (2010). [Erratum: Phys. Rev.D83,019901(2011)], p. 094006. DOI: 10.1103/PhysRevD.83.019901,10.1103/PhysRevD.82.094006. arXiv: 1008.3141 [hep-ph].

[172] K. Prasanth. "CP violation in D meson decays at Belle". In: *5th International Conference on New Frontiers in Physics Kolymbari, Crete, Greece, July 6-14, 2016.* 2016. arXiv: 1610.04771 [hep-ex]. URL: http://inspirehep.net/record/1492314/files/arXiv:1610.04771.pdf.

[173] Kristof De Bruyn et al. "Probing New Physics via the $B_s^0 \to \mu^+\mu^-$ Effective Lifetime". In: *Phys. Rev. Lett.* 109 (2012), p. 041801. DOI: 10.1103/PhysRevLett.109.041801. arXiv: 1204.1737 [hep-ph].

[174] Alexey A. Petrov. *Theory of rare D decays.* https://indico.tifr.res.in/indico/getFile.py/access?contribId=22&sessionId=11&resId=0&materialId=slides&confId=5095. 2016.

[175] Alexander Khodjamirian, Thomas Mannel, and Alexey A Petrov. "Direct probes of flavor-changing neutral currents in e^+ e-collisions". In: *JHEP* 11 (2015), p. 142. DOI: 10.1007/JHEP11(2015)142. arXiv: 1509.07123 [hep-ph].

[176] M. Beneke et al. "QCD factorization for exclusive, nonleptonic B meson decays: General arguments and the case of heavy light final states". In: *Nucl. Phys.* B591 (2000), pp. 313–418. DOI: 10.1016/S0550-3213(00)00559-9. arXiv: hep-ph/0006124 [hep-ph].

[177] Jernej F. Kamenik and Christopher Smith. "Tree-level contributions to the rare decays B+ —> pi+ nu anti-nu, B+ —> K+ nu anti-nu, and B+ —> K*+ nu anti-nu in the Standard Model". In: *Phys. Lett.* B680 (2009), pp. 471–475. DOI: 10.1016/j.physletb.2009.09.041. arXiv: 0908.1174 [hep-ph].

[178] S. Fajfer, Sasa Prelovsek, and P. Singer. "FCNC transitions $c \to u\gamma$ and $s \to d\gamma$ in $B_c \to B_u^*\gamma$ and $B_s \to B_d^*\gamma$ decays". In: *Phys. Rev.* D59 (1999). [Erratum: Phys. Rev.D64,099903(2001)], p. 114003. DOI: 10.1103/PhysRevD.59.114003,10.1103/PhysRevD.64.099903. arXiv: hep-ph/9901252 [hep-ph].

[179] Benjamin Grinstein and Dan Pirjol. "The CP asymmetry in B0(t) —> K(S) pi0 gamma in the standard model". In: *Phys. Rev.* D73 (2006), p. 014013. DOI: 10.1103/PhysRevD.73.014013. arXiv: hep-ph/0510104 [hep-ph].

[180] Ikaros I. Bigi and Ayan Paul. "On CP Asymmetries in Two-, Three- and Four-Body D Decays". In: *JHEP* 03 (2012), p. 021. DOI: 10.1007/JHEP03(2012)021. arXiv: 1110.2862 [hep-ph].

[181] Luigi Cappiello, Oscar Cata, and Giancarlo D'Ambrosio. "Standard Model prediction and new physics tests for $D^0 \to h^+h^-\ell^+\ell^-(h = \pi, K : \ell = e, \mu)$". In: *JHEP* 04 (2013), p. 135. DOI: 10.1007/JHEP04(2013)135. arXiv: 1209.4235 [hep-ph].

[182] Roel Aaij et al. "First observation of the decay $D^0 \to K^-\pi^+\mu^+\mu^-$ in the ρ^0-ω region of the dimuon mass spectrum". In: *Phys. Lett.* B757 (2016), pp. 558–567. DOI: 10.1016/j.physletb.2016.04.029. arXiv: 1510.08367 [hep-ex].

[183] Diganta Das et al. "The $\overline{B} \to \overline{K}\pi\ell\ell$ and $\overline{B}_s \to \overline{K}K\ell\ell$ distributions at low hadronic recoil". In: *JHEP* 09 (2014), p. 109. DOI: 10.1007/JHEP09(2014)109. arXiv: 1406.6681 [hep-ph].

[184] K. Azizi et al. "FCNC transitions of Lambdab(b,c) to nucleon in SM". In: *J. Phys.* G37 (2010), p. 115007. DOI: 10.1088/0954-3899/37/11/115007.

[185] Berin Belma Şirvanli. "Search for $c \to ul^+l^-$ transition in charmed baryon decays". In: *Phys. Rev.* D93.3 (2016), p. 034027. DOI: 10.1103/PhysRevD.93.034027.

[186] A. Khodjamirian et al. "Form Factors and Strong Couplings of Heavy Baryons from QCD Light-Cone Sum Rules". In: *JHEP* 09 (2011), p. 106. DOI: 10.1007/JHEP09(2011)106. arXiv: 1108.2971 [hep-ph].

[187] Cheng-Fei Li et al. "Analysis of the semileptonic decay $\Lambda_c \to ne^+\nu_e$". In: *J. Phys.* G44.7 (2017), p. 075006. DOI: 10.1088/1361-6471/aa68f1. arXiv: 1610.05418 [hep-ph].

[188] R. N. Faustov and V. O. Galkin. "Semileptonic decays of Λ_c baryons in the relativistic quark model". In: *Eur. Phys. J.* C76.11 (2016), p. 628. DOI: 10.1140/epjc/s10052-016-4492-z. arXiv: 1610.00957 [hep-ph].

[189] T. Blake, T. Gershon, and G. Hiller. "Rare b hadron decays at the LHC". In: *Ann. Rev. Nucl. Part. Sci.* 65 (2015), pp. 113–143. DOI: 10.1146/annurev-nucl-102014-022231. arXiv: 1501.03309 [hep-ex].

[190] S. Fajfer et al. "A Possible arena for searching new physics: The Gamma (D0 —> rho0 gamma) / Gamma (D0 —> omega gamma) ratio". In: *Phys. Lett.* B487 (2000), pp. 81–86. DOI: 10.1016/S0370-2693(00)00731-0. arXiv: hep-ph/0006054 [hep-ph].

[191] James Lyon and Roman Zwicky. "Anomalously large $\mathcal{O}_8$ and long-distance chirality from $A_{\rm CP}[D^0 \to (\rho^0, \omega)\gamma](t)$". In: (2012). arXiv: 1210.6546 [hep-ph].

[192] Gian Francesco Giudice, Gino Isidori, and Paride Paradisi. "Direct CP violation in charm and flavor mixing beyond the SM". In: *JHEP* 04 (2012), p. 060. DOI: 10.1007/JHEP04(2012)060. arXiv: 1201.6204 [hep-ph].

[193] Xing-Dao Guo et al. "Looking for New Physics via Semi-leptonic and Leptonic rare decays of D and D_s". In: (2017). arXiv: 1703.08799 [hep-ph].

[194] Cedric Delaunay et al. "Charming CP Violation and Dipole Operators from RS Flavor Anarchy". In: *JHEP* 01 (2013), p. 027. DOI: 10.1007/JHEP01(2013)027. arXiv: 1207.0474 [hep-ph].

[195] Ayan Paul, Alejandro De La Puente, and Ikaros I. Bigi. "Manifestations of warped extra dimension in rare charm decays and asymmetries". In: *Phys. Rev.* D90.1 (2014), p. 014035. DOI: 10.1103/PhysRevD.90.014035. arXiv: 1212.4849 [hep-ph].

[196] Suchismita Sahoo and Rukmani Mohanta. "New physics effects in charm meson decays involving $c \to u l^+ l^- (l_i^\mp l_j^\pm)$ transitions". In: *Eur. Phys. J.* C77.5 (2017), p. 344. DOI: 10.1140/epjc/s10052-017-4888-4. arXiv: 1705.02251 [hep-ph].

[197] Eugene Golowich et al. "Relating D0-anti-D0 Mixing and D0 —> l+ l- with New Physics". In: *Phys. Rev.* D79 (2009), p. 114030. DOI: 10.1103/PhysRevD.79.114030. arXiv: 0903.2830 [hep-ph].

[198] W. Buchmuller, R. Ruckl, and D. Wyler. "Leptoquarks in Lepton - Quark Collisions". In: *Phys. Lett.* B191 (1987). [Erratum: Phys. Lett.B448,320(1999)], pp. 442–448. DOI: 10.1016/S0370-2693(99)00014-3,10.1016/0370-2693(87)90637-X.

[199] I. Doršner et al. "Physics of leptoquarks in precision experiments and at particle colliders". In: *Phys. Rept.* 641 (2016), pp. 1–68. DOI: 10.1016/j.physrep.2016.06.001. arXiv: 1603.04993 [hep-ph].

[200] Gudrun Hiller and Ivan Nisandzic. "R_K and R_{K^*} beyond the Standard Model". In: (2017). arXiv: 1704.05444 [hep-ph].

[201] Martin Bauer and Matthias Neubert. "Minimal Leptoquark Explanation for the $\mathrm{R}_{D^{(*)}}$, R_K , and $(g-2)_g$ Anomalies". In: *Phys. Rev. Lett.* 116.14 (2016), p. 141802. DOI: 10.1103/PhysRevLett.116.141802. arXiv: 1511.01900 [hep-ph].

[202] Svjetlana Fajfer and Nejc Košnik. "Vector leptoquark resolution of R_K and $R_{D^{(*)}}$ puzzles". In: *Phys. Lett.* B755 (2016), pp. 270–274. DOI: 10.1016/j.physletb.2016.02.018. arXiv: 1511.06024 [hep-ph].

[203] Diganta Das et al. "Towards a unified explanation of $R_{D^{(*)}}$, R_K and $(g-2)_\mu$ anomalies in a left-right model with leptoquarks". In: *Phys. Rev.* D94 (2016), p. 055034. DOI: 10.1103/PhysRevD.94.055034. arXiv: 1605.06313 [hep-ph].

[204] Oleg Popov and Graham A White. "One Leptoquark to unify them? Neutrino masses and unification in the light of $(g-2)_\mu$, $R_{D^{(*)}}$ and R_K anomalies". In: (2016). arXiv: 1611.04566 [hep-ph].

[205] Damir Bečirević et al. "Palatable Leptoquark Scenarios for Lepton Flavor Violation in Exclusive $b \to s\ell_1\ell_2$ modes". In: *JHEP* 11 (2016), p. 035. DOI: 10.1007/JHEP11(2016)035. arXiv: 1608.07583 [hep-ph].

[206] Damir Bečirević and Olcyr Sumensari. "A leptoquark model to accommodate $R_K^{\rm exp} < R_K^{\rm SM}$ and $R_{K^*}^{\rm exp} < R_{K^*}^{\rm SM}$". In: (2017). arXiv: 1704.05835 [hep-ph].

[207] C. S. Kim et al. "Remarks on the Standard Model predictions for $R(D)$ and $R(D^*)$". In: *Phys. Rev.* D95.1 (2017), p. 013003. DOI: 10.1103/PhysRevD.95.013003. arXiv: 1610.04190 [hep-ph].

[208] Daniel Aloni et al. "Υ and ψ leptonic decays as probes of solutions to the $R_D^{(*)}$ puzzle". In: *JHEP* 06 (2017), p. 019. DOI: 10.1007/JHEP06(2017)019. arXiv: 1702.07356 [hep-ph].

[209] Heinrich Päs and Erik Schumacher. "Common origin of R_K and neutrino masses". In: *Phys. Rev.* D92.11 (2015), p. 114025. DOI: 10.1103/PhysRevD.92.114025. arXiv: 1510.08757 [hep-ph].

[210] F. F. Deppisch et al. "Leptoquark patterns unifying neutrino masses, flavor anomalies, and the diphoton excess". In: *Phys. Rev.* D94.1 (2016), p. 013003. DOI: 10.1103/PhysRevD.94.013003. arXiv: 1603.07672 [hep-ph].

[211] Ilja Doršner, Svjetlana Fajfer, and Nejc Košnik. "Leptoquark mechanism of neutrino masses within the grand unification framework". In: *Eur. Phys. J.* C77.6 (2017), p. 417. DOI: 10.1140/epjc/s10052-017-4987-2. arXiv: 1701.08322 [hep-ph].

[212] Ansgar Denner et al. "Feynman rules for fermion number violating interactions". In: *Nucl. Phys.* B387 (1992), pp. 467–481. DOI: 10.1016/0550-3213(92)90169-C.

[213] Gudrun Hiller, Dennis Loose, and Kay Schönwald. "Leptoquark Flavor Patterns & B Decay Anomalies". In: *JHEP* 12 (2016), p. 027. DOI: 10.1007/JHEP12(2016)027. arXiv: 1609.08895 [hep-ph].

[214] Sacha Davidson, David C. Bailey, and Bruce A. Campbell. "Model independent constraints on leptoquarks from rare processes". In: *Z. Phys.* C61 (1994), pp. 613–644. DOI: 10.1007/BF01552629. arXiv: hep-ph/9309310 [hep-ph].

[215] Sacha Davidson and Sebastien Descotes-Genon. "Minimal Flavour Violation for Leptoquarks". In: *JHEP* 11 (2010), p. 073. DOI: 10.1007/JHEP11(2010)073. arXiv: 1009.1998 [hep-ph].

[216] Jonathan M. Arnold, Bartosz Fornal, and Mark B. Wise. "Phenomenology of scalar leptoquarks". In: *Phys. Rev.* D88 (2013), p. 035009. DOI: 10.1103/PhysRevD.88.035009. arXiv: 1304.6119 [hep-ph].

[217] M. Hirsch, H. V. Klapdor-Kleingrothaus, and S. G. Kovalenko. "New low-energy leptoquark interactions". In: *Phys. Lett.* B378 (1996), pp. 17–22. DOI: 10.1016/0370-2693(96)00419-4. arXiv: hep-ph/9602305 [hep-ph].

[218] M. Hirsch, H. V. Klapdor-Kleingrothaus, and S. G. Kovalenko. "New leptoquark mechanism of neutrinoless double beta decay". In: *Phys. Rev.* D54 (1996), R4207–R4210. DOI: 10.1103/PhysRevD.54.R4207. arXiv: hep-ph/9603213 [hep-ph].

[219] Uma Mahanta. "Neutrino masses and mixing angles from leptoquark interactions". In: *Phys. Rev.* D62 (2000), p. 073009. DOI: 10.1103/PhysRevD.62.073009. arXiv: hep-ph/9909518 [hep-ph].

[220] Priyotosh Bandyopadhyay and Rusa Mandal. "Vacuum stability in an extended standard model with a leptoquark". In: *Phys. Rev.* D95.3 (2017), p. 035007. DOI: 10.1103/PhysRevD.95.035007. arXiv: 1609.03561 [hep-ph].

[221] Ilja Dorsner, Svjetlana Fajfer, and Nejc Kosnik. "Heavy and light scalar leptoquarks in proton decay". In: *Phys. Rev.* D86 (2012), p. 015013. DOI: 10.1103/PhysRevD.86.015013. arXiv: 1204.0674 [hep-ph].

[222] Ilja Dorsner and Pavel Fileviez Perez. "How long could we live?" In: *Phys. Lett.* B625 (2005), pp. 88–95. DOI: 10.1016/j.physletb.2005.08.039. arXiv: hep-ph/0410198 [hep-ph].

[223] Sergey Kovalenko and Ivan Schmidt. "Proton stability in leptoquark models". In: *Phys. Lett.* B562 (2003), pp. 104–108. DOI: 10.1016/S0370-2693(03)00544-6. arXiv: hep-ph/0210187 [hep-ph].

[224] Oscar J. P. Eboli, M. C. Gonzalez-Garcia, and J. K. Mizukoshi. "Z physics constraints on vector leptoquarks". In: *Phys. Lett.* B396 (1997), pp. 238–244. DOI: 10.1016/S0370-2693(97)00123-8. arXiv: hep-ph/9612254 [hep-ph].

[225] J. K. Mizukoshi, Oscar J. P. Eboli, and M. C. Gonzalez-Garcia. "Bounds on scalar leptoquarks from Z physics". In: *Nucl. Phys.* B443 (1995), pp. 20–36. DOI: 10.1016/0550-3213(95)00162-L. arXiv: hep-ph/9411392 [hep-ph].

[226] Johannes Blumlein, Edward Boos, and Alexander Kryukov. "Leptoquark pair production in hadronic interactions". In: *Z. Phys.* C76 (1997), pp. 137–153. DOI: 10.1007/s002880050538. arXiv: hep-ph/9610408 [hep-ph].

[227] Andreas Blumhofer and Bodo Lampe. "A Low-energy compatible SU(4) type model for vector leptoquarks of mass <= 1-TeV". In: *Eur. Phys. J.* C7 (1999), pp. 141–148. DOI: 10.1007/s100529900965. arXiv: hep-ph/9706454 [hep-ph].

[228] Michael Duerr, Pavel Fileviez Perez, and Mark B. Wise. "Gauge Theory for Baryon and Lepton Numbers with Leptoquarks". In: *Phys. Rev. Lett.* 110 (2013), p. 231801. DOI: 10.1103/PhysRevLett.110.231801. arXiv: 1304.0576 [hep-ph].

[229] Vardan Khachatryan et al. "Search for single production of scalar leptoquarks in proton-proton collisions at $\sqrt{s} = 8\ TeV$". In: *Phys. Rev.* D93.3 (2016). [Erratum: Phys. Rev.D95,no.3,039906(2017)], p. 032005. DOI: 10.1103/PhysRevD.95.039906,10.1103/PhysRevD.93.032005. arXiv: 1509.03750 [hep-ex].

[230] CMS Collaboration. "Search for pair-production of second-generation scalar leptoquarks in pp collisions at $\sqrt{s} = 13$ TeV with the CMS detector". In: (2016).

[231] Morad Aaboud et al. "Search for scalar leptoquarks in pp collisions at $\sqrt{s} = 13$ TeV with the ATLAS experiment". In: *New J. Phys.* 18.9 (2016), p. 093016. DOI: 10.1088/1367-2630/18/9/093016. arXiv: 1605.06035 [hep-ex].

[232] Ilja Dorsner, Svjetlana Fajfer, and Admir Greljo. "Cornering Scalar Leptoquarks at LHC". In: *JHEP* 10 (2014), p. 154. DOI: 10.1007/JHEP10(2014)154. arXiv: 1406.4831 [hep-ph].

[233] Vardan Khachatryan et al. "Search for pair production of first and second generation leptoquarks in proton-proton collisions at sqrt(s) = 8 TeV". In: *Phys. Rev.* D93.3 (2016), p. 032004. DOI: 10.1103/PhysRevD.93.032004. arXiv: 1509.03744 [hep-ex].

[234] L. Lavoura. "General formulae for f(1) —> f(2) gamma". In: *Eur. Phys. J.* C29 (2003), pp. 191–195. DOI: 10.1140/epjc/s2003-01212-7. arXiv: hep-ph/0302221 [hep-ph].

[235] Ivo de Medeiros Varzielas and Gudrun Hiller. "Clues for flavor from rare lepton and quark decays". In: *JHEP* 06 (2015), p. 072. DOI: 10.1007/JHEP06(2015)072. arXiv: 1503.01084 [hep-ph].

[236] C. D. Froggatt and Holger Bech Nielsen. "Hierarchy of Quark Masses, Cabibbo Angles and CP Violation". In: *Nucl. Phys.* B147 (1979), pp. 277–298. DOI: 10.1016/0550-3213(79)90316-X.

[237] Ivo de Medeiros Varzielas and Graham G. Ross. "SU(3) family symmetry and neutrino bi-tri-maximal mixing". In: *Nucl. Phys.* B733 (2006), pp. 31–47. DOI: 10.1016/j.nuclphysb.2005.10.039. arXiv: hep-ph/0507176 [hep-ph].

[238] Michael Carpentier and Sacha Davidson. "Constraints on two-lepton, two quark operators". In: *Eur. Phys. J.* C70 (2010), pp. 1071–1090. DOI: 10.1140/epjc/s10052-010-1482-4. arXiv: 1008.0280 [hep-ph].

[239] F. Gabbiani et al. "A Complete analysis of FCNC and CP constraints in general SUSY extensions of the standard model". In: *Nucl. Phys.* B477 (1996), pp. 321–352. DOI: 10.1016/0550-3213(96)00390-2. arXiv: hep-ph/9604387 [hep-ph].

[240] Sasa Prelovsek and D. Wyler. "c –> u gamma in the minimal supersymmetric standard model". In: *Phys. Lett.* B500 (2001), pp. 304–312. DOI: 10.1016/S0370-2693(01)00077-6. arXiv: hep-ph/0012116 [hep-ph].

[241] N. Carrasco et al. "$D^0-\bar{D}^0$ mixing in the standard model and beyond from N_f =2 twisted mass QCD". In: *Phys. Rev.* D90.1 (2014), p. 014502. DOI: 10.1103/PhysRevD.90.014502. arXiv: 1403.7302 [hep-lat].

[242] A. J. Bevan et al. "The UTfit collaboration average of D meson mixing data: Winter 2014". In: *JHEP* 03 (2014), p. 123. DOI: 10.1007/JHEP03(2014)123. arXiv: 1402.1664 [hep-ph].

[243] Mariana Frank and Shu-quan Nie. "Chargino contributions to epsilon-prime / epsilon in the left right supersymmetric model". In: *J. Phys.* G30 (2004), pp. 181–190. DOI: 10.1088/0954-3899/30/2/015. arXiv: hep-ph/0306020 [hep-ph].

[244] Gudrun Hiller and Alex Kagan. "Probing for new physics in polarized Λ_b decays at the Z". In: *Phys. Rev.* D65 (2002), p. 074038. DOI: 10.1103/PhysRevD.65.074038. arXiv: hep-ph/0108074 [hep-ph].

[245] Paul Singer and Da-Xin Zhang. "Two-body Cabibbo suppressed decays of charmed baryons into vector mesons and into photons". In: *Phys. Rev.* D54 (1996), pp. 1225–1228. DOI: 10.1103/PhysRevD.54.1225. arXiv: hep-ph/9603426 [hep-ph].

[246] Philipp Böer, Thorsten Feldmann, and Danny van Dyk. "Angular Analysis of the Decay $\Lambda_b \to \Lambda(\to N\pi)\ell^+\ell^-$". In: *JHEP* 01 (2015), p. 155. DOI: 10.1007/JHEP01(2015)155. arXiv: 1410.2115 [hep-ph].

[247] Thomas Gutsche et al. "Heavy-to-light semileptonic decays of Λ_b and Λ_c baryons in the covariant confined quark model". In: *Phys. Rev.* D90.11 (2014). [Erratum: Phys. Rev.D94,no.5,059902(2016)], p. 114033. DOI: 10.1103/PhysRevD.90.114033,10.1103/PhysRevD.94.059902. arXiv: 1410.6043 [hep-ph].

[248] T. Uppal and R. C. Verma. "Weak electromagnetic decays of charm baryons". In: *Phys. Rev.* D47 (1993), pp. 2858–2864. DOI: 10.1103/PhysRevD.47.2858.

[249] T. Aushev et al. "Physics at Super B Factory". In: (2010). arXiv: 1002.5012 [hep-ex].

[250] Adam F. Falk and Michael E. Peskin. "Production, decay, and polarization of excited heavy hadrons". In: *Phys. Rev.* D49 (1994), pp. 3320–3332. DOI: 10.1103/PhysRevD.49.3320. arXiv: hep-ph/9308241 [hep-ph].

[251] Mario Galanti et al. "Heavy baryons as polarimeters at colliders". In: *JHEP* 11 (2015), p. 067. DOI: 10.1007/JHEP11(2015)067. arXiv: 1505.02771 [hep-ph].

[252] Yevgeny Kats. "Measuring c-quark polarization in W+c samples at ATLAS and CMS". In: *JHEP* 11 (2016), p. 011. DOI: 10.1007/JHEP11(2016)011. arXiv: 1512.00438 [hep-ph].

[253] E. M. Aitala et al. "Mass splitting and production of sigma(c)0 and sigma(c)++ measured in 500-GeV pi- n interactions". In: *Phys. Lett.* B379 (1996), pp. 292–298. DOI: 10.1016/0370-2693(96)00471-6. arXiv: hep-ex/9604007 [hep-ex].

[254] G. Brandenburg et al. "Observation of two excited charmed baryons decaying into Lambda(c)+ pi+-". In: *Phys. Rev. Lett.* 78 (1997), pp. 2304–2308. DOI: 10.1103/PhysRevLett.78.2304.

[255] J. G. Korner, A. Pilaftsis, and M. M. Tung. "One Loop QCD Mass effects in the production of polarized bottom and top quarks". In: *Z. Phys.* C63 (1994), pp. 575–579. DOI: 10.1007/BF01557623. arXiv: hep-ph/9311332 [hep-ph].

[256] John K. Elwood. "Excited charmed baryon decays and their implications for fragmentation parameters". In: *Phys. Rev.* D53 (1996), pp. 4866–4874. DOI: 10.1103/PhysRevD.53.4866. arXiv: hep-ph/9511241 [hep-ph].

[257] Chi-Keung Chow. "Qualitative aspects of polarization distributions in excited heavy hadron productions". In: (1996). arXiv: hep-ph/9609514 [hep-ph].

[258] Mykhailo Lisovyi, Andrii Verbytskyi, and Oleksandr Zenaiev. "Combined analysis of charm-quark fragmentation-fraction measurements". In: *Eur. Phys. J.* C76.7 (2016), p. 397. DOI: 10.1140/epjc/s10052-016-4246-y. arXiv: 1509.01061 [hep-ex].

[259] David d'Enterria. "Physics case of FCC-ee". In: *Frascati Phys. Ser.* 61 (2016), p. 17. arXiv: 1601.06640 [hep-ex].

[260] Florian Herren and Matthias Steinhauser. "Version 3 of RunDec and CRunDec". In: (2017). arXiv: 1703.03751 [hep-ph].

[261] J. Charles et al. "CP violation and the CKM matrix: Assessing the impact of the asymmetric B factories". In: *Eur. Phys. J.* C41.1 (2005), pp. 1–131. DOI: 10.1140/epjc/s2005-02169-1. arXiv: hep-ph/0406184 [hep-ph].

[262] M. Ablikim et al. "Observation of the Singly Cabibbo-Suppressed Decay $D^+ \to \omega\pi^+$ and Evidence for $D^0 \to \omega\pi^0$". In: *Phys. Rev. Lett.* 116.8 (2016), p. 082001. DOI: 10.1103/PhysRevLett.116.082001. arXiv: 1512.06998 [hep-ex].

[263] S. Aoki et al. "Review of lattice results concerning low-energy particle physics". In: *Eur. Phys. J.* C77.2 (2017), p. 112. DOI: 10.1140/epjc/s10052-016-4509-7. arXiv: 1607.00299 [hep-lat].

[264] Aoife Bharucha, David M. Straub, and Roman Zwicky. "$B \to V\ell^+\ell^-$ in the Standard Model from light-cone sum rules". In: *JHEP* 08 (2016), p. 098. DOI: 10.1007/JHEP08(2016)098. arXiv: 1503.05534 [hep-ph].

[265] S. G. Porsev, K. Beloy, and A. Derevianko. "Precision determination of weak charge of ^{133}Cs from atomic parity violation". In: *Phys. Rev.* D82 (2010), p. 036008. DOI: 10.1103/PhysRevD.82.036008. arXiv: 1006.4193 [hep-ph].

[266] V. A. Dzuba et al. "Revisiting parity non-conservation in cesium". In: *Phys. Rev. Lett.* 109 (2012), p. 203003. DOI: 10.1103/PhysRevLett.109.203003. arXiv: 1207.5864 [hep-ph].

[267] Vincenzo Cirigliano and Ignasi Rosell. "Two-loop effective theory analysis of pi (K) —> e anti-nu/e [gamma] branching ratios". In: *Phys. Rev. Lett.* 99 (2007), p. 231801. DOI: 10.1103/PhysRevLett.99.231801. arXiv: 0707.3439 [hep-ph].

[268] Tatsumi Aoyama et al. "Tenth-Order Electron Anomalous Magnetic Moment — Contribution of Diagrams without Closed Lepton Loops". In: *Phys. Rev.* D91.3 (2015). [Erratum: Phys. Rev.D96,no.1,019901(2017)], p. 033006. DOI: 10.1103/PhysRevD.91.033006, 10.1103/PhysRevD.96.019901. arXiv: 1412.8284 [hep-ph].

[269] B. Graner et al. "Reduced Limit on the Permanent Electric Dipole Moment of Hg199". In: *Phys. Rev. Lett.* 116.16 (2016), p. 161601. DOI: 10.1103/PhysRevLett.116.161601. arXiv: 1601.04339 [physics.atom-ph].

[270] R. Huber et al. "Search for time reversal violation in the beta decay of polarized Li-8 nuclei". In: *Phys. Rev. Lett.* 90 (2003), p. 202301. DOI: 10.1103/PhysRevLett.90.202301. arXiv: nucl-ex/0301010 [nucl-ex].

[271] T. Suzuki, David F. Measday, and J. P. Roalsvig. "Total Nuclear Capture Rates for Negative Muons". In: *Phys. Rev.* C35 (1987), p. 2212. DOI: 10.1103/PhysRevC.35.2212.

[272] A. M. Baldini et al. "Search for the lepton flavour violating decay $\mu^+ \to e^+\gamma$ with the full dataset of the MEG experiment". In: *Eur. Phys. J.* C76.8 (2016), p. 434. DOI: 10.1140/epjc/s10052-016-4271-x. arXiv: 1605.05081 [hep-ex].

[273] A. M. Baldini et al. "MEG Upgrade Proposal". In: (2013). arXiv: 1301.7225 [physics.ins-det].

[274] Ann-Kathrin Perrevoort. "Status of the Mu3e Experiment at PSI". In: *EPJ Web Conf.* 118 (2016), p. 01028. DOI: 10.1051/epjconf/201611801028. arXiv: 1605.02906 [physics.ins-det].

[275] M. Fael, L. Mercolli, and M. Passera. "Radiative μ and τ leptonic decays at NLO". In: *JHEP* 07 (2015), p. 153. DOI: 10.1007/JHEP07(2015)153. arXiv: 1506.03416 [hep-ph].

[276] M. Fael and C. Greub. "Next-to-leading order prediction for the decay $\mu \to e\,(e^+e^-)\,\nu\,\overline{\nu}$". In: *JHEP* 01 (2017), p. 084. DOI: 10.1007/JHEP01(2017)084. arXiv: 1611.03726 [hep-ph].

[277] Yoshitaka Kuno. "A search for muon-to-electron conversion at J-PARC: The COMET experiment". In: *PTEP* 2013 (2013), p. 022C01. DOI: 10.1093/ptep/pts089.

[278] Hiroaki Natori. "DeeMe experiment - An experimental search for a mu-e conversion reaction at J-PARC MLF". In: *Nucl. Phys. Proc. Suppl.* 248-250 (2014), pp. 52–57. DOI: 10.1016/j.nuclphysbps.2014.02.010.

[279] Gianantonio Pezzullo. "The Mu2e experiment at Fermilab: a search for lepton flavor violation". In: *Nucl. Part. Phys. Proc.* 285-286 (2017), pp. 3–7. DOI: 10.1016/j.nuclphysbps.2017.03.002. arXiv: 1705.06461 [hep-ex].

[280] William A. Bardeen, A. J. Buras, and J. M. Gerard. "The K —> pi pi Decays in the Large n Limit: Quark Evolution". In: *Nucl. Phys.* B293 (1987), pp. 787–811. DOI: 10.1016/0550-3213(87)90091-5.

[281] Martin Gorbahn, Ulrich Haisch, and Mikolaj Misiak. "Three-loop mixing of dipole operators". In: *Phys. Rev. Lett.* 95 (2005), p. 102004. DOI: 10.1103/PhysRevLett.95.102004. arXiv: hep-ph/0504194 [hep-ph].

[282] Michal Czakon, Ulrich Haisch, and Mikolaj Misiak. "Four-Loop Anomalous Dimensions for Radiative Flavour-Changing Decays". In: *JHEP* 03 (2007), p. 008. DOI: 10.1088/1126-6708/2007/03/008. arXiv: hep-ph/0612329 [hep-ph].

[283] S. Fukae et al. "A Model independent analysis of the rare B decay B —> X(s) lepton+ lepton-". In: *Phys. Rev.* D59 (1999), p. 074013. DOI: 10.1103/PhysRevD.59.074013. arXiv: hep-ph/9807254 [hep-ph].

[284] S. Fukae, C. S. Kim, and T. Yoshikawa. "A Systematic analysis of the lepton polarization asymmetries in the rare B decay, B —> X(s) tau+ tau-". In: *Phys. Rev.* D61 (2000), p. 074015. DOI: 10.1103/PhysRevD.61.074015. arXiv: hep-ph/9908229 [hep-ph].

[285] H. H. Asatryan et al. "Complete gluon bremsstrahlung corrections to the process $b \to s l^+ l^-$". In: *Phys. Rev.* D66 (2002), p. 034009. DOI: 10.1103/PhysRevD.66.034009. arXiv: hep-ph/0204341 [hep-ph].

[286] Ian Richard Blokland et al. "Next-to-next-to-leading order calculations for heavy-to-light decays". In: *Phys. Rev.* D71 (2005). [Erratum: Phys. Rev.D79,019901(2009)], p. 054004. DOI: 10.1103/PhysRevD.79.019901,10.1103/PhysRevD.71.054004. arXiv: hep-ph/0503039 [hep-ph].

[287] Alexey Pak and Andrzej Czarnecki. "Heavy-to-heavy quark decays at NNLO". In: *Phys. Rev.* D78 (2008), p. 114015. DOI: 10.1103/PhysRevD.78.114015. arXiv: 0808.3509 [hep-ph].

[288] Ahmed Ali et al. "Power corrections in the decay rate and distributions in $B \to X_s l^+ l^-$ in the Standard Model". In: *Phys. Rev.* D55 (1997), pp. 4105–4128. DOI: 10.1103/PhysRevD.55.4105. arXiv: hep-ph/9609449 [hep-ph].

[289] H. M. Asatrian et al. "Complete bremsstrahlung corrections to the forward backward asymmetries in b —> X(s) l+ l-". In: *Mod. Phys. Lett.* A19 (2004), pp. 603–614. DOI: 10.1142/S0217732304013180. arXiv: hep-ph/0311187 [hep-ph].

[290] Ahmed Ali et al. "A Comparative study of the decays $B \to (K, K^{*)} \ell^+ \ell^-$ in standard model and supersymmetric theories". In: *Phys. Rev.* D61 (2000), p. 074024. DOI: 10.1103/PhysRevD.61.074024. arXiv: hep-ph/9910221 [hep-ph].

[291] S. Dobbs et al. "First Measurement of the Form Factors in the Decays $D^0 \to \rho^- e^+ \nu_e$ and $D^+ \to \rho^0 e^+ \nu_e$". In: *Phys. Rev. Lett.* 110.13 (2013), p. 131802. DOI: 10.1103/PhysRevLett.110.131802. arXiv: 1112.2884 [hep-ex].

[292] J. M. Flynn and Christopher T. Sachrajda. "Heavy quark physics from lattice QCD". In: *Adv. Ser. Direct. High Energy Phys.* 15 (1998), pp. 402–452. DOI: 10.1142/9789812812667_0006. arXiv: hep-lat/9710057 [hep-lat].

[293] J. Gill. "Semileptonic decay of a heavy light pseudoscalar to a light vector meson". In: *Nucl. Phys. Proc. Suppl.* 106 (2002), pp. 391–393. DOI: 10.1016/S0920-5632(01)01724-8. arXiv: hep-lat/0109035 [hep-lat].

[294] M. Ablikim et al. "Measurement of the form factors in the decay $D^+ \to \omega e^+ \nu_e$ and search for the decay $D^+ \to \phi e^+ \nu_e$". In: *Phys. Rev.* D92.7 (2015), p. 071101. DOI: 10.1103/PhysRevD.92.071101. arXiv: 1508.00151 [hep-ex].

[295] Gustavo Burdman and Gudrun Hiller. "Semileptonic form-factors from B —> K* gamma decays in the large energy limit". In: *Phys. Rev.* D63 (2001), p. 113008. DOI: 10.1103/PhysRevD.63.113008. arXiv: hep-ph/0011266 [hep-ph].

[296] Medina Ablikim et al. "Study of $D^+ \to K^- \pi^+ e^+ \nu_e$". In: *Phys. Rev.* D94.3 (2016), p. 032001. DOI: 10.1103/PhysRevD.94.032001. arXiv: 1512.08627 [hep-ex].

[297] Yue-Liang Wu, Ming Zhong, and Ya-Bing Zuo. "B(s), D(s) —> pi, K, eta, rho, K*, omega, phi Transition Form Factors and Decay Rates with Extraction of the CKM parameters |V(ub)|, |V(cs)|, |V(cd)|". In: *Int. J. Mod. Phys.* A21 (2006), pp. 6125–6172. DOI: 10.1142/S0217751X06033209. arXiv: hep-ph/0604007 [hep-ph].

[298] R. C. Verma. "Decay constants and form factors of s-wave and p-wave mesons in the covariant light-front quark model". In: *J. Phys.* G39 (2012), p. 025005. DOI: 10.1088/0954-3899/39/2/025005. arXiv: 1103.2973 [hep-ph].

[299] D. Melikhov and B. Stech. "Weak form-factors for heavy meson decays: An Update". In: *Phys. Rev.* D62 (2000), p. 014006. DOI: 10.1103/PhysRevD.62.014006. arXiv: hep-ph/0001113 [hep-ph].

[300] Svjetlana Fajfer and Jernej F. Kamenik. "Charm meson resonances and D —> V semileptonic form-factors". In: *Phys. Rev.* D72 (2005), p. 034029. DOI: 10.1103/PhysRevD.72.034029. arXiv: hep-ph/0506051 [hep-ph].

[301] Christoph Bobeth, Gudrun Hiller, and Danny van Dyk. "The Benefits of $\bar{B}- > \bar{K}^* l^+ l^-$ Decays at Low Recoil". In: *JHEP* 07 (2010), p. 098. DOI: 10.1007/JHEP07(2010)098. arXiv: 1006.5013 [hep-ph].

[302] R. Casalbuoni et al. "Effective Lagrangian for heavy and light mesons: Semileptonic decays". In: *Phys. Lett.* B299 (1993), pp. 139–150. DOI: 10.1016/0370-2693(93)90895-O. arXiv: hep-ph/9211248 [hep-ph].

[303] Hai-Yang Cheng. "Weak annihilation and the effective parameters a(1) and a(2) in nonleptonic D decays". In: *Eur. Phys. J.* C26 (2003), pp. 551–565. DOI: 10.1140/epjc/s2002-01065-6. arXiv: hep-ph/0202254 [hep-ph].

[304] Andrzej J. Buras. "QCD factors a1 and a2 beyond leading logarithms versus factorization in nonleptonic heavy meson decays". In: *Nucl. Phys.* B434 (1995), pp. 606–618. DOI: 10.1016/0550-3213(94)00482-T. arXiv: hep-ph/9409309 [hep-ph].

[305] Peter L. Cho and Mark B. Wise. "Comment on D(s)* —> D(s) pi0 decay". In: *Phys. Rev.* D49 (1994), pp. 6228–6231. DOI: 10.1103/PhysRevD.49.6228. arXiv: hep-ph/9401301 [hep-ph].

[306] C. C. Nishi. "Simple derivation of general Fierz-like identities". In: *Am. J. Phys.* 73 (2005), pp. 1160–1163. DOI: 10.1119/1.2074087. arXiv: hep-ph/0412245 [hep-ph].

[307] Jose F. Nieves and Palash B. Pal. "Generalized Fierz identities". In: *Am. J. Phys.* 72 (2004), pp. 1100–1108. DOI: 10.1119/1.1757445. arXiv: hep-ph/0306087 [hep-ph].

[308] Eugene Golowich and Alexey A. Petrov. "Short distance analysis of D0 - anti-D0 mixing". In: *Phys. Lett.* B625 (2005), pp. 53–62. DOI: 10.1016/j.physletb.2005.08.023. arXiv: hep-ph/0506185 [hep-ph].

[309] Alexey A Petrov. "Long-distance effects in charm mixing". In: *Proceedings, 6th International Workshop on Charm Physics (Charm 2013): Manchester, UK, August 31-September 4, 2013.* 2013. arXiv: 1312.5304 [hep-ph]. URL: http://inspirehep.net/record/1272720/files/arXiv:1312.5304.pdf.

[310] N. Carrasco et al. "S=2 and C=2 bag parameters in the standard model and beyond from N_f=2+1+1 twisted-mass lattice QCD". In: *Phys. Rev.* D92.3 (2015), p. 034516. DOI: 10.1103/PhysRevD.92.034516. arXiv: 1505.06639 [hep-lat].

[311] Chia Cheng Chang et al. "D-Meson Mixing in 2+1-Flavor Lattice QCD". In: *PoS* LATTICE2016 (2017), p. 307. arXiv: 1701.05916 [hep-lat].

[312] Jyoti Prasad Saha, Basudha Misra, and Anirban Kundu. "Constraining Scalar Leptoquarks from the K and B Sectors". In: *Phys. Rev.* D81 (2010), p. 095011. DOI: 10.1103/PhysRevD.81.095011. arXiv: 1003.1384 [hep-ph].

[313] J. S. Hagelin. "Mass Mixing and CP Violation in the $B^0 - \bar{B}^0$ system". In: *Nucl. Phys.* B193 (1981), pp. 123–149. DOI: 10.1016/0550-3213(81)90521-6.

[314] Amol Dighe, Anirban Kundu, and Soumitra Nandi. "Possibility of large lifetime differences in neutral B meson systems". In: *Phys. Rev.* D76 (2007), p. 054005. DOI: 10.1103/PhysRevD.76.054005. arXiv: 0705.4547 [hep-ph].

[315] Moira I. Gresham et al. "Confronting Top AFB with Parity Violation Constraints". In: *Phys. Rev.* D86 (2012), p. 034029. DOI: 10.1103/PhysRevD.86.034029. arXiv: 1203.1320 [hep-ph].

[316] Gautam Bhattacharyya, John R. Ellis, and K. Sridhar. "Bounds on the masses and couplings of leptoquarks from leptonic partial widths of the Z". In: *Phys. Lett.* B336 (1994). [Erratum: Phys. Lett.B338,522(1994)], pp. 100–106. DOI: 10.1016/0370-2693(94)00927-9,10.1016/0370-2693(94)90810-9. arXiv: hep-ph/9406354 [hep-ph].

[317] Rachid Benbrik and Chun-Khiang Chua. "Lepton Flavor Violating l —> l-prime gamma and Z —> l anti-l-prime Decays Induced by Scalar Leptoquarks". In: *Phys. Rev.* D78 (2008), p. 075025. DOI: 10.1103/PhysRevD.78.075025. arXiv: 0807.4240 [hep-ph].

[318] Jacques P. Leveille. "The Second Order Weak Correction to (G-2) of the Muon in Arbitrary Gauge Models". In: *Nucl. Phys.* B137 (1978), pp. 63–76. DOI: 10.1016/0550-3213(78)90051-2.

[319] King-man Cheung. "Muon anomalous magnetic moment and leptoquark solutions". In: *Phys. Rev.* D64 (2001), p. 033001. DOI: 10.1103/PhysRevD.64.033001. arXiv: hep-ph/0102238 [hep-ph].

[320] M. E. Pospelov and I. B. Khriplovich. "Electric dipole moment of the W boson and the electron in the Kobayashi-Maskawa model". In: *Sov. J. Nucl. Phys.* 53 (1991). [Yad. Fiz.53,1030(1991)], pp. 638–640.

[321] Andrzej Czarnecki and Bernd Krause. "Neutron electric dipole moment in the standard model: Valence quark contributions". In: *Phys. Rev. Lett.* 78 (1997), pp. 4339–4342. DOI: 10.1103/PhysRevLett.78.4339. arXiv: hep-ph/9704355 [hep-ph].

[322] Andreas Crivellin et al. "Renormalisation-group improved analysis of $\mu \to e$ processes in a systematic effective-field-theory approach". In: *JHEP* 05 (2017), p. 117. DOI: 10.1007/JHEP05(2017)117. arXiv: 1702.03020 [hep-ph].

[323] Ryuichiro Kitano, Masafumi Koike, and Yasuhiro Okada. "Detailed calculation of lepton flavor violating muon electron conversion rate for various nuclei". In: *Phys. Rev.* D66 (2002). [Erratum: Phys. Rev.D76,059902(2007)], p. 096002. DOI: 10.1103/PhysRevD.76.059902,10.1103/PhysRevD.66.096002. arXiv: hep-ph/0203110 [hep-ph].

[324] Vincenzo Cirigliano et al. "On the model discriminating power of mu —> e conversion in nuclei". In: *Phys. Rev.* D80 (2009), p. 013002. DOI: 10.1103/PhysRevD.80.013002. arXiv: 0904.0957 [hep-ph].

[325] Vincenzo Cirigliano, Sacha Davidson, and Yoshitaka Kuno. "Spin-dependent $\mu \to e$ conversion". In: *Phys. Lett.* B771 (2017), pp. 242–246. DOI: 10.1016/j.physletb.2017.05.053. arXiv: 1703.02057 [hep-ph].

[326] A. A. Gvozdev et al. "Muon decays with lepton number violation via vector leptoquark". In: *Phys. Lett.* B345 (1995), pp. 490–494. DOI: 10.1016/0370-2693(95)00003-4. arXiv: hep-ph/9411278 [hep-ph].

[327] Rachid Benbrik, Mohamed Chabab, and Gaber Faisel. "Lepton Flavour Violating τ and μ decays induced by scalar leptoquark". In: (2010). arXiv: 1009.3886 [hep-ph].

[328] Yuichi Uesaka et al. "Improved analyses for $\mu^- e^- \to e^- e^-$ in muonic atoms by contact interactions". In: *Phys. Rev.* D93.7 (2016), p. 076006. DOI: 10.1103/PhysRevD.93.076006. arXiv: 1603.01522 [hep-ph].

[329] Y Uchida et al. *COMET Phase-I Technical Design Report*. Tech. rep. 2015.

[330] J. Barranco et al. "Two Higgs doublet model and leptoquarks constraints from D meson decays". In: (2014). arXiv: 1404.0454 [hep-ph].

[331] Medina Ablikim et al. "Improved measurement of the absolute branching fraction of $D^+ \to \bar{K}^0 \mu^+ \nu_\mu$". In: *Eur. Phys. J.* C76.7 (2016), p. 369. DOI: 10.1140/epjc/s10052-016-4198-2. arXiv: 1605.00068 [hep-ex].

[332] Derek E. Hazard and Alexey A. Petrov. "Lepton flavor violating quarkonium decays". In: *Phys. Rev.* D94.7 (2016), p. 074023. DOI: 10.1103/PhysRevD.94.074023. arXiv: 1607.00815 [hep-ph].

[333] J. D. Jackson, S. B. Treiman, and H. W. Wyld. "Possible tests of time reversal invariance in Beta decay". In: *Phys. Rev.* 106 (1957), pp. 517–521. DOI: 10.1103/PhysRev.106.517.

[334] T. E. Chupp et al. "Search for a T-odd, P-even Triple Correlation in Neutron Decay". In: *Phys. Rev.* C86 (2012), p. 035505. DOI: 10.1103/PhysRevC.86.035505. arXiv: 1205.6588 [nucl-ex].

[335] A. Kozela et al. "Measurement of the Transverse Polarization of Electrons Emitted in Free Neutron Decay". In: *Phys. Rev. Lett.* 102 (2009), p. 172301. DOI: 10.1103/PhysRevLett.102.172301. arXiv: 0902.1415 [nucl-ex].

[336] E. G. Adelberger et al. "Positron neutrino correlation in the 0+ —> 0+ decay of Ar-32". In: *Phys. Rev. Lett.* 83 (1999). [Erratum: Phys. Rev. Lett.83,3101(1999)], pp. 1299–1302. DOI: 10.1103/PhysRevLett.83.1299. arXiv: nucl-ex/9903002 [nucl-ex].

[337] A. Gorelov et al. "Scalar interaction limits from the beta-ne correlation of trapped radioactive atoms". In: *Phys. Rev. Lett.* 94 (2005), p. 142501. DOI: 10.1103/PhysRevLett.94.142501. arXiv: nucl-ex/0412032 [nucl-ex].

[338] Frederik Wauters, Alejandro García, and Ran Hong. "Limits on tensor-type weak currents from nuclear and neutron decays". In: *Phys. Rev.* C89.2 (2014). [Erratum: Phys. Rev.C91,no.4,049904(2015)], p. 025501. DOI: 10.1103/PhysRevC.91.049904,10.1103/PhysRevC.89.025501. arXiv: 1306.2608 [nucl-ex].

[339] Wolfgang Altmannshofer et al. "Neutrino Trident Production: A Powerful Probe of New Physics with Neutrino Beams". In: *Phys. Rev. Lett.* 113 (2014), p. 091801. DOI: 10.1103/PhysRevLett.113.091801. arXiv: 1406.2332 [hep-ph].

[340] Morad Aaboud et al. "Search for high-mass new phenomena in the dilepton final state using proton-proton collisions at $\sqrt{s} = 13$ TeV with the ATLAS detector". In: *Phys. Lett.* B761 (2016), pp. 372–392. DOI: 10.1016/j.physletb.2016.08.055. arXiv: 1607.03669 [hep-ex].

Glossary

$\overline{\text{MS}}$ modified minimal subtraction. 9

ADM anomalous dimension matrix. 11

BLM Brodsky–Lepage–Mackenzie. 38

BRST Becchi–Rouet–Stora–Tyutin. 9

BSM beyond the standard model. 1

CKM Cabibbo–Kobayashi–Maskawa. 4

CL confidence/credibility level. 48

CLFQM covariant light front quark model. 130

CP charge parity. 1

CQM constituent quark model. 131

EOM equations of motion. 9

EW electroweak. 1

FCNC flavor changing neutral current. 5

GIM Glashow–Iliopolus–Maiani. 5

GPL generalized/Goncharov polylogarithm. 29

GSI gluon spectator interaction. 57

HPL harmonic polylogarithm. 29

HQE heavy quark expansion. 38

HQET heavy quark effective theory. 42

HSI hard spectator interaction. 47

IBP integration by parts. 15

IR infrared. 9

LCSR light cone sum rules. 57

LEET large energy effective theory. 43

LFU lepton flavor universality. 2

LFV lepton flavor violation. 52

LI Lorentz invariance. 25

LO leading order. 6

LQ leptoquark. 3

MI master integral. 23

MIA mass insertion approximation. 87

NLO next-to leading order. 9

NNLL next-to-next-to leading logarithmic. 2

NNLO next-to-next-to leading order. 2

NNNLL next-to-next-to-next-to leading logarithmic. 31

NNNLO next-to-next-to-next-to leading order. 101

OPE operator product expansion. 2

PC parity conserving. 53

PV parity violating. 53

QCD quantum chromodynamics. 2

QED quantum electrodynamics. 2

RG renormalization group. 2

RGE renormalization group equation. 3

SCET soft collinear effective theory. 47

SM standard model. 1

SUSY supersymmetric. 3

UV ultraviolet. 9

WA weak annihilation. 47